3rd International Conference on Sustainable Chemical & Environmental Engineering

ISBN: 978-618-86417-2-3

SUST ENG 2024

Proceedings

4th - 8th September 2024

Rethymno, Crete, Greece

hybrid event

www.susteng.tuc.gr

organizers

Design of Environmental Processes Lab

Technical University of Crete
School of Chemical and Environmental Engineering

co - organizers

Cyprus University of Technology

Dear friends and colleagues,

I am pleased to invite you to the 3rd International Conference on Sustainable Chemical and Environmental Engineering (SUSTENG 2024), which will be held in Rethymno, Crete, Greece, between 4th to 8th September 2024.

The conference is organized by the "Design of Environmental Processes Laboratory", of the School of Chemical and Environmental Engineering, Technical University of Crete and the Cyprus University of Technology.

The SUSTENG 2024 Conference will take place both with physical and virtual presence.

The conference aims to encourage the exchange of knowledge between academicians, scientists and engineers on hot issues and current developments in chemical and environmental engineering through sustainable perspective. The participants will have the opportunity to present their recent research findings on an extended spectrum of conference topics and be informed about new challenges, future trends, and technological innovations on sustainable processes following the principles of circular economy.

After the completion of the conference, all abstracts/full papers will be published in the SUSTENG 2024 Conference Proceedings with ISBN number, while selected manuscripts will be published to at least two Special Issues at high IF scientific journals (more information will be released soon).

The conference Chair

Petros Gikas

Professor

Head of the "Design of Environmental Processes Lab"

School of Chemical and Environmental Engineering

Technical University of Crete, Greece

SESSIONS OF SUSTENG 2024

Session 1: Solid waste management

Session 2: Wastewater management (I)

Session 3: Wastewater management (II)

Session 4: Biochemical engineering

Session 5: Materials science

Session 6: Water resources management

Session 7: Soil management

Session 8: Anaerobic digestion

Session 9: Water treatment

Session 10: Environmental management

Scientific committee:

Achille Ephrem Assogbadjo, University of Abomey-Calavi, Benin

Alexandros Katsaounis, University of Patras, Greece

Alexandros Stefanakis, Technical University of Crete, Greece

Anastasios Zouboulis, Aristotle University of Thessaloniki, Greece

Andreas Andreopoulos, National Technical University of Athens, Greece

Andrew Livingstone, Queens Mary University, UK

Anestis Vlysidis, National Technical University of Athens, Greece

Angela Gorgoglione, Universidad de la República, Uruguay

Antonios Kokosis, National Technical University of Athens, Greece

Antonios Papadakis, Region of Crete, Greece

Apostolos Giannis, Technical University of Crete, Greece

Apostolos Voulgarakis, Technical University of Crete, Greece

Aristeidis Koutroulis, Technical University of Crete, Greece

Artin Hatzikioseyian, National Technical University of Athens, Greece

Athanasia Tekerlekopoulou, University of Patras, Greece

Athanasios Kungolos, Aristotle University of Thessaloniki, Greece

Athanasios Stasinakis, University of the Aegean, Greece

Baoning Zhu, Beijing University of Chemical Technology, China

Christos Akratos, Democritus University of Trace, Greece

Constantinos Chrysikopoulos, Technical University of Crete, Greece

Cristina Trois, University of Kwa Zulu –Natal, South Africa

Dagmar Juchelkova, Technical University of Ostrava, Czech Republic

Danae Venieri, Technical University of Crete, Greece

Daniel Mamais, National Technical University of Athens, Greece

Despoina Vamvouka, Technical University of Crete, Greece

Dimitrios Dermantas, National Technical University of Athens, Greece

Dimitris Vayenas, University of Patras, Greece

Dinis Juizo, University of Eduardo Mondlane, Mozambique

Dionissios Mantzavinos, University of Patras, Greece

Dionysia Kolokotsa, Technical University of Crete, Greece

Dorothea Kasiteropoulou, University of Thessaly, Greece

Evan Diamantopoulos, Technical University of Crete, Greece

Ezio Ranieri, University of Bari, Italy

Elvis Tiburue, University of Ghana

Gagik Torosyan, State Engineering University of Armenia, Armenia

George Karatzas, Technical University of Crete, Greece

George Kyzas, International Hellenic University, Greece

George Papapolymerou, University of Thessaly, Greece

Isam Janajreh, Khalifa University, UAE

Jacek Dach, Poznan University of Life Sciences, Poland

Justin Chun-Te Lin, Feng Chia University, Taiwan

Keisuke Kuroda, Toyama Prefectural University Japan

Konstaninos Moustakas, National Technical University of Athens, Greece

Konstantinos Komnitsas, Technical University of Crete, Greece

Komi Agboka, University of Lome, Togo

Lazaros Papageorgiou, University College, UK

Lesly Tejeda, University of Cartagena, Colombia

Manish Kumar, University of Petroleum and Energy Studies, India

Maria Christina Fragkou, University of Chile, Chile

Maria Loizidou, National Technical University of Athens, Greece

Michael Fountoulakis, University of the Aegean, Greece

Michael Georgiadis, Aristotle University of Thessaloniki, Greece

Michael Kornaros, University of Patras, Greece

Michalis Koutinas, Cyprus Univeristy of Technology

Mohamed El Shaer, Zagazig University, Egypt

Mohamed Elhag, King Abdulaziz University, Saudi Arabia

Muhammad Arslan Ashraf, Government College University Faisalabad, Pakistan

Nicolas Kalogerakis, Technical University of Crete, Greece

Nikolaos Diangelakis, Technical University of Crete, Greece

Nikolaos Kiratzis, University of Western Macedonia, Greece

Nikolaos Nikolaidis, Technical University of Crete, Greece

Nikolaos Paranychianakis, Technical University of Crete, Greece

Noredine Loeid Mahdjoub, University of Kwa Zulu-Natal, South Africa

Okan Tarık Komesli, Atatürk University, Turkey

Panagiota Angeli, University College, UK

Partycja Pochwatka, University of Life Sciences in Lublin, Poland

Paraschos Melidis, Democritus University of Trace, Greece

Paraskevi Panagiotopoulou, Technical University of Crete, Greece

Petros Gikas, Technical University of Crete, Greece

Phillimon Odirile, University of Botswana, Botswana

Ruihong Zhang, University of California Davis, USA

Romain Lucas Glele Kakai, University of Abomey Calavi, Benin

Sema Sevinc Sengor, Middle East University, Turkey

Shan Yi, University of Auckland, New Zealand

Simona Di Gregorio, University of Pisa, Italy

Simos Malamis, National Technical University of Athens, Greece

George Tchobanoglous, University of California Davis, USA

Georgios Arampatzis, Technical University of Crete, Greece

Georgios Papadakis, Agricultural University of Athens, Greece

Gerasimos Lyberatos, National Technical University of Athens, Greece

Hassan Azaizeh, Tel-Hai College, Israel

Herve Boileau, University of Savoie Mont-Blanc, France

Hery Tiana Rakotondramiarana, University of Antananarivo, Madagascar

Ioannis Kalavrouziotis, Hellenic Open University, Greece

Ioannis Manariotis, University of Patras, Greece

Ioannis Tsanis, Technical University of Crete, Greece

Ioannis Vyrides, Cyprus University of Technology

Ioannis Yentekakis, Technical University of Crete, Greece

Spyridon Ntougias, Democritus University of Trace, Greece

Stergios Vakalis, University of the Aegean, Greece

Stratos Pistikopoulos, Texas A&M University, USA

Stylianos Rozakis, Technical University of Crete, Greece

Theocharis Tsoutsos, Technical University of Crete, Greece

Therese Lee Chan, The University of the West Indies, Trinidad and Tobago

Timothy Ginn, Washington State University, USA

Tonni Agustiono Kurniawan, Xiamen University, China

Vasileios Takavakoglou, Hellenic Agricultural Organization – DEMETER, Greece

Vassilios Tsihrintzis, National Technical University of Athens, Greece

Wei-Qin Zhuang, University of Auckland, New Zealand

Yaoyu Zhou, Hunan Agricultural University, China

SUST ENG 2024

SUSTENG 2024 - PROGRAMME AT A GLANCE

DAY 1 - Wednesday 4 September | Susteng 2024	
Rethymno Youth Center	
Registration	**19:30 - 20:00**
Welcome reception	**20:00 - 22:00**

DAY 2 - Thursday 5 September | Susteng 2024	
House of Culture	
Registration	**09:30 - 11:00**
Coffee break - Posters viewing	*10:45 - 11:00*
Greetings	**11:00 - 12:30**
PLENARY LECTURE: Prof. P. Gikas **Chair: K. Kuroda, A.E. Assogbadjo**	**12:30 - 13:15**
Lunch break	**13:15 - 14:45**
Session 1: Solid waste management	**14:45 - 16:30**
Session 2: Wastewater management (I)	**16:30 - 17:15**

DAY 3 - Friday 6 September | Susteng 2024	
House of Culture	
Session 3: Wastewater management (II)	**09:30 - 10:45**
Coffee break - Posters viewing	***10:45 - 11:00***
PLENARY LECTURE: Prof. T. Tsoutsos **Chair: P. Gikas, A.E. Assogbadjo**	**11:00 - 11:45**
Session 4: Biochemical engineering	**11:45 - 12:30**
Session 5: Materials science	**12:30 - 13:15**
Lunch break	***13:15 - 14:45***
PLENARY LECTURE: Prof. K. Kuroda **Chair: P. Gikas, T. Tsoutsos**	**14:45 - 15:30**
Session 6: Water resources management	**15:30 - 16:00**
Rethymno	
Field visit at Wastewater Treatment Plant of Rethymno	**18:30 - 19:30**
Gala dinner	**20:00 - 23:00**

DAY 4 - Saturday 7 September | Susteng 2024	
House of Culture	
Session 7: Soil management	**09:30 - 10:45**
Coffee break - Posters viewing	***10:45 - 11:00***
PLENARY LECTURE: Prof. A.E. Assogbadjo **Chair: P. Gikas, K. Kuroda**	**11:00 - 11:45**
Session 8: Anaerobic digestion	**11:45 - 12:30**
Session 9: Water treatment	**12:30 - 13:15**
Lunch break	***13:15 - 14:45***
Session 10: Environmental management	**14:45 - 16:15**
Closing ceremony	**16:15 - 17:00**

DAY 5 - Sunday 8 September | Susteng 2024	
Rethymno	
Conference excursion at the Historical Monastery of Arkadi and the Archeological Museum of Eleftherna (depending on participation)	**10:00 - 16:00**

SUST ENG 2024

SUSTENG 2024 PROGRAMME

DAY 1 - Wednesday 4 September | Susteng 2024	
Rethymno Youth Center	
Registration	**19:30 - 20:00**
Welcome reception	**20:00 - 22:00**

DAY 2 - Thursday 5 September | Susteng 2024	
House of Culture	
Registration	**09:30 - 11:00**
Coffee break	***10:45 - 11:00***
Greetings	**11:00 - 12:30**
PLENARY LECTURE: Prof. P. Gikas **Water reclamation and reuse: Opportunities and Challenges** **Chair: K. Kuroda, A.E. Assogbadjo**	**12:30 - 13:15**
Lunch break	**13:15 - 14:45**
Session 1: Solid waste management **Chair: A. Giannis, L. Afxentiou**	**14:45 - 16:30**
Technoeconomic assessment of pay as you throw system for the city of Chania **L. Afxentiou,** A. Giannis	14:45 - 15:00
The effect of biochar addition on the properties of alkali-activated materials produced from silicate tailings **K. Komnitsas,** V. Karmali, D. Vathi, A Kritikaki	15:00 - 15:15
A Review of EU refineries oily sludge waste production, management options and sustainability assessment of traditional and emerging oily sludges treatment techniques **E. Vaiopoulou,** A. Mianzan , W. Odle, K. Sakkalis	15:15 - 15:30
Biomass burning emissions from varying landuse over equatorial Southeast Asia (ESEA) **J. Sentian,** J.H. Chin, F.F. Adnan	15:30 - 15:45
Optimized location of electric vehicle batteries recycling center in Attica	15:45 - 16:00

A. Giannis, A. Lygizos, E. Kastanaki	
Current Trends, Challenges, and Future Opportunities in Biogas Production from Hospital Food Waste in Europe: Perspectives from the CaringNature Project **I. Vyrides**	16:00 - 16:15
Evaluation of the Physicochemical Properties and Ecotoxicological Impact of Municipal Biosolids for Agricultural Use **I. Giannakis, P.** Ntailiani, C. Emmanouil and A. Kungolos	16:15 -16:30
Session 2: Wastewater management (I) **Chair: E. Vaiopoulou, C. Rodriguez-Rodriguez**	**16:30 - 17:15**
Treatment of pharmaceutical-containing wastewater with a hybrid approach of advanced oxidation with persulphates/UV and biological removal by fungal pellets **C. Rodriguez-Rodriguez,** S. D. Villegas, M. D. Ramírez, G. V. Castro, M. M. Masís, R.C. Rodriguez	16:30 - 16:45
Effect of hydrogen peroxide on colour changes during the degradation of sulfamethoxazole by photo Fenton **U. Duoandicoechea,** A. De Luis, N. Villota	16:45 - 17:00
Domestic wastewater treatment by a high-rate anaerobic MBR system **E. Politou,** K. Azis, A. Makri, S. Ntougias, N. Remma, P. Melidis	17:00 - 17:15

DAY 3 - Friday 6 September | Susteng 2024	
House of Culture	
Session 3: Wastewater management (II) **Chair: G. Panayiotou, D. Gavrilescu**	**09:30 - 10:45**
Effect of iron catalyst on water quality parameters during the oxidation of diclofenac by photo-Fenton treatment **U. Duoandicoechea,** J. M. Lomas, N. Villota	09:30 - 09:45
Nutrient recovery from urine diverting dry toilets via pyrolysis **M. E. Koulouri,** M.R. Templeton, G. D. Fowler	09:45 - 10:00
Limassol District Local Government Organisation: Challenges and opportunities in sewage treatment **G. Panayiotou,** P. Marti	10:00 - 10:15
Advanced primary filtration process for the upgrade of overloaded activated sludge plants **K. Tsamoutsoglou,** P. Gikas	10:15 - 10:30
Preparation of biochar derived from olive mill solid waste in a circular economy approach for enhanced adsorption of trihalomethanes from water **S. Azerrad**, H. Azaizeh, E. Kurzbaum	10:30 - 10:45
Coffee break - Posters viewing	***10:45 - 11:00***
PLENARY LECTURE: Prof. T. Tsoutsos **Unlocking the potential of heritage-based innovation for sustainable development: The HI-EURECA-PRO project** **Chair: P. Gikas, A.E. Assogbadjo**	**11:00 - 11:45**
Session 4: Biochemical engineering **Chair: R. Konstantinou, T. Tsoutsos**	**11:45 - 12:30**

Enhancement of starch hydrolysis using immobilized cells and enzymes of two Aspergillus strains on oxidized carbonaceous materials **R. Konstantinou**	11:45 - 12:00
Bioprocess development for thermoplastic starch polyhydroxybutyrate biodegradation using algal-microbial co-cultures **F. Pyrilli,** E. Syranidou, G. Constantinides, M. Koutinas	12:00 - 12:15
A critical examination of macroalgae biomass utilization: Perspectives from life cycle assessments **C. Nikoloudakis,** A. Pantis, T. Tsoutsos	12:15 - 12:30
Session 5: Materials science **Chair: S. Azerrad, D. P. Gournis**	**12:30 - 13:15**
The green synthesis of irregular gold nanoparticles and their application in nanomedicine **R. Mariychuk,** R. Smolkova, L. Grishchenko, V. Lisnyak	12:30 - 12:45
Innovative bioprocess employing recyclable immobilized enzyme for paraoxon removal in water and effluents: Phosphotriesterase immobilized on Fe_3O_4-SiO_2-NH_2 magnetic nanocomposites **S. Azerrad**	12:45 - 13:00
2D Xenes of Group-14: New synthetic strategies and derivatives for environmental and energy applications **D. P. Gournis**	13:00 - 13:15
Lunch break	***13:15 - 14:45***
PLENARY LECTURE: Prof. K. Kuroda **Emerging contaminants in groundwater: threats in the 21st century** **Chair: P. Gikas, T. Tsoutsos**	**14:45 - 15:30**
Session 6: Water resources management **Chair: K. Tsamoutsoglou, E. Vaiopoulou**	**15:30 - 16:00**
From data to decision: understanding and mitigating uncertainty in watershed water quality models **A. Gorgoglione**	15:30 - 15:45
Water use and efficiencies in fuel refining sites **E. Vaiopoulou,** E. Fiddaman, S. Gibbons, S. Mackay, J. Shaw, L. Leclezio, J. Russel, M. Hjort, L. G. Guerrero	15:45 - 16:00
Rethymno	
Field visit at Wastewater Treatment Plant of Rethymno	**18:30 - 19:30**
Gala dinner	**20:00 - 23:00**

DAY 4 - Saturday 7 September | Susteng 2024	
House of Culture	
Session 7: Soil Management **Chair: F. J. Chadare, A. Stefanatou**	**09:30 - 10:45**
Soil improvement by electro carbonation induced calcite precipitation (ECICP) from the seawater **H. Abdeh Keykha,** M. Mavroulidou, H. Mohamadzadeh Romiani Hadi	09:30 - 9:45

Biocementation via microbial induced struvite precipitation: A mini review on cleaner method of soil stabilization **S. Joshi,** M. Mavroulidou, M. J. Gunn	09:45 - 10:00
PFAS soil treatment processes – a review of operating ranges and constraints **E. Vaiopoulou,** J. Hurst, S. Hale, J. Miles, E. Dall, W. Gevaerts , J. Burdick, M. Hjort	10:00 - 10:15
Effects of fungicides and bactericides on BVOC emissions in cypriot vineyard soils **K. Kaikiti,** S. Savvides, L. Philippot, I. Ioannides, A. Agapiou, M. Omirou	10:15 - 10:30
Use of residues generated from olive cultivation and olive oil production for the enhancement of soil quality **A. Stefanatou**, A. Kalampokidis, T. Maneka, G.E. Dimitriou, M. Pavlidis, M. Veloutsos, A. Galanidis, F. Galliou, T. Manios, D.F. Lekkas, P. Dimitrakopoulos, N. Fyllas, S. Vakalis, M. Fountoulakis	10:30 - 10:45
Coffee break - Posters viewing	***10:45 – 11:00***
PLENARY LECTURE: Prof. A.E. Assogbadjo **Review on ecosystems nature-based restoration initiatives in Africa** **Chair: P. Gikas, K. Kuroda**	**11:00 - 11:45**
Session 8: Anaerobic digestion **Chair: K. Tsamoutsoglou, G. Antonopoulou**	**11:45 - 12:30**
Environmental and energetic analysis of biogas plants supplied with different substrate scenarios **P. Pochwatka**, J. A. Kowalczyk, J. Mazurkiewicz, J. Pulka, K. Kupryaniuk, J. Dach	11:45 - 12:00
Designing sustainable processes for methane and hydrogen production using poplar woody sawdust biomass: The effect of chemical pretreatment **G. Antonopoulou,** I. Apostolopoulos, A. Tekerlekopoulou	12:00 - 12:15
Modelling hollow fibre membrane bioreactors for biogas purification **A. Hatzikioseyian,** J. Das, P. Lens	12:15 - 12:30
Session 9: Water treatment **Chair: A. Papadakis, T. Thodosiadis-Thomaidis**	**12:30 - 13:15**
The use of hyperspectral imaging in aquatic vegetation analysis **J. Kostecki,** S. Myszograj, E. Płuciennik-Koropczuk, I. Krupińska	12:30 - 12:45
Systematic environmental surveillance for legionella detection and treatment in a hospital water distribution system in the region of Crete during covid-19 era **A. Papadakis,** E. Koufakis, K. Tsamoutsoglou, N. Gikas, D. Chochlakis, A. Psaroulaki, P. Gikas	12:45 - 13:00
Unseen processes in freeze desalination: molecular dynamics of nucleation, crystal growth, and ion entrapment – a short review **I. Janajreh,** K. El Kadi	13:00 - 13:15
Lunch break	***13:15 - 14:45***
Session 10: Environmental Management **Chair: S. Lyle, A.E. Assogbadjo**	**14:45 - 16:15**

Pangaea.cubes - IoT low power challenges towards sustainability H/W - S/W design implementations and applications **T. Thodosiadis-Thomaidis,** G. Panagopoulou, V. Vorrias	14:45 - 15:00
Development of sustainable communication systems supported by high-impact environmental energy sources for people on the Move **S. Lyle,** K. Pappas, C. Lyle	15:00 - 15:15
Forest food resources back to the menu for enhancing food sovereignty in a context of high hybridation: case of Adansonia digitata and Irvingia gabonensis **F. J. Chadare,** F.T.K Fassinou, S. Ahouansou Montcho , M. Affonfere, A.E. Assogbadjo	15:15 - 15:30
Early-stage mathematical modeling of solution spray pyrolysis for the fabrication of functional ceramic films **N. Fotiadi,** D. Lazaridis, N. Rigakis, N. Kiratzis	15:30 - 15:45
Life cycle assessment to address key environmental impact elements of ERASE, an innovative in situ remediation technology **G. Beretta,** E. Sezenna, G. Dolci, L. Rigamonti, S. Saponaro, C. Carnabuci, D. Vezzoli	15:45 - 16:00
West african mangroves in the context of climate change: social-ecological dynamics, challenges and perspectives **R. Glèlè Kakaï**	16:00 - 16:15
Closing ceremony **Chair: P. Gikas, K. Kuroda, A.E. Assogbadjo, T. Tsoutsos**	**16:15 - 17:00**

DAY 5 - Sunday 8 September | Susteng 2024	
Rethymno	
Conference excursion at the Historical Monastery of Arkadi and the Archeological Museum of Eleftherna (depending on participation)	**10:00 - 16:00**

Posters
House of Culture-Upper Floor

Biogas potential of distillery stillage and evaluation of digestate as a potential fertilizer
I. Vaskina, R. Vaskin, M. Cieslik, A. Lewicki, L. Demkova, M. Skidanenko, S. Sydorenko

Modelling Methane Emissions Resulting from Municipal Solid Waste Management: Reduction Options and Environmental Impact
D. Petrisor, C. Cirjan , D. Gavrilescu, C. Teodosiu

Modeling of Waste Electrical and Electronic Equipment Generation Rate using Multiple Regression Analysis
M. Gavrilescu, D. Gavrilescu

Model development for a Renewable Energy Sources Thematic Park – RESTPark A synergistic approach to Water Management and Renewable Energy Systems (Bioclimatic architecture, Solar, Wind, Micro-Hydro, Geothermal & Biomass)
A. T. Thomaidis, T. T. Theodosiadis

Evaluation of Biochar from Sewage Sludge for Sustainable Carbon Adsorption
L. D. Tshenyego, P.T. Odirile, A. Giannis, P. Gikas

Unlocking the timeless wisdom of Athens: A journey towards sustainability through design
D. Tzourmakliotou, E. Sourli

Life Cycle Assessment of PLA/MXene Nanocomposite
V. Tzatzadakis, A.Thomos, F. Gojda, F. Krasanakis, K. Chrissopoulou, S. Anastasiadis, E. Patelarou, M. Stylianakis

Decarbonisation of asphalt mix production
A. Woszuk, S. Malinowski, R. Panek

Exploring innovative cathodes based on perovskites in Microbial Fuel Cells
L. Skopas, G. Bampos , I. Apostolopoulos, S. Bebelis, G. Antonopoulou

Hydrocyclone for the treatment of municipal primary wastewater
K. Tsamoutsoglou, A. Kechagias, P. Gikas

The impact of substrate extrusion on the energy and economic efficiency of biogas plant operation
K. Kupryaniuk, K. Witaszek, P. Pochwatka, J. Mazurkiewicz, I. Vaskina, D. Janczak, J. Dach

Quality criteria for water reuse in the Mediteranean basin
E. Gika, V. Tzika, F. Ranieri, A.C. Ranieri, E. Ranieri, P. Gikas

Carbon dioxide capture from actual industrial flue gas using microalgae
G. Makaroglou, D. Mitrogiannis, P. Gikas

Session 1: Solid waste management

Technoeconomic assessment of Pay As You Throw system for the city of Chania

L. Afxentiou[1] and A. Giannis[1]

[1]School of Chemical and Environmental Engineering, Technical University of Crete, University Campus, 73100 Chania, Greece
Corresponding author email: agiannis@tuc.gr

keywords: *Pay as you throw, waste management, recycling, optimization.*

Abstract

Waste management is a continuously evolving sector as it is at the forefront of the EU transition to a Circular Economy responsible future. The new EU directive imposes the implementation of "Pay As You Throw" (PAYT) system by member states based on "The Polluter Pays" Environmental Policy principle. This study evaluates the PAYT system implemented in the municipality of Aglantzia (Cyprus) and designs an economically viable PAYT system for the city of Chania (Greece). Through the implementation of PAYT system, the total cost of waste management is passed on to the municipality's residents, while providing financial incentives to encourage the separate collection of mixed waste, organic waste and recyclable materials, to reduce the amount of comingled waste sent for landfilling and thus reduce the overall cost of waste management services. At the same time, the fee amount (charge) is optimized for increased financial transparency as the cost of each individual step is calculated, making it easier to identify any problems, miscalculations, ineffectiveness of equipment, machinery, processes or facilities. The waste management data collected by DEDISA (local waste management authority) are used to calculate the projected amount of waste generation in the next three years (2025-2027), to create scenarios for the reduced quantity of collected mixed waste and the increased amount of recyclable materials, while estimating the yearly fee each household should pay for waste management. Two charge scenarios are analyzed: (1) the first scenario incorporates the municipality tax in its entirety to a prepaid bag (volume-based charge); and (2) the second scenario is a dual fee system including partial municipality tax and additional volume-based charge supplemented with the cost of the prepaid bag. The study proposes an innovative solution for streamlining yearly waste management costs utilizing IT, extracting the cost of prepaid bag and municipality tax for the dual charge system. The study also leverages the income generated from the sales of collected recyclable materials and the compost produced from separately collected biowaste to lower the overall waste management cost. Finally, the study provides guidelines for organizing, promoting and monitoring the implementation of the PAYT system in the city of Chania.

The effect of biochar addition on the properties of alkali-activated materials produced from silicate tailings

V. Karmali[1], D. Vathi[1], A. Kritikaki[1] and K. Komnitsas[1]

[1]School of Mineral Resources Engineering, Technical University of Crete, 73100 Chania, Greece
Corresponding author email: kkomnitsas@tuc.gr

Abstract

In this experimental study, the effect of biochar addition on the properties of alkali-activated materials (AAMs) produced from silicate tailings, that derive after flotation of sulphide ores, is investigated. The activating solution consists of potassium hydroxide (KOH) and sodium silicate (Na_2SiO_3) solutions. AAMs are produced by using different KOH molarity (4 mol/L, M), curing temperature (40 or 80 °C) and aging period (7 or 28 days). The effect of biochar type (produced from sewage sludge or walnut shells after pyrolysis at 350 or 500 °C) and percentage addition in the starting mixture (5% and 15% v/v) on the main properties (i.e. compressive strength, density, porosity and water absorption) of the produced AAMs is explored. The results indicate that the addition of biochar results in the production of specimens with decreased compressive strength and increased porosity and water absorption compared to the control specimens (produced with only the use of silicate tailings). X-ray diffraction (XRD) and Fourier transform infrared spectroscopy (FTIR) are used to characterize the raw materials, the produced biochars and selected AAMs. This study confirms the co-valorization potential of various by-product (waste) types (e.g. mining, municipal, agricultural) and the production of higher value-added products.

Keywords: *sewage sludge; walnut shells; mining waste; circular economy; SDGs.*

1. Introduction

The annual generation of solid mining waste reaches 20-25 billion tons, half of which is mine tailings (Kiventerä, et al., 2020). Although a share may be used in the construction sector, most of them are often disposed on land or in water reservoirs. Improper disposal practices can result in the solubilization of potentially hazardous elements (PTEs), causing significant environmental impacts (Bai et al., 2018; Bougara et al., 2018; Komnitsas et al., 2007). Ore beneficiation, involving mainly flotation, generates large volumes of tailings. Most of them are stored in tailing dams situated in the vicinity of mining sites/beneficiation plants. These tailings, if possible, may be also valorized for the recovery of critical and strategic elements (Kinnunen et al., 2018; Obenaus-Elmer et al., 2020; Perumal et al., 2020).

Alkali activation is a sustainable and quite well-established technology for the valorization of process by-products/wastes rich in silicon (Si) and aluminum (Al) for the production of secondary alkali activated materials (AAMs) with higher added value. It takes place when a strong alkaline solution (mainly NaOH or KOH) reacts with an aluminosilicate raw material. Al and Si ions are released, react and form alumino-silicate bonds, while the produced specimens develop a homogeneous microstructure and acquire beneficial mechanical properties (Komnitsas et al., 2019, 2020; Zaharaki et al., 2016).

Biochar is a porous material obtained from the pyrolysis of biomass, such as sewage sludge, agricultural wastes and various prunings. The addition of biochar in the starting mixture prior to alkali activation may result in the production of final products with modified microstructure and properties (Gupta et al., 2018; Praneeth et al., 2020; Zeidabadi et al., 2018). This study aims to investigate the effect of the addition of biochar on the properties of AAMs produced from silicate tailings. Parameters that are investigated include the molarity of KOH (4 and 6 M), curing temperature (40 or 80 °C), the type of biochar (produced from sewage sludge and walnut shells at two pyrolysis temperatures, 350 or 500 °C) and two percentages of biochar addition in the starting mixture (5% or 15% v/v).

2. Materials and Methods

The raw material used for alkaline activation is low-sulphur (FeS_2 content appr. 1 wt.%) silicate tailings (KST), obtained from the flotation plant of Kevitsa, in Finland. Prior to their characterization, KST were dried at 80 °C for 1 day and pulverized using a Sepor-type rod mill (Sepor, Los Angeles, CA, USA) and a Bico-type pulverizer

(Fritsch, Dresden, Germany) to less than 40 μm. The particle size distribution of the pulverized KST was determined using a laser particle size analyzer (Mastersizer S, Malvern Instruments, Malvern, UK). Chemical analysis of KST was carried out using an X-ray fluorescence energy dispersive spectrometer (XRF-EDS) S2 Range type (Bruker, Karlsruhe, Germany), while the loss on ignition (LOI) was determined after heating them at 1050 °C for 4 hours.

Two different feedstocks were selected for the production of biochar. Sewage sludge (SS), obtained from the Wastewater Treatment Plant of Chania (Crete, Greece) and walnut shells (WS) obtained from a farm in Lamia (central Greece). Prior to pyrolysis, SS and WS were oven dried (Carbolite, Germany) at 105 °C for 24 h to remove any residual moisture. The pyrolysis temperature, selected from earlier studies carried out at the laboratory, was 350 or 500 °C. The produced biochars were ground and sieved to size (d90) smaller than 75 μm prior to their use. The codes of the produced biochars are SS350, SS500, WS350, and WS500 (the first 2 letters denote the feedstock type and the last 3 digits the pyrolysis temperature).

Mineralogical analysis was performed using an X-ray diffractometer (Bruker AXS, D8-Advance, Bruker, Karlsruhe, Germany), DiffracPlus Software (EVA v 4.2, Bruker, Karlsruhe, Germany), Crystallographic Open Database (COD database); quantitative determination of mineralogical phases was done by the Rietveld software AutoQuan v.2.8 (Seifert GE). FTIR analysis was carried out in a PerkinElmer 1000 spectrometer (PerkinElmer, Akron, OH, USA), in the range of 400 to 4000 cm^{-1} using pellets produced by mixing the pulverized raw material with dry KBr at a ratio of 1:100 w/w.

AAMs were produced by (i) mixing KST with different percentages of SS and WS biochar (5 and 15 %v/v) for each pyrolysis temperature (350 or 550 °C), (ii) slow addition of the feed to the activating solution (KOH 4M and Na_2SiO_3 at 1:1 weight ratio) and mixing for 5 min at low speed for the production of a homogeneous paste. The paste was then cast into plastic cubic molds, with an edge of 4 cm, that vibrated for 1 min to remove air and then covered with parafilm to prevent moisture loss. After 24 h, a period that is considered sufficient for the initiation of the alkali activating reactions and the early development of alumino-silicate bonds, the specimens were removed from the molds and cured at 40 or 80 °C in an oven for 24h. Finally, the cured specimens were removed from the oven and left for aging at room temperature for a period of 7 or 28 days. The compressive strength of the produced AAMs, as the average value of three measurements, was determined with the use of an MST 815 (1600 KN) Rock Mechanics Test System with loading rate equal to 0.5-1 MPa/sec. Porosity, water absorption and density were also determined for selected AAMs, according to the BS EN 1936:2006 standard.

3. Results and discussion

3.1 Biochar characterization

Table 1 shows the values of selected properties of the feedstocks and the biochars. It is first seen that as pyrolysis temperature increases, pH also increases and yield decreases and this defines the economics of the process. All biochars exhibit pH values close to 9 or higher, indicating their alkaline nature and their potential for buffering the pH of acidic soils in agricultural applications. It is also seen that the specific surface area (m^2/g) of the produced biochars increases with temperature and this may affect the microstructure of the produced AAMs after alkali activation, as well as their water/nutrient/contaminant adsorption, depending on its use, potential.

Table 1. *Properties of feedstocks and biochars (pyrolysis temperature 350 or 500 °C).*

Parameter	Raw SS	SS350	SS500	Raw WS	WS350	WS500
pH	8.5	8.9	10.1	8.3	8.9	10.2
Dry Matter, TS (%)	31	93	94	89	93	88.0
Volatile Solids, VS (%)	49	66	50	97.2	89.2	75.1
Ash Content, AC (%)	24.4	34	55	2.8	10.7	32.4
Specific Surface Area, SSA (m^2/g)	1.2	12.8	24.9	2.1	19.6	29.8
Yield, %	-	27.2	18.3	-	35.3	14.1

3.2 KST characterization

The chemical composition of KST, in the form of oxides, is shown in **Table 2**. The main phases identified are SiO_2 (44.7 wt.%), MgO (21.8 wt.%), CaO (13.5 wt.%), Fe_2O_3 (11.5 wt.%) and Al_2O_3 (4.0 wt.%).

Table 2. *Chemical analysis (wt.%) of KST*

Oxide (wt.%)	SiO_2	MgO	CaO	Fe_2O_3	Al_2O_3	LOI*
	44.7	21.8	13.5	11.5	4.0	2.1

LOI: Loss on ignition at 1050 °C

The mineralogical analysis of KST is shown in **Figure 1**. The main phases present are tremolite $[Ca_2Mg_5Si_8O_{22}(OH)_2]$ 27 wt.%, diopside $(MgCaSi_2O_6)$ 26 wt.%, lizardite $[Mg_3(Si_2O_5)(OH)_4]$ 11 wt.%, albite $(NaAlSi_3O_8)$ 8 wt.%, clinochlore $[Mg_5Al(AlSi_3O_{10})(OH_8)]$ 8 wt.%, forsterite $[Mg_2SiO_4]$ 7 wt.%, biotite $[K(Mg,Fe)_3(AlSi_3O_{10})(F,OH)_2]$ 4 wt.%, magnetite (Fe_3O_4) 2 wt.% and pyrite (FeS_2) 1 wt.%.

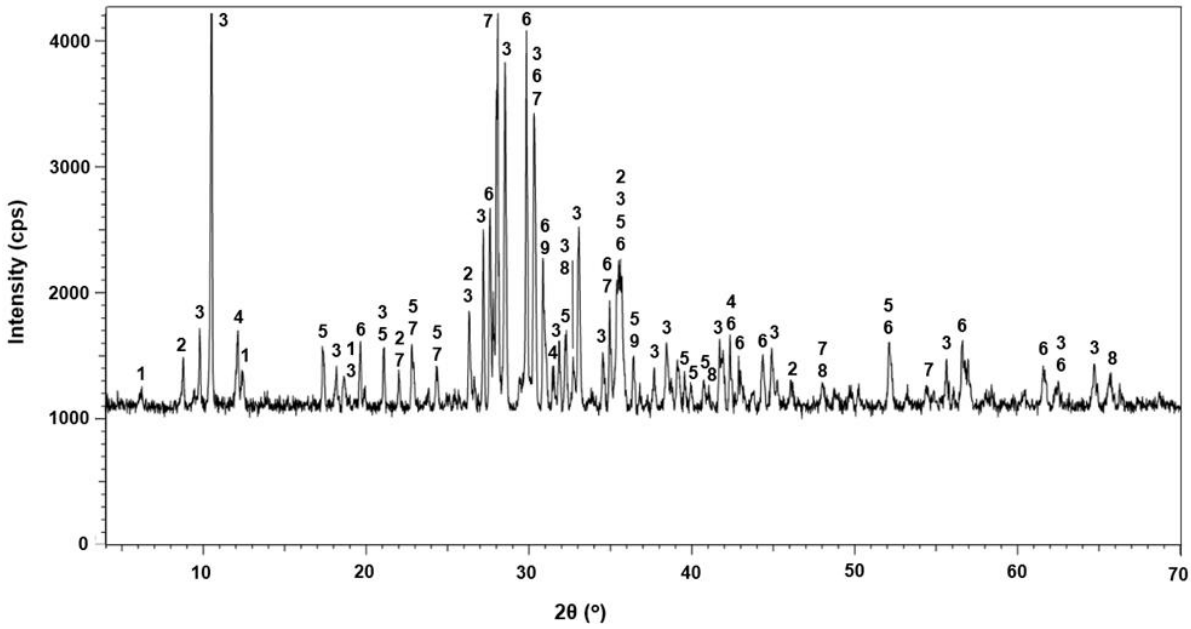

Figure 1. *XRD pattern of KST, 1-clinochlore, 2-biotite, 3-tremolite, 4-lizardite, 5-forsterite, 6-diopside, 7-albite, 8-pyrite, 9-magnetite.*

3.3 Effect of biochar addition on the compressive strength of the produced AAMs

Figures 2 shows the evolution of the compressive strength of the KST-based AAMs for two addition percentages (5 and 15% v/v) of SS biochar (**Fig. 2a**) and WS biochar (**Fig. 2b**) produced after pyrolysis at 350 or 500 °C. The compressive strength of control specimens, not involving the addition of biochar, is shown on the left part of each figure. It is first seen that the control specimens acquire a compressive strength of almost 20 MPa when the curing temperature is 80 °C. On the other hand, low curing temperature (40 °C) results in the production of specimens with low compressive strength (4 MPa), at least for the short aging period considered in this study (7 days).

The addition of biochar, regardless of its percentage and the feedstock type, does not substantially affect the compressive strength of the AAMs when the curing temperature is 40 °C. On the other hand, when the curing temperature is higher, 80 °C, the addition of biochar results in the production of AAMs with higher, compared to 40 °C, but reduced compressive strength compared to the control specimens. Higher decrease is noted when higher biochar addition percentage and lower pyrolysis temperature are used; for example, the addition of 15% v/v of SS350 biochar results in a specimen, after curing at 80 °C, with compressive strength value of almost 6 MPa (70% reduction compared to the control), while the addition of 5% v/v of WS500 biochar results in a specimen, after curing at 80 °C, with compressive strength value of 12.5 MPa (almost 35% reduction compared to the control). Furthermore, it is seen that the addition of WS biochar, for the same addition percentage, curing temperature and aging time, results in specimens with higher compressive strength when compared to those derived by the addition of SS biochar. This is probably due to the higher surface area of WS

biochar as well as its higher VS and lower AC content, compared to the SS biochar; however, this still has to be verified with additional experiments.

Table 3 shows the porosity (%), water absorption (%), and apparent density (g cm^{-3}) of the produced AAMs, with the addition of 15% v/v biochar, as well as their compressive strength values, to enable an easier comparison.

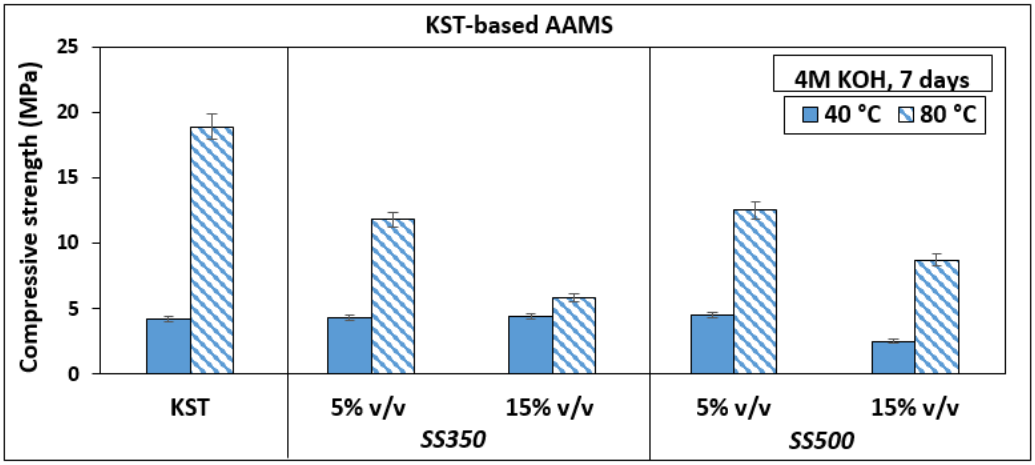

(a)

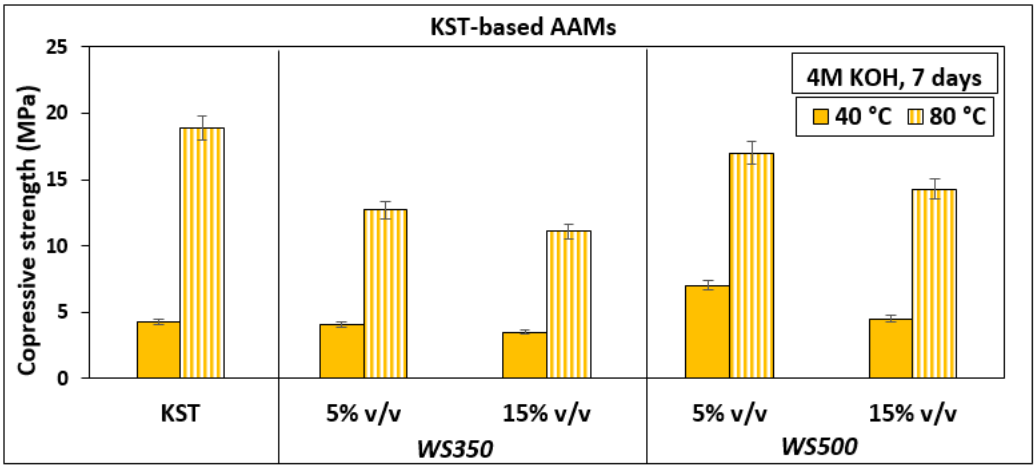

(b)

Figure 2. *Compressive strength of KST-based AAMs with 5 and 15% v/v biochar addition, produced after pyrolysis at 350 or 500 °C (a) SS, (b) WS biochar. Synthesis conditions: 4M KOH, curing temperature 40 or 80 °C, aging period 7 days; error bars derive from measurements of three specimens*

Table 3. *Physical properties of selected AAMs*.*

AAMs	Compressive strength (MPa)	Porosity (%)	Water absorption (%)	Apparent density (g cm^{-3})
KST	18.9	8.8	3.6	2.4
KST + 15% v/v SS350	5.8	13.4	4.1	2.1
KST + 15% v/v SS500	8.7	10.0	4.2	2.1
KST + 15% v/v WS350	11.1	13.5	6.0	2.2
KST + 15% v/v WS500	14.3	9.5	2.4	2.5

*activating solution (KOH 4M and Na_2SiO_3), curing at 80 °C and aging period for 7 days.

It is seen that the addition of 15% v/v of each biochar did not substantially affect these 3 properties. For example, the addition of WS500 biochar resulted in a slight increase of porosity to 9.5% and apparent density to 2.5%, as well as in decreased water adsorption (2.4%) compared to the control specimen (KST) values of 8.8%, 2.4% and 3.6% respectively. These two specimens exhibited also rather similar compressive strength

values, 14.3 and 18.9 MPa respectively. Another important result is the increased porosity of the AAMs produced with the addition of both biochars that derived after pyrolysis of the biomass at lower temperature, 350 °C (Piccolo et al., 2021; Gupta et al., 2018; Han et al., 2023).

4. Conclusions

The present study, that is in in line with the principles of circular economy, investigates the effect of biochar addition at low percentages, namely 5% and 15% v/v, on the properties of AAMs obtained after alkali activation of low-sulphur silicate tailings, obtained after flotation of sulphide ores. The biochars used were obtained after pyrolysis of sewage sludge and walnut shells at 350 or 500 °C.

The results indicate that (i) the addition of biochar regardless of the feedstock type and the addition percentage, does not practically affect the compressive strength of the produced AAMs, compared to the control, when the curing temperature is 40 °C, (ii) at higher curing temperature, 80 °C, the addition of biochar results in the production of AAMs with reduced compressive strength compared to the control; higher compressive strength values are obtained by the use of biochar produced at higher temperature (550 instead of 350 °C), (iii) addition of biochar produced at lower temperature (350 °C) results in the production of AAMs with higher porosity and water absorption; these products may be used in environmental applications, and (iv) the co-valorization of biochar and industrial by-products contributes to meeting several sustainable development goals (SDGs), including SDG 12 (Sustainable Consumption and Production) and SDG 11 (Sustainable Cities and Communities).

Future studies, involving different raw materials (e.g high sulphur flotation tailings), biochar addition percentage, pyrolysis temperature, alkaline solution (e.g NaOH), ratio of alkaline solution to Na_2SiO_3 solution (e.g 2:1 or 1:2) and longer aging times, are underway to optimize the properties and define the uses of the produced AAMs.

5. Acknowledgements

This research was carried out in the frame of ENICON project, “Sustainable processing of Europe’s low grade sulphidic and lateritic Ni/Co ores and tailings into battery grade metals”, https://enicon-horizon.eu/, and received funding from the European Union’s Framework Programme for Research and Innovation Horizon Europe under Grant Agreement No. 101058124.

REFERENCES

Bai, T., Song, Z.G., Wu, Y.G., Hu, X.D. and Hua, B., 2018. Influence of steel slag on the mechanical properties and curing time of metakaolin geopolymer. *Ceram. Int.*, 44 (13), 15706–15713. https://doi.org/10.1016/j.ceramint.2018.05.243.

Bougara, A., Lynsdale, C. and Milestone, N.B., 2018. The influence of slag properties, mix parameters and curing temperature on hydration and strength development of slag/cement blends. *Constr. Build. Mater.,* 187, 339–347. https://doi.org/10.1016/j.conbuildmat.2018.07.166.

Gupta, S., Kua, H.W. and Pang, S.D., 2018. Biochar-mortar composite: Manufacturing, evaluation of physical properties and economic viability. *Constr. Build. Mater.*, 167, 874–889. https://doi.org/10.1016/j.conbuildmat.2018.02.104.

Han, X., Jiang, N., Jin, F., Reddy, K.R., Wang, Y.; Liu, K. and Du, Y., 2023. Effects of biochar-amended alkali-activated slag on the stabilization of coral sand in coastal areas. *J. Rock Mech. Geotech. Eng.,* 15, 760–772. https://doi.org/10.1016/j.jrmge.2022.04.010.

Kinnunen, P., Ismailov, A., Solismaa, S., Sreenivasan, H., Räisänen, M.-L., Levänen, E. and Illikainen, M., 2018. Recycling mine tailings in chemically bonded ceramics – A review. *J. Clean. Prod.*, 174, 634–649. https://doi.org/10.1016/j.jclepro.2017.10.280.

Kiventerä, J., Perumal, P., Yliniemi, J. and Illikainen, M., (2020). Mine tailings as a raw material in alkali activation: A review. *Int. J Miner Metall. Mater.*, 27 (8), 1009–1020. https://doi.org/10.1007/s12613-020-2129-6.

Komnitsas, K. and Zaharaki, D., 2007. Geopolymerisation: A review and prospects for the minerals industry. *Miner. Eng.*, 20 (14), 1261–1277. https://doi.org/10.1016/j.mineng.2007.07.011.

Komnitsas, K., Petrakis, E., Bartzas, G. and Karmali, V., 2019. Column leaching of low-grade saprolitic laterites and valorization of leaching residues. *Sci. Total Environ,* 665, 347–357. https://doi.org/10.1016/j.scitotenv.2019.01.381.

Komnitsas, K., Yurramendi, L., Bartzas, G., Karmali, V. and Petrakis, E., 2020. Factors affecting co valorization of fayalitic and ferronickel slags for the production of alkali activated materials. *Sci. Total Environ.,* 721, 137753. https://doi.org/10.1016/j.scitotenv.2020.137753.

Obenaus-Emler, R., Falah, M. and Illikainen, M., 2020. Assessment of mine tailings as precursors for alkali-activated materials for on-site applications. *Constr. Build. Mater*., 246, 118470. https://doi.org/10.1016/j.conbuildmat.2020.118470.

Perumal, P., Niu, H., Kiventerä, J., Kinnunen, P. and Illikainen, M., 2020. Upcycling of mechanically treated silicate mine tailings as alkali activated binders. *Miner. Eng.,* 106587. https://doi.org/10.1016/j.mineng.2020.106587.

Piccolo, F., Andreola, F., Barbieri, L. and Lancellotti, I., 2021. Synthesis and Characterization of Biochar-Based Geopolymer Materials. *Appl. Sci.,* 11, 10945. https://doi.org/ 10.3390/app112210945.

Praneeth, S., Guo, R., Wang, T., Dubey, B.K. and Sarmah, A.K., 2020. Accelerated carbonation of biochar reinforced cement-fly ash composites: Enhancing and sequestering CO_2 in building materials. *Constr. Build. Mater*., 244, 118363. https://doi.org/10.1016/j.conbuildmat.2020.118363.

Zaharaki, D., Galetakis, M. and Komnitsas, K., 2016. Valorization of construction and demolition (C&D) and industrial wastes through alkali activation. *Constr. Build. Mater*., 121, 686–693. https://doi.org/10.1016/j.conbuildmat.2016.06.051.

Zeidabadi, Z. A., Bakhtiari, S., Abbaslou, H. and Ghanizadeh, A.R., 2018. Synthesis, characterization and evaluation of biochar from agricultural waste biomass for use in building materials. *Constr. Build. Mater*., 181, 301–308. https://doi.org/10.1016/j.conbuildmat.2018.05.271.

A Review of EU Refineries Oily Sludge Waste Production, Management Options and Sustainability Assessment of Traditional and Emerging Oily Sludges Treatment Techniques

Alfio Mianzan[1], William Odle[2], Jacob Oerig[2], Eleni Vaiopoulou[3], Konstantinos Sakkalis[4]

[1]NewFields UK, Bradford, United Kingdom
[2]NewFields LLC, Atlanta, United States
[3] Concawe, Brussels, Belgium
[4]bp, London, United Kingdom
Corresponding author email: Waste@Concawe.eu

Abstract

This study presents the results of a survey of EU refineries waste types' production, their sources and management options, with focus on oily sludges and a sustainability assessment of selected traditional versus emerging treatment options for oily sludges wastes. It provides a statistical analysis of waste production by Concawe[1] member company refineries in the years 2019, 2020 and 2021, based on survey data returned from 68 refineries (70.1% response rate) situated in the EU-27 countries + UK, Norway and Switzerland. It includes a breakdown of oily sludge waste tonnage according to its origin and how it was managed. A literature review of emerging and traditional oily sludges treatment technologies provided a selected list of treatment options for detailed assessment of their sustainability. The assessment consisted of a semi-quantitative multi-criteria analysis including criteria assigned to the three main pillars of sustainability: environment, social and economics. A fourth pillar (waste circularity) was added to assess technologies based on their preservation of resources and minimisation of waste generation. Each criterion was given a score with a higher score indicating technologies more favorable for each of the selected criteria. The scores were weighted allowing comparison of the assessed technologies for each of the four pillars. The assessment identified overall better sustainability performance for emerging technologies pyrolysis, solvent extraction and biopiles than for more traditional technologies such as incineration in municipal solid waste incinerators, at cement works and disposal to landfill.

Keywords: *refinery oily sludges, waste management options, waste treatment and disposal, sustainability*

1. Introduction

The European Commission (EC) has been adopting a 'Circular Economy package' aimed to develop a more circular economy (European Commission, 2020). Traditional oily sludge treatment/disposal technologies such as incineration and landfilling involve high treatment costs and sit low in the waste hierarchy. They are also becoming less desirable as environmental regulations become more stringent.

A previous review of European refineries waste data (Concawe Report 12/17) showed that Waste Water Treatment (WWT) and hydrocarbon sludges were the most significant part of refinery waste sludges in tonnages. A survey on oily sludges was undertaken of European refineries that reported waste production, sources and management options from 2019 to 2021. The survey identified current pre-treatment techniques and final management options for refinery oily sludges such as incineration, and landfill. These techniques are associated with adverse environmental and human health impacts and high costs. Also, oily sludges can be a potential energy source considering its production quantity and calorific value.

Energy recovery has received particular attention given that it can recover valuable resources as well as mitigate potential impacts by reducing disposal volumes of these type of waste. Recent developments present different treatment mechanisms, resource recovery performance, energy consumption and environmental impacts (Hu et al., 2013). Their success depends on the substantial reduction of oily sludge volumes, the recovery of energy from the sludge and the final treatment of the unrecoverable residue. Oily sludge treatment technologies can be divided into those that focus on the recovery of the oil contained in the oily

[1] Concawe is the technical branch of the Fuels Manufacturers Association operating in Europe.

sludges and those considered traditional disposal/treatment methods currently used by the industry (Figure 1).

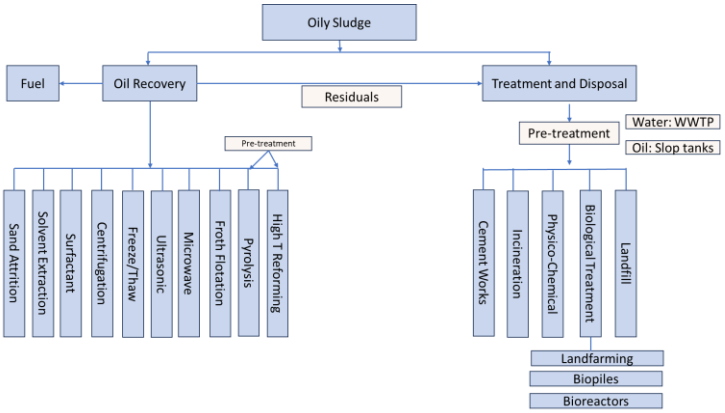

Figure 1. *Oil Sludge Treatment and Disposal Technologies (adapted from Murungi et al, 2022)*

As new technologies have been developed to recover oil in sludge, reduce the amount of waste needing additional treatment or disposal, and potentially having lower environmental and social impacts, to gain further insights into the overall sustainability of traditional vs emerging techniques, a sustainability assessment is undertaken herein considering the three pillars of sustainability: environment, social and economics. A fourth pillar, waste circularity, was added to assess technologies based on their preservation of resources and minimisation of waste generation.

2. Materials and Methods

Data on refinery waste production and management options were collected via a survey of European refineries who were asked to provide data for the years 2019, 2020 and 2022. Data was returned by 68 Concawe members' refineries (70.1% response rate) situated in the EU-27 countries + UK, Norway and Switzerland. Survey included questions on historic throughput and waste quantities reported were normalized to the years reported. Normality was tested using Q-Q plots. Waste data is presented as total waste tonnage (reflecting the environmental burden) and tonnes per kilotonne of refinery feedstock throughput (a measure of efficiency) and include an analysis of differences in waste production and management between different European regions. Wastes are reported based on their European Waste Catalogue codes (EWC codes). To identify emerging technologies for oily sludges treatment a thorough literature search was conducted using different sources. Also, interviews with technical experts from Concawe Member Companies were conducted to identify new technologies being sought or tested by refineries and to seek clarification on current technologies used. Findings are summarized in Figure 2.

To select technologies for the sustainability assessment, advantages and disadvantages of each technology were identified and their applicability evaluated to a refinery context and their stage of development (i.e., laboratory, field scale, fully implemented). The technologies selected were: pyrolysis, solvent extraction, cement works, biological treatment (biopiles), landfilling and incineration with energy recovery. A qualitative/semi-quantitative multicriteria analysis was chosen to undertake the sustainability assessment, broadly aligned with ISO 18504 (on sustainable contaminated soil remediation). This approach helped with the identification of relevant "categories of indicators" (assessment criteria) of the three pillars of sustainability plus the fourth pillar (waste circularity). Environmental, and some social indicators were selected from the EU Reference Document on Economics and Cross-Media Effects (ECME June 2006) along with indicators from US EPA's Tool for the Reduction and Assessment of Chemical and other environmental Impacts (EPA 2012). Indicators were global warming potential (GWP), acidification (AP) and eutrophication potential (EP), air quality indicators such as respiratory effects (RE) and smog formation (SM), ecotoxicity effects (ECT) and human toxicity/carcinogenic effects (CAR and NCAR) (Table 1). Weightings were applied between 0 and 5, where 0 was considered not specifically relevant or lacks data to make an assessment. One (1) indicates low importance or data were not conclusive, and 5 indicates high importance.

Table 1. *Assessment Criteria and Associated Weightings*

Pillar	Assessment Criteria	Media Affected	Assigned Weighting	Key Relevant Indicators
Environmental	Ozone Depletion Potential (ODP)	Air	0	Bromofluoroethanes, CFCs
	Global Warming Potential (GWP)	Air	5	CO_2 eq. per ton of sludge
	Acidification Potential (AP)	Air, water	1	SOx, NOx
	Euthrification Potential (EP)	Water	1	Phosphate, Nitrates
	Ecotoxicity Effects (ECT)	Air, water, soil	1	Metals, PAHs
	Further disposal/treatment of residues	Air, water, soil	5	N/A
	Energy Recovery (ER)		5	kW/h
Social	Onsite vs Offsite Treatment	N/A	3	Noise, Vibrations
	Carcinogenic Effects (CAR)	Air, water, soil	0	Cr VI
	Non-carcinogenic Effects (NCAR)	Air, water, soil	0	Metals, PAHs
	Respiratory Effects (RE)	Air	1	PM2.5, SOx
	Smog Formation (SM)	Air	1	NOx, O3
Financial	Commercial Availability	N/A	3	NA
	Disposal/Treatment Cost	N/A	5	€/ton of waste
Circularity Efficiency	Waste Hierarchy	N/A	5	Disposal, Recovery, Recycling

3. Results

3.1 European refineries oily sludges sources, quantities and management options

Sludges are semi-liquid residue from industrial processes and wastewater treatment. Different types of sludges are generated in refinery operations including crude and product tanks bottoms sludges, sludges from API separation units, flocculation and flotation units. (Best Available Techniques Reference Document for the Refining of Mineral Oil and Gas, 2015).

In total, the 68 refineries produced some 3600 kt of hazardous and non-hazardous waste between 2019-2021 thus, an average of 3.15 t of waste per kt of throughput. The largest amount of total waste originates from refinery operations (~62%), followed by re-construction works (~13%), diverse sources (~9.7%) and remediation activities (~8%). Non-hazardous soils and stones waste associated with construction works were the largest waste type produced in the period with ~850 kt. Sludges from waste water treatment containing hazardous substances (~240 kt), and soil and stones containing hazardous substances (~180 kt), were the second and third largest categories overall (Figure 2).

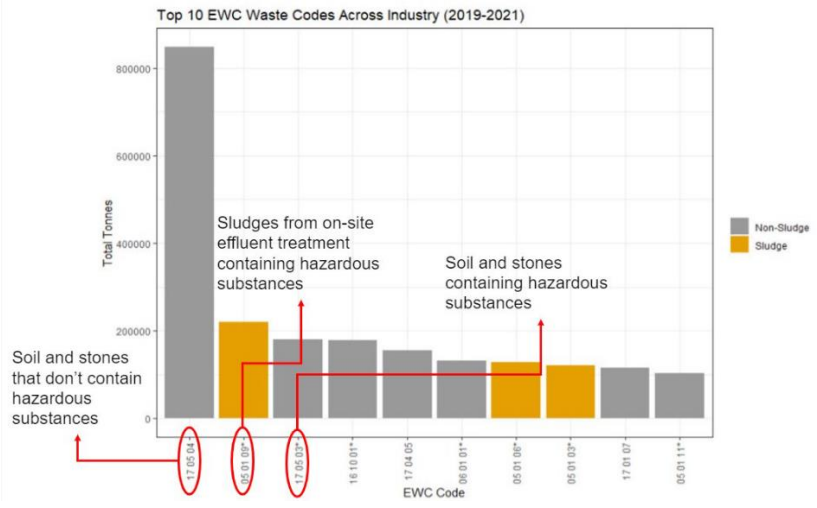

Figure 2. *Top Ten EWC Waste Categories by Tonnage (2019-2021)*

The percentages of sludges in relation to the total amounts of wastes produced were 22.17% (277,137 t) in 2019, 20.61% (237,466 t) in 2020 and 19.61 % (236,647 t) in 2021. The majority of the sludges produced (81.5%) were classified as hazardous. The greatest tonnage (~85%) of sludge wastes reported originated from refinery operations. The three largest waste sludge categories reported were sludge from waste water

treatment plants, oily sludges from maintenance operations and tank bottom sludges and represent 72% of the top ten waste sludge categories (62% of the total amount of sludges produced in the period).

The Waste Framework Directive (2008/98/EC) sets out a waste hierarchy, or priority order of what constitutes the best overall environmental option in waste legislation and policy. It places prevention then reuse, recycling, recovery and disposal from most to least desirable management option. To facilitate the analysis, sludge waste management options reported in the survey were grouped into disposal or recovery options to reflect the EU Waste Hierarchy. As such, disposal categories included incineration (D10), landfill (D1/5) and treatment (such as D9 for physicochemical treatment). Recovery options included incineration with energy recovery (R1), recycling (R3/R4/R5 for recycling and R9 for reuse) and recovery other such as regeneration (R2/R6).

Hazardous sludges constituted the majority of the waste sludge. Incineration and incineration with energy recovery were the two largest management options by weight. Only 2.6 % of the sludges managed by these options were classified as non-hazardous. These two incineration options were followed by landfill, recycling and treatment, all with similar tonnages of hazardous sludges and less amounts of non-hazardous sludges. The recovery-other option is the only option with a larger quantity of non-hazardous sludges in relation to the hazardous fraction (Figure 3).

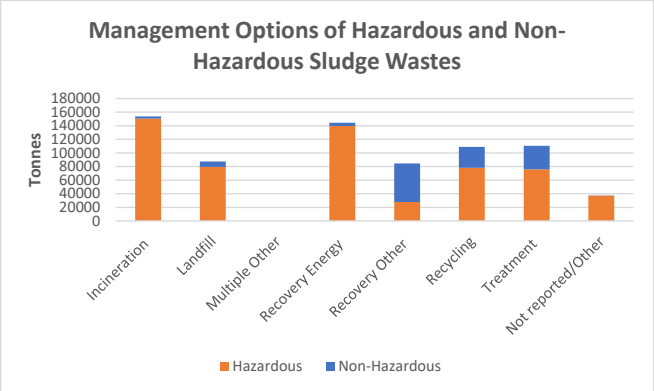

Figure 3. *Hazardous and Non-Hazardous Sludge Wastes by Management Option*

There are regional differences in the management options, this might reflect the availability of waste management options and local policy enforced. Approximately 44% of the wastewater treatment (WWT) sludges received no treatment prior to final disposal or the information was not provided. All regions reported a mixture of treatment/separation and no treatment prior to final disposal with the exception of UK/Ireland/Northern Europe which reported all WWT sludges treated by thickening (centrifugal, flotation and gravity thickening). Energy recovery (R1) was the main management option for this type of sludge waste with a reported 25.2% of the total volume. This was followed by physico-chemical treatment (~14.4%) and recycling (~6.8%)[2]. Disposal into landfill constituted only 1.7% of the total. Overall, more volume of waste water sludge was treated than not treated prior to incineration (D10) and energy recovery (R1), while more sludge volume was not treated than treated when the management option selected was physicochemical treatment (D9).

The largest management option (~15%) for maintenance sludges was physico-chemical treatment (D9), followed in decreasing volume by recycling (R3/4/5), energy recovery (R1), incineration (D10) and oil re-refining (R9), with percentages of between approximately 10% and 13%. The disposal into landfill (D1/5) was low, with approximately 1.8% of the total maintenance sludge managed by this option (in UK/Ireland/Northern Europe, Central/Eastern Europe and Iberia Country Regions). For maintenance sludges it is unclear the pattern in final management options and sludge separation or lack of separation onsite.

The highest tonnage of tank bottom sludges was managed by Landfill (25%) followed by Incineration (24%) and Energy Recovery (23%). Recycling was the main management option for maintenance sludges (26%) followed by Landfill (24%) and Treatment (18%). Wastewater sludges were mainly managed by Incineration (34%) and Energy Recovery (26%), followed by Treatment (16 %) and Recycling (11%).

[2] Examples of category D9, physico-chemical treatment, includes oxidation/reduction, precipitation, neutralisation, immobilisation, etc. Examples of recycling options include composting, anaerobic digestion, gasification and pyrolysis.

3.2 Sustainability assessment of traditional and emerging refinery oily sludges management options

The sustainability assessment consisted of a comparison between traditional oily sludge treatment/disposal technologies and emerging technologies. The assessment used does not follow a Life Cycle Assessment (LCA) method, but helps identifying system boundaries of the selected management options helping to better understanding of which parts of the alternatives are responsible for the higher impacts. In general, the processes considered are those from the beginning of the oily sludge treatment to the final landfilling or treatment of the residual solids. The technologies assessed included incineration, landfilling, solvent extraction, pyrolysis, biopiles and cement kilns.

The scores were applied on a relative basis, with reference to the relevant indicators in Table 1. The scores range between 1 and 5, where 1 represents the least favorable technique and 5 is the most favorable for that particular criterion (i.e., causes the least impact, has the lower cost, etc). For each pillar (environmental, social, finance and waste circularity) a percentage score was calculated (percentage of maximum possible score, reflecting the number of assessment criteria). The assessment then combined (and normalised) the score for the four pillars, to provide a balanced overall score for each management option. For a given option, this balance overall score can be compared against the other options and assists with the identification of the most favorable options. The results of the assessment are shown in Figure 4. The most favorable management options are biopiles, followed by solvent extraction and pyrolysis. These options are more favorable from a sustainability and circularity point of view than traditional options such as landfilling, cement works and incineration with energy recovery. However, these are considered as emerging techniques and their degree of application to refineries varies, with some technologies only tested at laboratory or pilot scale. Therefore, a conclusion can only be drawn once their availability, cross media effects and applicability restriction are determined.

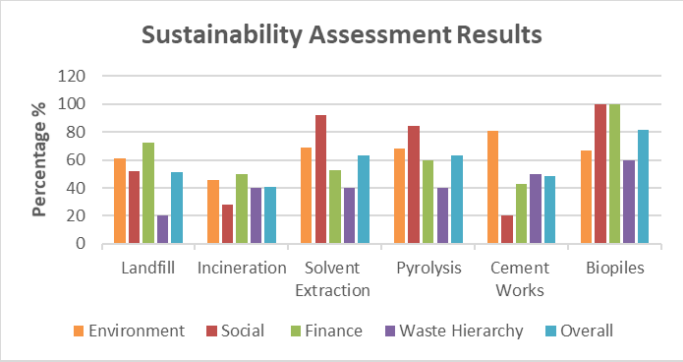

Figure 4. *Sustainability Assessment Results (High bar is judged more sustainable)*

Regarding the environmental pillar, the emission of greenhouse gases is an important environmental impact for all options, primarily associated with CO_2 emissions from combustion and biological degradation, and methane emissions in the case of landfilling. Biological degradation options are favourable with some 300 kg of CO_2 eq. per ton of sludge (Tsiligiannis et al 2020), while incineration is the least favourable option with 1000 to 2000 kg/ton of CO_2 eq. per ton of sludge and much higher when the use of auxiliary fuels to achieved required combustion temperatures is considered. Pyrolysis also scores less favourable when combustion of py-gas and py-oil is considered together with the energy required to maintain the temperature in the pyrolysis reactor. Environmental criteria of Ecotoxicity criteria (ECT), Acidification potential (AP) and Eutrophication potential (EP) were given low weightings given the lack of quantified data encountered during the literature review. The final treatment/disposal of solid residues considers the additional potential environmental impacts from the need to dispose/treat residues (ash, wastewater, solids) from the selected management options. Pyrolysis and cement works resulted the most favourable options. Solids residues from pyrolysis are essentially a char that can be used for soil conditioning while in cement works solid residues are incorporated into clinker. Biopiles have no solid residues since after degradation in the biopiles the remaining soil can be used as a soil conditioner. However, biopiles and landfill produce leachate that requires treatment. Incineration and solvent extraction scored the least favourable due to the amounts of solid residues produced by these options (between 10 and 20% of the original sludge) and the amounts of separated water that needs

to be treated in a waste water treatment plant in the case of solvent extraction. Finally, the Energy Recovery criterion includes the use of energy from waste as a substitute for fossil fuel. Landfill (without CH_4 capture) and biopiles are the least favourable, whilst incineration and cement works obtained higher scores with over 1300 kW/h of produced energy per ton of sludge. Solvent extraction and pyrolysis result in similar production of grid electricity of between 1000 and 1150 kW/h per ton of (oily) sludge using the heat energy from the combustion of recovered oil.

Regarding the social pillar, criteria refer to impacts to people due to emissions. Emissions refer not only to emissions to air and water but also nuisance issues such as noise, vibrations and odours. As such, options requiring offsite transport were selected as the least favourable ones as they can cause additional nuisance due to transport such as noise, dust, vibrations, etc. Onsite treatment was not considered to increase existing refinery impacts on neighbourhoods in any significant way. Most oily sludges are currently disposed or treated offsite. However, handling more waste onsite has the potential to increase overall sustainability and circularity as long as proper management of the waste can be achieved in a cost-effective way. Options such as solvent extraction and pyrolysis can be scaled up to operate within a refinery depending on permitting requirements given contractors are available who can build these plants to various capacities. Biopiles are already used by one Company Member, but availability of space in the refinery is paramount to make them viable. Incineration, cement works, and landfilling are clearly offsite options unlikely to be viable or permitted in refineries and therefore received a lower score. Air emissions causing air quality issues with consequences for people, such as respiratory effects and/or smog formation, were also considered in this category. Cement works was found to be the least favourable option with landfill and biopiles the most favourable. Toxic, carcinogenic effects of emissions from the selected management options are criteria commonly used in LCA studies. However, these criteria were not considered for the assessment.

Regarding the financial pillar, gate costs for disposal or treatment of hazardous waste are difficult to calculate without actual analysis of the waste received by waste managers. Consequently, costs (in €/ton of waste) were obtained from interviews that provided ranges of costs for disposal of oily sludges in general. Other costs were obtained from the literature review and do not necessarily represent commercial rates. Costs for solvent extraction and pyrolysis are operational costs and exclude capital costs (no information). Biopiles assigned costs also represents operational costs only. Solvent extraction costs are based on pilot tests. Commercial availability was not considered, because some options (landfill, incineration) are widespread available to compare against selected emerging options. The low scores in solvent extraction are linked to lack of information and lesser widespread availability.

Re the circularity pillar, each Waste Hierarchy was allocated a score of 1 to 5 in ascending order, i.e., 1 for disposal and 5 for prevention. In this way, landfill (D1/5) was provided a score of 1 and incineration with energy recovery (R1) a score of 2. Incineration without energy recovery (D10) would have been assigned a score of 1. Pyrolysis (R3) and solvent extraction (R3) also falls into the recovery hierarchy and are assigned a score of 2. The co-processing of wastes in cement kilns is a mix of recycling and thermal recovery. The mineral portion of the waste is reused during the process and replaces virgin raw materials. At the same time, the energy content of the waste is very efficiently recovered into thermal energy (R1), thus saving conventional fuels. Therefore, in the waste hierarchy co-processing of waste in cement works generally has a position just below recycling (R5, recycling of inorganic materials) as it is more beneficial than incineration with energy recovery (Cement Sustainability Initiative, CSI). Accordingly, the cement works option was assigned a score of 2.5.

4 Conclusions

Oily sludges are significant wastes in refinery operations in the 2019-2021 period, oily sludges in European refineries ranged between 19.6 and 22.2 wt% of total produced wastes. The main three types of oily sludges produced by weight were tank bottom sludges, refinery maintenance sludges and WWTP sludges. Incineration with and without energy recovery, followed by landfill, treatment and recycling were the main management options.

The sustainability assessment indicated that biopiles are the most favourable management option, followed by solvent extraction and pyrolysis. However, these are considered as emerging techniques and their degree of application to refineries varies, with some technologies only tested at laboratory or pilot scale. Therefore, a conclusion can only be drawn once their availability, cross media effects and applicability restriction are determined, and the specificities of the refinery are taken into account.

Finally, the sustainability assessment provided a rapid, semiquantitative method to compare overall sustainability of different technologies. More quantitative sustainability appraisal tools, such as LCA tools, can be beneficial in the understanding of impacts and benefits from emerging technologies in comparison to traditional approaches. They can also help quantify possible cross-media effects and avoid unintended consequences of improving one or more of the evaluated pillars to the detriment of others.

References

A new Circular Economy Action Plan for a cleaner and more competitive Europe, European Commission COM 2020 (98).

Best Available Techniques (BAT) Reference Document for the Refining of Mineral Oil and Gas, 2015, and its accompanied BAT, 2014.

Best Available Techniques (BAT) Reference Document for Common Wastewater and Waste Gas Treatment/Management Systems in the Chemical Sector, 2010.

Best Available Techniques (BAT) Reference Document for Waste Incineration, 2019.

Best Available Techniques (BAT) Reference Document for the Production of Cement, Lime and Magnesium Oxide, 2013.

Best Available Techniques (BAT) Reference Document for Waste Treatment, 2018.

Best Available Techniques (BAT) Reference Document for Large Combustion Plants, 2017

Concawe (2017). 2013 Survey of Waste Production and Management at European Refineries. Concawe Report No 12/17.

Concawe Waste Survey Data 2019-2021 (Report in preparation).

Directive (EU) 2018/851 of the European Parliament and of the Council of 30 May 2018 amending Directive 2008/98/EC on waste.

Directive 2010/75/EU of the European Parliament and of the Council of 24 November 2010 on industrial emissions (integrated pollution prevention and control).

Directive 2008/50/EC of the European Parliament and of the Council of 21 May 2008 on ambient air quality and cleaner air for Europe.

EPA, 2012. Tool for the Reduction and Assessment of Chemical and other Environmental Impacts (TRACI).

EU Council Directive on the landfill of waste, 1999.

EU Reference Document on Economics and Cross-Media Effects, June 2006.

ISO, 2017. ISO 18504:2017, Soil Quality: Sustainable Remediation. ISO, Geneva

Murungi P.I., Sulaimon A. A., 2022. Petroleum sludge treatment and disposal techniques: a review. *Environmental Science and Pollution Research (2022) 29:40358-40372. https://doi.org/10.1007/s11356-022-19614-z.*

Tsiligiannis A., Tsiliyannis C., 2020. Oil refinery sludge and renewable fuel blends as energy sources for the cement industry. *Renewable Energy 157 (2020), https://doi.org/10.1016/j.renene.2020.03.129.*

United Nations, 2020. CCET guideline series on intermediate municipal solid waste treatment technologies: Waste-to-Energy Incineration.

Biomass Burning Emissions from Varying Landuse Over Equatorial Southeast Asia (ESEA)

J. Sentian[1,2], J.H. Chin[1,2] and F.A.F. Adnan [2,3]

[1]Faculty of Science and Natural Resources, University Malasyia Sabah, Kota Kinabalu, Sabah, Malaysia
[2]Climate Change Research Laboratory, Universiti Malaysia Sabah, Kota Kinabalu, Sabah, Malaysia
[3]Small Island Research Centre, Universiti Malaysia Sabah, Kota Kinabalu, Sabah, Malaysia
Corresponding author email: jsentian@ums.edu.my

Keywords: *Air pollutants; biomass burning; Landuse; MODIS; remote sensing.*

Introduction

Equatorial Southeast Asia (ESEA) plays a crucial role in global climate dynamics and is susceptible to the influences of El Niño-Southern Oscillation (ENSO) and monsoons. During El Niño events, biomass burning in this region intensifies, leading to a significant deterioration in air quality. Despite its significance, comprehensive records of biomass burning emissions within ESEA regions are still lacking and needed, making it difficult to monitor air quality and create accurate emission inventories. Regional discrepancies in global fire emissions inventories indicate that existing data may not accurately represent actual emissions in specific regions like ESEA. This study aims to establish a detailed emission inventory specifically designed for ESEA, highlighting estimated emissions and sources of biomass burning at a regional scale to enhance climate and air quality management in the region. The primary objective of this research is to develop an emissions inventory for 11 specific pollutants, namely namely SO_2, NO_x, $PM_{2.5}$, PM_{10}, OC, EC, CO_2, CO, NH_3, NMVOC, and CH_4 covering the ESEA regions in 2021.

Materials and methods

Each of the five countries that made up ESEA (Malaysia, Indonesia, Singapore, Brunei and Timor Leste) had a unique distribution of land cover and conditions for biomass burning. The emissions under Non-El Niño conditions were estimated by using the bottom-up approach, to estimate emissions at the source level. Burned area and land cover data are important variables affecting biomass burning and emissions in the study area. Both data were acquired from Moderate Resolution Imaging Spectroradiometer (MODIS) and processed by using ArcGIS. In addition, this study specifically focused on emissions emitted from five vegetation burning, namely, cropland, wetland, shrubland, savannah, and forest burning, which are categorized under seven land cover. The amount of biomass burned, in (Mg/year), from respective land covers was calculated as the product of the burned area, fuel load (FL) and combustion factor (CF), using Equation 3.2 as follows (Zhou et al., 2017).

Estimating biomass burning emissions using the bottom-up method involves calculating emissions based on activity data and emission factors. This method is commonly used when specific data on the amount of biomass burned and emission factors for different types of biomasses are available. The emission factor (EF), commonly expressed in units of g/kg, represents the amount of a specific pollutant released into the atmosphere per unit of activity or process (McMeeking et al.,2008; Akagi et al.,2011).

Results and discussion

Table 1 presents the emission levels of 11 species, including CO_2, CO, PM_{10}, $PM_{2.5}$, SO_2, NO_x, CH_4, NMVOC, NH_3, OC, and EC, released from biomass burning in 2021. CO_2 was the most prevalent species emitted during biomass burning, followed by CO. CO_2 emissions were estimated at 987463.1 Mg/year, with CH_4 emissions at 2386.73 Mg/year. Despite CH_4 being a relatively minor contributor to biomass burning (<10%), its greenhouse gas impact can be approximately 50 times greater than that of CO_2. The third most common species emitted during biomass burning were non-methane volatile organic compounds (NMVOCs), with an estimated 9604.66 Mg/year. Shrubland and evergreen forests were the primary sources of ESEA biomass burning emissions, jointly contributing around 50% of the total emissions. Notably, the burning of evergreen forests was the main source of PM emissions, resulting in 22986 Mg/year for PM_{10} and 4290 Mg/year for $PM_{2.5}$ in 2021. Conversely, cropland burning produced comparatively lower PM_{10} and $PM_{2.5}$ emissions, with 93 Mg/year and 74 Mg/year in 2013, and 27 Mg/year and 21 Mg/year in the same year.

Table 1: *ESEA biomass burning emissions (Mg/year) estimate by different land covers in 2021*

	CO_2	CO	PM_{10}	$PM_{2.5}$	SO_2
Evergreen Forest	550725.5	30837.95	4290.50	3418.99	150.83
Deciduous Forest	25194	1576.557	197.84	190.11	15.46
Mixed Forest	5759.21	360.392	54.94	43.46	13.25
Shrubland	327995.20	12997.48	1624.69	1510.00	129.97
Savannah	62848.22	2191.516	367.73	234.01	25.26
Wetland	9023.69	480.4459	63.90	57.24	4.08
Cropland	5917.243	332.6946	27.54	21.86	1.74
Total	**987463.1**	**48777.04**	**6627.14**	**5475.67**	**340.59**

	NO_x	CH_4	NMVOC	NH_3	OC	EC
Evergreen Forest	837.99	1709.49	8044.68	254.74	1575.41	167.59
Deciduous Forest	20.09	77.28	170.02	23.18	142.19	9.27
Mixed Forest	14.31	27.38	49.46	15.02	32.55	2.12
Shrubland	745.44	496.96	917.47	229.36	1261.52	95.56
Savannah	104.00	55.71	345.44	18.57	96.56	14.85
Wetland	10.73	7.67	34.75	3.07	32.20	2.65
Cropland	12.67	12.24	42.84	6.12	8.74	2.75
Total	1745.23	2386.73	9604.66	550.06	3149.17	294.79

Conclusions

During the specific time frame, an increased number of fires were observed, particularly in June and July of 2021, with these months recording the largest areas of burned land. The fires that occurred during the dry season led to significant emissions from the burning of shrubland and evergreen forests, which were the main sources of emissions during that year. While the savannah accounted for a larger portion of the burned land, the emissions and biomass burned from savannah fires were less significant compared to those from evergreen forest fires. Notably, emissions of NH_3, SO_2, and NOx were highest from shrubland fires, while greenhouse gas emissions were primarily attributed to evergreen forest fires due to their high capacity for carbon sequestration.

Acknowledgements: This study is supported by the SEARRP Fund (GLA0013-2018) for the regional study on greenhouse gas emissions.

References

Akagi, S. K., Yokelson, R. J., Wiedinmyer, C., Alvarado, M. J., Reid, J. S., Karl, T. & Wennberg, P. O. 2011. Emission factors for open and domestic biomass burning for use in atmospheric models. *Atmospheric Chemistry and Physics*, 11(9): 4039–40

McMeeking, G. R. (2008). *The optical, chemical, and physical properties of aerosols and gases emitted by the laboratory combustion of wildland fuels*, PhD Dissertation, Department of Atmospheric Sciences, Colorado State University, 109–113

Zhou, Y., Xing, X., Lang, J., Chen, D., Cheng, S., Wei, L., Wei, X., and Liu, C. (2017). A comprehensive biomass burning emission inventory with high spatial and temporal resolution in China, *Atmos. Chem. Phys*., 17, 2839–2864, https://doi.org/10.5194/acp-17-2839-2017,

Optimized location of electric vehicle batteries recycling center in Attica

A. Lygizos[1], E. Kastanaki[1] and A. Giannis[1]

[1]School of Chemical and Environmental Engineering, Technical University of Crete, University Campus, 73100 Chania, Greece
Corresponding author email: agiannis@tuc.gr

keywords: *Electric vehicle batteries; collection system; recycling center; optimized location.*

Abstract

The management of end-of-life electric vehicle batteries (EoL EVBs) is an urgent matter in-line with circular economy principles. According to estimates, the lithium-ion batteries (LIBs) in electric vehicles have a lifespan of ten to fifteen years. Once they reach the EoL, these batteries are classified as waste. The implementation of strategies such as recycling, reuse, and remanufacturing should be considered from both economic and environmental perspectives. In Greece, there is no established network for the collection and recycling of EoL EVBs due to insufficient quantities to support such infrastructure. This study proposes an integrated system for the collection, recycling, and remanufacturing of LIBs from electric vehicles in the Region of Attica. Considering the national and European initiatives focused on advancing electromobility and taking into consideration the historical data of electric vehicle sales in Greece, the projected waste quantities are estimated. Initially, this approximation is made on a nationwide scale and subsequently refined to the region of Attica. Two different scenarios (Early loss-EL and Regular loss-RL) are examined until the year 2040 to assess current and future waste amounts. Based on the EL and RL scenarios, it is anticipated that the region of Attica will have to manage between 4,300 and 7,300 tonnes of EoL LIBs by 2040, respectively. Subsequently, the optimized location of collection centers and recycling facilities are formulated, ultimately leading to the selection of the most economically and environmentally advantageous option. The operational costs, transport and processing costs, as well as the CO_2 emission tax imposed by the European Union, are estimated to present a comprehensive overview of the integrated network. Further technoeconomic analysis is performed to determine the revenue of the recycling network, derived from the recovery of valuable metals present in LIBs and the sale of reassembled batteries meeting the required market specifications. Based on the calculations and approximating the investment costs needed for implementing the network, a holistic design is presented. The payback period for the network investment falls within the range of 6 to 8 years, which proves highly advantageous since it is considerably shorter than the planning period for such an installation. This study is characterized by its multifaceted nature as it takes into consideration numerous factors and data, ultimately optimizing an integrated network for managing EVBs in Attica.

Current Trends, Challenges, and Future Opportunities in Biogas Production from Hospital Food Waste in Europe: Perspectives from the CaringNature Project

I. Vyrides[1]

[1]Department of Chemical Engineering, Cyprus University of Technology, Anexartisias 57 Str., 3603, Limassol, Cyprus

Corresponding author: ioannis.vyrides@cut.ac.cy

Summary:
As part of the CaringNature Project, which is supported by the European Union's Horizon Europe research and innovation programme under Grant Agreement n°101137340, the initiative aims to develop ten innovative solutions targeting the reduction of the healthcare sector's environmental footprint. This ambitious project collaborates with 19 partners (including Cyprus University of Technology, Department of Chemical Engineering) from 11 EU countries, employing a multidisciplinary approach to address challenges in waste management, energy efficiency, and sustainable healthcare operations without compromising patient care or safety. In this study, it was highlighted that food waste in hospitals is a significant concern, comprising up to 50% of total waste, mainly from meal preparation, unused meals, and patient leftovers. Effective strategies for waste segregation and management were emphasized, focusing on waste minimization, energy conversion, and other sustainable practices like anaerobic digestion. Practical applications of these strategies in hospitals have been instrumental in reducing greenhouse gas emissions and enhancing operational efficiency. This demonstrates the project's impact on promoting sustainable waste handling practices within the healthcare sector across Europe. Moreover, the CaringNature Project also focuses on innovative wastewater treatment practices, particularly in handling wastewater from hospital operations. The project explores the feasibility of on-site wastewater treatment systems that integrate advanced biotechnological processes. These systems aim to purify wastewater while recovering valuable resources, such as biogas, thus contributing to the project's overarching goals of sustainability and reduced environmental impact.

Evaluation of the Physicochemical Properties and Ecotoxicological Impact of Municipal Biosolids for Agricultural Use

I. Giannakis[1]*, P. Ntailiani[2], C. Emmanouil[2] and A. Kungolos[1]

[1]School of Civil Engineering, Aristotle University of Thessaloniki, 54124 Thessaloniki, Greece

[2]School of Spatial Planning and Development, Aristotle University of Thessaloniki, 54124 Thessaloniki, Greece

Corresponding author email: iogianna@civil.auth.gr

keywords: *Biosolids, circular economy, soil amendments, bioassays, metals.*

Introduction

The 17 Sustainable Development Goals (SDGs) of the United Nations emphasize the importance of ensuring soil quality, reversing soil degradation, and using soil resources efficiently. In this context, developing and utilizing technologies for sustainable waste management, along with promoting sustainable construction in technical projects and infrastructures, is essential.Considering the new Action Plan for the Circular Economy and the establishment of specifications and requirements for secondary materials and sustainable products, as well as the principles of the European Green Deal for carbon border adjustment, the main objective of this research is to enhance the soil microbiome to meet the agricultural needs of modern society using circular economy principles. This involves converting waste into valuable products and replacing outdated, environmentally harmful methods with new techniques that have a smaller environmental footprint. Additionally, this research aims to substitute chemical plant protection agents with non-chemical biological agents derived from BS.By focusing on these goals, this research contributes to sustainable agricultural practices, improve soil health, and reduce the environmental impact of traditional methods, thereby supporting global efforts to combat climate change and ensure sustainable resource management.

Materials and methods

Anaerobically digested sludge samples were collected from three different Wastewater Treatment Plants (Table 1). Subsequently, the samples were subjected to the EN 12457-2 stage leaching test (CEN 2002). Basic physicochemical parameters, such as pH and electrical conductivity, were measured in the leachates. Additionally, the organism *Daphnia magna* was exposed to the leachates following OECD guidelines (OECD 2004). When it was possible, the parameter EC50 was calculated and the results were transformed into toxic units (TU) according to Persoone et al. (2003). The concentrations of heavy metals, as specified in Directive 86/278/EEC, were measured both within the biosolids (BS) and in their leachates.

Table 1. *Sludge samples*

WWTP	Treatment procedure	Sampling date	Humidity (%)
Nea Michaniona	Dehydrated	12/02/2024	81.6
Sindos	Thermal hydrolysis/ dehydrated	15/12/2023	70.4
Kozani	Dehydrated	18/12/2024	88.1

Results

The detectable amounts of metals for both BS and leachates were, in all cases, much lower than the limit values for heavy-metal concentrations in sludge for use in agriculture as set by Directive 86/278/EEC. The pH, electrical conductivity, and toxicity of the leachates from the sludge samples of Nea Michaniona and Sindos are presented in Table 2. It should be noted that the leaching test could not be conducted for the sludge sample from Kozani. According to the classification system devised by Persoone et al. (2003), the sludge samples demonstrated acute toxicity to the tested organism.

Table 2. *Parameters measured in sludge leachates*

WWTP	pH	Electrical conductivity (mS/cm)	TU
Nea Michaniona	7.35	5.11	2.1
Sindos	7.36	5.07	8

Discussion and conclusions

In this study, the toxic responses of the leachates to *D. magna* were categorized into acute toxicity classes, comparable to the values observed in *D. magna* after exposure to sludge leachates in the study by Fang et al. (2017), which reported toxicity units (TU) ranging from 2.99 to 5.65 over 48-hour values. Notably, the sample from Sindos, where the sludge undergoes thermal hydrolysis to produce a higher quality and safer product for agricultural use, showed the highest toxicity to this organism. However, to draw safer conclusions, additional sampling with more toxicity indicator organisms is recommended. The BS examined in this study also demonstrated very low concentrations of heavy metals, both in the BS themselves and in their leachates. These concentrations were significantly lower than the limits set by Directive 86/278/EEC for soil, indicating the suitability of these specific BS for agricultural use.

Acknowledgements:

GREEN FUND

BIOSOIL-Development and utilization of soil improvement methods using biosolids from Wastewater Treatment Plants and bio-reinforcement techniques in the context of circular economy and citizen science- Green Fund Research and Application- "Natural Environment and Novel Actions 2023"; FUNDING: GREEN FUND 200,000 euros; beneficiary: Aristotle University of Thessaloniki

References

CEN (2002). EN12457-2. Characterization of Waste–Leaching–Compliance Test for Leaching of Granular Waste Material and Sludge-Part 2: One Stage Batch Test at a Liquid to Solid Ratio of 10L/kg With Particle Size below 4mm (Without or With Size Reduction). European Committee for Standardization.

Fang B., Guo J., Li F., Giesy J. P., Wang L., Shi W. (2017). Bioassay directed identification of toxicants in sludge and related reused materials from industrial wastewater treatment plants in the Yangtze River Delta. Chemosphere 168, 191-198.

OECD GUIDELINE 202 FOR TESTING OF CHEMICALS (1984). *Daphnia* sp., Acute Immobilisation Test and Reproduction Test.

Persoone G., Marsalek B., Blinova I., Törökne A., Zarina D., Manusadzianas L., Nałęcz-Jawecki G., Tofan L., Stepanova N., Tothova L., Kolar B. (2003). A practical and user-friendly toxicity classification system with microbiotests for natural waters and wastewaters. Environ Toxicol, 18(2003), 395-402.

Session 2: Wastewater management (I)

Treatment of pharmaceutical-containing wastewater with a hybrid approach of advanced oxidation with persulphates/UV and biological removal by fungal pellets

D. Villegas-Solano[1], D. Ramírez-Morales[1], V. Castro-Gutiérrez[1], M. Masís-Mora[1] and C.E. Rodríguez-Rodríguez[1]

[1]Research Center for Environmental Pollution (CICA), University of Costa Rica, San José, Costa Rica
Corresponding author email: carlos.rodriguezrodriguez@ucr.ac.cr

keywords: *pharmaceuticals; advanced oxidation; biodegradation; ecotoxicity.*

Introduction

Pharmaceuticals are considered as contaminants of emerging concern, and their occurrence has been described in different aquatic matrices, including ground and surface water, and effluents from hospitals and wastewater treatment plants (WWTP) (Chaturvedi et al., 2021). The conventional treatments applied in WWTP are designed for the removal of dissolved carbon, phosphorus, and nitrogen, however, they do not completely remove pharmaceuticals, even though the most biodegradable compounds can be eliminated to a great extent. For this reason, the development of new approaches aimed at the removal of pharmaceuticals from polluted effluents is of great interest from the environmental engineering point of view. In this respect, physicochemical strategies such as advanced oxidation processes (AOP) have been studied to achieve the removal of micropollutants, including ozonation, Fenton or photo-Fenton processes and their variations (Pandis et al., 2022). One such variation makes use of persulfates (instead of peroxide) coupled to UV and has shown promising efficiency for the removal of organic pollutants. Similarly, several biological approaches employing ligninolytic fungi, such as biofilters/biobarriers and reactor configurations using biomass in the form of pellets, resulted in significant micropollutant removal, thanks to the action of their unspecific enzymatic complexes and adsorption processes (Zhuo and Fan, 2021). Taking into account the advantages of both kinds of approaches, this work aims to evaluate a hybrid treatment for pharmaceutical-containing wastewater (synthetic/real), based on the advanced oxidation with UV/persulfates in a falling film reactor and the biological removal with fungal biomass of *Trametes versicolor* in a stirred tank reactor.

Materials and methods

Synthetic wastewater was prepared using distilled water spiked with a mixture of 11 pharmaceuticals (acetaminophen, caffeine, codeine, diclofenac, diphenhydramine, doxycycline, fluoxetine, gemfibrozil, ibuprofen, lovastatin, ofloxacin) at a working concentration of 1 mg/L each. Real wastewater was collected from the effluent of a local psychiatric hospital. Advanced oxidation of synthetic/real wastewater was performed in a falling film reactor (CE 584 advanced oxidation, G.U.N.T.), using UV/persulfates. The working volume was 5 L, and the system was operated with 40 mg/L persulfate, at a recirculating flow of 240 L/h for 60 min. The biological treatment was applied for 4 d in batch mode in a stirred tank bioreactor (BioFlo 120, Eppendorf), at a working volume of 5 L, inoculated with 400 g pellets of *T. versicolor* and 50 g rice husk as a lignocellulosic substrate. The wastewater was first treated by the AOP, and the resulting effluent was subsequently treated in the bioreactor (treatment AOP-B). The inverse sequence of treatment (biological and then AOP, i.e. B-AOP) was also assayed for comparison purposes.

Samples were collected for the analysis of pharmaceuticals (times 0, 5, 10, 30 and 60 min for AOP; 0, 1, 2, 3 and 4 d for biological) and ecotoxicological determinations (times 0, 30 and 60 min for AOP; 0, 2 and 4 d for biological). Pharmaceutical quantification was done with a multiresidue method by LC-MS/MS (Ramírez-Morales et al., 2020); ecotoxicological evaluation was performed with tests on three benchmark organisms: immobilization in *Daphnia magna*, bioluminescence inhibition in *Vibrio fischeri*, and germination of *Lactuca sativa* (Lizano-Fallas et al., 2017; Rodríguez-Castillo et al., 2019). Chemical oxygen demand (COD) was analyzed during the treatment of real wastewater.

Results and discussion

Overall removal values of pharmaceuticals were 87.5% and 98.0% for the treatments AOP-B and B-AOP, respectively, when synthetic wastewater was employed. Controls at flask scale with heat-inactivated biomass suggest that most of the removal by biological means can be ascribed to adsorption, although biological transformation provides additional removal for some compounds, and may take place after adsorption. Detoxification was achieved in all bioindicators in B-AOP, while on the contrary, the residual toxicity increased in every case in AOP-B. The addition of $CuSO_4$ to enhance fungal enzymatic activity had an adverse effect as it increased the toxicity in the biological subtreatments; hence it was not used in assays with real wastewater.

A different toxicological profile was observed when the real wastewater was treated. The treatment AOP-B resulted in global detoxification and higher COD removal compared to B-AOP. However, the B-AOP treatment produced a more toxic effluent, likely due to the formation of toxic transformation products during the AOP; such products are probably adsorbed to fungal biomass in the subsequent biological treatment in AOP-B. The quantification of pharmaceuticals is still pending in the assays with real wastewater.

Conclusions

The treatment APO-B represents a promising configuration for a tertiary treatment of hospital effluents, according to its detoxification performance in real wastewater. The analysis of the pending quantification of pharmaceuticals in the assays with real wastewater is necessary to evaluate to a better extent the success of the process in removing pharmaceuticals and to correlate pharmaceutical content with ecotoxicological variations.

Acknowledgements: This study is supported by Vicerrectoría de Investigación (Project 802-B8-510) from the University of Costa Rica and the Ministry of Science, Technology and Telecommunications of Costa Rica (MICITT) (Project FI-197B-17).

References

Chaturvedi, P., Shukla, P., Giri, B. S., Chowdhary, P., Chandra, R., Gupta, P. and Pandey, A., 2021. Prevalence and hazardous impact of pharmaceutical and personal care products and antibiotics in environment: A review on emerging contaminants. *Environ. Res*., 194, 110664.

Lizano-Fallas, V., Masís-Mora, M., Espinoza-Villalobos, D., Lizano-Brenes, M. and Rodríguez-Rodríguez, C. E., 2017. Removal of pesticides and ecotoxicological changes during the simultaneous treatment of triazines and chlorpyrifos in biomixtures. *Chemosphere*, 182, 106-113.

Pandis, P. K., Kalogirou, C., Kanellou, E., Vaitsis, C., Savvidou, M. G., Sourkouni, G., Zorpas, A.A. and Argirusis, C., 2022. Key points of advanced oxidation processes (AOPs) for wastewater, organic pollutants and pharmaceutical waste treatment: A mini review. *ChemEngineering*, 6, 8.

Rodríguez-Castillo, G., Molina-Rodríguez, M., Cambronero-Heinrichs, J. C., Quirós-Fournier, J. P., Lizano-Fallas, V., Jiménez-Rojas, C., Masís-Mora, M., Castro-Gutiérrez, V., Mata-Araya, I. and Rodríguez-Rodríguez, C. E., 2019. Simultaneous removal of neonicotinoid insecticides by a microbial degrading consortium: Detoxification at reactor scale. *Chemosphere*, 235, 1097-1106.

Zhuo, R. and Fan, F., 2021. A comprehensive insight into the application of white rot fungi and their lignocellulolytic enzymes in the removal of organic pollutants. *Sci. Total Environ*., 778, 146132.

Effect of hydrogen peroxide on colour changes during the degradation of sulfamethoxazole by photo Fenton

U. Duoandicoechea[1], J.M. Lomas and N. Villota[1]

[1]Department of Environmental and Chemical Engineering, Faculty of Engineering Vitoria-Gasteiz, University of the Basque Country, Vitoria-Gasteiz, Spain
Corresponding author email: natalia.villota@ehu.eus

keywords: *colour; kinetic modelling; photo-Fenton; sulfamethoxazole*

Introduction

During the oxidation of sulfamethoxazole (SMX) applying photo-Fenton technology, based on the radical reaction mechanism between hydrogen peroxide and UV light catalysed by iron salts, aromatic intermediates are generated. They contain chromophore groups causing intense tint (varies between yellow and brown) and turbidity in the water. During oxidation, it is found that the concentration of oxygen dissolved in water (DO, mg/L) decreases as hydrogen peroxide is consumed in the process, until reaching a stable value close to zero. When water doped with SMX is oxidized by using UV radiation catalysed by iron salts, a dark brown hue and high turbidity (7.5 NTU) is generated and the water presents high aromaticity and mineralization yields (TOC, mg/L) of around 67 %. By enhancing the treatment with hydrogen peroxide, these water quality indicators decrease with the dose of oxidant. Then, carrying out the treatment with molar ratios of 1 mol SMX : 10 H_2O_2 : 0.045 mol Fe^{2+}, colourless waters appear with low turbidity (<1 NTU) and mineralization yields of 93%.

Materials and methods

The oxidation assays by a photo-Fenton treatment were conducted with aqueous solutions of sulphamethoxazole $[SMX]_0$=50.0 mg·L^{-1} (Fragon, $C_{10}H_{11}N_3O_3S$ 100,6%) using a 150W UV combined with the ferrous ion dosage $[Fe(II)]_0$=0.5 mg L^{-1} (Panreac, $FeSO_4$ $7H_2O$ 99.0%), and varying the hydrogen peroxide $[H_2O_2]_0$=0-3.0 mM (Panreac, H_2O_2 30% w/v). Colour expressed in Absorbance Units (AU) was analyzed at λ=455 nm using a Spectrophotometer UV/Vis (Jasco V-730 Bio).

Results and discussion

Based on the results, a kinetic modelling of colour formation as a function of the oxidant concentration has been proposed, following a series reaction model, where SMX degrades to reaction intermediates of a coloured nature, which are species of a more aromatic nature and containing chromophore groups, according to a first-order kinetic constant $k_{colour,f}$ (1/min). If the oxidation conditions are sufficiently oxidizing, the coloured intermediates are decomposed to colourless species of biodegradable nature, according to a first-order kinetic constant $k_{colour,f}$ (1/min). The variable $[Colour]_\infty$ (UA) has been included, corresponding to the remaining colour that persists in the treated water, and a parameter α that relates SMX concentration to the colour absorbance units.

Model of series reaction:

$$SMX \xrightarrow{k\ colour,\ f} \text{Coloured intermediates} \xrightarrow{k\ colour,d} \text{Uncoloured species} \quad (1)$$

Mass balance for sulfamethoxazole oxidation:

$$-\frac{d\,[SMX]}{dt} = k_{SMX}[SMX] \quad (2)$$

Kinetic equation for sulfamethoxazole degradation:

$$[SMX]=[SMX]_0 \ \exp(-k_{SMX}\,t) \quad (3)$$

Kinetic constat of firt-order for sulfamethoxazole oxidation :

$k_{SMX} = -0.0628\ [H_2O_2]_0^2 + 0.2318\ [H_2O_2] + 0.1554 \quad (r^2=0.9726)$ (4)

Mass balance for colour changes:

$$\frac{d\,[Colour]}{dt} = k_{colour,f}\ \alpha\ [SMX] - k_{colour,d}\ ([Colour] - [Colour]_\infty)$$ (5)

Kinetic equation for colour changes:

$$[Colour] = [Colour]_\infty + \left[\frac{k_{colour,f}\ [SMX]_0}{k_{colour,d} - k_{SMX}}\right]\ \left[\alpha \exp(-k_{SMX}\ t) - \exp(-k_{colour,d}\ t)\right]$$ (6)

Parameter that relates SMX concentration to the colour absorbance units:

$$\alpha = \lambda_{455}/\lambda_{260}$$ (7)

$\alpha = 0.2098\ [H_2O_2]_0^2 - 0.9689\ [H_2O_2] + 2.0639 \quad (r^2=0.9932)$ (8)

Kinetic constant of first-order for colour formation:

$k_{colour,f} = -0.0002\ [H_2O_2]_0^2 + 0.0008\ [H_2O_2] + 0.0001 \quad (r^2=0.9889)$ (9)

Kinetic constant of first-order for colour degradation:

$k_{colour,d} = -0.0017\ [H_2O_2]_0^2 + 0.0154\ [H_2O_2] + 0.028 \quad (r^2=0.9744)$ (10)

Final colour of water solution treated:

$[Colour]_\infty = -0.0014\ [H_2O_2]_0^3 + 0.0191\ [H_2O_2]_0^2 - 0.0713\ [H_2O_2]_0 + 0.08 \quad (r^2=0.9684)$ (11)

Acknowledgements: This study is supported by the Basic and/or Applied Research projects (PIBA): "Degradation of emerging contaminants (drugs) that cause high turbidity and color in water using ultraviolet light and ozone", PIBA 2023 1 0032 University of the Basque Country. Department of Education of the Basque Government.

References

Villota, N., Jankelevitch, S., Lomas, J.M., 2022. Kinetic modelling of colour and turbidity formation in aqueous solutions of sulphamethoxazole degraded by UV/H_2O_2. *Environ. Technol.,* 45, 2, 349-359. https://doi.org/10.1080/09593330.2022.2109997.

Domestic wastewater treatment by a high-rate anaerobic MBR system

E. Politou, K. Azis, A. Makri, S. Ntougias, N. Remmas, P. Melidis[1]
[1]Laboratory of Wastewater Management and Treatment Technologies, Department of Environmental Engineering, Democritus University of Thrace, Xanthi, Greece
Corresponding author email: pmelidis@env.duth.gr

keywords: *domestic wastewater; anaerobic treatment; EGSB; MBR; zero energy wwtp.*

Introduction

The critical need to conserve natural resources and energy is propelling humanity towards adopting a circular economy model, with wastewater treatment playing a crucial role. In recent years, research has increasingly focused on developing effective wastewater treatment methods that not only decontaminate but also harness wastewater as an energy source. One such method is the anaerobic membrane bioreactors (AnMBRs)(Kanafin et al., 2021).

AnMBR systems offer a novel approach to municipal wastewater treatment by combining the advantages of traditional anaerobic digestion with membrane filtration. In these systems, anaerobic microorganisms biodegrade the organic matter in the wastewater, producing biogas that can be used for energy, avoiding the consumption of oxygen (Vinardell et al., 2020). Additionally, the membrane filtration ensures the treated wastewater is free of solids, making it rich in essential nutrients like nitrogen and phosphorus, which are beneficial for crop growth. This nutrient-rich effluent is suitable for irrigation providing environmental and economic benefits. AnMBRs also generate significantly less sludge compared to conventional aerobic systems (Kanafin et al., 2021).

In this study, an expanded granular sludge bed (EGSB) reactor was paired with an ultrafiltration membrane system to treat municipal wastewater sustainably (Chu et al., 2005) . Initially, acetic acid was used during the startup phase to help the anaerobic bacteria acclimate. The system then transitioned to treating municipal sewage.

Materials and methods

The anaerobic system used consisted of an Expanded Granular Sludge Bed (EGSB) reactor and an ultrafiltration membrane system. In the experiments that were conducted, it was examined the influence of changing temperature conditions on the performance of the anaerobic membrane bioreactor (AnMBR) system. Specifically, it was investigated the impact of temperature variations on, biogas production, biodegradation of the organic load, the response and performance of the membranes under these operating conditions.

The hydraulic residence time (HRT) of the anaerobic reactor was maintained at 48 hours. During the experiments, the average organic loading rate (OLR) was 0.3 g COD/m^3/d. It was examined the performance of the anaerobic system under three different temperature conditions ranging from 20 to 38°C.

Key operational parameters, such as biogas production, organic matter removal efficiency, and effluent quality, were closely monitored and analyzed under each of the temperature regimes investigated.

In addition to monitoring the operational parameters, it was also closely tracked the water quality and process performance indicators like COD, BOD_5, Transmembrane Pressure (TMP), P-PO_4^{3-}, NH_4^+-N, TKN-N, total alkalinity and FOS/TAC ratio, pH, Total and Volatile Solids (TS, VS).

Results and discussion

By closely monitoring the investigated key parameters, we could be able to assess how the AnMBR system adapted and performed under different temperature regimes. This allowed us to gain valuable insights into the operational characteristics and limitations of the system, as well as identify optimal temperature conditions for efficient biogas generation and organic matter removal.

The comprehensive evaluation of the system's response to temperature changes provides important information for the design, operation, and optimization of EGSB reactor, which is crucial for enhancing their overall performance and energy recovery capabilities.

The anaerobic reactor operated with an average influent total COD (Chemical Oxygen Demand) of 627 mg/L ± 200 mg/L. The organic loading rate (OLR) was 0.3 g COD/L/d. The temperature conditions ranged from mesophilic (38°C) to psychrophilic (20°C). The average biogas production was 0.73 ± 0.26, 0.54 ± 0.16, 0.54 ± 0.15, 0.43 ± 0.22 L biogas/gCOD removed at 38°C, 30°C, 25°C and 20°C respectively, with the COD effluent averaging 47±10, 39±22, 38±11 and 18± 11 mg/L for the same temperature conditions.

A critical operational parameter for the membrane component of the anaerobic membrane bioreactor (AnMBR) system was the transmembrane pressure (TMP). This parameter was closely monitored in real-time during the experiments. The TMP is a measure of the pressure difference across the membrane, and it provides valuable insights into the membrane's performance and fouling behavior. By continuously monitoring the TMP, we were able to track any changes or increases in the membrane's resistance, which can indicate the need for membrane cleaning (De Vela, 2021).

As required, we performed chemical cleaning of the membranes to maintain their performance and restore their permeability. This proactive maintenance of the membrane system is crucial for ensuring the long-term reliable operation of the AnMBR process (Lin et al., 2013).

Conclusions

The COD reduction and the corresponding biogas production provides an overview of the operating conditions and performance of the anaerobic reactor under different temperature regimes, highlighting the impacts on biogas production and effluent quality.

By evaluating the system's behavior across the temperatures range of 20 – 38 °C, it was able to assess the impact of temperature variations on the overall performance of the anaerobic reactor.

The TMP monitoring was crucial for evaluating the membrane filtration performance and identifying any potential fouling or clogging issues.

This multifaceted monitoring approach enabled to evaluate the system's response to the changing temperature conditions and optimize the overall performance of the anaerobic membrane bioreactor.

Acknowledgements: This research received no specific grant from any funding agency in the public, commercial, or not-for-profit sectors.

References

Chu, L.-B., Yang, F.-L., Zhang, X.-W., 2005. Anaerobic treatment of domestic wastewater in a membrane-coupled expended granular sludge bed (EGSB) reactor under moderate to low temperature. Process Biochem. 40, 1063–1070. https://doi.org/10.1016/j.procbio.2004.03.010

De Vela, R.J., 2021. A review of the factors affecting the performance of anaerobic membrane bioreactor and strategies to control membrane fouling. Rev. Environ. Sci. Biotechnol. 20, 607–644. https://doi.org/10.1007/s11157-021-09580-2

Kanafin, Y.N., Kanafina, D., Malamis, S., Katsou, E., Inglezakis, V.J., Poulopoulos, S.G., Arkhangelsky, E., 2021. Anaerobic Membrane Bioreactors for Municipal Wastewater Treatment: A Literature Review. Membranes 11, 967. https://doi.org/10.3390/membranes11120967

Lin, H., Peng, W., Zhang, M., Chen, J., Hong, H., Zhang, Y., 2013. A review on anaerobic membrane bioreactors: Applications, membrane fouling and future perspectives. Desalination 314, 169–188. https://doi.org/10.1016/j.desal.2013.01.019

Vinardell, S., Astals, S., Peces, M., Cardete, M.A., Fernández, I., Mata-Alvarez, J., Dosta, J., 2020. Advances in anaerobic membrane bioreactor technology for municipal wastewater treatment: A 2020 updated review. Renew. Sustain. Energy Rev. 130, 109936. https://doi.org/10.1016/j.rser.2020.109936

Session 3: Wastewater management (I I)

Effect of iron catalyst on water quality parameters during the oxidation of diclofenac by photo-Fenton treatment

U. Duoandicoechea[1], A. De Luis[2] and N. Villota[1]

[1] Department of Environmental and Chemical Engineering, Faculty of Engineering Vitoria-Gasteiz, University of the Basque Country, Vitoria-Gasteiz, Spain
[2] Department of Environmental and Chemical Engineering, Bilbao School of Engineering, University of the Basque Country, Bilbao, Spain
Corresponding author email: natalia.villota@ehu.eus

keywords: *Colour, diclofenac, photo-Fenton, turbidity.*

Introduction

Diclofenac, DCF ($C_{14}H_{11}Cl_2NO_2$) is a non-steroidal anti-inflammatory drug (NSAID) used to treat pain and inflammation. This drug can enter the environment through a variety of pathways, including waste disposal from factories that produce it, excretion from people and animals that consume it, and improper disposal of expired or unused medicines. Once DCF enters the environment, it can be difficult to remove, and many studies have detected it in rivers and groundwater.

In this situation, Advanced Oxidation Processes (AOPs) emerge as an alternative for the removal of DCF from water, due to their high efficiency in the degradation of a wide variety of recalcitrant organic compounds. Among all the AOPs, UV light irradiation and its combination with hydrogen peroxide catalysed by iron salts, known as photo-Fenton technology, stand out. The decomposition of these pollutants by AOPs can significantly reduce the environmental impact of wastewater and effluents, improving water quality and reducing risks to public health and the environment.

Materials and methods

To carry out the oxidation reactions of the DCF-doped aqueous solutions, a 1.0 L photocatalytic reactor containing a 150 W half-power mercury UV lamp (Heraeus, 85.8 V, 148.8 W, 1.79 A, 95% transmission between 300 and 570 nm) was used, which was agitated by means of a magnetic stirrer. The reactor is fed with the aqueous samples of diclofenac sodium (Fragon, >99.5%) of concentration $[DCF]_0$=50.0 mg/L. Then the concentration of ferrous sulphate catalyst estimated for each test $[Fe(II)]_0$=0-5.0 mg/L and oxidant $[H2O2]_0$=1.0 mM is added. All reactions have been carried out at the natural pH of water (around $[pH]_0$=6.5). During the reaction, the temperature of the reaction mixture is kept within a range of 30-35°C using a heating bath (Frigiterm- P Selecta). During the 120 minutes of the test, the following variables were analysed: pH was measured with a pH meter (Kent EIL9142). Water turbidity was measured in nephelometric turbidity units (NTU) with a turbidity meter (Hanna Instruments HI88703). Aromaticity and colour were analysed using a UV/Vis spectrophotometer (Jasco V-630) measuring at λ=254 and 455 nm. Dissolved oxygen and temperature were measured with a portable oxygen meter (Hanna Instruments HI 9142). A TOC analyser (Shimadzu TOC-V) was used to measure total organic carbon (TOC, mg/L). The determination of DCF was carried out using a high-performance liquid chromatography (Waters 2695) coupled with a dual λ absorbance detector (Waters 2487).

Results and discussion

During the degradation of DCF there is a strong increase in the aromaticity of the water, because DCF degrades to species with a higher degree of aromaticity than the pollutant itself. These aromatic intermediates are very stable and UV light is not able to degrade them, so they remain in the treated water. By combining hydrogen peroxide with UV light, the treatment is able to completely degrade these aromatic intermediates. However, when using the photo-Fenton process, the aromaticity remains in the water because the iron is able to react with some of the intermediate species generating metal complexes. These complexes would be highly stable and would therefore persist, generating colour and turbidity in the treated water.

On the other hand, during the degradation of DCF, a strong yellow colour is generated in the water. When the oxidation process is carried out with UV light, the colour is maintained. By combining the treatment with hydrogen peroxide, water with a colourless appearance, low turbidity (<1 NTU) and [DO]=8.1 mg/L is obtained, which means that the water is of very good quality. However, when the iron treatment is boosted, a brown colour and high turbidity (30 NTU) persist, showing that the turbidity of the water increases proportionally with the iron dose. In addition, the dissolved oxygen levels are lower than [DO] < 2.0 mg/L, which indicates that the water is of poor quality. This is because iron can react with DCF degradation intermediates to generate metal complexes of a coloured nature. In other words, iron would be a colour activator, thus worsening the quality of the treated water. Therefore, it would be advisable to use the UV/H_2O_2 combination to obtain water with a colourless appearance that meets the quality requirements established in the environmental legislation.

Maximum turbidity is achieved when using a stoichiometric ratio of 1 mol Fe: 3 mol DCF. Because the molecular structure of diclofenac sodium has a carboxylic group that can be easily coordinated to a metal centre to give a coordination compound, it is an ideal ligand for the formation of coordination complexes, where the iron ion is coordinated with three deprotonated ligands, so that the charge is compensated. These ligands are coordinated via the oxygen atoms of the carboxylate groups. By increasing the iron dosage above this stoichiometric ratio, the iron is in excess and precipitates in the form of ferric hydroxide, which causes a decrease in the turbidity of the water.

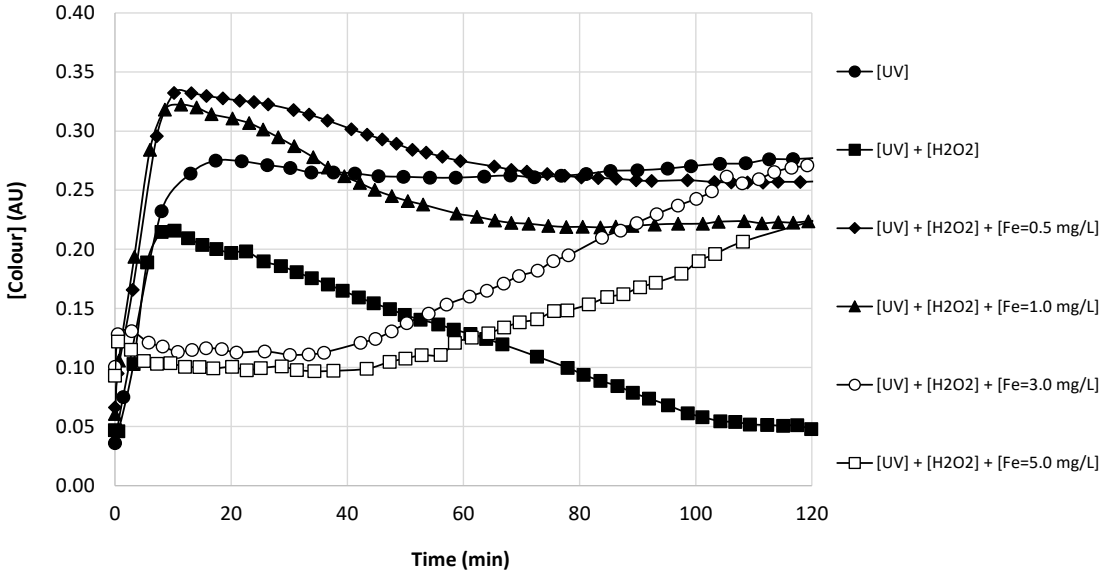

Figure 1. Colour changes during the DCF degradation by photo-Fenton. Experimental conditions: $[DCF]_0$=50.0 mg/L; [UV]=150W; $[H2O2]_0$=1.0 mM; $[pH]_0$=6.5; [T]=30ºC.

Acknowledgements: This study is supported by the Basic and/or Applied Research projects (PIBA): "Degradation of emerging contaminants (drugs) that cause high turbidity and colour in water using ultraviolet light and ozone", PIBA 2023 1 0032 University of the Basque Country. Department of Education of the Basque Government.

References

Villota, N., Jankelevitch, S., Lomas, J.M., 2022. Kinetic modelling of colour and turbidity formation in aqueous solutions of sulphamethoxazole degraded by UV/H2O2. Environ. Technol., 45, 2, 349-359. https://doi.org/10.1080/09593330.2022.2109997.

Nutrient recovery from urine diverting dry toilets via pyrolysis

M.E. Koulouri*, M.R. Templeton, G.D. Fowler
Department of Civil and Environmental Engineering, Imperial College London, UK, SW7 2AZ
*Corresponding/presenting author email: maria.koulouri17@imperial.ac.uk

keywords: *nutrient recovery, biochar, urine diversion, faecal sludge, adsorption*

Introduction

The rising urban population, especially in developing countries, creates challenges related to resource scarcity and sustainable human waste management (Trimmer et al., 2019). These parallel issues create an opportunity for sanitation-driven resource recovery, particularly for outputs of on-site dry toilets that are more nutrient-dense compared to other wastewater sources. It is currently estimated that 3.7 billion people globally rely on on-site facilities to access sanitation services (WHO/UNICEF, 2023). While sewered sanitation infrastructure usually involves mixing of human excreta with large amounts of flush water and other wastewater streams, decentralised dry toilets provide opportunities to recover valuable resources from pure human excreta and are often urine diverting (Martin et al., 2020).

This study investigated nutrient recovery from on-site, dry, urine diverting toilets via pyrolysis. Firstly, benefits of urine diversion were quantified by comparing biochars produced from mixed urine and faeces (MUF) and source separated faeces (SSF) for their agricultural properties. Further enhancement of SSF biochars with urine-derived nutrients was investigated via adsorption and precipitation to produce combined fertilisers and soil amendments. Findings of this research can be used to inform global sanitation waste management, particularly for container-based and composting toilets used in remote islands, developing countries or emergency contexts. Ultimately, resource recovery benefits create meaningful incentives to ensure universal access to safely managed sanitation, in line with the UN Sustainable Development Goal 6.

Materials and methods

The study experimental design is summarised in **Figure 1**. Samples of source separated faeces (SSF) and urine (SSU) were collected from 12 volunteers in the UK and transferred to Imperial College London (ICL). Aliquots of SSU samples were stored for a period of 6 months. The MUF samples were prepared by blending fresh SSF and SSU samples at a ratio representative of that of daily excretion (1g:10mL) (Rose et al., 2015). For biochar production, slow pyrolysis (10°C/min) was carried out on a rotary furnace under N_2, at three prescribed temperatures (450, 550, 650°C) for 30min. The biochars were analysed for their thermal properties, inorganic composition and surface properties. Analytical methods are described in Koulouri et al. (2024, 2023).

Batch adsorption experiments were performed to investigate NH_4^+ adsorption from stored SSU onto SSF-derived biochars, as well as combined N and P recovery via precipitation induced by MgO addition. The effect of the biochar dose was investigated by adding 0.5–2g of biochar to 20mL urine (n=5) and shaking on a reciprocal shaker at 150rpm for 72h in order to reach equilibrium.

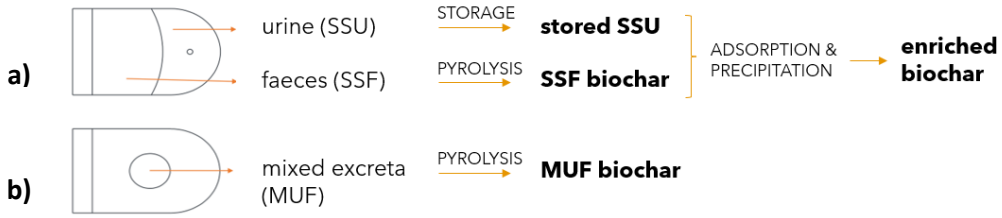

Figure 1: Schematic of experimental design scenarios with (a) and without (b) urine diversion.

Results and discussion

Preliminary results highlighted the different thermal decomposition behaviour of SSF and MUF samples during pyrolysis. Both SSF and MUF biochars were found to have good nutrient recovery potential (**Figure 2**). While MUF biochars had higher concentrations of P and K, their high measured salinity may place limitations on agricultural applications to salt sensitive plants. Urine diversion significantly benefited N recovery (70% of total N volatilisation losses during pyrolysis avoided) and resulted in SSF biochars with higher liming potential.

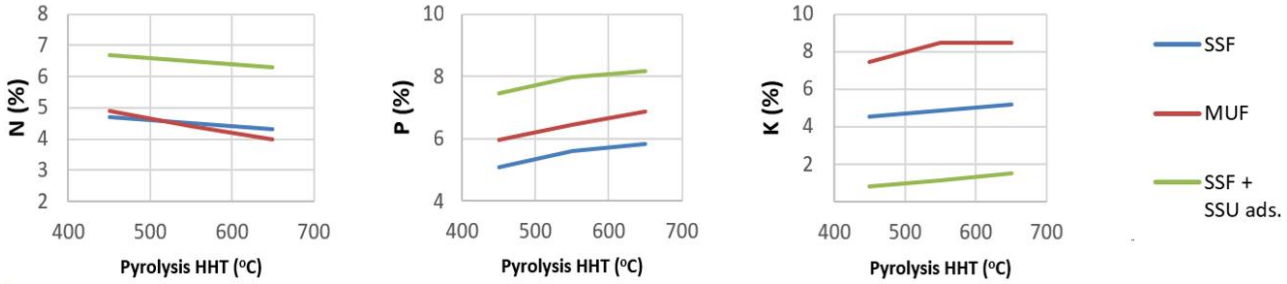

Figure 2: NPK concentrations (%) for biochars produced at 450, 550, 650°C from source-separated faeces (SSF) and mixed urine and faeces (MUF), and for enriched SSF biochars after adsorption from stored urine (SSF + SSU ads.).

For urine samples, storage in sealed containers was found to successfully prevent N losses and urea hydrolysis lead to equilibrium between NH_3 and NH_4^+ phases. NH_4^+ adsorption onto faecal-derived biochars was feasible and the capacity of the biochar was 19.8 mg NH_4–N/g. Experimental data exhibit a good fit to both the Freundlich and Langmuir isotherm models and the rate of the reaction was well described by pseudo 2nd-order kinetics. The main NH_4^+ recovery mechanism was attributed to exchange reactions with K^+ ions (up to 30% N recovery), while the main P recovery mechanism was precipitation of struvite/struvite-K and substituted hydroxyapatite, as identified by SEM-EDX (>98% P recovery) (**Figure 3**). The combination of MgO addition (Mg:P = 1.5) with the lower biochar dose tested (25g/L) produced the most NP-rich combined fertiliser and soil amendment product which was easily separated from urine (**Figure 2**).

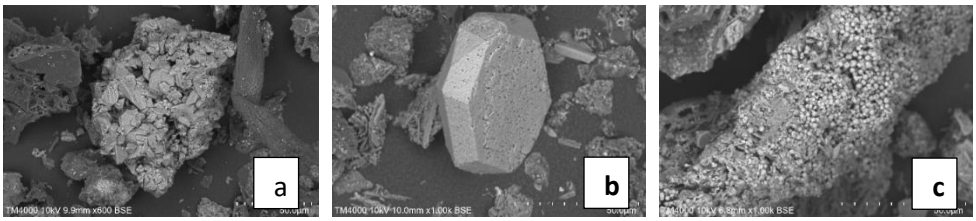

Figure 3: SEM analysis for faecal-derived biochars after treatment with stored human urine and MgO (Mg:P=1.5), showing crystals identified by EDX as struvite (a), struvite-K (b) and substituted hydroxyapatite (c).

Conclusions

Overall, results indicate that urine diversion can optimise soil improving properties of produced biochars, while also allowing the separate recovery of nutrients from urine. Combined recovery of NH_4^+ and precipitates from urine to produce NP-enriched biochar fertilisers is feasible.

This research paves the way for the production of marketable human excreta-derived fertilisers that can compete with, or exceed the performance of, commercial fertilisers associated with heavy environmental burdens. Future studies should aim to further optimise and simplify treatment and reuse technologies, in parallel with efforts to establish these systems within formal and informal institutions and stakeholders.

Acknowledgements

The authors thank ICL for the donation of a scholarship and the Society of Chemical Industry for financially supporting this work. This project was also supported by the Royal Academy of Engineering under the Research Chairs and Senior Research Fellowships programme. Approvals for human excreta collection were obtained via the ICL Research Governance and Integrity Team (21IC6817) and the ICL Tissue Bank (ICHTB).

References

Koulouri et al., 2024. Enhancing the nitrogen and phosphorus content of faecal-derived biochar via adsorption and precipitation from human urine. J. Environ. Manage. 352, 119981.

Koulouri et al., 2023. Source separation of human excreta: Effect on resource recovery via pyrolysis. J. Environ. Manage. 338, 117782.
Martin et al., 2020. Human urine-based fertilizers: A review. Crit. Rev. Environ. Sci. Technol. 0, 1–47.
Rose et al., 2015. The Characterization of Feces and Urine: A Review of the Literature to Inform Advanced Treatment Technology. Crit. Rev. Environ. Sci. Technol. 45, 1827–1879.
Trimmer et al., 2019. Resource recovery from sanitation to enhance ecosystem services. Nat. Sustain.2.
WHO/UNICEF, 2023. Progress on household drinking-water, sanitation and hygiene 2000-2022.

Limassol District Local Government Organisation: Challenges and opportunities in sewage treatment

Yiannis Tsouloftas[1], Socrates Metaxas[1], Michalis Vrionides[1], Pierina Marti[1] and Gregoris Panayiotou[1]

[1] Limassol District Local Government Organisation, Limassol, Cyprus
Corresponding author email: gregoris.panayiotou@eoalemesos.org.cy

keywords: *Limassol, sewage, biological treatment plants*

On 1st July 2024 the Limassol District Local Government Organisation (LDLGO) was founded and started operations under Law 37(I)/2022. This was a huge step in Cypriot reality since a number of important services and responsibilities have been assigned to the new organisation. More specifically, the new organisation has undertaken the following operating activities:

- Potable Water – previously handled by the Water Board of Limassol
- Sewage and Rain Water Drainage systems – previously handled by the Sewerage Board of Limassol - Amathus,
- Solid Waste Management – previously handled by the Limassol Waste Management Board,
- Issuance of Building and Town Planning Permits – previously handled by various local authorities, the Government Town Planning and Housing Department and the District Administration Office.

The main aim of this Local Government reform was to create a single point of service for the people of each district, and in our case the people of the Limassol District.

The new organisation is facing huge challenges, especially during its first stages of operation, since the services and responsibilities gathered under its umbrella are of vital importance for the development in the Limassol District and the wellbeing of the citizens.

In particular regarding the sewage treatment in the new era, after 1st July 2024, the LDLGO in addition to the two main Sewage Treatment Plants located in Moni and Kato Polemidia, has undertaken the responsibility for another seven (7) Sewage Treatment Plants/facilities in the mountainous communities/villages of Platres, Agros, Kyperounta, Pelendri, Alassa, Kyvides and Troodos. Previously these facilities were under the responsibility of Communal Sewage Boards and the Government Water Development Department of Cyprus. The initial general state of these facilities when taken over by LDLGO was as follows:

- good in 4 cases,
- bad in 1 case and
- very bad in the other 2 cases.

When LDLGO undertook the responsibility for the maintenance and operation of these facilities, immediate remedial actions were carried out, primarily to eliminate any health and safety issues that were present and to improve accordingly the biological treatment process and thus the quality of the recovered water. These actions are of course only the first steps of a long process and additional actions and modifications are planned to be carried out in the near future so as to improve the level of services provided. Moreover, these actions and measures will improve the protection of the environment and contribute towards the success of the newly founded organisation.

Advanced primary filtration process for the upgrade of overloaded activated sludge plants

K. Tsamoutsoglou[1] and P. Gikas[1]

[1] School of Chemical and Environmental Engineering, Technical University of Crete, 73100 Chania, Greece
Corresponding author email: pgikas@tuc.gr

keywords: *wastewater; microsieve; energy savings;*

In recent years, energy use in Wastewater Treatment Plants (WWTPs) has increased due to the application of advanced wastewater and sludge treatment methods as well as the management of higher volumes of waste (Siatou et al., 2020). Many WWTPs operate with increased hydraulic flows or increased inlet load, resulting in incomplete wastewater treatment. The phenomenon is intense during the summer months, in WWTPs serving tourist areas (Tsamoutsoglou et al., 2024). Innovative primary filtration systems for the treatment of municipal wastewater with low cost and energy could be a solution to the above-mentioned problems. The innovation of primary filtration systems lies in the early removal of suspended solids from raw wastewater, before their entry into the aeration tank. In this way, existing and new WWTPs can be upgraded, without the need for conventional expansion. The Advanced Primary filtration (APF) process has been implemented at Kyperounda WWTP (Figure 1).

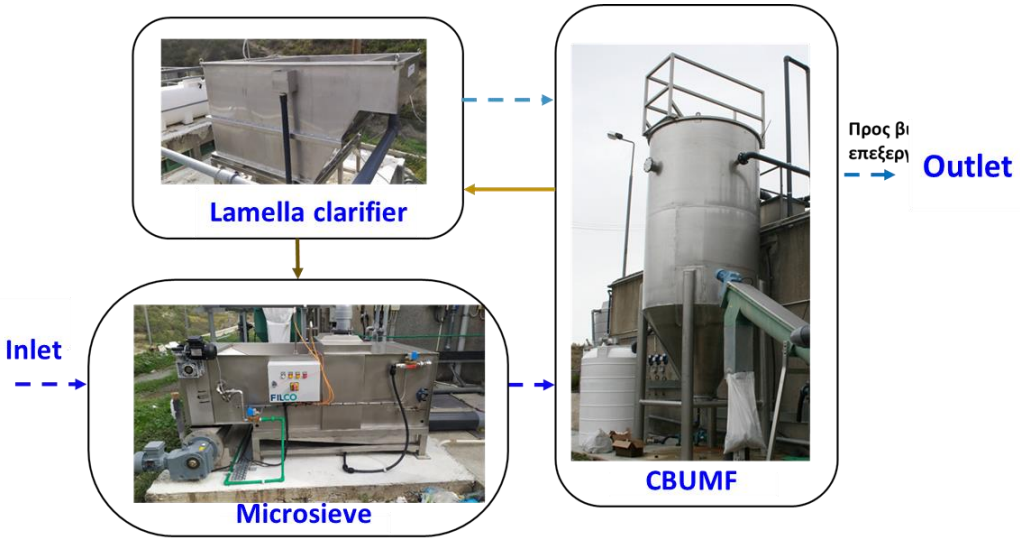

Figure 1: APF process at WWTP of Kyperounda, Cyprus.

The APF process has been designed for maximum a capacity of 1,800 m^3/d. The pilot unit consist in series of: microsieves and Continuous Backwash Upflow Media Fitler (CBUMF), while the condensate of the CBUMF is treated in a lamella clarifier. The APF process demonstrated: (i) an average total suspended solids (TSS) removal rate of 52%, yielding effluent TSS concentrations between 290 and 375 mg/L, without coagulants; (ii) an average biological oxygen demand (BOD5) removal rate of 46%, resulting in effluent BOD_5 concentrations ranging from 195 to 375 mg/L; and (iii) an average chemical oxygen demand (COD) removal rate of 43%, with effluent COD concentrations between 328 and 485 mg/L.

References

Siatou, A., Manali, A., Gikas, P., 2020. Energy consumption and internal distribution in activated sludge wastewater treatment plants of Greece. Water 12, 1204.

Tsamoutsoglou, K., Katzourakis, V.E., Chrysikopoulos, C. V, Gikas, P., 2024. Performance evaluation and parameter estimation of the advanced primary filtration (APF) process in wastewater treatment plants. Sep. Purif. Technol. 127106.

Preparation of biochar derived from olive mill solid waste in a circular economy approach for enhanced adsorption of trihalomethanes from water

Sara Azerrad[1,3], Hassan Azaizeh[2], Shilat Parsha[3], Eyal Kurzbaum[3]

[1] The Natural Resources and Environmental Research Center-NRERC, University of Haifa, Mount Carmel, 3498838 Haifa, Israel
[2] Tel Hai College, Department of Environmental Science, Upper Galilee, 12208, Israel
[3] Department of Geography and Environmental Studies, University of Haifa, Mount Carmel, 3498838 Haifa, Israel

email: saraa@gri.org.il

keywords: Biochar, circular economy, adsorption, trihalomethanes

Introduction

Agricultural waste, generated annually in substantial volumes, comprises by-products from agriculture and crop residues. Effective management of this waste is crucial for sustainable practices, aiming to produce value-added products while minimizing environmental pollution. Within the Mediterranean basin, olive tree cultivation for oil production stands as a significant agricultural activity. The solid waste resulting from oil extraction, known as olive mill solid waste (OMSW), constitutes a blend of skin, pulp, and seeds (Abdelhadi et al., 2017; Peer et al., 2023). Pyrolysis, a process involving heating with limited oxygen supply at temperatures ranging from 300° to 800°C, offers a means to convert agricultural waste into biochar (BC). BC boasts several beneficial properties, including high cation exchange capacity, a large surface area, and a stable structure (Wang and Wang, 2019).

In drinking water treatment, chlorine disinfection stands as the predominant and cost-effective method for eliminating pathogens, thus averting waterborne diseases. However, chlorine-based disinfectants yield undesirable disinfection by-products (DBPs), such as trihalomethanes (THMs), which are closely monitored due to their suspected adverse effects on human health (Valdivia-Garcia et al., 2016). The European Union Drinking Water Directive stipulates a maximum allowable concentration of total THMs in drinking water at 100 µg/L, while the US EPA regulates THMs with a maximum allowable annual average level of 80 µg/L (Valdivia-Garcia et al., 2016).

This study focuses on the preparation of OMSW-derived BC, comparing various pyrolysis temperatures as well as physical (thermal) and chemical activation methods. The investigation aims to optimize the adsorption capacity of OMSW-derived BC, thereby enhancing its efficacy in water treatment. The different types of BC prepared herein are characterized, and their ability to remove THMs is evaluated.

Materials and methods

Biochar was synthesized from OMSW via pyrolysis at temperatures ranging from 400 to 600°C. Additionally, thermal activation was performed using an oven at 900°C under a nitrogen atmosphere (BC-T), while chemical modification involved treatment after thermal activation with a mixture of iron and zinc as transition metals (BC-Zn/Fe) or a potassium hydroxide solution. (BC-KOH). Additionally, two types of commercial activated carbon (AC) were tested in order to compare the performance of our BC. AC-A (Hydraffin XC 30) is produced from Bituminous coal and AC-B (Hydraffin CC 30) is produced from coconut shells, both possess a surface area ~1000 m^2/g. Batch adsorption experiments were carried out by spiking THMs into phosphate buffer to attain initial concentrations of 150-200µg/L. The experiments were conducted in borosilicate bottles (250 mL) filled with 200 mL of water solutions. Biochar was added to each bottle to achieve a concentration of 300 mg/L, followed by mixing on an orbital shaker at 150 rpm and 25°C. Aliquots were withdrawn at different time intervals for further analysis. Batch experiments were performed in triplicate, and mean values along with standard deviations were reported. THMs concentration was measured using headspace gas chromatography coupled to a mass spectrometer (HS-GC-MS).

Results and Conclusions

Initially, the performance of BC derived solely from pyrolysis at temperatures of 450°C and 600°C was compared with BC subjected to further chemical/thermal activation (BC-T, BC-KOH, and BC-Zn/Fe), along with two types of commercial AC. The adsorption of THMs was evaluated by expressing their relative concentration (Ce/Co) (Fig. 1). Results revealed that BC produced solely through pyrolysis exhibited limited effectiveness in adsorbing THMs, achieving a maximum adsorption of only 10% at 600°C. In contrast, the further activated BCs showed enhanced THM adsorption, with BC-T demonstrating the highest efficacy, followed by BC-KOH and BC-Zn/Fe. Notably, BC-T (21 m^2/g) exhibited a lower SSA compared to BC-KOH (70 m^2/g) and BC-Zn/Fe (456 m^2/g), suggesting that functional groups within BC may play a crucial role in adsorption, potentially surpassing the significance of surface area alone. This observation was consistent with the behavior observed in the two types of commercial activated carbon, which possessed significantly higher SSAs (~1000 m^2/g) but exhibited lower THM adsorption compared to BC-T. Among the two types of commercially available activated carbon, type A (bituminous coal) exhibited slightly higher efficiency than type B (coconut shell), yet BC-T demonstrated superior THM adsorption compared to both types of commercial activated carbon.

THMs exhibited preferential adsorption onto BC with the adsorption sequence being bromoform > chlorodibromomethane (CDBM) > bromodichloromethane (BDCM) > chloroform. At a BC-T concentration of 300 mg/L, adsorption efficiencies were achieved for chloroform (41.2% ± 4.9), BDCM (55.6% ± 3.6), CDBM (64.6% ± 3.2), and bromoform (74.1% ± 3.6) after a 4-hour treatment period. The utilization of agriculture waste-derived BC for THM adsorption in water represents a promising avenue in the field of water treatment, aligning with principles of circular economy for agricultural waste utilization.

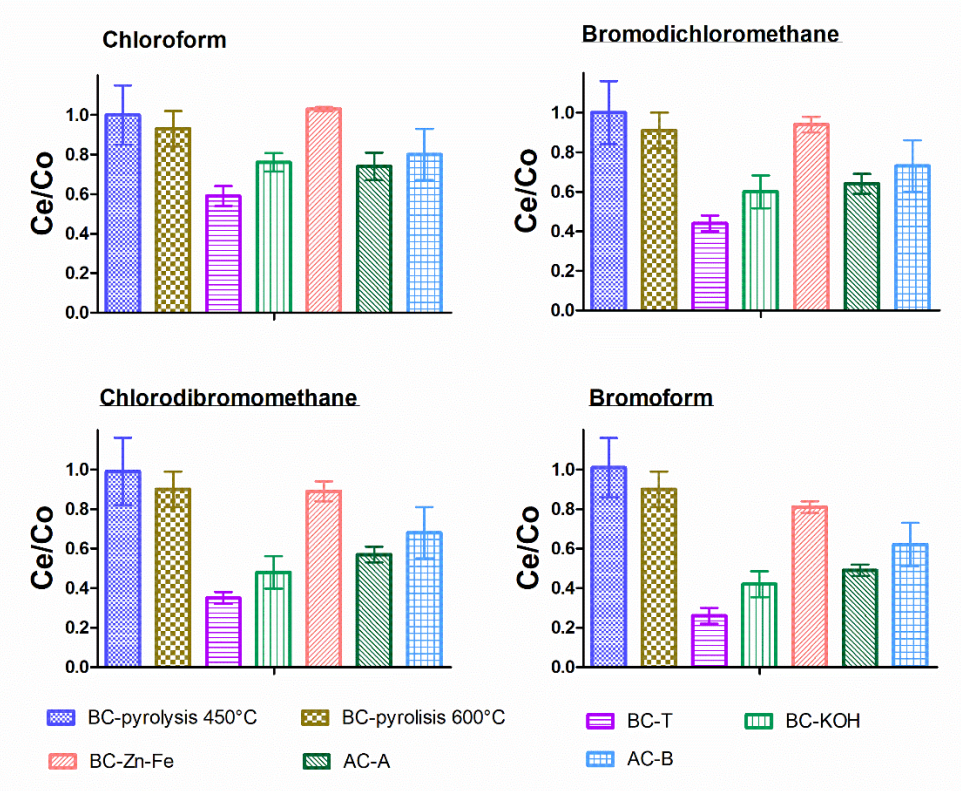

Fig.2. Adsorption of THMs by the different types of BC. Initial concentration THMs: 150-200 μg/L each, Biochar concentration:300 mg/L, Adsorption time: 4h, Water matrix: Buffer phosphate (50mM) pH 7.

References

Abdelhadi, S.O., Dosoretz, C.G., Rytwo, G., Gerchman, Y. and Azaizeh, H. (2017) Production of biochar from olive mill solid waste for heavy metal removal. Bioresource Technology 244, 759–767.

Peer, G., Azaizeh, H., Kurzbaum, E., Shahar, B., Mattar, N. and Azerrad, S.P. (2023) Valorization of olive mill solid waste-derived biochar: An efficient approach for simultaneous adsorption and oxidation of micropollutant in surface water. Journal of Water Process Engineering 56, 104461.

Valdivia-Garcia, M., Weir, P., Frogbrook, Z., Graham, D.W. and Werner, D. (2016) Climatic, Geographic and Operational Determinants of Trihalomethanes (THMs) in Drinking Water Systems. Scientific Reports, 6, 35027.

Wang, J. And Wang, S., (2019) Preparation, modification and environmental application of biochar: A review. Journal of Cleaner Production 227, 1002–1022.

Session 4: Biochemical engineering

Enhancement of starch hydrolysis using immobilized cells and enzymes of two *Aspergillus* strains on oxidized carbonaceous materials

R. Konstantinou[1], M. Patsalou [1], E. Hatdjikyprianou[2], A. J. Tasiopoulos[2], G. Constantinides[3], M. Koutinas[1,]

[1]Department of Chemical Engineering, Cyprus University of Technology, Limassol, Cyprus
[2]Department of Chemistry, University of Cyprus, Aglandjia, Nicosia, Cyprus
[3]Department of Mechanical Engineering and Materials Science and Engineering, Cyprus University of Technology, Limassol, Cyprus
Corresponding author email: michail.koutinas@cut.ac.cy

keywords: *Starch hydrolysis; Aspergillus strains; char; oxidized biochar; immobilization.*

Introduction

The worldwide production of starchy crops is increasing every year, while starch is considered as a crucial renewable resource, which should be completely hydrolyzed during saccharification to enable its use as feedstock in industrial biotechnology applications (Bansal et al., 2020). Among the processes employed for starch hydrolysis, enzyme hydrolysis could be performed in the presence of amylolytic enzymes, while biocatalyst immobilization on carbonaceous materials (e.g. biochar) has effectively enhanced productivity in different bioprocess (Hermida and Agustian, 2022; Kyriakou et al., 2019). Adsorption of the biocatalyst (cells, enzymes) on the material is affected by the carrier's surface chemistry and morphology (He et al., 2022). The current work has optimized the starch hydrolysis bioprocess using oxidized biochar as immobilization carrier, focusing on the chemistry of the surface of the material aiming to increase oxygen functional groups (e.g. carbonyl, carboxyl and hydroxyl) and thus, enhance the formation of hydrogen bonds during immobilization.

Materials and methods

As starch-based feedstock, potato (cv. Spunta) was obtained from a local potato producer (Nicosia, Cyprus). Characterization of potato was performed employing standard analytical methods including Kjeldahl nitrogen analysis, as well as ash, starch and fibre (cellulose, hemicellulose) content quantification.

A. niger MUCL 28817 and *A. awamori* MUCL 28815 were employed both for amylolytic enzyme production and as cells directly involved in the enzyme hydrolysis process, while carbonaceous materials, char and biochar, obtained via pyrolysis of recycled car tyres and pistachio shells respectively, were used as immobilization carriers.

Oxidized biochar was prepared following pyrolysis via oxidation of the material using the following oxidizing agent treatments: 0.2 M and 1 M nitric acid (HNO_3), 0.2 M and 1 M phosphoric acid (H_3PO_4), as well as 1% (v/v) and 30% (v/v) hydrogen peroxide (H_2O_2).

The structural, physical and chemical characteristics of char and biochar were assessed through scanning electron microscopy (SEM) and energy-dispersive X-ray spectroscopy (EDS). The surface areas of the materials were determined using the Brunauer-Emmett-Teller (BET) method.

Starch saccharification efficiency was determined in enzyme hydrolysis via analysis of reducing sugars' concentration through 3,5-dinitrosalicylic acid (DNS) method (Miller et al., 1959) and High Pressure Liquid Chromatography (HPLC) analysis depending on the requirements of each experiment.

Results and discussion

During the present work, preliminary studies were performed including the characterization of the raw material. Potato constituted 16.55% dry matter, 0.82% total nitrogen, 5.10% protein, 7.56% ash, 12.57% starch, 12.92% hemicellulose and 1.30% cellulose. Based on the enzyme kinetics determined, experiments were maintained for 3 d prior harvesting of cells/enzymes in subsequent trials. Furthermore, characterization of the immobilization carrier microstructure was performed using BET, SEM and EDS analyses. The BET surface area and porosity of materials in nanoscale showed that the materials treated using 1% H_2O_2 and 0.2 M HNO_3 displayed BET values of 38 and 44 $m^2\ g^{-1}$, which were higher as compared to pristine biochar (30 $m^2\ g^{-1}$). SEM images showed that all the carbonaceous materials assessed were characterized by porosity. Biochar oxidized

using 0.2 M HNO_3, 0.2 M H_3PO_4, 1 M HNO_3 and 1 M H_3PO_4 were characterized by similar pore sizes compared to parental materials, in contrast to biochar oxidized using 1% and 30% H_2O_2 which presented smaller pore sizes (2.860 μm and 0.724 μm respectively). The immobilization of fungi (cells, biofilm) to the surface of the carrier was confirmed via electron micrographs. The elemental EDS analysis of the materials showed that the chemical oxidation increased the oxygen percentage on the surface of the materials. Biochar oxidation using 30% H_2O_2 increased by 10% the oxygen content (30.53%) as opposed to untreated biochar (20.86%), while biochar oxidized using 1% H_2O_2 contained 26.01% of oxygen. Additionally, experiments aiming to determine the most efficient content and particle size of the immobilization carrier required in fermentations were performed, showing that the highest final concentration of reducing sugars was achieved at 24 h using 3.2% (w/v) biochar comprised diameters between 0.3-0.5 cm. Batch, repeated batch and fed-batch experiments were carried out to determine the most efficient mode of operation for the bioprocess. The maximum reducing sugars concentration in enzyme hydrolysis of 45% (w/v) and 90% (w/v) potato solid content was achieved following 6 h of hydrolysis using *A. niger* as immobilized carrier and following 72 h using the co-culture of the two strains. Repeated batch trials were initially performed via removal of any residual substrate and products as well as addition of 90% potato solids at 6 and 14 d, while an additional repeated batch experiment was conducted without removal of the media. The maximum yield achieved was 0.61 $g_{glucose}$ g_{starch}^{-1} using attached cells of *A. niger* at 6 d following the removal of residual substrate and products.

Experiments of commercial starch hydrolysis were performed using oxidized biochar as immobilization carrier. The results showed that *A. niger* immobilized on biochar oxidized using 1% (v/v) H_2O_2 achieved the highest yield 0.78 $g_{glucose}$ g_{starch}^{-1} demonstrating 70.3% of the maximum theoretical yield, while the concentration of the sugars released was 12.5 g L^{-1}. Significant improvement of the bioprocess was additionally achieved employing biochar oxidized using 0.2 M HNO_3, which substantially increased the glucose content accumulated (9.9 g L^{-1}) as compared to untreated biochar (4 g L^{-1}).

Conclusions

The substantial improvement of bioprocess performance achieved using oxidation of the biomaterial could have been potentially stimulated by the combined effect of specific surface area and oxygen content increase monitored. Oxidation of biochar using 1% (v/v) H_2O_2 increased glucose production by a factor of 3 relative to the use of the untreated material and enhanced the surface area and the oxygen content on the surface of the material. Moreover, the use of 0.2 M HNO_3 for biochar oxidation additionally enhanced the bioprocess by a factor of 2 regarding glucose accumulation. The study has shown that engineering the properties of biochar through chemical treatment could serve as a novel strategy towards development of advanced industrial biotechnology applications.

Acknowledgements: This work was supported by the Cyprus Research and Innovation Foundation (RIF, Cyprus) [grant number ENTERPRISES/0223/Sub-Call1/0245].

References

Bansal, R., Katalyal, P., Jain, D., 2021. Enzymatic and acidic hydrolysis of cull potatoes for production of fermentable sugars. Starch, 74, 2100202.

Hermida, L., Agustian, J., 2022. The application of conventional or magnetic materials to support immobilization of amylolytic enzymes for batch and continuous operation of starch hydrolysis processes. *Rev. Chem. Eng*. 40, 1-34.

Kyriakou, M., Chatziiona, VK., Costa, CN., Kallis, M., Koutsokera, M., Constantinides, G., Koutinas, M., 2019. Biowaste-based biochar: a new strategy for fermentative bioethanol overproduction via whole-cell immobilization. *Appl. Energy*, 480-491.

He, X et al., 2022. The effects of H_2O_2- and HNO_3/ H_2SO_4-modified biochars on the resistance of acid paddy soil to acidification. *Environ. Pollut*, 293, 118588.

Miller, G.L., 1959. Use of dinitrosalicylic acid reagent for determination of reducing sugar. *Anal. Chem*. 31, 426–428.

Bioprocess Development for Thermoplastic Starch And Polyhydroxybutyrate Biodegradation Using Algal-Microbial Co-Cultures

F. Pyrilli[1], E. Syranidou[1], G. Constantinides[2] and M. Koutinas[1*]

[1]Department of Chemical Engineering, Cyprus University of Technology, Limassol, Cyprus
[2]Department of Mechanical Engineering and Materials Science and Engineering, Cyprus University of Technology, Limassol, Cyprus
*michail.koutinas@cut.ac.cy

keywords: *Bioplastics, Thermoplastic Starch, Polyhydroxybutyrate, Aerobic biodegradation, Microalgae*

Introduction

Bioplastics are considered as the environmental friendly substitute of fossil-based plastics (Calabrò & Grosso, 2018), and their production rate is foreseen to increase in the coming years. Manufacturing of plastics using biogenic resources could reduce greenhouse gas emissions by up to 225% compared to conventional plastics (Benavides et al., 2020). Therefore, defining sustainable end-of-life routes for these materials constitutes a matter of outmost importance. Biological recycling is considered as the most favourable option for a range of popular bioplastics such as thermoplastic starch (TPS) and polyhydroxybutyrate (PHB). The current study presents preliminary findings relevant to the application of microalgal-microbial co-cultures for PHB and TPS biodegradation.

Materials and methods

Batch experiments were performed in shake flasks under mesophilic conditions employing bioplastic pellets and films as carbon source, while an acclimated microbial community was inoculated. Optimisation methods included *Chlorella vulgaris* co-cultures conducted under 12h:12h light-dark cycles. Physicochemical modifications of the biopolymer along with shifts in the microbial community composition were monitored to understand the underlying mechanisms that controlled the biodegradation process.

Results and discussion

TPS removal experiments resulted in 14.8% ± 0.3 weight reduction following 10 d of incubation using pellets, while films demonstrated higher reduction that reached slightly over 30% at 15 d. Evidence is provided demonstrating that the biodegradation of TPS pellets/ films displayed a two-phase pattern with different degradation rates, where biodegradation in the first phase was high and decelerated in the second phase reaching a plateau. Specific bacterial families were dominant in the attached communities depending on biofilm formation and degradation stages. The genera *Microbacterium* and *Achromobacter* played important roles in the biofilm of TPS pellets, while *Bacillus* was dominant in films. The genera *Fusarium* and *Neocosmospora* displayed the highest abundance in all fungal assemblages.

Addition of the microalgae in the co-culture slightly increased TPS biodegradation from 18.6 % to 21.4%. Co-cultures conducted using PHB further improved the biodegradation process given that weight reduction increased from 25% to 33.4%. Control biodegradation experiments conducted using only the microalgae exhibited that although 4.7% TPS weight reduction could be achieved by *C. vulgaris*, the microalgae could not biodegrade PHB. This study highlights the potential of the microbial community to be exploited for the development of TPS and PHB waste treatment technologies.

Conclusions

The results demonstrated the significant potential for TPS waste treatment in an industrial environment compared to composting and anaerobic digestion. The bioprocess displayed a two-phase pattern incorporating different biodegradation rates, which remained high in the first phase (pellets: 5.8 mg d^{-1} degradation rate) and decelerated (pellets: 0.2 mg d^{-1} degradation rate) in the second phase. Additionally, higher weight reduction was observed in TPS films compared to pellets. Distinct bacterial assemblages were formed in the TPS biodegradation process. In contrast, PHB microbial degradation reached a steady weight reduction rate. Notably, *C. vulgaris* enhanced weight reduction in both TPS and PHB pellets.

Acknowledgements: The support from the Horizon 2020 Framework Programme H2020 – MSCA/ERA-IF-Postdoctoral Fellowships - 2021 under REA grant agreement n°101065005 is highly appreciated.

References

Calabrò, P.S., Grosso, M., 2018. Bioplastics and waste management. *Waste Manag*. 78, 800–801.

Benavides, P.T., Lee, U., Zare-Mehrjerdi, O., 2020. Life cycle greenhouse gas emissions and energy use of polylactic acid , bio-derived polyethylene , and fossil-derived polyethylene. *J. Clean. Prod*. 277, 124010.

A Critical Examination of Macroalgae Biomass Utilization: Perspectives from Life Cycle Assessments

C. Nikoloudakis[1], A. Pantis[1], and T. Tsoutsos[1]

[1] Renewable and Sustainable Energy Systems Laboratory, School of Chemical and Environmental Engineering, Technical University of Crete, Chania, Greece
Corresponding author email: ttsoutsos@tuc.gr

keywords: *macroalgae; biorefinery; life cycle assessment; SWOT*

Introduction

Recent studies have been exploring the use of macroalgae biomass within the Blue Economy framework, leading to the creation of products for sectors such as energy, food, agriculture, pharmaceuticals, and chemicals [1]. These innovations contribute to multiple United Nations Sustainable Development Goals outlined in the 2030 Agenda for Sustainable Development. The European Union's aquaculture policies promote the cultivation of macroalgae as a strategy to combat climate change, in line with the European Green Deal, and advocate for the use of Life Cycle Assessment (LCA) techniques to improve overall system efficiency [2]. One of the current challenges faced by this industry is the large volumes of residual by-products, which are typically repurposed as fertilizers or disposed of in soil. This study aims to illuminate the existing practices for adding value to macroalgae, with a focus on the intermediary steps and end products, while also emphasizing the energy-intensive areas previously identified in LCA studies of various processes.

Materials and methods

The study involved a comprehensive review of literature that detailed the various methods of macroalgae valorization, including a Life Cycle Assessment (LCA) of the biorefinery systems in question. It was conducted using the Scopus database, covering the years 2014 to 2024. The initial query, based on specific criteria such as LCA, yielded 123 articles. These were then filtered to align with the main goal of the review, eliminating those without a clear depiction of the biorefinery system being evaluated. This refinement process narrowed the field to 23 relevant publications.

Conducting an LCA on biorefinery systems enables the industry to pinpoint environmental 'hotspots'—stages in the process that consume significant energy amounts, like biomass drying using electricity or the fossil fuels heavy use in farming and harvesting. Addressing these energy-intensive areas and lessening the environmental footprint of macroalgae biorefineries are crucial towards a sustainable production model. Additionally, further research may uncover new ways to optimize key processes and enhance product output [3].

Furthermore, the pathways under study were subjected to a SWOT analysis to evaluate the present state of macroalgae use in biorefineries and to bring attention to existing challenges. By identifying internal strengths and weaknesses, as well as external opportunities and threats, a SWOT analysis aids industries in setting achievable objectives and developing effective strategies to advance their biorefinery operations.

Results and discussion

The bioethanol production from macroalgae encompasses essential steps like hydrolysis, fermentation, and distillation. Typical preliminary treatments involve the drying and mincing of the wet biomass. Recovery of ethanol and other heavier alcohols is achieved through hydrolysis and fermentation, or alternatively, by combining partial anaerobic digestion with hydrogenation. The resultant solid waste from these processes can be repurposed as fertilizer or animal feed. Life Cycle Assessment (LCA) studies suggest that macroalgae-based bioethanol is a more environmentally friendly alternative to traditional gasoline [4],[5].

For biogas production, six different methods were examined, all employing anaerobic digestion. The produced biogas powers combined heat and power (CHP) systems to generate electricity, with the steam from turbines also warming the feed for the anaerobic digesters. Some approaches have adopted a zero-waste philosophy, making use of the leftover materials from alginate extraction and production. These practices

underscore the feasibility of sustainable energy generation from macroalgae, which carries environmental advantages like the reduction of climate change effects and marine eutrophication [6]. Nevertheless, to overcome challenges such as the presence of phenols, heavy metals, salts, sulfides, and volatile acids that can hinder methanogenesis, enhancements in the pretreatment and harvesting of macroalgae are necessary [7].

Additionally, macroalgae-derived products for human and animal nutrition hold significant value. These production methods generally involve chopping, dehydrating, drying, fermenting, pasteurizing, and other hydrothermal treatments. An acidic pretreatment might be required before enzymatic hydrolysis to decompose cellulose. As a result, high-value protein supplements are generated, either as main products or by-products. Macroalgae biorefineries stand as a lucrative prospect in the market for high-value oils, bolstering the expansion of the Blue Economy. LCA reviews point out that these production chains positively impact climate change mitigation and address marine eutrophication. However, to further diminish the environmental footprint, there's a call for improved efficiency in the drying processes [8].

Conclusions

While macroalgae holds promise for generating high-value products, aiding in carbon capture, and flourishing in extreme environments, it also presents considerable obstacles. These hurdles include the demanding labor required for harvesting, fluctuating biomass availability, underdeveloped technology, and a lack of understanding regarding large-scale operations. Moreover, life cycle assessments (LCAs) are often plagued by significant uncertainties. To harness the burgeoning interest in macroalgae within the Blue Circular Bioeconomy, it's crucial to address these challenges. The implementation of supportive policies, cultivation of a knowledgeable workforce, and execution of thorough environmental impact assessments are imperative to surmount the barriers of high expenses, geographical constraints, and stringent regulations. Such measures will pave the way for macroalgae to fulfill its potential in diminishing pollution and fostering sustainable development.

Acknowledgements: *The results and the research methodology presented in this paper are part of the Horizon Europe program "iCULTURE" (contract number 101082010). The sole responsibility for the content of this publication lies with the authors. It does not necessarily reflect the opinion of the European Union. Neither the REA nor the European Commission is responsible for any use that may be made of the information contained therein.*

References

1. Hossain, M. A., Islam, M. N., Fatima, S., Kibria, M. G., Ullah, E., & Hossain, M. E. (2024). Pathway toward sustainable blue economy: Consideration of greenhouse gas emissions, trade, and economic growth in 25 nations bordering the Indian ocean. *Journal of Cleaner Production*, *437*, 140708. https://doi.org/10.1016/j.jclepro.2024.140708
2. European Commission (2021). *Strategic guidelines for a more sustainable and competitive EU aquaculture for the period 2021 to 2030*, COM/2021/236 final.
3. Pravin, R., Baskar, G., Rokhum, S. L., & Pugazhendhi, A. (2023). Comprehensive assessment of biorefinery potential for biofuels production from macroalgal biomass: Towards a sustainable circular bioeconomy and greener future. Chemosphere, 339, 139724. https://doi.org/10.1016/j.chemosphere.2023.139724
4. Foteinis, S., Antoniadis, A. G., Tsoutsos, T. (2018). Life cycle assessment of algae-to-biodiesel shallow pond production systems in the Mediterranean: influence of species, pond type, by-product valorisation and electricity mix, *Biofuels, Bioproducts & Biorefining*, 12(4), July/August 2018, pp 542-558
https://doi.org/10.1002/bbb.1871
5. Fasahati, P., Dickson, R., Saffron, C., Woo, H., & Liu, J. J. (2022). Seaweeds as a sustainable source of bioenergy: Techno-economic and life cycle analyses of its biochemical conversion pathways. Renewable & Sustainable Energy Reviews, 157, 112011. https://doi.org/10.1016/j.rser.2021.112011
6. Nilsson, A. E., Bergman, K., Barrio, L. P. G., Cabral, E. M., & Tiwari, B. K. (2022). Life cycle assessment of a seaweed-based biorefinery concept for production of food, materials, and energy. Algal Research, 65, 102725. https://doi.org/10.1016/j.algal.2022.102725
7. Seghetta, M., Romeo, D., D'Este, M., Alvarado-Morales, M., Angelidaki, I., Bastianoni, S., & Thomsen, M. (2017). Seaweed as innovative feedstock for energy and feed – Evaluating the impacts through a Life Cycle Assessment. Journal of Cleaner Production, 150, 1–15. https://doi.org/10.1016/j.jclepro.2017.02.022
8. Zhang, X., & Thomsen, M. (2021). Techno-economic and environmental assessment of novel biorefinery designs for sequential extraction of high-value biomolecules from brown macroalgae Laminaria digitata, Fucus vesiculosus, and Saccharina latissima. Algal Research, 60, 102499. https://doi.org/10.1016/j.algal.2021.102499

Session 5: Material science

The Green Synthesis of Irregular Gold Nanoparticles and Their Application in Nanomedicine

R. Mariychuk[1], R. Smolkova[1], L.M. Grishchenko[2], and V.V. Lisnyak[3]

[1]Department of Ecology/Faculty of Humanities and Natural Sciences, University of Presov, Presov, Slovakia
[23]Department of Physical Chemistry/Faculty of Chemistry, Taras Shevchenko National University of Kyiv, Kyiv, Ukraine
[3]Department of Analytical Chemistry/Faculty of Chemistry, Taras Shevchenko National University of Kyiv, Kyiv, Ukraine

Corresponding author email: ruslan.mariychuk@unipo.sk

keywords: *phytosynthesis; biocompatibility; irregular shape; plasmonic photothermal therapy.*

Introduction

The impressive development and application of nanomaterials in different areas has been noticed due to their unique physical and chemical properties in recent decades. Nanoparticles (NPs) have been observed to be prospective for applications in many fields, such as electronics, optics, catalysis, water treatment, agriculture, food science, pharmacy, and medicine. Such interest has initiated the rapid development of various synthesis methods. Modern chemistry can offer numerous trustworthy protocols for the synthesis of NPs using various reducing and capping agents, including biochemicals, i.e., chemical compounds from natural sources (plants, microorganisms, or fungi). This group of methods received the name “green method” due to their low toxicity of reactants and products, simplicity, cost-efficiency, and energy efficiency [1].

The ability of conducting NPs to absorb light due to surface plasmon resonance (SPR) has generated many applications, such as biomedicine and biosensing. Optical properties depend not only on the size of NPs but also on their shape. If regular (spherical) Au NPs absorb the radiation in the visible range (520–540 nm), for irregularly shaped nanotriangles, nanohexagons, nanostars, etc., the SPR maximum shifts to a near-infrared (NIR) range (>700 nm). This makes Au NPs prospective for use as photothermal and drug delivery agents [2].

Irregularly shaped (spherical, hexagonal, and nanotriangle) Au NPs were synthesized using various plant extracts: leaves of *Solidago canadensis* [3], and *Mentha piperita* [4], fruits of *Sambucus nigra* [5], etc. However, the development of trustable and reproducible protocols for the phytosynthesis of irregular Au NPs is complicated due to the complexity of the chemical composition of plant extracts. This problem can be solved using isolated phytochemicals, preferably major components of medicinal plants (polyphenols and sugars).

Therefore, this report is dedicated to a review of available publications and our own experiments in the synthesis of irregularly shaped Au NPs with responses in the NIR range using extracts of selected plants and isolated phytochemicals.

Materials and methods

Peppermint leaf and elderberry fruit extracts were prepared using previously published procedures [4] and [5], respectively. Namely, phytochemically mediated AuNPs were prepared by direct interaction of aqueous solutions: 0.5 mg/mL extracts and gallic acid and 1 mM $HAuCl_4$ with continuous stirring using a magnetic bar.

The characterization of AuNP nanocolloid solutions was carried out through UV-Vis spectroscopy using a Shimadzu UV-1800 spectrophotometer (Japan). The morphology analysis of Au NPs was conducted via transmission electron microscopy (TEM) using a JEOL JEM-2100F instrument.

The photothermal effects of nanocolloid solutions were studied using infrared lasers provided by Laserland and Jolooyo, China, with λ_{ex} of 808 and 850 nm with powers of 500 and 1000 mW, respectively, and the temperature changes were measured using an infrared thermometer (MLX90614, Melexis, Belgium). The stability of the nanocolloid solutions was followed by three heating-cooling cycles.

Results and discussion

Three samples of Au NPs were obtained using extracts of elderberry fruits, peppermint extract, and gallic acid as representative polyphenolic compounds identified in many plant extracts. It was observed that the optical

properties of nanocolloid solutions depend on the nature of the composition of phytochemicals (Fig. 1) and the shape of the NPs. Thus, NPs mediated in elderberry extract show an absorbance of 530 nm, typical for spherical Au NPs. Using peppermint extract led to the formation of NPs with absorption both at 530 and 1050 nm. TEM shows the presence of regular spherical and triangular NPs. Gallic acid-mediated Au NPs show the broad absorbance maximum at 620 nm that is produced by urchin-shaped Au NPs.

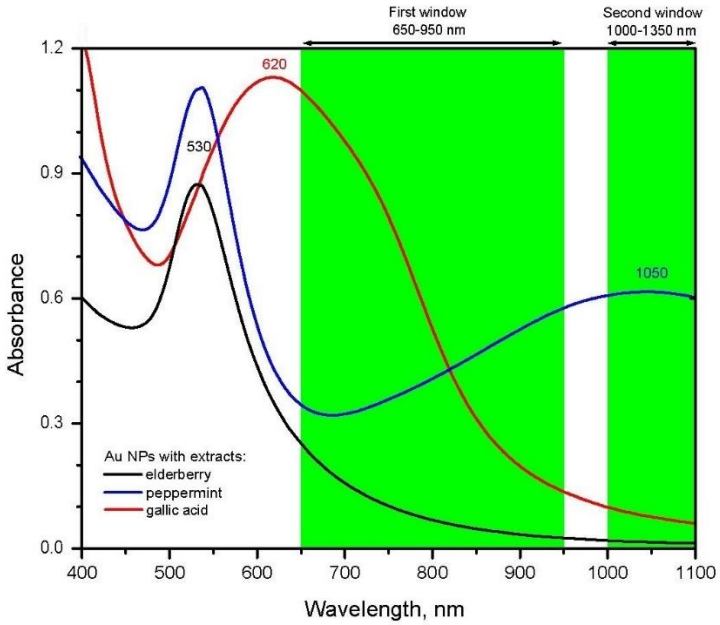

Figure 1. *UV-Vis spectra of different-shaped Au NPs were prepared using aqueous plant extracts: elderberry berries (black), peppermint leaves (blue), and gallic acid (red).*

Since the main point of interest was the obtaining of NPs with responses in the NIR range, peppermint-mediated NPs were tested by irradiation with lasers of different wavelengths within the above-mentioned bio-optical windows (Fig. 1). The samples showed a stable and consistent photothermal response without any photodegradation when irradiated with 808 and 850 nm lasers with DT in the range of 5 to 11 °C.

Conclusions

In this review, we presented the recent achievements in the green synthesis of Au NPs, with particular focus on obtaining irregularly shaped NPs with a response to the NIR range. In several examples, we have shown that the size and shape, which means control over optical properties, of Au NPs can be tuned by the selection of phytochemicals and synthesis conditions. Obtained Au NPs solutions exhibited reliable photothermal responses when exposed to lasers at 808, and 850 nm. Au NPs represent a promising option for bioimaging or hyperthermic applications due to their advantageous optical properties and potential for biocompatibility.

Acknowledgements: This study is supported by the Slovak Research and Development Agency under the project APVV SK-PL-23-0032: “Microbial response to phytosynthesized metal nanoparticles”.

References

1. Poudel, D.K. et al., 2022. Plant-Mediated Green Synthesis of Ag NPs and Their Possible Applications: A Critical Review. *J. Nanotech.*, 2022, 2779237.
2. Malekzadeh, R. et al., 2023. Nanoarchitecture-based photothermal ablation of cancer: A systematic review. *Envir. Res.*, 236, 116526.
3. Mariychuk, R. et al. 2020. Green synthesis of non-spherical gold nanoparticles using *Solidago canadensis* L. extract. *Appl. Nanosci*. 10, 4817–4826.
4. Mariychuk, R. et al., 2020. Green synthesis of stable nanocolloids of monodisperse silver and gold nanoparticles using natural polyphenols from fruits of *Sambucus nigra* L. *Appl. Nanosci*., 10, 4545–4558.
5. Mariychuk, R. et al., 2022. The regularities of the *Mentha piperita* L. extract mediated synthesis of gold nanoparticles with a response in the infrared range. *Appl. Nanosci*., 12 (4), 1071–1083.

Innovative bioprocess employing recyclable immobilized enzyme for paraoxon removal in water and effluents: Phosphotriesterase immobilized on Fe_3O_4-SiO_2-NH_2 magnetic nanocomposites

Sara Azerrad [1, 2], Shilat Parsha[1]

[1] Shamir Research Institute, P.O Box 97, 1290000 Katzrin, Israel
[2] The Natural Resources and Environmental Research Center-NRERC, University of Haifa, Mount Carmel, 3498838 Haifa, Israel
Corresponding author email: saraa@gri.org.il

keywords: *magnetic nanoparticles, nanocomposites, pesticides, water treatment, water reuse*

Introduction

Pesticides are widely used in agriculture to increase crop production as well as to reduced insect-borne diseases. It has been reported that around 2 million tons of pesticides have been used annually worldwide (Sharma et al. 2019). The wide use of pesticides represents some challenges since they can be widespread in the environment contaminating different water sources such as groundwater, surface water due to runoff and leaching from agricultural fields. Furthermore, the urban use of pesticides mainly in-house gardening for pest control is an important source of pesticide contamination in water (Syafrudin et al. 2021, Torres-Palma and Serna-Galvis 2018). In this research, it was developed a biocatalysis process for the comprehensive removal of paraoxon (pesticide model compound) from water and effluents. The enzyme phosphotriesterase (PTE) was immobilized onto Fe_3O_4-SiO_2-NH_2 nanocomposites (MNCs) to create a reusable biocatalyst. Paraoxon removal, enzyme activity, biocatalyst stability, reusability parameters were evaluated.

Materials and methods

Magnetite nanoparticles were synthesized via chemical co-precipitation using $FeCl_2$ and $FeCl_3$ as precursor salts. To ensure stability and prevent chemical degradation, a silica (SiO_2) shell was applied to the magnetite nanoparticles. The silica coating was achieved by adding tetraethyl orthosilicate (TEOS) and ammonium hydroxide (NH_4OH). Subsequently, the Fe_3O_4-SiO_2 nanoparticles were functionalized with amino groups using 3-aminopropyltriethoxysilane (APTES) to facilitate enzyme immobilization. The enzyme, PTE, was covalently attached to the nanoparticles using glutaraldehyde as a cross-linker as illustrated in Figure 1.

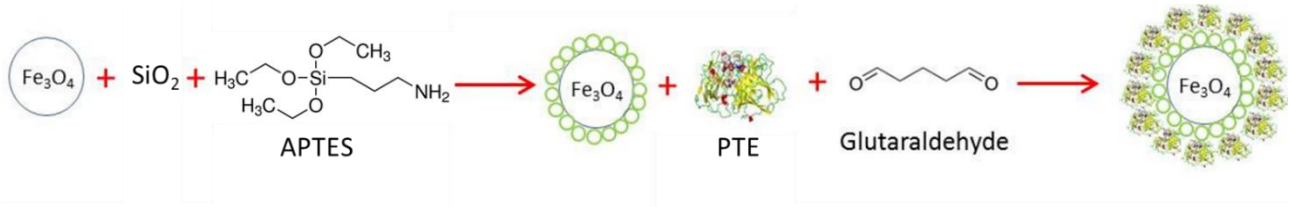

Figure 1. Schematic representation of the immobilization process

Experiments were performed in batch using buffer phosphate (50 mM, pH 7) as well as secondary effluents. The performance of free and immobilized enzyme was compared. Samples were incubated at 25 °C on an orbital shaker (150 rpm), and aliquots were withdrawn at different time intervals. All experiments were conducted in triplicate to ensure reproducibility and reliability of the results.

Results and discussion

The results demonstrate effective paraoxon removal by PTE enzyme immobilized onto Fe_3O_4-SiO_2 nanoparticles in buffer phosphate solution. After a 15-minute treatment, immobilized enzyme achieved higher removal efficiencies compared to free enzyme (98.1% vs. 95.6%, respectively) as presented in Fig.2. Importantly, while free enzyme activity decreased by 34%, immobilized enzyme activity remained stable, indicating enhanced enzymatic stability on the nanocomposite surface. The reduction in paraoxon

concentration corresponded with an increase in p-nitrophenol formation, consistent with the hydrolysis mechanism of paraoxon catalyzed by PTE (Zhang et al., 2009).

Initial assessment of enzyme reusability in buffer phosphate revealed consistent paraoxon removal efficiencies exceeding 99% across three cycles. Although enzymatic activity decreased modestly by 10% after repeated use, the immobilized enzyme maintained high stability and efficacy. Similar results were observed in secondary effluent tests, highlighting sustained enzyme stability and efficient paraoxon removal over multiple cycles.

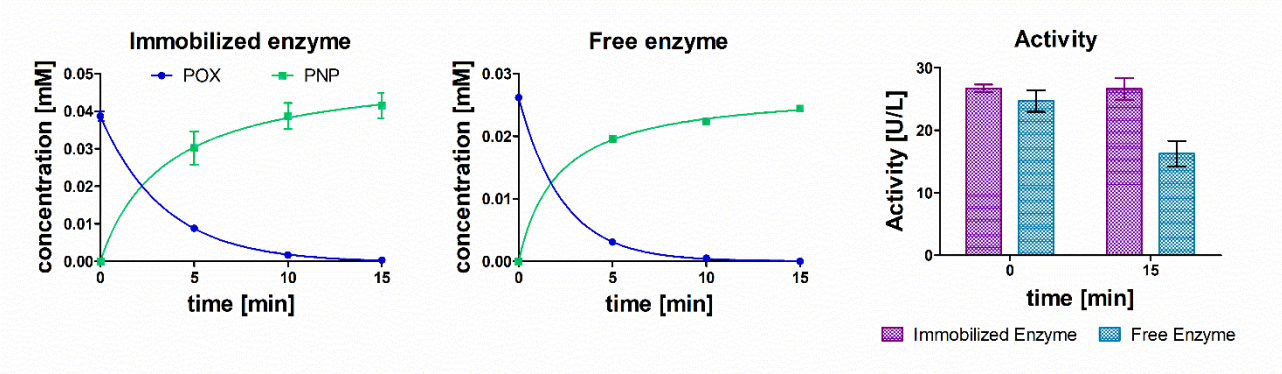

Figure 2. Paraoxon removal by PTE enzyme immobilized onto MNCs in buffer phosphate. PTE concentration: 24.7± 1.7 U/L (free enzyme) and 26.7±0.6 U/L (immobilized enzyme). POX concentration: 10 mg/L. POX: paraoxon, PNP: p-nitrophenol

Experiments performed in humic acid (2 mg/L as TOC) and sodium chloride solutions (600 mg/L) showed a notoriously inhibitory effect of chlorides on free PTE enzyme, after 22h incubation the enzyme was completely deactivated. However, immobilized enzyme maintained 80% of its residual activity after 22 h. Humic acid exhibited a lower effect in enzyme deactivation, ~ 40% residual PTE activity was obtained for free enzyme whereas for immobilized PTE ~80% residual activity was maintained after 22h incubation. Our results clearly indicate that immobilized PTE onto MNCs possess an enhanced stability to water solution components than free enzyme even at less favorable conditions.

Conclusions

The immobilization of PTE onto these nanoparticles demonstrated high enzyme loading efficiency (85%) and stability, crucial for enzymatic catalysis in the hydrolysis of paraoxon.

In buffer phosphate and secondary effluents, immobilized PTE showed superior stability over free enzyme, maintaining its activity. This stability led to consistent paraoxon removal efficiencies exceeding 95% and significant reusability for at least four cycles without substantial loss of activity.

Overall, the results highlight the potential of Fe_3O_4-SiO_2-NH_3 magnetic nanoparticles as efficient carriers for PTE immobilization, offering robust enzymatic performance suitable for practical applications in water treatment and environmental remediation.

Acknowledgements: This study is supported by the Israeli Ministry of Science and Technology, Research number 3-16807.

References

Sharma, A., Kumar, V., Shahzad, B., Tanveer, M., Sidhu, G.P.S., Handa, N., Kohli, S.K., Yadav, P., Bali, A.S., Parihar, R.D., Dar, O.I., Singh, K., Jasrotia, S., Bakshi, P., Ramakrishnan, M., Kumar, S., Bhardwaj, R. and Thukral, A.K. (2019) Worldwide pesticide usage and its impacts on ecosystem. SN Applied Sciences 1(11), 1446.

Syafrudin, M., Kristanti, R.A., Yuniarto, A., Hadibarata, T., Rhee, J., Al-Onazi, W.A., Algarni, T.S., Almarri, A.H. and Al-Mohaimeed, A.M. (2021) Pesticides in Drinking Water-A Review. International journal of environmental research and public health 18(2), 468.

Zhang, X., Wu, R., Song, L., Lin, Y., Lin, M., Cao, Z., Wu, W. and Mo, Y. (2009) Molecular dynamics simulations of the detoxification of paraoxon catalyzed by phosphotriesterase. Journal of computational chemistry 30(15), 2388-2401.

2D Xenes of Group-14: New synthetic strategies and derivatives for environmental and energy applications

Dimitrios P. Gournis[1]

[1]School of Chemical and Environmental Engineering, Technical University of Crete (TUC)& Institute of GeoEnergy, Foundation for Research and Technology - Hellas (FORTH) GR-73100, Chania, Crete, Greece
e-mail: dgournis@tuc.gr

Abstract

Much of the research effort on 2D materials focuses on its use as building block for the development of novel hybrid structures with well-defined dimensions and behavior suitable for applications among else in gas storage, heterogeneous catalysis, gas/liquid separations, nanosensing and biology. Towards this aim, tailored *nanostructured materials* (including pillared layered structures) based on *2D Xenes of group-14 such as germanane (GeH),*[1-6] *silicane (siloxane)*,[7] *stanane*,[8] and various *graphene-based matrices* (graphene, graphene oxide and graphite nitrate)[9-18] with high surface area, tunable pore size and functionalities have been synthesized and studied by using top-down (bulk synthesis) and bottom-up (by combining the Langmuir-Schaefer and the self-assembly techniques) synthetic approaches. Hybrid materials were characterized by a combination of analytical techniques. Representative case studies addressing cutting edge processes of great importance in environment and energy such as the use of these hybrid nanostructures as catalysts, phase change materials, cytotoxic agents, effective adsorbents for environmental remediation, and gas (H_2 and CO_2) storage materials will be discussed.

References

1. T. Giousis, G. Potsi, A. Kouloumpis, et al.. *Angew. Chem.- Inter. Ed.,* **2021**, *60*, 360.
2. Q. Chen, L. Liang, G. Potsi, et al. *Nano Letters,* **2019**, *19*, 1520.
3. A. Kouloumpis, A. V. Chatzikonstantinou, N. Chalmpes, et al. *ACS Appl. Nano Mater.,* **2021**, *4*, 2333
4. B. N. Madhushankar, A. Kaverzin, T. Giousis, et al. *2D Materials* **2017,** *4*, 021009
5. T. Giousis, S. Fang, M. Miola, et. al. *J. Environm. Chem. Engineer*. **2023**, *11*, 109784
6. T. Giousis, P. Zygouri, N. Karouta, et al. *Small* **2024**, https://doi.org/10.1002/smll.202403277
7. A. Kouloumpis, G. Potsi, T. Giousis, et al. *Solid State Phenom*. **2022**, *336*, 63
8. A. Vaso, E. Tengelidi, A. S. Kaloudi et al. *Chem. Mater*. **2024** subm.
9. E. Thomou, V. Sakavitsi, G. K. Angeli, et al. *RSC Advances,* **2021**, *11*, 13743
10. K. Spyrou, L. Kang, E.K. Diamanti, et al. *Carbon*, **2013**, *61*, 313.
11. T. Tsoufis, G. Tuci, S. Caporali, et al. *Carbon*, **2013**, *59*, 100.
12. K. Spyrou, G. Potsi, E.K. Diamanti, et al. *Adv. Funct. Mater.*, **2014**, *24*, 5841.
13. K. Spyrou, M. Calvaresi, E.A.K. Diamanti, et al. *Adv. Funct. Mater.*, **2015**, *25*, 263.
14. T. Tsoufis, Z. Syrgiannis, N. Akhtar, et al. *Nanoscale*, **2015**, *7*, 8995.
15. V. Georgakilas, A. Demeslis, E. Ntararas et al. *Adv. Funct. Mater.*, **2015**, *25*, 1481.
16. A. Kouloumpis, K. Spyrou, K. Dimos et al. *Front. Mater.*, **2015**, *2*, art. 10.
17. N. Chalmpes, M. Patila, A. Kouloumpis et al. *ACS Appl. Mater. Interfac*. **2022**, *14*, 26204.
18. F. Yan, E.M. Alfinsin, P. Ngene, et al. *Nanoscale* **2024**, https://doi.org/10.1039/D4NR01524J

session

Session 6: Water resources management

From Data to Decision: Understanding and Mitigating Uncertainty in Watershed Water Quality Models

A. Gorgoglione[1]

[1]Department of Fluid Mechanics and Environmental Engineering, School of Engineering, Universidad de la República, Montevideo, Uruguay
Corresponding author email: agorgoglione@fing.edu.uy

keywords: *uncertainty; water quality; modeling; watershed.*

Introduction

Water quality models are essential tools for understanding, managing, and predicting the impacts of various factors on the quality of water within a watershed (Russo et al., 2023). These models play a crucial role in environmental management, informing policies and decisions related to water resources, pollution control, and ecosystem conservation. However, the accuracy and reliability of these models are often challenged by various sources of uncertainty, which can significantly affect their predictive capabilities and confidence in their outputs (Gorgoglione et al., 2019).

The objective of this paper is to identify and analyze the sources of uncertainty in water quality models at the watershed scale. By doing so, we aim to provide a comprehensive understanding of the factors that contribute to uncertainty and offer insights into how these uncertainties can be managed or mitigated. Understanding these uncertainties is critical for improving model performance, enhancing decision-making, and ultimately achieving better outcomes for water resource management.

Sources of Uncertainty

Model Structure Uncertainty

Conceptual Models: Model structure uncertainty arises from the conceptualization of the processes within the watershed. Different models may conceptualize hydrological and biogeochemical processes in various ways, leading to differences in model structure. For instance, some models may represent nutrient cycling with a higher level of detail, while others might simplify these processes. These differences can result in varying outputs and predictions.

Model Simplifications: Simplifications and assumptions made during model development contribute significantly to structural uncertainty. For example, assumptions about homogeneous soil properties or uniform land use within a watershed can simplify the modeling process but may not accurately reflect the true variability present in the natural environment. These simplifications can lead to discrepancies between modeled and actual water quality.

Input Data Uncertainty

Data Quality: The quality of input data is a major source of uncertainty. Input data such as precipitation, temperature, soil characteristics, and land use are often subject to measurement errors, gaps, and inaccuracies. Poor quality or incomplete data can lead to significant deviations in model outputs.

Spatial and Temporal Resolution: The spatial and temporal resolution of input data also plays a critical role in determining model accuracy. High-resolution data can capture more detailed variations within the watershed, but such data are often unavailable or impractical to obtain. Conversely, low-resolution data might overlook important local variations, introducing uncertainty into the model predictions.

Parameter Uncertainty

Parameter Estimation: Water quality models require numerous parameters, many of which cannot be directly measured and must be estimated. The process of parameter estimation introduces uncertainty due to the variability and limited availability of data. Different estimation techniques can yield different parameter values, affecting model outcomes.

Sensitivity Analysis: The sensitivity of model outputs to parameter changes is another important aspect of parameter uncertainty. Some parameters may have a greater influence on model results than others.

Conducting sensitivity analyses helps identify these critical parameters and understand how their uncertainty propagates through the model.

Calibration and Validation Uncertainty

Calibration Processes: Model calibration involves adjusting model parameters to match observed data. This process is inherently uncertain due to the limited availability and quality of observational data. Overfitting the model to specific datasets can also reduce its generalizability to other conditions.

Validation Techniques: Validation of water quality models is performed by comparing model outputs to independent observed data. The choice of validation techniques and datasets introduces uncertainty, as discrepancies between observed and modeled data can arise from various sources, including measurement errors and model limitations.

Model Boundary and Initial Conditions

Boundary Conditions: Defining model boundaries accurately is essential but challenging. Uncertainty arises when the boundaries of the watershed are not well-defined or when external inputs (e.g., upstream inflows) are not accurately characterized. Misrepresenting boundary conditions can lead to significant errors in model predictions.

Initial Conditions: Setting initial conditions for model simulations introduces uncertainty, especially when historical data are incomplete or not representative of the current state of the watershed. Incorrect initial conditions can propagate through the model, affecting long-term predictions.

External Factors

Climate Change: Climate change projections introduce significant uncertainty into water quality models. Changes in temperature, precipitation patterns, and extreme weather events can alter hydrological and biogeochemical processes in ways that are difficult to predict. Incorporating climate change scenarios into models is essential but adds another layer of uncertainty.

Land Use Changes: Land use and management practices within the watershed can change over time, influencing water quality. Predicting future land use changes and their impacts on water quality is fraught with uncertainty due to the complex interactions between human activities and natural processes.

Policy and Management Scenarios: Different policy and management scenarios, such as agricultural practices and conservation efforts, can have varying impacts on water quality. The uncertainty in predicting the outcomes of these scenarios stems from the complex and often nonlinear interactions between multiple factors.

Future Directions

Addressing the sources of uncertainty in water quality models requires a multifaceted approach. Future research should focus on developing models that better represent the complex processes within watersheds, thereby reducing structural uncertainty. This includes integrating advances in hydrological and biogeochemical sciences into model frameworks. Additionally, enhancing data collection methods through the use of remote sensing technologies, citizen science, and other innovative approaches can improve the quality and availability of input data. Employing advanced techniques such as machine learning for parameter estimation can better capture the variability and uncertainty of model parameters. Conducting comprehensive sensitivity and uncertainty analyses will provide deeper insights into the key drivers of model uncertainty and guide efforts to reduce it. Improving the accuracy of climate and land use change projections and incorporating them into models can enhance the ability to predict future water quality scenarios. Finally, encouraging interdisciplinary collaboration among hydrologists, ecologists, climate scientists, and policymakers is essential for developing more holistic and effective solutions for managing water quality under uncertainty.

References

Gorgoglione, A., Bombardelli, F.A., Pitton, B.J., Oki, L.R., Haver, D.L., Young, T.M., 2019. Uncertainty in the parameterization of sediment build-up and wash-off processes in the simulation of sediment transport in urban areas. *Environ. Model. Softw.,* 111, 170–181.

Russo, C., Castro, A., Gioia, A., Iacobellis, V., Gorgoglione, A., 2023. Improving the sediment and nutrient firstflush prediction and ranking its influencing factors: An integrated machine-learning framework. *Journal of Hydrology*, 616:128842.

Water Use and Efficiencies in Fuel Refining Sites

E. Vaiopoulou[1], E. Fiddaman[2], S. Gibbons[2], S. Mackay[2], J. Shaw[2], L. Leclezio[2], J. Russell[2], M. Hjort[1] and G. Guerrero-Limón[1]

[1]Concawe, Brussels, Belgium
[2]Environmental Resources Management, UK
Corresponding author email: WaterQuality@Concawe.eu

keywords: *water; reuse; efficiency; refinery; fuel.*

Introduction

Under the Industrial Emissions Directive (IED) (2010/75/EU), the European Commission is required to undertake a process of drawing up and reviewing Best Available Techniques (BAT) for relevant industry sectors. The European Environment Agency (EEA) reports that one third of European countries or associated river basins have a relatively low availability of water. Industry use remains the largest abstractor of water in Europe, with agriculture being the largest consumer. It is expected that precipitation will continue to change in future years, with an increase in mean annual precipitation in northern Europe and a decrease in southern Europe, along with prolonged periods of drought and episodes of more intense rainfall.

This work aims to describe current water use in EU refineries, establishing the refining water footprint, and examining alternatives practices which may help to reduce current and future stress on freshwater resources.

Materials and methods

A combination of desk-based literature reviews, data visualization techniques, member interviews, and digital surveys have been used to describe trends in water stress and scarcity in Europe up to 2030, evaluate available water stress tools, identify and define common water metrics, review Concawe member water data (2019), and collate information about members experience with water use, water efficiency techniques, and other related topics.

The desk-based literature review focused on the current thinking and planning within Europe to summarise the current and projected types of water stresses in Europe, magnitude of water stresses in Europe, and the geographical distribution of different types of water stresses. Secondly, a high-level evaluation of the strengths and weaknesses of the various water scarcity tools used in Europe and relevant global tools was also conducted. Finally, interviews were conducted with 6 refinery companies where it was discussed their experience with current, planned and considered, water reduction/efficiency practices and techniques, reasoning for adoption or abandonment of efficiency techniques, water metric terminologies, water metric targets and other reporting indices (e.g. intensity of water use), experience at operations with water stress, both existing and anticipated in the future, and key operational sensitivities.

Results and discussion

A matrix of definitions was created and cross-checked with members during the interviews and via the digital survey. It was found that while Concawe members often broadly follow the same definitions of water terminology, with many subscribing to the IPIECA definition of 'freshwater', there are variations which are often dependent on the local environment (source of water) and requirements. For many other water-related terms, members have no official internal definitions, and no industry wide standard exists. Also, interviewed sites reported that monitoring presented it set of challenges as flows are not well-monitored, there are tracking difficulties in regards the source of the wastewater.

Based on 2019 Concawe members' survey, the total intake volume for all refineries was 2,178,736 dam3. Of this, 464,479 dam3 was freshwater and 1,714,257 dam3 was salt/brackish water. Sites located in areas of extremely high water stress use a lower proportion of salt/brackish water than sites located in areas of high water stress. Once-Through Cooling Water is the highest use of water (64%) in refineries (Figure 1).

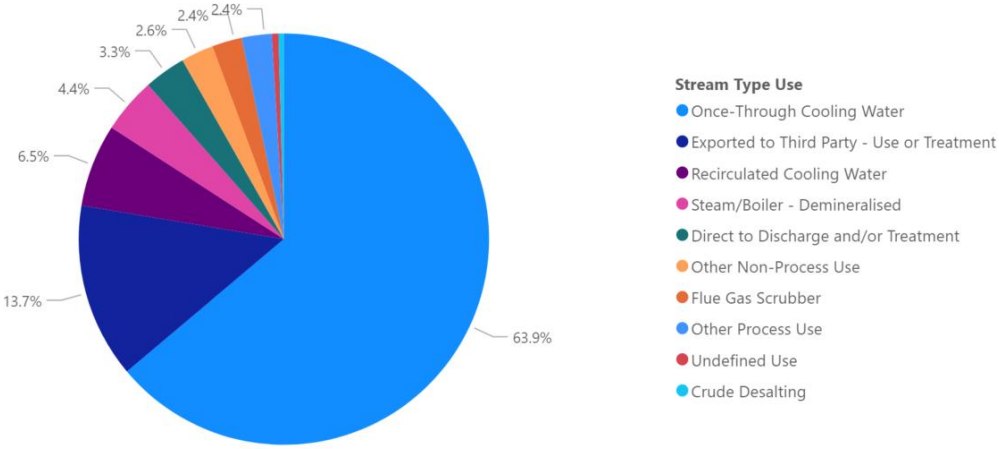

Figure 1. *Proportions of All Water Used based on 2019 Concawe members' survey.*

The study has investigated the potential vulnerability around water availability from both a climate change perspective by using Aqueduct 4.0 to consider the changing stresses across different parts of Europe and from regulatory pressures which may evolve around reducing freshwater consumption, increasing recycling and efficiency and increasing/improving the treatment methods for wastewater. Alongside the analysis of potential challenge, the study also considered the opportunities that exist with the survey revealing a wide range of existing business opportunities for sourcing grey water and improving efficiency at refineries.

Conclusions

The projected reduction in oil demand is expected to lead to an important reduction in water use. However, this review highlighted some potentially significant challenges – not least in the need to consider cross-media effects with increased efficiency leading to potentially greater power demands and a resulting concentrating effect in wastewater making permit adherence for discharges potentially more challenging.

References

Concawe (2022), *Definition Guidelines of Water Reuse, Recycling and Reclamation for European Refinery Sector.* Report No. 4/22. Brussels: Concawe

European Environment Agency, 2021b. Report No. 12/2021. *Water resources across Europe — confronting water stress: an updated assessment.* Luxembourg: Publications Office of the European Union, 2021

European Environment Agency, 2022. *Water abstraction by source and economic sector in Europe.* (europa.eu) accessed 15 November 2022.

IPIECA, 2014. *Efficiency in water use – guidance document for the upstream onshore oil and gas industry.* IPIECA October 2014

Medarac, H., Magagna, D. and Hidalgo González, I., 2018. P*rojected fresh water use from the European energy sector*, EUR 29438 EN, Publications Office of the European Union, Luxembourg, 2018.

Session 7: Soil management

Soil Improvement by Electro Carbonation Induced Calcite Precipitation (ECICP) from the Seawater

Hamed Abdeh Keykha[1], Maria Mavroulidou[1]*, Hadi Mohamadzadeh Romiani[2]

[1] Division of Civil and Building Services Engineering, BEA, London South Bank University, 103 Borough Road, London, SE1 0AA, UK
[2] Departments of Civil Engineering, Buein Zahra Technical University, Buein Zahra, Qazvin, Iran

Corresponding author email: mavroum@lsbu.ac.uk

Abstract

This paper explores the potential of using captured CO_2 to generate carbonates, towards the production of sustainable binders for soil stabilization. In this study, seawater was used in an electrokinetic process to produce sodium hydroxide, which reacted with CO_2 in the presence of Ca^{+2}, resulting in the precipitation of $CaCO_3$. A downward flow injection method was employed to introduce carbonate produced from CO_2 and calcium solutions into sand column specimens. Permeability and unconfined compressive strength (UCS) tests were conducted to evaluate the effectiveness of the method as soil stabiliser. Scanning electron microscope (SEM) images and energy dispersive X-ray spectroscopy (EDX) spectra confirmed the precipitation of calcite crystals in soil pores, thereby enhancing strength. This method has the potential of using captured industrial CO_2 to rapidly produce high concentrations of $CaCO_3$, which can potentially serve as a sustainable soil binder.

Keywords: Carbon dioxide, Electro-carbonation, Calcite, Soil stabilization.

Biocementation via microbial induced struvite precipitation: A mini review on cleaner method of soil stabilization

Sumit Joshi, Maria Mavroulidou* and Michael J Gunn

School of Build Environment and Architecture, London South Bank University, SE1 0AA, London, U.K
Corresponding author email: mavroum@lsbu.ac.uk
keywords: *biomineralization; struvite; ammonium; phosphate; soil improvement.*

Introduction

Biological mineralization is a widespread natural phenomenon, in which over sixty distinct biominerals of biogenic origin are produced. A novel and effective research method that draws inspiration from nature is microbially induced calcium carbonate precipitation (MICP). A wide range of MICP based engineering applications have been studied, including soil stabilisation, stone monument restoration and improving the durability properties of concrete. To date, ureolysis-based metabolic process of urease producing bacteria is the most widely used for rapid and controlled precipitation of calcium carbonate as a cementing agent. Despite the benefit of being a biomimetic and potentially sustainable process, the MICP process using enzymatic hydrolysis of urea generates ammonia (NH_4^+ (aq) & NH_3 (g)) posing threat to groundwater and ecosystems. To overcome this, a novel technique known as the microbial induced struvite precipitation (MISP) mechanism has recently been developed to manage the ammonium and ammonia byproducts. In MISP treatment, ammonium ions are utilized in the presence of magnesium and phosphate ions to precipitate bio-struvite minerals that have shown promise of providing effective cementation in construction materials and geotechnical applications. In this comprehensive review, bio-struvite through phosphate biomineralization is presented as an alternative and efficient breakthrough in ammonia free bio-cementation.

Struvite – Mechanism of precipitation

Struvite, is a white colored, orthorhombic crystalline mineral formed of Mg^{2+}, NH_4^+ and PO_4^{3-} ($MgNH_4PO_4{\cdot}6H_2O$) in equal molar concentrations. As the concentration of phosphates, magnesium, and ammonium exceeds the solubility product in an alkaline environment, struvite precipitation occurs (Hao et al, 2013). Struvite is the most ideal mineral obtained chemically or biologically usually from the wastewater treatment plants, showing the recovery of 51.8% of phosphates based on its chemical composition. The chemical equation of the formation of struvite is given below:

$$Mg^{2+} + NH_4^+ + PO_4^{3-} + 6H_2O \rightarrow MgNH_4PO_4.6H_2O$$

The method of biological struvite is proposed as a key route to recover phosphorous and ammonium from the waste water. It has the advantage of no pH-adjustment and recovering PO_4^{3-}/NH_4^+ even at low concentrations when compared with conventional chemical precipitation. A diverse range of microbial strains have been documented to modify solution chemistry (such as pH and NH_4^+) through their metabolic processes, hence fostering supersaturation conditions that lead to the formation of bio-struvite. In the next section, application of bio-struvite in geotechnical engineering is discussed.

Bio-struvite – Application in geotechnical engineering

In the field of soil biocementation, the potential of phosphate biomineralization generated by microbes has been demonstrated. Biogenic struvite minerals have advantages over ureolytic-based MICP as: (a) bio-struvite precipitation does not entail ammonium byproducts, (b) bio-struvite crystals have low solubility and (c) there is potential of using waste phosphorous resources to bioprecipitate struvite.

To improve the engineering properties of construction materials through MISP, different studies proposed by researchers are discussed below.

The use of *Sporoscarcina pasteurii* bacterial strain to biocement loose sand using microbially produced struvite was reported (Yu et al, 2016). Biocementation was carried out in a sand column using solutions comprising $MgCl_2$, urea, and $K_2HPO_4.3H_2O$ in varying concentrations. The microbial struvite precipitation led to a considerable decrease in ammonia and an increase in strength (1.59 MPa) in biocemented loose sand. The wind erosion of loose sand was reported to be significantly suppressed as a bio-struvite crust formed a

solidified layer on the sand. In a different study, spraying treatments with *Sporoscarcina pasteurii* and solutions comprising urea, $MgCl_2$, and $K_2HPO_4.3H_2O$, resulted into the suppression of desert sand following cementation with bio-struvite precipitation. Significant improvements in the mechanical properties and decreased porosity of biocemented desert sand were reported after three times of media spraying treatment (Yu et al, 2019a). An average wind speed of 12.0 m/s was used to measure wind erosion for the biocemented desert sand. The wind erosion rate of untreated desert sand was reported to be 798 g/m^2/h. However, after 3 spray treatment of media and *S. pasteurii* culture results into 0 g/m^2/h wind erosion rate of biocemented desert sand.

The optimization of bio-magnesium phosphates for the treatment of sand particles was also reported, in which a ratio of 1:2:2 for bio-carbonate cement: $MgCl_2$: $K_2HPO_4.3H_2O$, respectively was recommended (Yu et al, 2019b). In this study, a reduction in the average permeability and a strength gain of the sand cemented by bio-struvite was reported. This study also reported the fixation of 88% of ammonia into struvite crystals.

In another bio-struvite study, columns made of Ottawa sand were treated with the microbially induced struvite precipitation also employing the *S. pasteurii* strain (Yu et al, 2022). The bacterial culture was injected into a two-stage injection treatment in which a first cycle using 2M dipotassium hydrogen phosphate was followed by a second cycle using 1M urea and 2M magnesium chloride solution after 6 hours. Bio-struvite precipitation was found to be quicker, more effective in reducing specimen porosity, and needed less injection cycles when compared to microbially produced $CaCO_3$ precipitation.

The combined effects of a one-phase MICP treatment and a two-phase microbial struvite treatment were documented in a recent study on Ottawa sand columns (Yu and Yang, 2023). A grown culture of *S. pasteurii* containing a solution of urea and calcium chloride/calcium acetate at low pH 6 was introduced into the sand column during the MICP treatment. The collected effluent, referred to as the "biocementation waste solution," was utilized to create two distinct solutions of $K_2HPO_4.3H_2O$ and $MgCl_2$. The prepared solutions were then injected into the sand columns to induce struvite by bacteria. It has been reported that the struvite and calcium carbonate crystals effectively precipitated in the sand grains and greatly decreased the permeability of the biocemented sand.

Conclusions

Microbially induced struvite precipitation has emerged as a feasible and promising alternative to the ureolytic pathway of biocementation by calcite precipitation for geotechnical applications. The literature study indicates that MISP-based soil treatments are still in their infancy. Some encouraging results of bio-struvite precipitation during laboratory-scale studies have given rise to novel ideas about how to solve the geotechnical issues in an environmentally responsible and sustainable manner.

Acknowledgements: This paper is supported by the UKRI-funded MSCA-PF project "BIOPHILIC: BIOprecipitated PHosphates for Improved Low-carbon Innovative Cements" (EP/Y029615/1).

References

Hao, X., Wang, C., Van Loosdrecht, M. C., Hu, Y., 2013. Looking beyond struvite for P-recovery. *Environ. Sci. Technol.,* 47, 4965-4966.

Yu, X., Qian, C., Xue, B., 2016. Loose sand particles cemented by different bio-phosphate and carbonate composite cement. *Constr Build. Mater*., 113, 571-578.

Yu, X., Qian, C., Jiang, J., 2019a. Desert sand cemented by bio-magnesium ammonium phosphate cement and its microscopic properties. *Constr Build. Mater*., 200, 116-123.

Yu, X., Zhan, Q., Qian, C., Ma, J., Liang, Y. 2019b. The optimal formulation of bio-carbonate and bio-magnesium phosphate cement to reduce ammonia emission. *J. Clean. Prod*., 240, 118156.

Yu, X., Yang, H., Wang, H., 2022. A cleaner biocementation method of soil via microbially induced struvite precipitation: A experimental and numerical analysis. *J. Environ. Manage*., 316, 115280.

Yu, X., Yang, H., 2023. One-phase MICP and two-phase MISP composite cementation. *Constr Build. Mater*., 409, 133724.

PFAS Soil Treatment Processes – A Review of Operating Ranges and Constraints

J. Hurst[1], S. Hale[1], J. Miles[1], E. Dal[1], W. Gevaerts[2], J. Burdick[3], E. Vaiopoulou[4] and M. Hjort[4]

[1]Arcadis UK
[2]Arcadis Belgium
[3]Arcadis US
[4]Concawe
Corresponding author email: jake.hurst@arcadis.com

keywords: *PFAS (per- and polyfluoroalkyl substances); soil treatment technologies; firefighting foam; remediation; comparative evaluation*

Introduction

The wide use, e.g., in certain firefighting foams, as well as the unique and diverse properties of Per- and Polyfluoroalkyl Substances (PFAS) represent complexity and challenges for traditional soil remediation technologies. Thus, there is the need to identify robust, cost effective and sustainable options which are acceptable to all stakeholders.

A total of 13 treatment technologies have been systematically evaluated including destructive, non-destructive and pathway management approaches considering technical, operational and commercial factors as well as identify current knowledge gaps. The technologies were then further sub-divided into 'field deployed' and 'innovative' based on their approximate Technology Readiness Level as well as whether there are established/ plausible treatment mechanisms.

Materials and methods

The evaluation was informed by a literature review of published scientific research and other documents as well as a vendor liaison process incorporating current implementation experience and results. Relevant treatment scenarios, treatment trains and material types and treatment goals were also discussed and considered during the review.

The report was undertaken by a global team of Arcadis PFAS experts working closely with the Concawe Soil and Groundwater Taskforce.

Results and discussion

This presentation details the findings of this evaluation and aims consolidate current global practice to increase understanding and support soil experts and/ or practitioners to identify effective and resource-efficient soil treatment technologies for PFAS.

In summary, look-up tables were produced in order to easily compare the technologies per the following categories:

- Suitability to treatment scenarios
- Treatment efficacy vs. treatment goals
- Treatment efficacy for different PFAS
- Suitability to soil properties
- Suitability to co-contamination
- Potential impact on site operations
- Requirement for ongoing management
- Technology development / commercial availability
- Cost
- Durability and residual liability
- Sustainability / energy & chemical usage

The resulting look-up tables in conjunction with a report that details the findings of each technology will help both to identify suitable 'ready-to-use' technologies as well is to inform were additional research is needed in order to further advance brining innovative technologies into application. In addition, the depth and breadth of review has enabled overarching insights and conclusions to be developed.

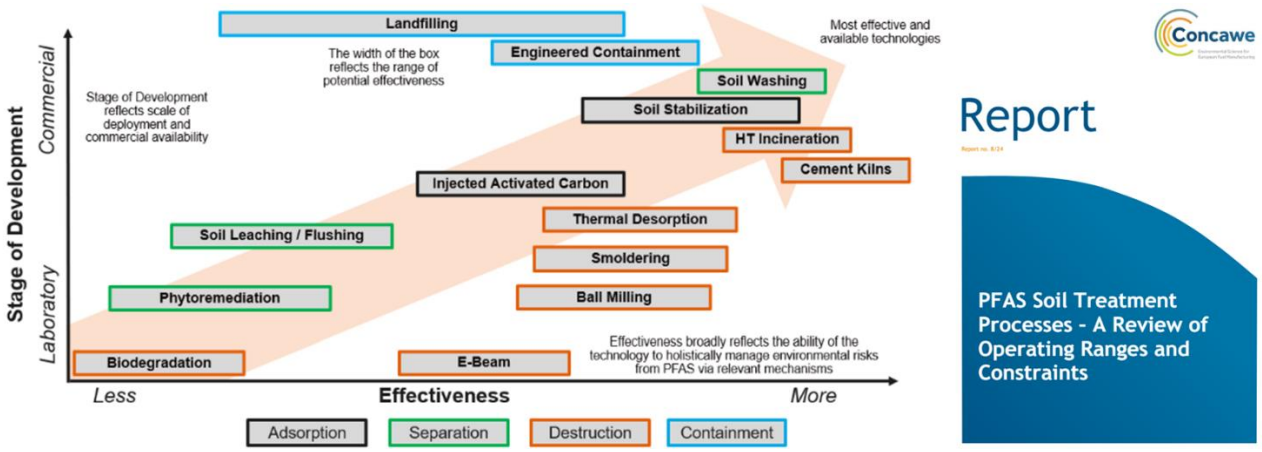

Conclusions

The conclusions highlight the need to accept and optimise existing soil treatment technologies with no 'game changing' technologies evident at least in the short term. There is a need to ensure remediation goals are achievable and sustainable and align with practical performance limits in real world applications and matrices. Data gaps are identified which speak to the need to holistically consider the types of PFAS present and the ultimate fate of PFAS within treatment by-products.

References

Concawe (2024), *PFAS Soil Treatment Processes – A Review of Operating Ranges and Constraints.* Report No. 8/24. Brussels: Concawe

Effects of fungicides and bactericides on BVOC emissions in Cypriot vineyard soils

Kyriaki Kaikiti[1], Savvas Savvides[3], Laurent Philippot[4], Ioannis M. Ioannides[2], Agapios Agapiou[1]*, Michalis Omirou[2]*

(1) Department of Chemistry, University of Cyprus, P.O.Box 20537, 1678 Nicosia, Cyprus,

agapiou.agapios@ucy.ac.cy

(2) Department of Agrobiotechnology, Agricultural Research Institute, P.O.Box 22016, Nicosia 1516, Cyprus

(3) Department of Fruit Trees, Agricultural Research Institute, P.O.Box 22016, Nicosia 1516, Cyprus

(4) Université Bourgogne Franche-Comté, INRAE, AgroSup Dijon, Agroécologie, Dijon, France

keywords: *soil BVOCs, vineyard soil, pesticide treatments, HS-SPME-GC-MS analysis*

Introduction

This study investigates the impact of different types of fungicides and bactericides on the emissions of biogenic volatile organic compounds (BVOCs) in vineyard soils. Soil samples were collected from three distinct wine-making regions in Cyprus, each with known variations in BVOC emissions. We aimed to explore how the application of these chemicals influences BVOC profiles and soil microbial communities. Previous research suggests that fungicides and bactericides can alter microbial dynamics, potentially affecting BVOC production and release. By comparing BVOC emissions before and after fungicides and bactericides application, we seek to understand the microbial responses in different type of chemicals. Previous research by Amelie et al. [1] demonstrated that fungicide application on plants did not significantly change the overall emission rates of BVOCs. However, a trend towards increased emissions was observed, particularly with fungicides. In contrast, bactericides showed minimal impact. It was also suggested that fungi might inhibit BVOC emissions by metabolizing these compounds or that the fungicide had potential adverse effects on plant emissions. Additionally, other studies [2] revealed that soil microbial communities play a crucial role in the production and consumption of BVOCs, influencing soil health and plant growth. Similarly, Peñuelas et al. [3] found that BVOCs are critical in plant-microbe interactions, with significant implications for ecosystem functions and agricultural practices.

This study explores the dynamics of BVOC emissions in vineyard soils subjected to different chemical treatments. Understanding these interactions is crucial for developing strategies that mitigate negative environmental impacts while promoting soil health and productivity.

Materials and methods

Soil samples from vineyards in three villages across Cyprus were subjected to different treatments to investigate the impact of BVOC emissions. The treatments included fungicide and bactericide applications. The cycloheximide (≥ 95%, Sigma-Aldrich, Switzerland) was used as the fungicide, while ampicillin (Merck, USA) and bacitracin (Sigma-Aldrich, Switzerland) were used as bactericides (antibiotic-1 and antibiotic-2, respectively). The BVOCs were analyzed using Headspace Solid-Phase Microextraction Gas Chromatography-Mass Spectrometry (HS-SPME-GC-MS), employing a 95 µm Carbon Wide Range/Polydimethylsiloxane (CWR/PDMS) smart SPME fiber and an Agilent GC 7890A/MS 5975C analytical system equipped with a PAL RSI 85 autosampler (CTC Analytics AG, Switzerland). This methodology allowed for the comprehensive assessment of how fungicides and bactericides influence BVOC emissions.

Results and discussion

In Soil 1, untreated samples resulted in 28 BVOCs with a total normalized area of 57.96. One day post-treatment, the fungicide-treated soil showed the highest increase, with 39 BVOCs and a total normalized area of 135.03, while bacitracin and ampicillin treatments had lower emissions. After 14 days, all treatments showed

a decrease in BVOCs and total normalized areas, with the fungicide treatment still maintaining the highest total normalized area of 44.14. For Soil 2, untreated samples emitted 29 BVOCs with a total normalized area of 85.00. After one day, ampicillin-treated soil showed the highest total area (122.23), followed by bacitracin (78.48) and fungicide (65.27). By 14 days, BVOC emissions significantly dropped across all treatments. Soil 3 initially had 10 BVOCs with a total area of 9.33. After one day post-treatment, all treated soils showed a significant increase, with fungicide-treated soil having the highest total area (92.02). After 14 days, BVOC emissions decreased notably in all treatments. These results suggest that fungicides and bactericides significantly affect BVOC emissions, initially increasing them but leading to a decline over time, supporting the hypothesis that fungicides and bactericides disturb the soil microbial community and change the BVOCs emissions from agricultural soils.

References

[1] A. Saunier, P. Mpamah, C. Biasi, J.D. Blande, Microorganisms in the phylloplane modulate the BVOC emissions of Brassica nigra leaves, Plant Signal. Behav. 15 (2020). https://doi.org/10.1080/15592324.2020.1728468.

[2] H. Insam, M.S.A. Seewald, Volatile organic compounds (VOCs) in soils, Biol. Fertil. Soils 46 (2010) 199–213. https://doi.org/10.1007/s00374-010-0442-3.

[3] J. Peñuelas, D. Asensio, D. Tholl, K. Wenke, M. Rosenkranz, B. Piechulla, J.P. Schnitzler, Biogenic volatile emissions from the soil, Plant, Cell Environ. 37 (2014) 1866–1891. https://doi.org/10.1111/pce.12340.

Use of residues generated from olive cultivation and olive oil production for the enhancement of soil quality

A. Stefanatou[1], A. Kalampokidis[1], T. Maneka[1], G-E. Dimitriou[1], M. Pavlidis[2], M. Veloutsos[2], A. Galanidis[1], F. Galliou[3], T. Manios[3], D-F Lekkas[1], P. Dimitrakopoulos[1], N. Fyllas[4], S. Vakalis[1] and M.S. Fountoulakis[1]

[1]Department of Environment, University of the Aegean, Mytilene, Greece
[2]Agricultural cooperative of Petra, Petra, Greece
[3]Department of Agriculture, Hellenic Mediterranean University, Heraklion, Greece
[4]Department of Biology, National and Kapodistrian University of Athens, Athens, Greece

Corresponding author email: estefanatou@env.aegean.gr

keywords: *compost, soil additive, olive trees, pruning, circularity, wastewater*

Introduction

Among the European countries, Greece is one of the largest producers of olive oil worldwide, with over 200,000,000 olive trees (Skiada et al. 2019). However, there is a lack of management regarding the wastes that derive from olive cultivation and its production as well. More specifically, liquid waste either end up illegally in the environment without any processing or are usually processed with hydrated lime, ending in evaporation ponds (Enaime et al. 2024). On the other hand, solid residues from tree pruning, are burned in forested areas, releasing large quantities of gas such as carbon dioxide and an increased risk of wildfires (Castillo-ruiz et al. 2021). Thus, the aim of this project was the resolution of these urgent problems by utilizing the residues from olive cultivation and the liquid waste from olive mills to produce compost and soil additives. These substances will then be distributed to olive groves to increase soil fertility.

Materials and methods

The experiment took place in an olive grove on Lesvos Island, renowned for its rich tradition in olive cultivation. Specifically, three distinct soil additives were generated and employed. Firstly, olive leaves from a three-phase olive mill were co-composted with olive mill wastewater (OMW) pretreated by sedimentation (**Figure 1a**). Additionally, shredded residues from olive tree prunings were composted on-site, utilizing the liquid fraction of olive mill wastewater (LFOMW) for moisture control (**Figure 1b**). Furthermore, biochar, the residue derived from producing charcoal from coarse olive wood, was also utilized as a soil additive.

Samples of the different mixtures of composts were collected before and after their stabilization, for the determination of their chemical and physical characteristics. More specifically, measurement of total Kjeldahl nitrogen, humidity, total solids, volatile solids as well as total phenols were conducted. Regarding the characterisation of the olive groves soil, samples before the application of the soil additive and after, were collected in specific olive trees, for the investigation of the soil additives' contribution to carbon and macronutrients increase. Moreover, flora samples that grow at the understory of the olive trees were collected before and after the use of the soil additives. Through this, the effect of the different mixtures of soil additives that may have in the understory vegetation of the olive trees, were investigated.

Results and discussion

In both compost mixtures, the initial pH was mainly acidic, ranging from 5.3 to 6.1. Compost that contained olive leaves and liquid waste was characterized by higher initial electrical conductivity as well as

humidity compared to the compost that contained shredded olive prunings and liquid waste. Moreover, the compost with the shredded olive prunings and liquid waste was characterized by higher initial percentages of TS and VS compared to the other mixture (**Table 1**).

Table 1. *Initial physical and chemical characteristics of the two different compost mixtures.*

type of soil additive	number of container	pH	Electrical conductivity (μS/cm)	Humidity (%)	TS (%)	VS (%)
olive leaves + OMW	1	6.1	826	66	34	88
olive leaves + OMW	2	5.9	756	62	38	86
shredded olive prunings + LFOMW	1	5.5	633	35	65	96
shredded olive prunings + LFOMW	2	5.3	626	37	63	96

Figure 1. *Compost containers in which olive leaves (left, **1a**) and shredded olive prunings (right, **1b**) in combination with the liquid waste were used.*

Conclusions

The main aim of this project was the production of compost and soil additives by utilizing the residues from olive cultivation and the liquid waste from olive mills, in order to increase the concentration of carbon and macronutrients in the studied olive groves. Through this practice, the olive groves will become more resilient against erosion.

Acknowledgements: This project was funded by the Rural Development Program (RDP) 2014-2020 within the framework of Action 2 of Submeasure 16.1-16.5 "Cooperation for environmental projects, environmental practices and actions for climate change, MEASURE 16 "COOPERATION" (M16SYN2-00346).

References

Castillo-ruiz FJ, Colmenero-martinez JT, Bayano-tejero S, et al (2021) Methodology for olive pruning windrow assessment using 3d time-of-flight camera. Agronomy 11:1–11. https://doi.org/10.3390/agronomy11061209

Enaime G, Dababat S, Wichern M, Lübken M (2024) Olive mill wastes: from wastes to resources. Environ Sci Pollut Res 31:20853–20880. https://doi.org/10.1007/s11356-024-32468-x

Skiada V, Tsarouhas P, Varzakas T (2019) Preliminary study and observation of “kalamata PDO” extra virgin olive oil, in the messinia region, southwest of peloponnese (Greece). Foods 8:. https://doi.org/10.3390/foods8120610

Session 8: Anerobic digestion

Environmental and energetic analysis of biogas plants supplied with different substrate scenarios

P. Pochwatka[1], A. Kowalczyk-Juśko[1], J. Mazurkiewicz[2], J. Pulka[2], K. Kupryaniuk[2] and J. Dach[2]

[1]Department of Environmental Engineering and Geodesy, University of Life Sciences in Lublin, Lublin, Poland
[2]Department of Biosystems Engineering, Poznań University of Life Sciences, Poznań, Poland
Corresponding author email: patrycja.pochwatka@up.lublin.pl

keywords: *by-product; biomethane; anaerobic digestion; biomass.*

Introduction

In line with the prevailing trends in Europe, caused by the European Green Deal, applicable directives, among others: RED II (Appendix IX), the promoted substrates for biogas plants should be those that are waste biomass, e.g. straw, manure, pomace, cobs cleaned of maize grains. However, most agricultural biogas plants in Europe still use maize silage as a substrate, which is not waste and could be used as animal food.

Many more types of by-product biomass are produced on farms and processing plants than those listed in European directives. Many of them pose a problem for farmers and processors because they are subject to disposal, which is often subject to a fee. The solution to this problem may be an investment in biogas plants, which will not only eliminate the "problem", but also be a source of income for the farm or processor. Several scenarios should be considered where biogas will be burned in a cogeneration engine and the product will be electricity and heat sold or used for own needs, as well as scenarios where the produced biogas will be purified into biomethane, injected into the network, or compressed into bio-CNG. In all scenarios, the obtained byproduct – digestate, can be used as fertilizer, thanks to which the farm can save on the purchase of artificial fertilizers, and the processor can sell or give the digestate to nearby farmers.

An aspect worth considering is reducing the product's carbon footprint. In Polish reality, hard coal and lignite are still the basis of the national energy system. Agri-food products produced using energy and heat from sources with a high carbon footprint may be unattractive to consumers and may even be avoided by retail chains following Green Deal trends. Investments in RES in Poland are mostly uncontrollable energy sources – windmills, photovoltaics. Biogas plants, apart from being a stable source of energy, are controllable because they can produce energy in the so-called energy peak(s) (Pochwatka et al., 2023). In addition, the electricity produced from biogas has a low, and even negative carbon footprint when using some substrates.

The aim of this work is the environmental, energy and economic analysis of using waste biomass as the substrates for biogas plants. The work analyzed scenarios for the use of various waste biomass as a substrate for biogas plants and their benefits.

Materials and methods

The first stage of the work was testing the biogas efficiency of waste substrates, on which the analyzed scenarios of biogas plant operation were to be based. Biogas efficiency tests were performed at Ecotechnologies Laboratory (EL) – the largest Polish biogas laboratory. This laboratory is located at the Poznan University of Life Science (PULS) and, in addition to conducting laboratory research, manages 8 biogas plants located on 3 experimental farms belonging to PULS and in the first half of 2024 will launch the first Polish biomethane plant (capacity 1 million m^3/year) on the experimental farm Brody.

Substrate tests were carried out in EL according to the German standards DIN 38 414/S8 and VDI 4630. Calculations of energetic efficiency of biogas plant operation for individual variants of substrates were carried out according to the methodology described in Pochwatka et al. (2020). All prices and costs included in the analysis came from actually operating biogas installations.

Results and discussion

The work analyzed the operation of biogas plants fed with substrates in three different variants – traditional variant (the most popular in Europe): slurry and maize silage and waste variants: cow manure and waste whey;

maize straw and distillery stillage. Conducted tests showed that substrates had very different biogas efficiencies (table 1).

Table 1. *Characteristics of tested substrates*

Type of substrate	TS [% FM]	VS [% TS]	Biogas production [m^3/Mg FM]	Methane content [%]	Methane production [m^3/Mg FM]
Slurry	2.46	70.35	11.05	69.77 %	7.71
Maize silage	34.32	96.12	220.85	51.67 %	114.12
Cow manure	15.11	85.04	48.81	65.72 %	32.08
Whey	13.72	84.37	96.82	46.05 %	44.59
Maize straw	77.82	89.87	422.04	51.93 %	219.15
Distillery stillage	8.05	74.45	42.31	53.18 %	22.50

The substrates used had very different dry matter contents, methane production efficiency, and purchase prices – which consequently influenced the operational parameters of the biogas plant (especially economic ones). It should be emphasized that the analysis was performed for the same installations with a capacity of 0.5 MW generating 4,200 MWh of electricity per year – and this required the supply of completely different amounts of substrates in individual variants and resulted in different masses of the produced digestate.

Conclusions

The analyzes carried out showed that in each of the variants, the investment in a biogas plant with a capacity of up to 0.5 MW is profitable (assuming a guaranteed price for electricity from the biogas plant), although the payback period is different. The least profitable option is to use a mixture of maize silage and slurry, which results from the high cost of purchasing the silage. This traditional variant should be forgotten due to the fact that in the face of the RED II and RED III regulations, maize silage as the main crop should not be used for energy production.

References

Pochwatka, P., Kowalczyk-Juśko, A., Sołowiej, P., Wawrzyniak, A., Dach, J. 2020. Biogas Plant Exploitation in a Middle-Sized Dairy Farm in Poland: Energetic and Economic Aspects. *Energies*, 13(22), 6058. https://doi.org/10.3390/en13226058.

Pochwatka, P., Rozakis, S., Kowalczyk-Juśko, A., Czekała, W., Qiao, W., Nägele, H.-J., Janczak, D., Mazurkiewicz, J., Mazur, A., Dach, J. 2023. The energetic and economic analysis of demand-driven biogas plant investment possibility in dairy farm. *Energy*, 283, 129165. https://doi.org/10.1016/J.ENERGY.2023.129165.

RED II. 2018. Directive (EU) 2018/2001 of the European Parliament and of the Council of 11 December 2018 on the promotion of the use of energy from renewable sources. http://data.europa.eu/eli/dir/2018/2001/oj.

Environmental and energetic analysis of biogas plants supplied with different substrate scenarios

P. Pochwatka[1], A. Kowalczyk-Juśko[1], J. Mazurkiewicz[2], J. Pulka[2], K. Kupryaniuk[2] and J. Dach[2]

[1]Department of Environmental Engineering and Geodesy, University of Life Sciences in Lublin, Lublin, Poland
[2]Department of Biosystems Engineering, Poznań University of Life Sciences, Poznań, Poland
Corresponding author email: patrycja.pochwatka@up.lublin.pl

keywords: *by-product; biomethane; anaerobic digestion; biomass.*

Introduction

In line with the prevailing trends in Europe, caused by the European Green Deal, applicable directives, among others: RED II (Appendix IX), the promoted substrates for biogas plants should be those that are waste biomass, e.g. straw, manure, pomace, cobs cleaned of maize grains. However, most agricultural biogas plants in Europe still use maize silage as a substrate, which is not waste and could be used as animal food.

Many more types of by-product biomass are produced on farms and processing plants than those listed in European directives. Many of them pose a problem for farmers and processors because they are subject to disposal, which is often subject to a fee. The solution to this problem may be an investment in biogas plants, which will not only eliminate the "problem", but also be a source of income for the farm or processor. Several scenarios should be considered where biogas will be burned in a cogeneration engine and the product will be electricity and heat sold or used for own needs, as well as scenarios where the produced biogas will be purified into biomethane, injected into the network, or compressed into bio-CNG. In all scenarios, the obtained byproduct – digestate, can be used as fertilizer, thanks to which the farm can save on the purchase of artificial fertilizers, and the processor can sell or give the digestate to nearby farmers.

An aspect worth considering is reducing the product's carbon footprint. In Polish reality, hard coal and lignite are still the basis of the national energy system. Agri-food products produced using energy and heat from sources with a high carbon footprint may be unattractive to consumers and may even be avoided by retail chains following Green Deal trends. Investments in RES in Poland are mostly uncontrollable energy sources – windmills, photovoltaics. Biogas plants, apart from being a stable source of energy, are controllable because they can produce energy in the so-called energy peak(s) (Pochwatka et al., 2023). In addition, the electricity produced from biogas has a low, and even negative carbon footprint when using some substrates.

The aim of this work is the environmental, energy and economic analysis of using waste biomass as the substrates for biogas plants. The work analyzed scenarios for the use of various waste biomass as a substrate for biogas plants and their benefits.

Materials and methods

The first stage of the work was testing the biogas efficiency of waste substrates, on which the analyzed scenarios of biogas plant operation were to be based. Biogas efficiency tests were performed at Ecotechnologies Laboratory (EL) – the largest Polish biogas laboratory. This laboratory is located at the Poznan University of Life Science (PULS) and, in addition to conducting laboratory research, manages 8 biogas plants located on 3 experimental farms belonging to PULS and in the first half of 2024 will launch the first Polish biomethane plant (capacity 1 million m^3/year) on the experimental farm Brody.

Substrate tests were carried out in EL according to the German standards DIN 38 414/S8 and VDI 4630. Calculations of energetic efficiency of biogas plant operation for individual variants of substrates were carried out according to the methodology described in Pochwatka et al. (2020). All prices and costs included in the analysis came from actually operating biogas installations.

Results and discussion

The work analyzed the operation of biogas plants fed with substrates in three different variants – traditional variant (the most popular in Europe): slurry and maize silage and waste variants: cow manure and waste whey; maize straw and distillery stillage. Conducted tests showed that substrates had very different biogas efficiencies (table 1).

Table 1. *Characteristics of tested substrates*

Type of substrate	TS [% FM]	VS [% TS]	Biogas production [m^3/Mg FM]	Methane content [%]	Methane production [m^3/Mg FM]
Slurry	2.46	70.35	11.05	69.77 %	7.71
Maize silage	34.32	96.12	220.85	51.67 %	114.12
Cow manure	15.11	85.04	48.81	65.72 %	32.08
Whey	13.72	84.37	96.82	46.05 %	44.59
Maize straw	77.82	89.87	422.04	51.93 %	219.15
Distillery stillage	8.05	74.45	42.31	53.18 %	22.50

The substrates used had very different dry matter contents, methane production efficiency, and purchase prices – which consequently influenced the operational parameters of the biogas plant (especially economic ones). It should be emphasized that the analysis was performed for the same installations with a capacity of 0.5 MW generating 4,200 MWh of electricity per year – and this required the supply of completely different amounts of substrates in individual variants and resulted in different masses of the produced digestate.

Conclusions

The analyzes carried out showed that in each of the variants, the investment in a biogas plant with a capacity of up to 0.5 MW is profitable (assuming a guaranteed price for electricity from the biogas plant), although the payback period is different. The least profitable option is to use a mixture of maize silage and slurry, which results from the high cost of purchasing the silage. This traditional variant should be forgotten due to the fact that in the face of the RED II and RED III regulations, maize silage as the main crop should not be used for energy production.

References

Pochwatka, P., Kowalczyk-Juśko, A., Sołowiej, P., Wawrzyniak, A., Dach, J. 2020. Biogas Plant Exploitation in a Middle-Sized Dairy Farm in Poland: Energetic and Economic Aspects. *Energies*, 13(22), 6058. https://doi.org/10.3390/en13226058.

Pochwatka, P., Rozakis, S., Kowalczyk-Juśko, A., Czekała, W., Qiao, W., Nägele, H.-J., Janczak, D., Mazurkiewicz, J., Mazur, A., Dach, J. 2023. The energetic and economic analysis of demand-driven biogas plant investment possibility in dairy farm. *Energy*, 283, 129165. https://doi.org/10.1016/J.ENERGY.2023.129165.

RED II. 2018. Directive (EU) 2018/2001 of the European Parliament and of the Council of 11 December 2018 on the promotion of the use of energy from renewable sources. http://data.europa.eu/eli/dir/2018/2001/oj.

Designing sustainable processes for methane and hydrogen production using poplar woody sawdust biomass: The effect of chemical pretreatment

I. Apostolopoulos[1], A. Tekerlekopoulou[2], G. Antonopoulou[2]*

[1]Department of Chemical Engineering, University of Patras, Caratheodory 1, GR 26504, Patras, Greece
[2] Department of Sustainable Agriculture, University of Patras, 2 Georgiou Seferi str., GR 30100, Agrinio, Greece
Corresponding author email: geogant@upatras.gr

keywords: *biofuels, chemical pretreatment, woody biomass, hydrogen, methane*

Introduction

In the present study, different chemical pretreatment methods such as alkaline and acid were applied on woody biomass such as poplar woody sawdust (PWS). The impact of each pretreatment method on the structural and chemical composition of the lignocellulosic content (cellulose, hemicellulose, lignin) was evaluated. In the sequel, the pretreated feedstocks were further evaluated for biofuel production such as biohydrogen and biogas, under different process schemes.

Materials and methods

PWS was chopped, milled, and then sieved to a powder, before being air-dried at ambient temperature. For all pretreatment methods the solids loading, expressed as total solids (TS), was 5% w/v, (5 g of TS in 100 mL water or acid or alkali). Acid pretreatment was conducted by the use of H_2SO_4 and HCl, at 2,10 and 20 g/100 gTS, at 121°C for 1 h, while the alkaline, using NaOH at the same concentrations, but at lower temperature and longer time (80°C, 24h). Blank experiments, in which only thermal treatment (121°C for 1h or 80°C for 24 h) without any chemical addition, were carried out, for comparative reasons. After pretreatment, the whole pretreated biomass was separated through vacuum filtration (0.7 μm pore size) and two fractions (a liquid and a solid one) were obtained. A detailed physicochemical and structural characterization was performed in both fractions based on Antonopoulou et al. (2020). Both fractions, as well as the whole pretreatment slurry (without separation), were used to produce methane, through batch biochemical methane potential (BMP) tests and hydrogen, through biochemical hydrogen production (BHP) tests.

BMP tests were performed either at the whole slurry or at the separated fractions, obtained after pretreatment, based on Antonopoulou et al. (2020).

BHPs were conducted at meshophilic conditions, using heat treated mixed anaerobic sludge, as microbial inoculum, with the addition of commercial enzymes (40 FPU/gTS) via a SSF (simultaneous saccharifiacation and fermentation) process. For the best pretreatment conditions (H_2SO4 10 g /100 gTS) different schemes were evaluated, such as: a) fermentation without enzymes addition and b) hydrolysis (using enzymes) at a separate step, prior to fermentation (SHF). In addition, the separation of the whole pretreatment slurry and the use of the separated fraction for BHP was also assessed

Results and discussion

The main characteristics of PWS were: total solids (TS): 93.2%, cellulose: 32.7 % of TS, hemicellulose: 16.8% TS, lignin: 34.2 % TS, extractives: 5% TS. From Figure 1, where the effect of pretreatments on the lignocellulosic fraction is presented, it can be seen that 10 or 20 g HCl /100 gTS caused a reduction of hemicellulose by 69.6 and 97.6 %, respectively, while the use of H_2SO_4 at the higher concentration of 20 g/100 gTS, the hemicellulose fraction was reduced by 58.5 %. The lignin fraction was significantly affected only by alkaline pretreatment and the higher the NaOH concentration, the higher was the lignin removal efficiency observed. From Figure 2, where the effect of different pretreatment methods on the BMP of PWS when the whole pretreatment slurry (Fig.2a) or the separated fractions obtained after pretreatment (Fig.2b) are presented, it is obvious that alkali pretreatments enhance the methane production, at both cases. Regarding BHPs of the whole slurry at SSF (Fig.2c), 10 g /100 gTS HCl or H_2SO_4 led to a higher hydrogen yield.

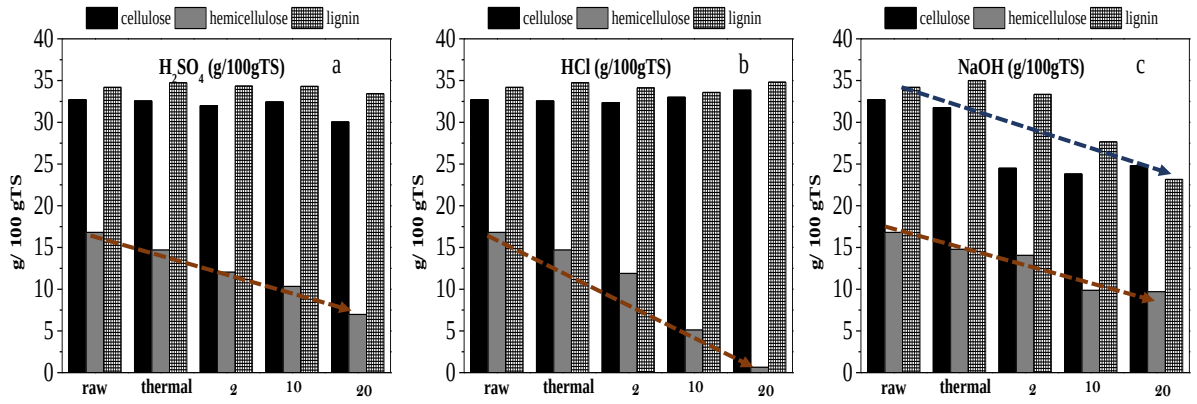

***Figure 1**. The lignocellulosic content (g/100 gTS initial) of the raw, thermally pretreated, acid pretreated (H_2SO_4 (a), HCl (b)) and alkali pretreated (NaOH (c)) PWS.*

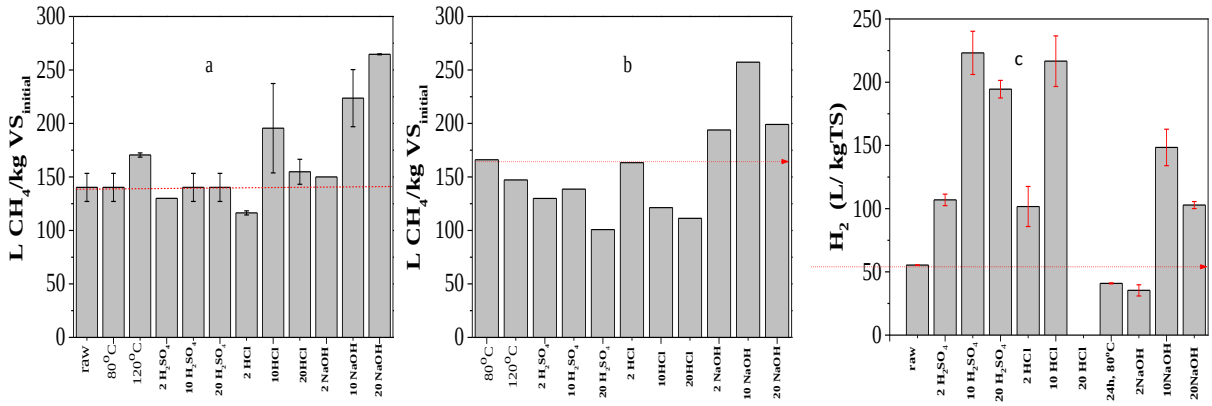

Performing alternative BHP tests for PWS pretreated with 10 g H_2SO_4/ 100 gTS the main results are concentrated in Table 1. The possible scenario for the best pretreatment approach and biofuel generation is presented in Table 2, where the energy gained in each process, is calculated.

***Table 1.** BHP s for the different concepts for PWS pretreated with 10 g H_2SO_4/ 100 gTS*

Scheme		L H_2/kgTS
Whole biomass	No enzymes	14.81 ± 0.89
Whole biomass	40 FPU /gTS at SHF	134.61 ± 14.56
Whole biomass	40 FPU /gTS at SSF	223.16 ± 14.68
Separation of both fractions	Solids with 40 FPU /gTS at SSF	76.24 ± 5.70

***Tabl2 2 1.** The energy gained for each process and biofules production .*

Scheme	Energy MJ_2/kgTS

Whole biomass	10 g/100 gTS H_2SO4, H_2, SSF	2.83
Whole biomass	20 g /100 gTS NaOH, CH_4	9.63
Separation of both fractions	10 g/100 gTS H2SO4, H_2, solids at SSF	0.97
Separation of both fractions	20 g /100 gTS NaOH, CH_4	9.37

Acknowledgements: This work has been financed by the funding programme "MEDICUS", of the University of Patras.

References

- Antonopoulou, G., Vayenas, D and Lyberatos, G. (2020) Biogas production from physicochemically pretreated grass lawn waste: comparison of different process schemes. Molecules,25, 296

Modelling Hollow Fibre Membrane Bioreactors for Biogas Purification

A. Hatzikioseyian[1], J. Das[2] and P.N.L. Lens[2]

[1]Laboratory of Environmental Science and Engineering, School of Mining and Metallurgical Engineering, National Technical University of Athens (NTUA), Greece
[2]University of Galway, Galway H91 TK33, Ireland
Corresponding author email: artin@metal.ntua.gr

keywords: *HFMB; modelling; biogas; ammonia; hydrogen sulphide.*

Introduction

Biogas, produced from the anaerobic digestion of organic matter, is a promising renewable energy source. However, before it can be utilized, particularly for applications such as electricity generation, heating, or as fuel, purification and upgrading processes are essential. Raw biogas typically contains significant amounts of impurities, notably hydrogen sulphide (H_2S) and ammonia (NH_3), which pose several challenges. Hydrogen sulphide, which is toxic and corrosive, can damage equipment and create hazardous conditions, while its combustion produces sulphur dioxide, a harmful environmental pollutant. Ammonia, on the other hand, contributes to the formation of nitrogen oxides (NO_x) during combustion, further exacerbating air pollution problems. Various technologies and methods have been proposed to remove H_2S and NH_3. These include adsorption, chemical scrubbing, and biological processes. Hollow fibre membrane bioreactors (HFMBs) represent a combination of membrane technology and biological processes for the purpose of biogas upgrading. HFMBs are made up of an array of hollow fibres that are immersed in an aqueous phase contained within an outer shell. These membranes provide a substantial surface area for efficient mass transfer. Microbial cells can be attached to the outer surface of the membrane or retained within the shell side of the bioreactor. Substances present in the lumen side can diffuse through the fibre walls, thereby supporting microbial growth and removal of contaminants. This work summarises the development of a mathematical model to describe the fluid dynamics, transport phenomena, and chemical and microbial processes that govern the operation and efficiency of a hollow fibre membrane bioreactor.

Materials and methods

The reactor prototype used for this model is described in detail in previous studies (Das 2022; Das and Lens 2022; Das et al. 2022a; Das et al. 2022b, c). Two laboratory HFMBs were set up in parallel under abiotic conditions (control experiment without the use of inoculum) and biotic conditions (inoculated reactor). The reactor is shown in Fig. 1(a) with the characteristic bundle of ten hollow fibres. The shell side of the reactor where the tubes are submerged in water is also shown along the inlet-outlet and various sampling ports.

Model development

The model of the reactor was implemented in COMSOL Multiphysics®. A typical workflow used for computational fluid dynamics (CFD) models was followed consisting of: (a) setting up the model environment; (b) building the geometry of the hollow fibre membrane bioreactor; (c) defining the parameters - functions; (d) specifying the materials and their properties; (e) defining the physics of the model as well as the boundary conditions; (f) creating a mesh; (g) running the simulation under dynamic conditions (transient study); and (h) post-processing the results. The 3D geometry of the reactor is presented in Fig. 1(b), while the generated tetrahedral mesh is shown in Fig. 1(c). The chemistry module was used to include the gas species (i.e., CH_4, CO_2, H_2S, NH_3, N_2, O_2, H_2, CO) as well as the bio/chemical species (i.e., biomass, NH_4^+, HS^-, HCO_3^-, H^+ and OH^-). The laminar flow module was used to describe the continuity and momentum of the fluids, while the transport of concentrated species module was used to study the mass transfer processes within the tubes, along with the porous properties of the membrane. Additionally, the diluted species module was used to describe the chemical/biochemical reactions as well as the mass transfer of the species in the liquid phase.

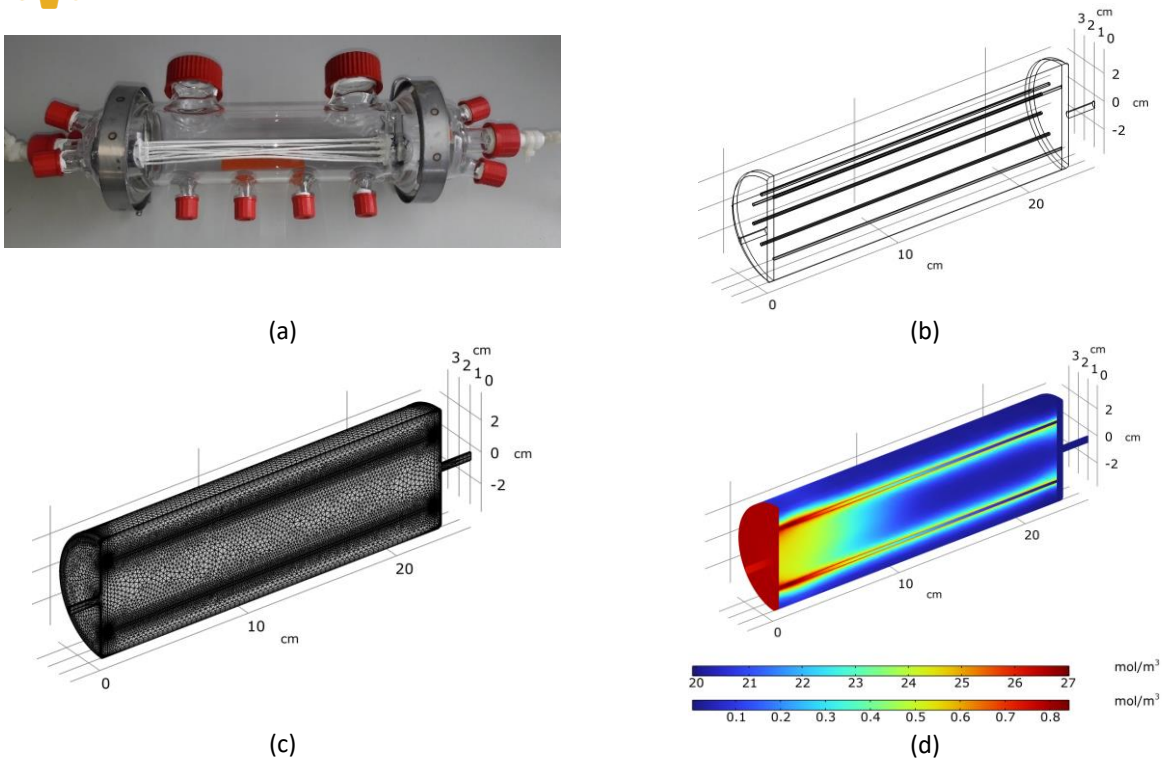

Figure 1. *(a) Picture of the HFMB prototype; (b) A cross section of the 3D geometry of the reactor; (c) Meshing of the geometry; (d) Indicative distribution of CH_4 concentration in the gas and liquid domain.*

Results and discussion

The dynamics of HFMB were simulated under three diverse operating conditions: (a) at constant biogas residence time/constant inlet composition; at progressively reduced biogas residence time/variable inlet composition under (b) abiotic and (c) biotic conditions. Our study reveals the importance of abiotic processes along with the biological processes carried out by autotrophic sulphide oxidizing bacteria (SOB) and autotrophic ammonium oxidizing bacteria (AOB). Fig. 1(d) presents an indicative simulation of the CH_4 concentration in the gas stream and aqueous phase after a step feed of raw biogas in the HFMB.

Conclusions

The results of our research work contribute to the understanding and advancement of sustainable biogas purification technologies based on membrane technology combined with biological methods. Our analysis also provides valuable insights for HFMB design and process optimisation.

References

Das, J., 2022. Biogas clean-up using a novel hollow fibre membrane bioreactor for end-use applications. Ph.D. Thesis, National University of Ireland Galway (NUI Galway).

Das, J. and Lens, P.N.L., 2022. Resilience of hollow fibre membrane bioreactors for treating H_2S under steady state and transient conditions. *Chemosphere*, 307(Pt 4), 136142.

Das, J., Nolan, S. and Lens, P.N.L., 2022a. Simultaneous removal of H_2S and NH_3 from raw biogas in hollow fibre membrane bioreactors. *Environmental Technology & Innovation*, 28, 102777.

Das, J., Ravishankar, H. and Lens, P.N.L., 2022b. Biological biogas purification: Recent developments, challenges and future prospects. *Journal of Environmental Management*, 304, 114198.

Das, J, Ravishankar, H. and Lens, P.N.L., 2022c. Biological removal of gas-phase H_2S in hollow fibre membrane bioreactors. *Journal of Chemical Technology & Biotechnology* 97(5), 1149-1161.

Session 9: Water treatment

The use of hyperspectral imaging in aquatic vegetation analysis

J. Kostecki[1], S. Myszograj[1], E. Płuciennik-Koropczuk[1], I. Krupińska[1]

[1]Institute of Environmental Engineering /University of Zielona Gora, Zielona Gora, Poland
Corresponding author email: j.kostecki@iis.uz.zgora.pl

keywords: *aquatic plants; hyperspectral image; hyperspectral analysis; water pollution.*

Introduction

Aquatic plants play a key role in the functioning of aquatic ecosystems, performing many important functions. Among the most important are primary production, water filtration, climate regulation and bank stabilisation. The protection and sustainable use of these resources is essential to maintain healthy and functioning aquatic ecosystems (Zhao et al 2022).

The standard surveys used to analyse the presence of species, whether common, endangered or invasive, use traditional monitoring methods that still present many challenges that affect both their effectiveness and accuracy. These include the availability of vegetation (water depth, density of cover, variable environmental conditions). Sampling for further analysis can also be problematic. Traditional methods may not provide sufficiently detailed information on species, biomass, health and distribution of aquatic plants. They are also limited by the size of water bodies and the availability of researchers (Lewis and Thursby 2018).

Hyperspectral imaging technology is an innovative tool that has the potential to revolutionise aquatic plant analysis. Compared to traditional monitoring methods, hyperspectral imaging offers a number of significant advantages, including the level of data accuracy and detail, remote monitoring, the ability to collect data under different lighting conditions, and integration with GIS and ecological models (Eshkabilov et al. 2021, Sarić et al. 2022). Conventional digital photography captures images in three channels: red, green and blue (RGB). Hyperspectral imaging allows images to be recorded in hundreds of narrow spectral bands, each band corresponding to a specific wavelength of light, providing much more detailed information. Hyperspectral imaging can be used to identify specific species, assess the biomass and cover of a water body, the presence of pollutants and plant pathogens, the availability of nutrients and progressive eutrophication, and the influence of environmental factors. (O'Hare et al 2018).

Materials and methods

The study analysed selected plant species collected from 2 sites: the Laczna River and the Czerwiensk Lagoon, Poland (52°00'10.1 "N 15°25'12.6 "E). Samples were collected manually using a scoop, transported to the laboratory where they were analysed using a SPECIM FX10e hyperspectral camera.

Results and discussion

Differences between RGB and hyperspectral images has been shown in table 1. Comparing the two figures, a higher reflectance in the 500-600 nm range was observed for *Typha angustifolia* (about 20%). It contains more chlorophyll (both a and b). The reflectance of *Elodea canadensis* is much lower (about 10%).

Leaf pigments and cellulose are transparent to near infrared wavelengths (700-1300 nm) and leaf absorption is low. Most of the energy is transmitted and reflected, depending on the structural features of the leaf, resulting in a high near infrared (NIR) plateau. High reflection can be seen in both images (in the 700-1000 nm range).

The combination of low visible and high near-infrared reflectance is characteristic of most plants. When the condition of the plant deteriorates, e.g. due to water shortage, it starts to reflect more visible light and less near-infrared light. This can also be observed in autumn, when the leaves turn yellow and red due to seasonal changes.

Table 1. *Experimental results*

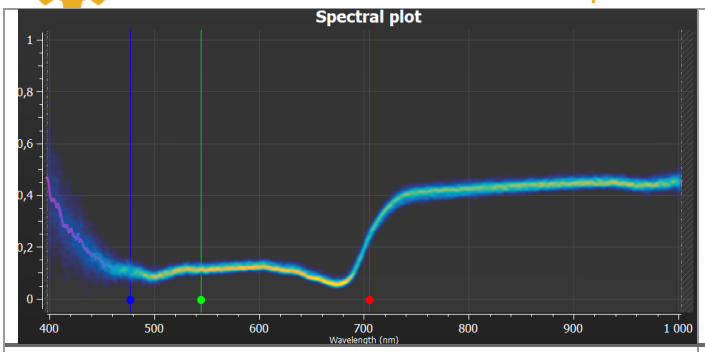

Hiperspectral image of *Elodea canadensis* Michx. | *Elodea canadensis* Michx.

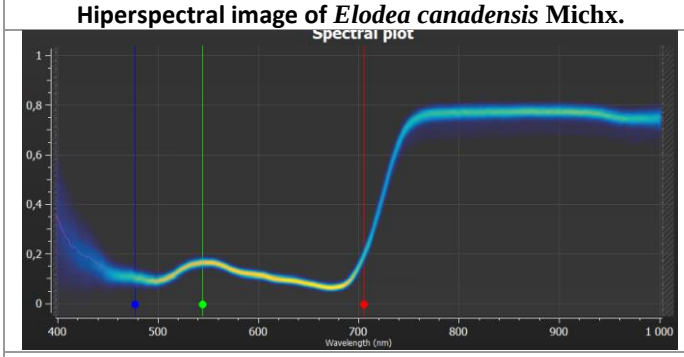

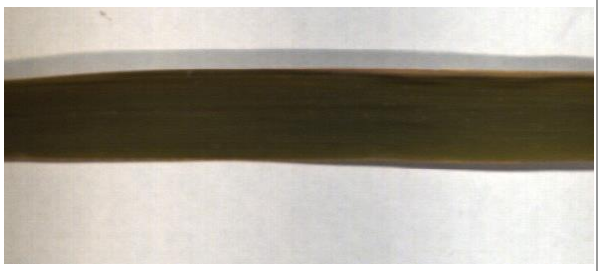

Hiperspectral image of *Typha angustifolia, L.* | *Typha angustifolia, L.*

Conclusions

Based on the results obtained, hyperspectral imaging technology was found to be useful in the analysis of selected aquatic plant species. Unfortunately, the cost of its application is currently too high to be used on a large scale. It is necessary to rely on other available techniques. Given the potential benefits for science and environmental protection, further research is advisable.

Acknowledgements: This study is supported by the HYDROSTRATEG1/001/T/2022 (acronym HIPER). Co-financed by NCBiR within the framework of the 1st Government Strategic Program HYDROSTRATEG, POLAND, 1.10.2023 – 30.09.2026. A comprehensive system for monitoring the quality of surface waters and coastal areas using a multi-sensor system with the hyperspectral cameras.

References

Eshkabilov, S., Lee, A., Sun, X., Lee, C.W., Simsek, H. 2021. Hyperspectral imaging techniques for rapid detection of nutrient content of hydroponically grown lettuce cultivars, Computers and Electronics in Agriculture, 181, 105968, https://doi.org/10.1016/j.compag.2020.105968.

Lewis, M., Thursby, G. 2018. Aquatic plants: Test species sensitivity and minimum data requirement evaluations for chemical risk assessments and aquatic life criteria development for the USA, Environmental Pollution, 238, 270-280. https://doi.org/10.1016/j.envpol.2018.03.003.

Liu, Y., Ndirangu, L., Li, W., Pan, J., Cao, Y., Jeppesen, E. 2024. Response of Functional Traits of Aquatic Plants to Water Depth Changes under Short-Term Eutrophic Clear-Water Conditions: A Mesocosm Study. *Plants*, *13*, 1310. https://doi.org/10.3390/plants13101310.

O'Hare, M.T., Aguiar, F.C., Asaeda, T. et al. 2018. Plants in aquatic ecosystems: current trends and future directions. Hydrobiologia, 812, 1–11. https://doi.org/10.1007/s10750-017-3190-7.

Sarić, R., Viet D. Nguyen, Burge, T., Berkowitz, O., Trtílek, M., Whelan, J., Lewsey, M.G., Čustović, E.. 2022. Applications of hyperspectral imaging in plant phenotyping, Trends in Plant Science, 27(3), 301-315. https://doi.org/10.1016/j.tplants.2021.12.003.

Zhao, J., Liu, C., Li, H., Liu, J., Jiang, T., Yan, D., Tong, J., Dong, L. 2022. Review on Ecological Response of Aquatic Plants to Balanced Harvesting. Sustainability, 14, 12451. https://doi.org/10.3390/su141912451.

Systematic environmental surveillance for Legionella detection and treatment in a hospital water distribution system in the Region of Crete during COVID-19 era

A. Papadakis[1,2], E. Koufakis[3], K. Tsamoutsoglou[4], N. Gikas[4], D. Chochlakis[1,5] A. Psaroulaki[1,5] and P. Gikas[4]

[1] Lab of Food, Water & Environment Microbiology, Department of Clinical Microbiology and Microbial Pathogenesis, School of Medicine, University of Crete, Voutes—Staurakia, 71110 Heraklion, Crete, Greece
[2] Directorate of Public Health of the Region of Crete, 71201 Heraklion, Crete, Greece
[3] Regional Coordinator of Civil Protection Office, Region of Crete, Heraklion, Greece
[4] School of Chemical and Environmental Engineering, Technical University of Crete, 73100, Chania. Greece
[5] Regional Public Health Laboratory of Crete, Voutes—Staurakia, 71110 Heraklion, Crete, Greece

Corresponding author email: apapadakis@crete.gov.gr

keywords: *Legionella; microbiological agents; water distribution system; hospital; chlorine dioxide; Covid-19*

Introduction

Legionnaires' disease can manifest as severe respiratory tract infection with a high mortality rate and is sometimes associated with a healthcare-associated outbreak by a contaminated water supply. Certain measures, including disinfection by chlorination, maintaining increased temperatures are usually undertaken to prevent Legionella outbreaks (Papadakis *et al.*, 2018; 2021). However, these preventive strategies are not always effective, since there are several factors (e.g., synergistic interactions with other microbes, physico-chemical factors, biofilm formation) that promote survival and proliferation of the pathogen in water pipes (Kumar *et al.*, 2022).

The aim of the research was to study the risk factors and the possible colonization of *Legionella spp.* in a hospital facility, due to the increased risk of secondary infection of patients with COVID-19, the poor maintenance for reasons related to COVID-19 as well as the temporary shutdown of parts of the buildings resulting in stagnant water conditions. In addition, the safety and efficacy of an on-site chlorine dioxide (ClO_2) water treatment system in controlling *Legionella* was assessed.

Materials and methods

165 water samples were collected from a hospital water system in the Region of Crete for a prolonged period between 2021 and 2024, during COVID-19 pandemic. The samples were collected in 1 L sterile containers containing sufficient sodium thiosulphate (20 mg) to neutralize any chlorine or other oxidizing biocides. In each sample the presence of Legionella species along with environmental parameters such as water temperature, pH and free chlorine were tested.

According to European technical guidelines, 10 inspections and 121 electronic check lists were performed, where other epidemiological factors were recorded including water pressure, stagnation of water, physicochemical properties of water, and proximity of sampling point to the boiler among others.

Finally, following installation of a chlorine dioxide water treatment system, an inspection sampling was performed for water cultures of the same hospital water supply.

Results and discussion

Based on the data analysis, over 49% of the samples were positive to the presence of *Legionella* species (>=50 CFU/L). Specifically, the annual positivity in 2021 was 17/19 samples (namely 89%), in 2022 27/55 samples (49%), in 2023 23/63 samples (37%) and in 2024 14/28 samples (50%) (Figure 1). *Legionella pneumophila* serogroup 1, 65/165 (39%) max 10,000 CFU/L and serogroup 3, 5/165 (3%) max 14,000 CFU /L species were isolated. Additionally, the inspections revealed the existence of an intense periodic coloring of the water, and low temperatures for the water flow in the vicinity of the boiler (<60ºC), as well as in the rooms, where totally 52 cases were found between 22.2-49ºC. Finally, 115 measurements for the estimation of residual chlorine

were found to be outside the national legal regulation limits of <0.2 mg/L. Table 1 shows the significant parameters that calculated for hot water temperature <50 °C, and chlorine concentrations <0.2 mg/L.

Table 1. *Experimental results for water samples during Covid-19.*

Hot water temperature <50 °C		***Chlorine concentrations <0.2 mg/L***	
Relative risk (R.R.)	4.1311	Relative risk (R.R.)	2.4120
95% CI	1.1528 to 14.8046	95% CI	1.3635 to 4.2669
z statistic	2.178	z statistic	3.025
Significance level	P = 0.0294	Significance level	P = 0.0025
NNT (Harm)	1.916	NNT (Harm)	3.187
95% CI	4.104 (Harm) to 1.250 (Harm)	95% CI	6.629 (Harm) to 2.098 (Harm)

According to the latest inspection after the employment of an on-site chlorine dioxide system before the internal water supply network, the positivity was dropped to 3/19 samples (namely 16%) (Figure 1) comprising a promising approach towards nosocomial Legionella within the hospital water supply. Chlorine Dioxide treatment may be used as a secondary disinfectant in hospitals and other facilities due to the effectiveness of chlorine dioxide in controlling pathogens such as *Legionella pneumophila, Stenotrophomonas maltophilia*, and *Mycobacterium avium* complex.

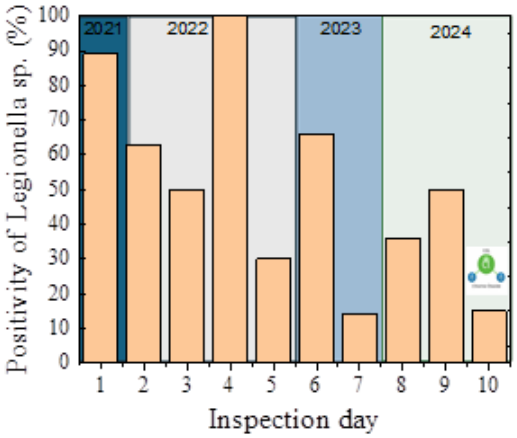

Figure 1. Positivity of Legionella sp. Within the water supply during 2021-2024 after several inspections (1-9) and in 2024 (10) after the employment of chlorine dioxide disinfection system.

Conclusions

To conclude, despite the increased preventive measures against HAI due to the Covid-19 pandemic, the case hospital was found incapable to respond to them, despite technical interventions such as the replacement of the boiler and occupation of filters. Aging facility piping increases the risk of colonization and requires immediate replacement. The risk assessment of the water supply network in conjunction with the creation of a water safety plan (WSP), and other sanitation procedures such as chemical disinfection with a complementary chlorination method, are required to control Legionella outbreaks associated with water distribution systems. The results of this work indicate that the operation of a chlorine dioxide system effectively reduced Legionella species from a hospital water supply which hold promise as an efective preventative solution to the *Legionella* contamination in hospitals.

Acknowledgements: This study is supported by the Region of Crete and the Regional Laboratory of Public Health of Crete, School of Medicine, University of Crete. We would like to thank all the environmental health inspectors of the Local Public Health Authorities of the Crete Island for collecting the environmental samples.

References

Papadakis A, Chochlakis D, Sandalakis V, Keramarou M, Tselentis Y and Psaroulaki A, 2018. Legionella spp. Risk Assessment in Recreational and Garden Areas of Hotels. *Int. J. Environ. Res. Public Health.*, 15(4), 598.

Papadakis, A.; Keramarou, M.; Chochlakis, D.; Sandalakis, V.; Mouchtouri, V.A.; Psaroulaki, A. Legionella spp. Colonization in Water Systems of Hotels Linked with Travel-Associated Legionnaires' Disease. Water 2021, 13, 2243. https://doi.org/10.3390/w13162243.

Kumar M, Gikas P, Kuroda K, and Vithanage M, 2022. Tackling water security: A global need of cross-cutting approaches, *J. Environ. Management.*, 306, 114447.

Unseen Processes in Freeze Desalination: Molecular Dynamics of Nucleation, Crystal Growth, and Ion Entrapment – A Short Review

Khadije El Kadi[1,2] and Isam Janajreh[1,2]

[1]Mechanical and Nuclear Engineering Department, Khalifa University, Abu Dhabi, United Arab Emirates
[2]Center for Membrane and Advanced Water Technology, Khalifa University, Abu Dhabi, United Arab Emirates
Corresponding author email: isam.janajreh@ku.ac.ae

ABSTRACT
Freeze desalination (FD) presents a promising path for sustainable and energy-efficient freshwater production. This emerging technology leverages the physical principles of crystallization to form ice crystals from supercooled saline solutions, followed by the melting of ice to produce freshwater. Despite its potential, FD faces challenges related to capital costs and more importantly to its process complexity. Understanding the intricate freezing process is essential for optimizing FD efficiency. Molecular dynamics (MD) simulations offer a powerful tool to study FD phenomena at the molecular level, providing insights into ice nucleation, crystal growth, and surface interactions. This short review highlights recent advancements in MD simulations for FD, categorizing them into three main areas: crystal growth and salt ion rejection, homogeneous ice nucleation kinetics, and freezing on solid surfaces. While MD simulations hold promise for enhancing FD understanding, significant knowledge gaps persist. Future research directions include investigating the dynamics of hydrogen bonding during ice nucleation, elucidating ion entrapment mechanisms, and quantifying ion rejection rates during ice growth.
Keywords: Molecular dynamics; Freeze desalination; Ice nucleation; Ion entrapment; Ice crystallization.

1. NTRODUCTION

While several desalination methods are currently mature and abundant, freeze desalination (FD) is an emerging technology that has the potential to be a more sustainable and energy efficient alternative. FD is a freezing-melting process in which ice crystals are formed from a supercooled saline solution and further melted to produce freshwater. The technology is based on the physical nature of crystallization in which impurities, e.g., salts and dissolved solids, are excluded during the formation of ice lattice (Saji et al., 2020). One notable advantage of FD is the potential for brine valorization in the form of salt hydrates, particularly when operating at the eutectic point condition, i.e., highly concentrated brine (Nathoo et al., 2009; Pangborn, 1963; Stepakoff et al., 1974). This offers another possibility of utilizing the byproduct of the current desalination plants in a valuable way, contributing to the overall sustainability of the operation. Meanwhile, the capital cost and complexity of the process are two factors affecting the deployment of FD in the desalination industry (Kucera, 2019). The process of freezing saline water follows the NaCl-water binary phase diagram, depicted in ***Figure 4***. As the temperature drops below the liquidus line, ice crystals emerge in the liquid phase, expelling out salt ions and forming a concentrated brine solution. Conversely, if the salt-water mixture exceeds the solubility line at a given temperature, it becomes supersaturated, indicating an excess of dissolved salt. This can occur through cooling, such as in FD, or through evaporation, causing salt crystals to precipitate from the solution. When saline water cools, salt hydrates crystallize, a phenomenon referred to as eutectic point freezing at the eutectic point temperature. The shape of the ice, the degree of ice growth, and the rejection of brine hinge on various factors, including the mixture's composition, initial salinity, cooling/heat removal speed, and physical traits such as density, viscosity, surface tension, and temperature.

Understanding the freezing process is crucial for optimizing FD. Heat and mass transfer occur simultaneously between solid and liquid phases, particularly at the interface. Heat transfer triggers phase change, forming ice. The rate of heat removal influences phase transition and ice formation patterns. Kinetic factors at the ice-liquid interface impact ice growth quality and thickness. Mass transfer of solutes during freezing alters liquid composition and final ice appearance. Comprehending interconnected mass and heat transfer at the interface is vital for controlling ice quality (Elif Genceli Güner et al., 2015; Kalista et al., 2018).

Continuum approaches commonly used to describe freezing processes often fail to accurately capture the intricate transport phenomena at the ice-liquid interface, which typically spans several molecular diameters

(Slattery et al., 2007). These approaches assume fluid continuity and homogeneity, overlooking the non-uniform nature of the ice-liquid interface. Moreover, they rely on assumptions to approximate the complex phenomena of ice nucleation at nano-time and space scales, a stochastic process involving the formation and aggregation of water molecule clusters into ice crystals. In contrast, molecular dynamics (MD) simulations offer a promising tool to study freezing processes at the molecular level, capturing individual molecule behavior. MD simulations provide insights into thermodynamics and kinetic factors at the interface, including ice nucleation and growth, by considering intermolecular and intramolecular forces. They offer valuable information that is not easily predictable or easy to capture through continuum models or experiments, such as nucleation and recalescence. Thus, MD simulations complement experimental and numerical continuum studies, enhancing understanding of parameters in saline water freezing and facilitating more efficient and sustainable desalination processes.

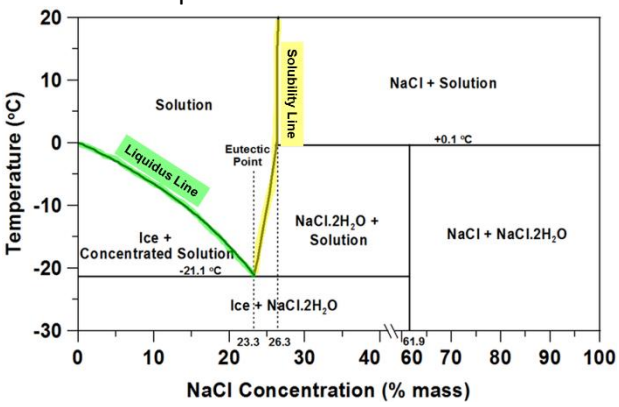

Figure 4. *Phase diagram of NaCl-H_2O mixture*

2. MD for FD

MD simulation has emerged as a powerful tool for studying phenomena occurring during ice crystallization process, which has been of particular interest in various applications such as desalination, cryopreservation, food concentration, and pharmaceutical purposes (Englezos, 1994; Izutsu, 2018; Sánchez et al., 2009; Whaley et al., 2021; Williams et al., 2015). Recent advances in MD simulations for FD technology are highlighted in this work. Literature review categorizes MD work into three areas: (1) crystal growth and salt ion rejection, (2) homogeneous ice nucleation kinetics, and (3) solid surface freezing effects. Despite some studies, significant knowledge gaps persist in simulating seawater freezing using MD.

2.1. Crystal growth and Ion rejection

Studying the behavior of ions and impurities during ice growth is an important aspect to understand the FD process and determining their mechanisms and eventually efficiency. In such MD studies, the simulation box is typically initiated with two distinct equilibrated regions, namely an ice region and a liquid water region, as seen in Figure 5. This approach has been widely adopted by researchers in this field (Conde et al., 2018; Rozmanov and Kusalik, 2011; Tsironi et al., 2020; Wu et al., 2017). For instant, (Vrbka and Jungwirth, 2005) have performed extensive MD simulations of ice growth in an aqueous sodium chloride (NaCl) solution. They have reported the change in water oxygen density and ion density profiles along the direction of crystal growth. Similarly, (Carignano et al., 2006) have investigated the growth of hexagonal ice structure from a brine solution. (Fatemi and FOROUTAN, 2016) were able to simulate crystal growth in a brine solution (salinity = 14%) using the coarse-grained mono-atomic water (mW) model, where radial distribution function (RDF) was utilized to describe the relationship between oxygen water molecules and dissolved ions. It was found that Na+ ions are more likely to be closer to liquid molecules than Cl- ions. Additionally, Na^+-ice interactions were much weaker than Na^+-water interactions (Luo et al., 2021). These results suggest higher entrapment of Cl- ions in the ice phase compared to Na+, similar findings were reported by (Luo et al., 2021; Tsironi et al., 2020). For NaCl-water mixture, it was found that ice growth rate is slower at higher concentrations due to the ion-water interactions. Other results revealed that the accumulation of specific anions, e.g., F^-, on the ice-liquid interface critically influence ice structure and growth rates (Zhang et al., 2021).

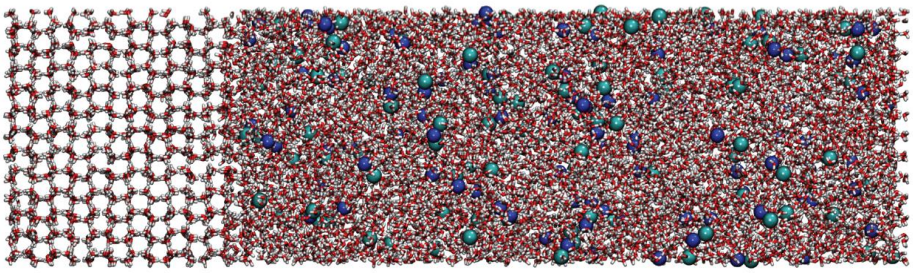

Figure 5. *Initial simulation setup of ice crystal (left) growth in a 0.53M saline water solution (right) with PBC (Color codes: Na+: Dark blue, Cl-: Light blue, H: White, O: Red). Retrieved from* (Tsironi et al., 2020).

2.2. Ice nucleation and surface interactions

Information about the structure and morphology of ice nuclei, the kinetics of nucleation, as well as the role of impurities are important factors in determining the FD performance and can be obtained through MD simulations. However, simulating the nucleation process accurately can be computationally challenging, and many factors can influence the outcome of simulations. This is because ice nucleation exhibits a stochastic nature, with a characteristic time of orders of magnitude longer than those of classical MD simulations (Limmer and Chandler, 2013; Naullage et al., 2020). To initiate the nucleation process in pure water, either deep supercooling or rare event simulations (via enhanced sampling methods) are necessary to overcome the large free energy barriers associated with ice nucleation (Naullage et al., 2020). Water stays supercooled, trapped in a high-energy state (state A), even below the melting point, hindered by an energy barrier (ΔG) from transitioning to stable ice (state B) (Barahona, 2015) (see **Figure 6 (a)**). One of the early studies on homogenous ice nucleation using MD was conducted by Matsumoto et al. (Matsumoto et al., 2002). In this study, water was firstly thermalized at a high temperature, followed by quenching it to a low temperature of 230 K at time t = 0 resulting in a supercooled state of water. As seen in **Figure 7 (a)**, the freezing process of water went into four stages: (1) a long quiescent period (supercooled water), (2) a slow decrease in potential energy, (3) a rapid decrease in potential energy, and a (4) final period where the ice structure fully forms, with intermittent collective motions and energy fluctuations associated with hydrogen bond rearrangements (see **Figure 7 (b)**) occurring during the supercooled liquid state in the quiescent period.

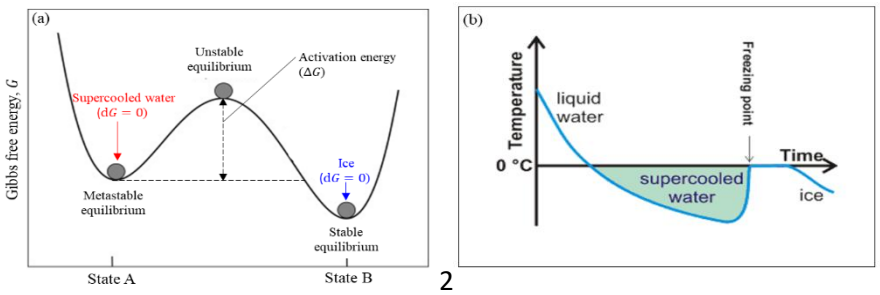

Figure 6. *(a) Free energy as a function of the arrangement of atoms in phases: State A: metastable configuration (supercooled water), State B: stable configuration (ice), (b) cooling curve of pure water*

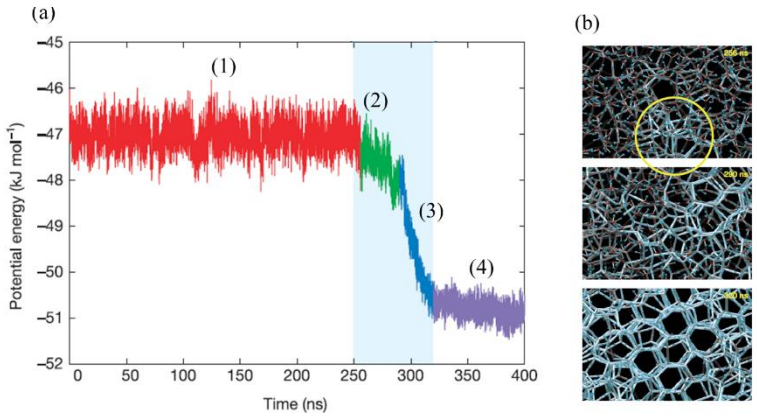

Figure 7. *(a) The total potential energy of the system showing the four stages of water freezing, and (b) the development of "long lasting" hydrogen bond network as developed by* (Matsumoto et al., 2002)

Despite that, if ice nucleation occurs heterogeneously, meaning water is no longer pure and contains dissolved ions/particles or in a direct contact with solid surface, the formation of a metastable state may be inhibited (Langham et al., 1997). In this case, ions can provide nucleation sites to form ice crystals, thus reducing the free energy barrier. Understanding the interaction between the solid surface and the saltwater solution during freezing can help in the design and optimization of FD processes, more specifically for the indirect FD configuration. The surface morphology and properties, e.g., wettability and surface roughness, can affect the ice nucleation (heterogenous nucleation) and growth process, and therefore, the efficiency of the desalination process. Despite the potential of MD simulations in providing atomic-level insights into such phenomenon, the literature on this topic is still relatively scarce. Only a few studies have focused on the behavior of freezing of saline water on solid surfaces using MD (Li et al., 2018; Metya et al., 2016; Metya and Singh, 2018; Moore et al., 2010; Naullage et al., 2020; Ren et al., 2020; Sayer and Cox, 2019; Zielke et al., 2016). This highlights the need for further research efforts to address the knowledge gap in this area and to fully utilize the capabilities of MD simulations in elucidating the underlying physics of FD.

The group of (Metya et al., 2016; Metya and Singh, 2018) have explored the nucleation behavior of a supercooled water (pure water droplet (Metya et al., 2016) and saline bulk solution (Metya and Singh, 2018)) on a nanotextured (Metya et al., 2016) and smooth (Metya and Singh, 2018) graphene surfaces. They found that the ice nucleation rate is enhanced with increasing surface fraction for the Cassie-Baxter state, while the nucleation rate decreases for the Wenzel state with increasing surface fraction (see ***Figure 8***). Moreover, ice adhesion was found to be significantly higher for the Wenzel states compared to the Cassie-Baxter states. Such different wetting states of rough surfaces can give a sense of surface wettability. The authors also showed that a hydrophobic surface is a better nucleating surface when the salinity is above 5%. Heterogeneous ice nucleation occurs at the liquid-solid interface, leading to phase-segregated brine near the liquid-vapor interface. On the other hand, Li et al. (Li et al., 2018) found that the presence of nanogrooves on a surface can have a significant impact on the ice nucleation rate, either enhancing or delaying nucleation depending on the width of the grooves. The study provides critical insights for designing surfaces that can effectively control ice nucleation (Li et al., 2018).

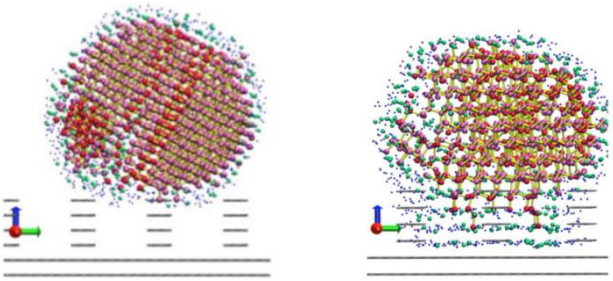

Figure 8. *Water droplet interaction with Cassie-Baxter (left) and Wenzel (right) rough surfaces during ice nucleation* (Metya et al., 2016).

Another important factor that can affect ice formation on surfaces is the presence of ice-nucleating agents (also referred as Ice-binding molecules (IBMs)), which are substances that promote the formation of ice nuclei and facilitate the transition of liquid water to solid ice by lowering the energy barrier for ice nucleation (Abdelmonem et al., 2015; Naullage et al., 2020; Qiu et al., 2019). Ren et al. (Ren et al., 2020) investigated the influence of inorganic salts (LiI, LiCl, NaI, NaCl, KI, KCl, and NH_4I) on the heterogeneous ice nucleation on kaolinite surface ($Al_2Si_2O_5(OH)_4$). The interaction between salts and ice-binding surfaces was found to be relatively weak and non-specific, which can improve the quality of frozen ice. Both Zielke et al. (Zielke et al., 2016) and Sayer et al. (Sayer and Cox, 2019) have investigated ice nucleation on AgI surface using the all-atom TIP4P/2005 water model. The presence of ions (Na^+ and Cl^-) at a water/solid interface have significantly impact the mechanism of ice formation by stabilizing a proton ordered contact layer, potentially leading to more efficient ice nucleation (Sayer and Cox, 2019).

The exact effect of ions on the nucleation process is dependent on several factors, including the ion concentration composition, as well as the temperature and pressure conditions. For instance, it was found that the nucleation rate slows down with salt due to a significant increase in the ice-fluid interfacial free energy, despite the higher thermodynamic driving force for ice nucleation in salty water for a given supercooling (Soria et al., 2018). In another earlier study (Bauerecker et al., 2008), antifreeze effect of adding salt (NaCl: 1 M) on ice nucleation and freezing was investigated, and the molecular mechanisms behind the

corresponding slow down were revealed. On the other hand, Espinosa et al. (Espinosa et al., 2017) reported that increasing operating pressure and solute concentration hinder ice formation by increasing the energy requirement of creating the ice-liquid interface.

3. FUTURE DIRECTIONS

Despite significant advancements in the application of MD simulations to study FD, several research gaps persist, offering substantial opportunities for further exploration. While MD simulations have elucidated the formation and rearrangement of hydrogen bonds of water molecules during the formation of ice crystals, the intricate details of these processes during different stages of freezing require further investigation. Firstly, the transient dynamics of hydrogen bonding during ice nucleation and growth, particularly under varying salinity and temperature conditions, remain underexplored. Secondly, the mechanisms underlying ice entrapment of ions, such as the preferential entrapment of certain ions over others, are not yet fully understood. Identifying the specific molecular interactions and conditions that influence ion entrapment is critical. This includes examining the roles of different ionic species, concentrations, and impurities present in the water. Advanced MD simulations, supplemented with experimental validation, could help elucidate the precise conditions that promote or inhibit ion entrapment during ice crystallization. In addition, there is a need to investigate the rejection rates of various ions during the ice growth process. The interplay between ion-water interactions and hydration energy significantly impacts these rates. Current studies have highlighted that ion-water interactions slow down ice growth at higher concentrations, but a comprehensive understanding of how these interactions affect different ions under diverse operational conditions is lacking. Future research should aim to quantify the impact of specific ion-water interactions on rejection rates and crystal growth dynamics, potentially leading to optimized desalination processes.

MD simulations also have the potential to provide detailed information about ice nucleation and growth on surfaces and the behavior of water molecules and ions at the interface. The knowledge gained from such simulations can be applied to optimize FD processes and mitigate scaling effects caused by impurities. However, simulating freezing on surfaces using MD is computationally challenging, and many factors can influence the simulation results. Despite the promising capabilities of MD, the literature on this topic is still relatively limited, indicating the need for further research efforts. Such efforts will bridge existing knowledge gaps and advance the understanding and efficiency of FD processes.

4. CONCLUSIONS

In conclusion, the application of MD simulations has provided valuable insights into freeze desalination processes, ranging from crystal growth dynamics to surface interactions. However, substantial research gaps remain, necessitating further exploration to unlock the full potential of MD in advancing FD technology. Future research efforts should focus on unraveling the transient dynamics of hydrogen bonding, and explaining ion entrapment mechanisms for various ionic compositions and concentrations. By addressing these knowledge gaps, MD simulations can play a pivotal role in optimizing FD processes and advancing sustainable freshwater production.

5. ACKNOWLEDGEMENTS

This publication is based on the work supported by the Khalifa University under Award No. ESIG-2023-013/847001 and Award No. RIG-2023-107

REFERENCES

Abdelmonem, A., Lützenkirchen, J., Leisner, T., 2015. Probing ice-nucleation processes on the molecular level using second harmonic generation spectroscopy. Atmos. Meas. Tech. 8, 3519–3526. https://doi.org/10.5194/amt-8-3519-2015

Barahona, D., 2015. Thermodynamic derivation of the activation energy for ice nucleation. Atmos Chem Phys 15, 13819–13831. https://doi.org/10.5194/acp-15-13819-2015

Bauerecker, S., Ulbig, P., Buch, V., Vrbka, L., Jungwirth, P., 2008. Monitoring Ice Nucleation in Pure and Salty Water via High-Speed Imaging and Computer Simulations. The Journal of Physical Chemistry C 112, 7631–7636. https://doi.org/10.1021/jp711507f

Carignano, M.A., Baskaran, E., Shepson, P.B., Szleifer, I., 2006. Molecular dynamics simulation of ice growth from supercooled pure water and from salt solution. Ann Glaciol 44, 113–117.

Conde, M.M., Rovere, M., Gallo, P., 2018. Molecular dynamics simulations of freezing-point depression of TIP4P/2005 water in solution with NaCl. J Mol Liq 261, 513–519.

Elif Genceli Güner, F., Wåhlin, J., Hinge, M., Kjelstrup, S., 2015. The temperature jump at a growing ice–water interface. Chem Phys Lett 622, 15–19. https://doi.org/10.1016/J.CPLETT.2015.01.013

Englezos, P., 1994. The freeze concentration process and its applications. Developments in Chemical Engineering and Mineral Processing 2, 3–15.

Espinosa, J.R., Soria, G.D., Ramirez, J., Valeriani, C., Vega, C., Sanz, E., 2017. Role of Salt, Pressure, and Water Activity on Homogeneous Ice Nucleation. J Phys Chem Lett 8, 4486–4491. https://doi.org/10.1021/acs.jpclett.7b01551
Fatemi, S.M., FOROUTAN, M., 2016. Molecular dynamics simulations of freezing behavior of pure water and 14% water-NaCl mixture using the coarse-grained model.
Izutsu, K., 2018. Applications of freezing and freeze-drying in pharmaceutical formulations. Survival Strategies in Extreme Cold and Desiccation: Adaptation Mechanisms and Their Applications 371–383.
Kalista, B., Shin, H., Cho, J., Jang, A., 2018. Current development and future prospect review of freeze desalination. Desalination 447, 167–181. https://doi.org/10.1016/j.desal.2018.09.009
Kucera, J., 2019. Desalination: water from water. John Wiley & Sons.
Langham, E.J., Mason, B.J.-N., Bernal, J.D., 1997. The heterogeneous and homogeneous nucleation of supercooled water. Proc R Soc Lond A Math Phys Sci 247, 493–504. https://doi.org/10.1098/rspa.1958.0207
Li, C., Tao, R., Luo, S., Gao, X., Zhang, K., Li, Z., 2018. Enhancing and Impeding Heterogeneous Ice Nucleation through Nanogrooves. The Journal of Physical Chemistry C 122, 25992–25998. https://doi.org/10.1021/acs.jpcc.8b07779
Limmer, D.T., Chandler, D., 2013. Corresponding states for mesostructure and dynamics of supercooled water. Faraday Discuss 167, 485–498. https://doi.org/10.1039/C3FD00076A
Luo, S., Jin, Y., Tao, R., Li, H., Li, C., Wang, J., Li, Z., 2021. Molecular understanding of ion rejection in the freezing of aqueous solutions. Physical Chemistry Chemical Physics 23, 13292–13299.
Matsumoto, M., Saito, S., Ohmine, I., 2002. Molecular dynamics simulation of the ice nucleation and growth process leading to water freezing. Nature 416, 409–413. https://doi.org/10.1038/416409a
Metya, A.K., Singh, J.K., 2018. Nucleation of Aqueous Salt Solutions on Solid Surfaces. The Journal of Physical Chemistry C 122, 8277–8287. https://doi.org/10.1021/acs.jpcc.7b12495
Metya, A.K., Singh, J.K., Müller-Plathe, F., 2016. Ice nucleation on nanotextured surfaces: the influence of surface fraction, pillar height and wetting states. Physical Chemistry Chemical Physics 18, 26796–26806. https://doi.org/10.1039/C6CP04382H
Moore, E.B., de la Llave, E., Welke, K., Scherlis, D.A., Molinero, V., 2010. Freezing, melting and structure of ice in a hydrophilic nanopore. Physical Chemistry Chemical Physics 12, 4124–4134. https://doi.org/10.1039/B919724A
Nathoo, J., Jivanji, R., Lewis, A.E., 2009. Freezing your brines off: eutectic freeze crystallization for brine treatment, in: International Mine Water Conference. pp. 431–437.
Naullage, P.M., Metya, A.K., Molinero, V., 2020. Computationally efficient approach for the identification of ice-binding surfaces and how they bind ice. J Chem Phys 153, 174106. https://doi.org/10.1063/5.0021631
Pangborn, J.B., 1963. Observations of the eutectic freezing of salt solutions. Report to AJ Barduhn, Department of Chemical Engineering, Syracuse University.
Qiu, Y., Hudait, A., Molinero, V., 2019. How Size and Aggregation of Ice-Binding Proteins Control Their Ice Nucleation Efficiency. J Am Chem Soc 141, 7439–7452. https://doi.org/10.1021/jacs.9b01854
Ren, Y., Bertram, A.K., Patey, G.N., 2020. Effects of Inorganic Ions on Ice Nucleation by the Al Surface of Kaolinite Immersed in Water. J Phys Chem B 124, 4605–4618. https://doi.org/10.1021/acs.jpcb.0c01695
Rozmanov, D., Kusalik, P.G., 2011. Temperature dependence of crystal growth of hexagonal ice (I h). Physical Chemistry Chemical Physics 13, 15501–15511.
Saji, V.S., Meroufel, A.A., Sorour, A.A., 2020. Corrosion and fouling control in desalination industry. Springer.
Sánchez, J., Ruiz, Y., Auleda, J.M., Hernández, E., Raventós, M., 2009. Freeze concentration in the fruit juices industry. Food Science and Technology International 15, 303–315.
Sayer, T., Cox, S.J., 2019. Stabilization of AgI's polar surfaces by the aqueous environment, and its implications for ice formation. Physical Chemistry Chemical Physics 21, 14546–14555. https://doi.org/10.1039/C9CP02193K
Slattery, J.C., Sagis, L., Oh, E.-S., 2007. Interfacial transport phenomena. Springer Science & Business Media.
Soria, G.D., Espinosa, J.R., Ramirez, J., Valeriani, C., Vega, C., Sanz, E., 2018. A simulation study of homogeneous ice nucleation in supercooled salty water. J Chem Phys 148, 222811.
Stepakoff, G.L., Siegelman, D., Johnson, R., Gibson, W., 1974. Development of a eutectic freezing process for brine disposal. Desalination 15, 25–38.
Tsironi, I., Schlesinger, D., Späh, A., Eriksson, L., Segad, M., Perakis, F., 2020. Brine rejection and hydrate formation upon freezing of NaCl aqueous solutions. Physical Chemistry Chemical Physics 22, 7625–7632.
Vrbka, L., Jungwirth, P., 2005. Brine rejection from freezing salt solutions: A molecular dynamics study. Phys Rev Lett 95, 148501.
Whaley, D., Damyar, K., Witek, R.P., Mendoza, A., Alexander, M., Lakey, J.R.T., 2021. Cryopreservation: an overview of principles and cell-specific considerations. Cell Transplant 30, 0963689721999617.
Williams, P.M., Ahmad, M., Connolly, B.S., Oatley-Radcliffe, D.L., 2015. Technology for freeze concentration in the desalination industry. Desalination 356, 314–327.
Wu, S., Zhu, C., He, Z., Xue, H., Fan, Q., Song, Y., Francisco, J.S., Zeng, X.C., Wang, J., 2017. Ion-specific ice recrystallization provides a facile approach for the fabrication of porous materials. Nat Commun 8, 15154.
Zhang, S., Zhang, C., Wu, S., Zhou, X., He, Z., Wang, J., 2021. Ion-specific effects on the growth of single ice crystals. J Phys Chem Lett 12, 8726–8731.
Zielke, S.A., Bertram, A.K., Patey, G.N., 2016. Simulations of Ice Nucleation by Model AgI Disks and Plates. J Phys Chem B 120, 2291–2299. https://doi.org/10.1021/acs.jpcb.5b06605

Session 10: Environmental management

Pangaea.cubes - IoT Low Power Challenges towards Sustainability. H/W - S/W Design implementations and applications.

T. Thomaidis-Theodosiadis[1], G. Panagopoulou[2] and V. Vorrias[2]
[1] Gridnet S.A., Volos, Greece, [2] Pangaea R&D, Larisa, Greece
Corresponding author email: thomaidistv@gmail.com

keywords: *IoT; Sustainability; Smart Cities; Smart Agriculture; .*

Introduction

The current "Pangaea IoT.Cubes" design proposal yields as a result of the common effort of startups Pangaea and Gridnet R&D teams to create innovative Low Power IoT wireless smart-autonomous devices towards supporting the United Nations Sustainable Development Goals (1) for Sustainability. Emphasis has been given on four particular goals that are related to cities and sustainability, as follows, Goal 7: Affordable and clean energy, Goal 11: Sustainable Cities and Communities, Goal 13: Climate Action and Goal 15: Life on Land. It should be emphasized that "The creativity, knowhow, technology and financial resources from all of society is necessary to achieve the SDGs in every context"**.** Pangaea R&D and Gridnet SA as IoT solution providers - among others - for precision agriculture, are supporting farmers and agronomists all over Greece.

Vision and Technology

The vision of Pangaea R&D is a modern multidisciplinary approach towards the development of intelligent and environmentally friendly solutions in accordance with the current state of the art industrial developments. Among Pangaea R&D goals are the development and implementation of technological innovations and know-how, in the modern rural and urban areas, through collaboration with academic and research institutes, via networking, coordination and collaborative actions of complementary disciplines, thus covering the fields of smart agriculture, smart cities, maritime informatics, telematics and innovative production technologies. In that respect our vision is to embed the new features/capabilities of SotA technologies (i.e. nRF9160) as compact, smart and low power System in Package (SiP) with integrated LTE-M / NB-IoT modem and GNSS, with advanced processing and security capabilities, accessible and easy to use aggregated to "a family" of single devices of low power cellular IoT designs, namely: Pangae.IoT.cubes. The efficient utilisation of our technologies are strongly related to cloud continuum, ranging from centralised cloud data centres through fog and edge nodes to IoT devices, playing a crucial role in the implementation of advanced data-driven applications, including emerging AI and machine-learning-based applications, beyond the 5G era.

Current research/experimentation

During this realisation, valuable insight has been gained, among various research programmes, of the FED4Fire–Field Research on Precision Agriculture With LoRa, via the PAWL experimentation research (2021) where open field precision agriculture applications investigated the performance of LoRa (low-power wide-area network modulation technique) vs to ZigBee based solutions, optimising the cost effectiveness and reliability of the provided IoT solutions on various aspects like coverage, throughput and energy efficiency. (https://pan-gaea.gr/fed4fire/).

Currently our research is conducted via the Raft4CC project. With its distributed and federated model, the cloud continuum helps to address the pressing challenges of exploiting data generated at the network edge and by IoT devices. The efficient operation of this distributed model requires a consensus protocol, such as Raft, in order to coordinate the geo-distributed sites. In that respect Raft4CC project pioneered the development of an efficient consensus mechanism to support top-tier distributed applications on the computing continuum. A comprehensive series of experiments were conducted in authentic scenarios that were implemented in SLICES. The SLICES resources, which were distributed, were used to deploy Raft-operated systems that spanned multiple locations across Europe.

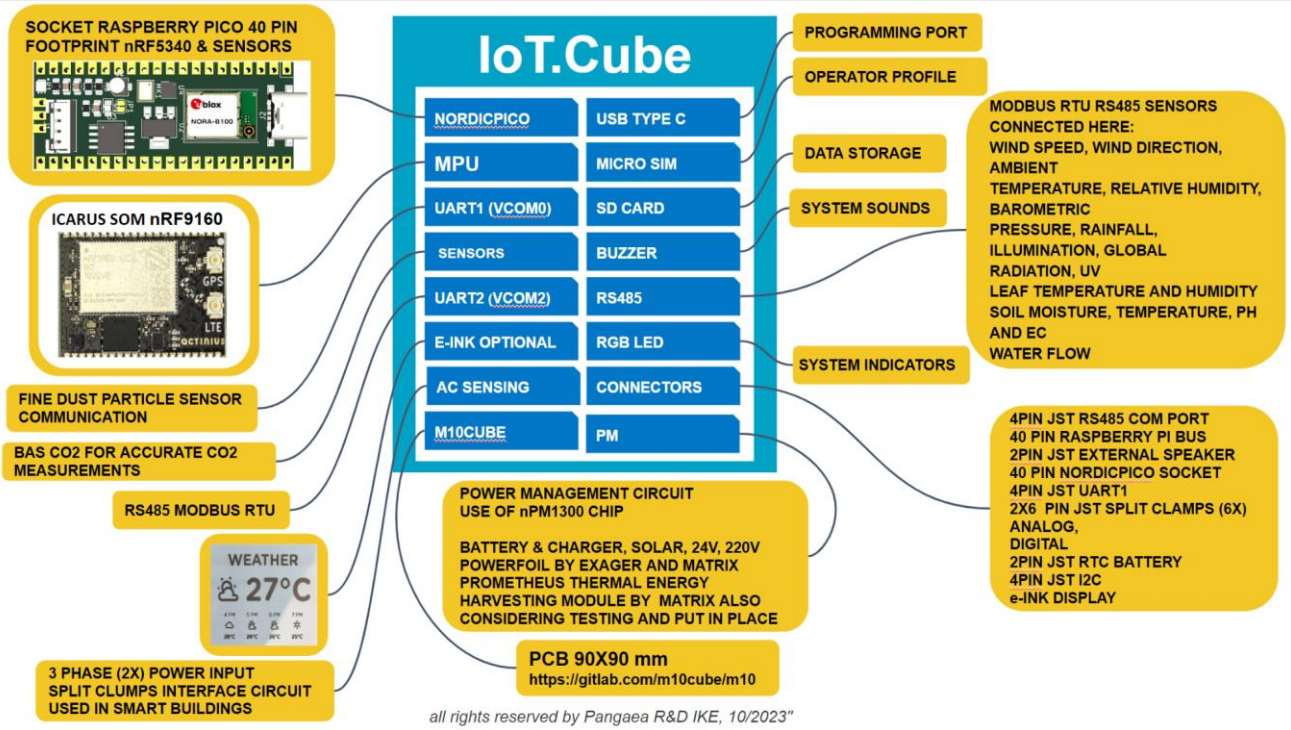

Figure 1. *Pangae.IoT.cube: A compact, smart and low power self sustained System in Package (SiP) with integrated LTE-M / NB-IoT modem and GNSS, with advanced processing and security capabilities.*

Pangaea.IoT.Cubes leverage concurrently deployed, multi-protocol communication capabilities (WiFi6, Bluetooth Low Energy (BLE) Mesh, Thread, Matter, Zigbee, LTE, LTE-M, NB-IoT) based on advanced federated Raft4CC models, enabling their application in diverse commercial fields.

Acknowledgements: This study is supported by:
-The SLICES-SC EU Horizon 2020 research and innovation programme under grant agreement No 101008468
-GRIDNET sa, as pioneer developers of communication and internet technology solutions, wireless communications, software-defined networking, distributed sensors networking and energy management, https://gridnet.gr/

References

Theodosiadis-Thomaidis, T., Panagopoulou, G and Pistikopoulos, S. 2022, SUSTENG 2022, 31 Aug – 04 Sep 2022, Rethymno, Crete, Greece ISBN: 978-618-86417-0-9, p.p.283-284, “Development of computational tools for criticality analysis of process systems, utilizing Industrial IoTs”

United Nations Sustainable Development Goals (SDGs) - Global Goals
https://www.undp.org/sustainable-development-goals

The Fed4FIRE+ project: a continuation of Fed4FIRE’s “best-in-town” federation of experimentation facilities for the Future Internet Research and Experimentation initiative.
SLICES-SC Open Call, The Winners,1st round The CAP BABEL MACHINE Project - https://slices-sc.eu/slices-sc-open-call-id-call-2-the-winners/

Development of Sustainable Communication Systems Supported by High-Impact Environmental Energy Sources for People on the Move

Stacey D. Lyle, PhD, Professor of Practice[1], Pappas, Konstantinos, PhD, Assistant Director[2] and Cynthia Lyle, Senior Research Development Officer[3]

[1] Zachry Department of Civil and Environmental Engineering Texas A&M University, College Station, Texas USA
[2] Energy Institute, Texas A&M University, College Station, Texas USA
[3] Energy Institute, Texas A&M University, College Station, Texas USA

Corresponding author email: stacey.lyle@tamu.e4du

keywords: *geothermal energy, communication networks, population*

Abstract

With the number of international migrants estimated to be nearly 281 million globally, more people are on the move than ever before. Globally, more than 108 million people are forcibly displaced by conflict, violence, human rights violations, and disasters. Hazardous events, amplified by compound risk factors such as ecosystem degradation, climate change, conflict, epidemics and pandemics, and underlying conditions, such as weak governance, corruption, and violence – will increase displacement in the years to come and compel millions to migrate within and across borders. People on the move often rely on mobile communication devices to seek their basic needs - safety, shelter, first aid, and food. In 2016, the United Nations Refugee Agency reported that refugees and migrants, speaking various languages, accessed and disseminated critical information through mobile cellular devices. However, poor internet connectivity resulting from downed communication cellular towers remains a significant challenge. Reliable cellular towers use backup power sources, such as generators, but these require continuous refueling. Poorly functioning cellular towers can disrupt communication during critical times. Wind and solar energy have been proposed as alternatives, but their production varies due to environmental weather conditions. An alternative solution is to power cellular towers using continuous renewable geothermal energy. Geothermal energy harnesses heat from the Earth's interior, making it a clean and sustainable resource. Properly managed geothermal plants have minimal environmental impact. Leveraging geothermal energy could offer a resilient and environmentally friendly solution to power communication infrastructure for people on the move. Establishing partnerships among scientists, engineers, government agencies, energy companies, communication providers, and non-governmental organizations is crucial in order to reduce environmental impact, while promoting energy efficiency for sustainable communication networks. By working together, we can create a more efficient and reliable network that supports those in need. This presentation will lay the foundation for implementing a collaborative plan aimed at reducing environmental impacts and enhancing energy efficiency in sustainable communication networks.

References

Atkinson, C., James, K., 2009. *Green gone wrong, Deutsche Welle, Retrieved from https://www.dw.com/en/green-good-intentions-cause-chaos-in-two-german-towns/a-4473382*

UNHCR, 2015. Increasing two-way communication with refugees on the move in Europe., : UNHCR Innovation Service: Year in Review 2016 Report, Retrieved from https://www.unhcr.org/innovation/increasing-two-way-communication-with-refugees-on-the-move-in-europe/

Lyle, W., 2024. *Using Geospatial Technologies to Lower Carbon Intensity at Chevron, 2024 ESRI Energy Resources GIS Conference, Houston, Texas* https://www.esri.com/en-us/about/events/esri-energy-resources-gis-conference/overview

Daher B., Pappas K., Lavell A. (2023) White Paper A Systems Approach for Disaster Risk Reduction: Exploring the Nexus of Energy, Food, and Human Mobility in the Northern Countries of Central America. Disaster Risk Reduction, United Nations Office for Disaster Risk Reduction (UNDRR) https://www.undrr.org/publication/white-paper-systems-approach-disaster-risk-reduction-exploring-nexus-energy-food-and

Forest food resources back to the menu for enhancing food sovereignty in a context of high hybridation: case of *Adansonia digitata* and *Irvingia gabonensis*

Flora Josiane Chadare[1], Finagnon Toyi Kevin Fassinou[1], Simon Ahouansou Montcho[2], Marius Affonfere[1], Achille Assogbadjo[3]

[1]Laboratoire de Sciences et Technologie des Aliments et Bioressources et de Nutrition Humaine, Ecole des Sciences et Techniques de Conservation et de Transformation des Produits Agricoles, Centre Universitaire de Sakété, Université Nationale d'Agriculture, Sakété, République du Bénin
[2.] Ecole d'Aquaculture, Centre Universitaire d'Adjohoun, Université Nationale d'Agriculture, République du Bénin
[3]Faculty of Agronomic Sciences, University of Abomey-Calavi, République du Bénin
Corresponding author email: fchadare@gmail.com

keywords: Food security; Baobab; Mutchayan; food and nutritional value; non timber forest products.

Introduction

Food and nutritional security have been threatened by several issues including climatic, geopolitical and sanitary crisis. Indeed, after remaining relatively stable up to 2015, the proportion of hungry people increased from 6% in 2019 to reach 9.8% of the world population in 2021.
It is foreseen that more than 670 million people (8% of word population) are still hungry in 2030 even with economic recovery. Africa comes out as one to be the most affected part of the world which is mainly explained by its dependency vis a vis of the exogenous resources. As such, the food sovereignty of African population looks more and more hindered.

At the same moment, in most tropical countries, the Non Timber Forest Products (NTFPs) play an important role in the daily life and well-being of the local population (Babalola & Agbeja, 2009). Among them, the Baobab, Adansonia digitata is key economic tree used daily by local populations in Africa. The baobab fruit pulp are known very used to make a gruel, the sour dough and the beverage (Kaboré et al., 2011). The fruit pulp has high nutritional value and its products are reported used to improve food security (De Caluwé et al., 2010). In West and Central African, the *Irvingia gobonensis* tree are a preferred tree and a valuable source of income for local population (Ayuk et al., 1999, Babalola & Agbeja, 2009). Its seed is reported to be a good source of protein, minerals and fats (Atawodi, 2011). Though some studies were conducted within *Adansonia digitata* and *Irvingia gabonensis* plant part nutritional values (Chadare, 2010, Giami et al., 1994, Oboh & Ekperigin, 2004), nutritional values on their derived products were poorly investigated. This study aims at characterizing baobab (*Adansonia digitata*) and African bush mango (*Irvingia gabonensis*) fruits pulp and theirs most important derived product nutritional values as reported by local populations.

Materials and methods

The paper presents an investigation on food and nutritional non-timber forest products with a focus on baobab and african bush mangoe and their derived products. Selected factors affecting food sovereignty has been analysed including heavy food importations and non-timber forest products are proposed as alternative to food sovereignty. To analyse the food and nutritional value of non-timber forest products, field survey was conducted to check the consumption frequency of baobab and African bush mango fruit pulp and their derived products. The most important derived products were selected for each species and the processing follow up on its derived product was performed. Laboratory analysis was conducted on the BFP and ABMF and their derived products. The survey was carried out in two biogeographical zones of Benin mainly Sudanian zone (Materi and Tanguiéta) and Guinean zone (Come and Azove) where baobab and/or African bush mango naturally occur and used by populations (Assogbadjo *et al*., 2005, Vihotogbe, 2012). Collected data were related to consumption frequency daily and per week, the proportion of informants using foods derived from baobab pulp or african bush mangoe and processing techniques of derived products. Most important products were selected by using weighted derived product score. Physico-chemical and nutritional value of the raw

material (baobab pulp or african bush mangoe pulp) and the most important derived product were evaluated using standard methods.

Results and discussion

While Food security requires having enough food of the right quality available and accessible to everyone, food sovereignty promotes local and sustainable food production, protects the environment and natural resources, and preserves food and cultural traditions. It aims to ensure that populations can feed themselves autonomously, without excessive dependence on food imports or external decisions regarding agriculture and food. In such a context, excessive dependency of exogenous foods and goods somehow hinders the food sovereignty of local population especially in urban areas where food mostly consumed by populations are not always aligned with their culture and whose production circumstance are not controlled by themselves. For instance, cereals and fertilizers importations by two countries from sub-Sahara Africa namely Senegal and Benin showed that they have imported in 2022 cereals for USD 350,000 thousands for Senegal and for about USD 400,000 thousand for Benin, mainly rice followed by wheat (Figure 1).

Though rice production is a reality in Senegal and Benin, the local production which may respect cultural and sustainability needs are not enough always enough to feed the demand of rice consumption in the targeted countries where there seems to be a shift of diet. Wheat which is not produced by both countries looks also well consumed by the population in Senegal and Benin. An alternative to enhance food sovereignty is the promotion of non-timber forest foods whose derived products should be back in the menu. Examples of African bush mangoe and baobab are presented in this paper. Muchayan, a paste made of cereal dough and baobab pulp comes out as the most important product from baobab fruit pulp followed bu moukou-moukou and prorridge (cereal based enriched with baoab pulp). No derived product was found from African bush mango fruit pulp at local level in Benin. Mutchayan is mostly used as tonifying drink. Its nutritional value is 12.16±0.08g/100g dw for carbohydrate and 1.77±0.48g/100g dw for protein. Mutchayan iron, calcium and zinc content were respectively 1.75±0.02mg/100g dw, 0.10±0.01mg/100g dw and 0.35±0.04mg/100g (dw). African bush mango is consumed just as a fruit and its pulp (ABMF) contains 12.56±0.10g/100g dw of carbohydrate and 1.32±0.24g/100g dw of protein content. The iron content of ABMF is 0.29±0.07mg/100g dw and its calcium and zinc content were respectively 0.02±0.01mg/100g dw and 0.09±0.03mg/100g dw. Its vitamin A content was 500±0.01µg/100g (dw) (Table 1). Stabilisation and increased production of Mutchayan is a channel for entrepreneurship of young women and men.

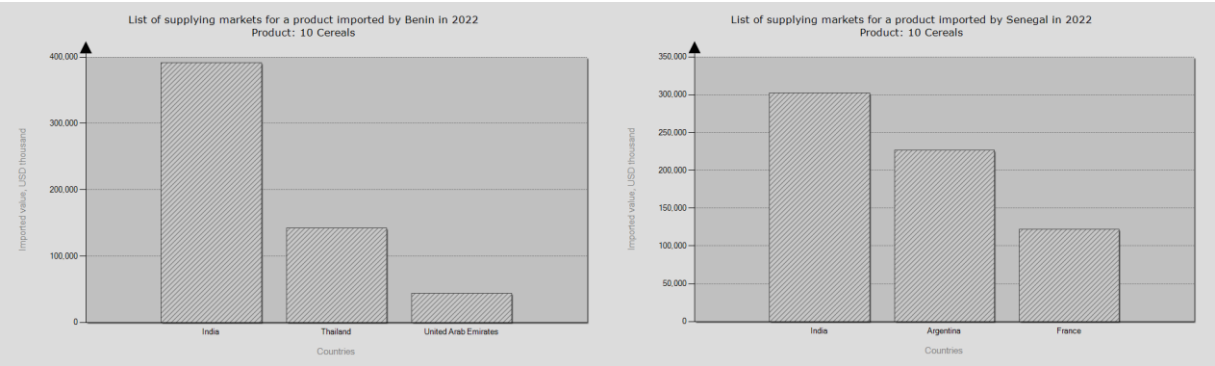

Figure 1. Importation of cereals by Benin and Senegal

Sources: ITC calculations based on Institut National de la Statistique et de l'Analyse Economique du Bénin statistics. // ITC calculations based on Agence Nationale de la Statistique et de la Démographie du Sénégal statistics.

Conclusions.

Endogenous foods are integrated to the food habit and culture of local populations. As a result of hybridation, there is a shift in diet occuring mainly in African urbam area. Forest foods should be back to the menu to reduce food importation by African countries and consequently promote food sovereignty.

Acknowledgements. This study is supported by the mastercard foundation through Tagdev2.0 project.

References. Mbaeyi-Nwaoha, et.al 2017, *Food Science and Technology* **5,** 56-69

Early-stage Mathematical Modeling of Solution Spray Pyrolysis for the Fabrication of Functional Ceramic Films

N. Fotiadi[2], D. Lazaridis[1], N.Rigakis[3] and N. Kiratzis[1]

[1]Laboratory of Advanced Materials and Electrochemical Technology (ElectrocheMat Lab)/Department of Mineral Resources Engineering/School of Engineering, University of Western Macedonia, Kozani, Greece
[2]Department of Chemical Engineering/School of Engineering, University of Western Macedonia, Kozani, Greece
[3]1st General Secondary Education Lyceum of Grevena, Grevena, Greece
Corresponding author email: nkiratzis@uowm.gr

keywords: *Ceramic film; Spray Pyrolysis; Mathematical Modeling;.*

Introduction

Ceramic or composite ceramic-metallic membranes (cermets) are widely used as electrodes in various devices such as ceramic fuel cells or electrolyzers, gas sensors, and ceramic membranes. Parameters such as membrane thickness, porosity, and tortuosity regulate the extent and relative contribution of concentration and activation polarization losses in electrochemical reactions in ceramic fuel cells and electrolyzers. It is crucial during the fabrication of such structures to control the morphology of the produced film structure to achieve optimal values of electrochemical reaction and diffusion rates.

Recent research efforts in developing the aforementioned devices have focused on innovative fabrication methods that allow control over the morphological characteristics of the produced thin ceramic membranes according to their required functional properties. Such methods mainly belong to the category of molecular deposition methods where the film formation is determined by a series of physicochemical processes of the precursor molecules suitably regulated by the deposition method parameters in such a way that the fabricated film acquires the required morphological and functional characteristics.

One of the promising methods in this category is the technique of solution spray pyrolysis (SAT), which essentially involves the preparation of thin simple and/or mixed inorganic oxide films by spraying a solution of salts with appropriate ions in suitable molecular ratios within a thermal field and on a suitable substrate for the time required for the decomposition of salts into the appropriate oxides. A typical experimental set-up is shown in Figure 1. The advantages of the method, besides its low cost, lie in its simplicity since it operates in an open atmosphere, precise control of stoichiometry at a droplet level, and the direct correlation of the solution's physicochemical properties and the process parameters with the properties of the final ceramic film (morphology, particle size). Modeling efforts of this technique have not been widely documented in the literature, with perhaps the most significant being the physical-chemical mechanisms of Messing et al. and Jayanthi et al.

In this work, we extend the mathematical model of the above authors to simulate the spray pyrolysis of an aqueous solution for depositing ZrO_2, CeO_2, and $LaMnO_3$ films using the Wolfram Mathematica software. Mass and heat transfer equations are applied at the droplet level, and we focus on the initial stages of the process. The theoretical results, in the form of concentration profiles of the dissolved substance inside the droplet, are compared with the morphology of experimental membranes.

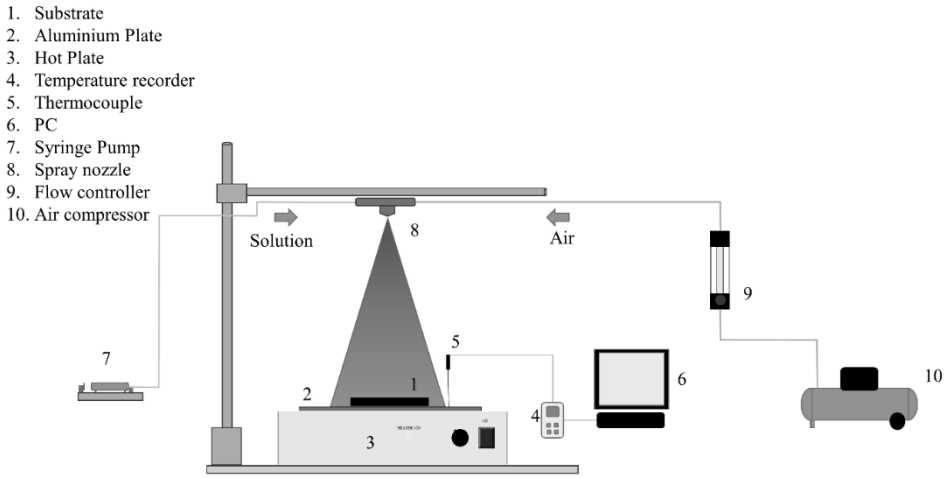

Figure 1. *A typical Experimental Set-up of the Solution Spray Pyrolysis (SAT) process.*

References

He W, Yoon KJ, Eriksen RS, Gopalan S, Basu SN, and Pal UB. (2010). *Journal of Power Sources*, 195:532-535

He W and Goodenough JB. (2014). *Journal of Power Sources*, 251:108-112.

Kiratzis NE. (2016). Ionics, 22:751-770.

Krestou A, Giozis I, Maroulis G, Barbatsis A, Tsanaktsidis C, Kyriakou V and Kiratzis NE.(2018). *ECS Journal of Solid State Science and Technology*, 7 (11): P660-P670.

Messing GL, Zhang S-C, Jayanthi GV. (1993). *J Am Ceram Soc*, 76(11):2707 – 2726.

Jayanthi GV, Zhang S-C, Messing GL.(1993). *Aerosol Science and Technology* (1993) 19: 478-490.

Life Cycle Assessment to address key environmental impact elements of ERASE, an innovative in situ remediation technology

Gabriele Beretta[1], Elena Sezenna[1], Giovanni Dolci[1], Lucia Rigamonti[1], Sabrina Saponaro[1], Claudio Carnabuci[2], Daniele Vezzoli[2]

[1]Department of Civil and Environmental Engineering, Politecnico di Milano, Milano, Italy
[2]HPC Italia srl, Milano
Corresponding author email: gabriele.beretta@polimi.it

keywords: *Electrode-aided remediation; soil; LCA; sustainable remediation.*

Introduction

Soil is a non-renewable resource and, together with groundwater, needs to be preserved for the next generations and eventually restored from negative impacts through appropriate remedial measures and interventions.

The main goal of soil and groundwater sustainable remediation is to mitigate contamination and effectively reduce/control the associated risks, considering the potential environmental impacts that may arise from remediation activities to maximize the overall benefits of the intervention.

In the framework of the Polluted Site Decontamination Pre-Commercial Procurement (POSIDON PCP), HPC Italia srl and Politecnico di Milano – Civil and Environmental Engineering Department proposed and developed, from the laboratory proof of concept up to field testing, an in situ remediation technique (ERASE - ElectRode-Aided Soil rEmediation). ERASE is based on the integration and simultaneous exploitation of physical, chemical, and biological mechanisms induced by properly powering at least one pair of electrodes installed in a porous medium (heterogeneous soil/backfilling materials, under saturated or unsaturated conditions), contaminated by organic and inorganic pollutants.

Contemporaneity to the technology development process a Life Cycle Assessment (LCA) of the proposed solution was performed to evaluate its environmental impacts. The LCA identified key impact factors (electrodes life cycle and electricity consumption) as the most relevant environmental burdens (Beretta et al. 2023). This paper focuses on the outcomes of pilot testing in Bilbao and comparing through LCA different electrode materials and different electrical energy sources.

Materials and methods

Overview of pilot test in Bilbao

The ERASE pilot testing in Bilbao (ES) took place in a small portion of the former Zorrotzaurre industrial area, highly contaminated with Total Petroleum Hydrocarbons (TPHs), Polycyclic Aromatic Hydrocarbons (PAHs), and Inorganics (i.e., As, Pb, and Cd). The pilot plant consisted of an electrical unit (i.e., 18 electrode pairs and the power supply system), a hydraulic unit (i.e., injection/extraction systems), and a monitoring unit (to monitor electrical parameters, saturated and unsaturated porous medium).

The field strategy was structured according to the following phases: a) installation of the plant, preliminary checks, and tuning; b) DC operation and dosing of persulfate, to promote electrokinetic transport mechanisms of inorganic pollutants and the distribution of the oxidant; c) AC operation to heat the soil to 30° - 40°C and thermally activate the oxidant.

Life Cycle Assessment method

The LCA was performed according to the ISO 14044 and 14040 standards (ISO, 2006a; ISO, 2006b). The selected functional unit (FU) was the overall pilot test including preliminary activities, operational activities, and the decommissioning of the pilot plant.

The Environmental Footprint 3.0 (Fazio et al., 2018) method, that includes 16 impact categories on human health and environment, was selected. Normalization and weighting stages were not performed.

Based on the pilot test data, performed by using titanium electrodes and the national power grid as the electricity source, the assessment aimed to investigate the effects of the electrode material and the electricity

source on the environmental performance of the cleanup system. The ecoinvent database (version 3.8 allocation, cut-off by classification system model) was used to support the analysis (ecoinvent centre, 2021). The systems were modeled with the SimaPro software (9.3 version).

Results and discussion

Regarding the impacts related to the production of one electrode (unit impact) for the different electrode materials considered, the analysis has shown that: - when chromium steel is used compared to titanium, impacts decrease in all the impact categories with reductions in the range of 9.8 - 97%. Greater reductions, between 61.5 and 99.8%, are obtained by using graphite. However, graphite is poorly resistant to corrosion during the process, and, despite the use of thicker electrodes, testing would be required especially in the DC phase.

The use of photovoltaic energy (totally or mixed with a national grid source) allows for the reduction of potential impacts in all the impact categories excluding "Resource use, mineral and metals" (RUM). RUM impact category is strictly related to the production of photovoltaic panels (PPs) and might be mitigated by reusing PPs for other reclamation interventions.

From the detailed analysis of the impact categories of each stage of the pilot plant, considering chromium steel electrodes and electricity source as a mix of on-site PPs and national grid, the most relevant burden is related to "Electricity consumption", followed by "Production, installation, decommissioning, end-of-life of electrodes" (stage A) and "Production and use of chemicals". About stage A, most of the potential impacts are related to the production of the electrodes. The choice of on-site renewable energy can, however, partially mitigate the impacts of this electrode material.

Conclusions

LCA allowed the identification of the field-scale pilot test key elements (Electricity consumption", "Production, installation, decommissioning, and end-of-life of electrodes" and "Production and use of chemicals") that might be improved to reduce the environmental impacts and increase the ERASE technology's environmental performance. Useful suggestions came from the outcomes of the comparison of different electrode materials (titanium, chromium steel, and graphite) and electricity sources (grid energy, photovoltaic energy, or a combination of them). Chromium steel electrodes and energy partially from renewable sources (photovoltaic panels) ensure a significant reduction in the potential impacts of the remediation intervention (up to -74%, titanium electrodes powered by the national grid).

Acknowledgements: This work was part of the POSIDON project, which received funding from the Horizon 2020 research and innovation program of the European Union (under grant agreement No. 776838). It reflects only the views of the authors.

References

Beretta G., Sezenna E., Dolci G., Rigamonti L., Saponaro S., Carnabuci C., and Vezzoli D. (2023). LCA in the development of an in-situ innovative remediation technology: the case of ERASE-ElectRode-Aided Soil rEmediation. In L'innovazione per la sostenibilità ambientale nell'epoca della multitransizione (pp. 377-380). Cnr Edizioni.

Fazio S., Castellani V., Sala S., Schau E.M., Secchi M., and Zampori L. (2018) Supporting information to the characterization factors of recommended EF Life Cycle Impact Assessment methods. EUR 28888 EN, European Commission, Ispra, 2018, ISBN 978-92-79-76742-5, JRC109369

Ecoinvent centre (2021) Ecoinvent Version 3.8 database. Available at: http://www.ecoinvent.org/

Joint Research Center, EU Science HUB, Photovoltaic Geographical Information System (PVGIS) tools. Available at: https://re.jrc.ec.europa.eu/pvg_tools/en/

West African Mangroves in the Context of Climate Change: Social-Ecological Dynamics, Challenges and Perspectives

Romain Glèlè Kakaï

Laboratoire de Biomathématiques et d'Estimations Forestières, Faculty of Agronomic Sciences, University of Abomey-Calavi, 04 BP 1525, Cotonou, Republic of Benin
glele.romain@gmail.com

***Keywords**: Coastal ecosystems, Conservation, Participative management, Economic value, Traditional beliefs.*

Abstract

Mangroves are coastal ecosystems composed of shrub and tree species communities which only develop in the tidal zone of tropical and sub-tropical regions. They constitute natural barriers against storm surges, tsunamis, sea level rise and erosion and stock five times more carbon than other forest ecosystems. They cover less than 1% of the globe but provide important ecosystem services to humanity. They are, however, declining and threatened by anthropogenic activities and climate change. Around 50% of mangroves in Benin were lost in less than five decades. Several restoration projects have been initiated to restore the degraded sites, but the successes recorded are generally not commensurate with the investments. Diagnostics suggest that this is partly due to the poor understanding and consideration of socio-ecological aspects and the biology of mangroves in restoration and management projects. Furthermore, research on mangroves in West Africa is low, resulting in a very low contribution of West Africa to the global literature on mangroves despite being home to 13.2% of mangroves globally. This presentation focuses on (i) providing scientific data and knowledge for the sustainable management of mangroves, (ii) Contributing to the integrated conservation of mangroves to achieve the resilience of the West African coasts, and (iii) contributing to regional and global scientific knowledge on mangroves. Some main topics related to mangroves are highlighted, such as spatio-temporal dynamics, ecosystem services and their economic values. In addition, some other aspects are developed like the impacts of anthropogenic activities on the stand structure of mangrove forests, the impacts of climate change on mangrove ecosystems, the development of specific and local allometric equations for a more precise estimate of carbon stock, eco-physiological responses of mangrove species to salinity in nurseries and natural environments, and the effectiveness of traditional systems (local deities) and participatory management on the conservation of mangroves. This presentation will summarize this exciting journey and present the perspectives and challenges.

SUSTENG 2024

SUSTENG 2024

PROGRAMME

Posters

Biogas potential of distillery stillage and evaluation of digestate as a potential fertilizer

I. Vaskina[1,2], R. Vaskin[2], M. Cieslik[1], A. Lewicki[1], L. Demkova[3], M. Skidanenko[2], S. Sydorenko[2]

[1]Department of Biosystems Engineering, Poznan University of Life Sciences, Poznan, Poland
[2]Department of Ecology and Environmental Protection Technologies, Sumy State University, Sumy, Ukraine
[3]Department of Ecology, Presov University, Presov, Slovak Republic

Corresponding author email: iryna.vaskina@up.poznan.pl

keywords: *anaerobic fermentation, fertilizers, bioethanol, sustainable agriculture, waste.*

Introduction

The hostilities in Ukraine and Israel and the uncertain global situation affect the possibility of sustainable development in the nearest future and cause emergencies in all spheres of life, especially high risks in global energy and food security. Therefore, solutions for fighting these risks are extremely important. The issue of food security is deeply connected with the limitation of grain export (Ukraine is one of the biggest world exporters) and, on the other hand, with the quality of agricultural soils affected by the continuous shelling of the Ukrainian territory. Due to the damage to the port infrastructure of Ukraine by Russia, more and more Ukrainian agricultural producers can't export harvested grain (wheat, corn etc.) and looking for other solutions. That's why, processing of the grains into bioethanol is becoming increasingly popular.

Producing the bioethanol leads to the formation of large amounts of waste (distillery stillage) - 12-15 dm^3 of waste per 1 dm^3 of alcohol, so it makes a significant impact on the environment. Stillage is usually used to feed farm animals (due to high protein levels). On the other hand, it contains different mineral substances - phosphates, nitrates, sulfates, and potassium - which could affect the soil properties. However, direct application on the field is limited because of specific smell due to the presence of sulfur-containing compounds (indole, skatole). Another important characteristic of stillage is high levels of chemical oxygen demand (COD) - 60-150 g/dm^3) and biochemical oxygen demand (BOD) - 35-60 g/dm3 (Mikucka and Zielińska, 2020) which is also an obstacle to its unlimited application on agricultural lands.

Anaerobic digestion is a very beneficial process of stillage treatment. It will allow to recovery of energy from it in the form of biogas, reduce the abovementioned parameters, and obtain digestible fertilizer. So, the study of processing the waste after bioethanol production and the safe use of the digestate as an organic fertilizer or as a soil improver is relevant and forms the main purpose of this work.

Materials and methods

The studies were provided in the Ecotechnologies Laboratory at the Poznan University of Life Sciences (Poland) within the MSCA4Ukraine project "Biogas Solutions in Overcoming the Energy, climate and food crisis in EU and Ukraine" in cooperation with Presov University. The distillery stillage from biogas plants of IMA Polska (Murowane Goślina) and Agri Plis (Kramplewicy) was used.

The studies of the methane efficiency of the substrates were carried out using batch culture technology, based on the adapted standards DIN 38 414-S8 and VDI 4630. Biogas composition was determined using a GA5000 (GeoTech) biogas analyzer. The organic matter content (OM) was determined according to the PN-EN 15169:2011 standard. The contents of nitrogen, carbon, and sulfur were determined using the dynamic combustion method in an EA Vario EL IIIP elemental analyzer. The content of macroelements and heavy metals was determined in the obtained digestate by standard methods. The macroelements in the soil samples were examined before and after digestate application.

Results and discussion

The conducted studies showed a high yield of biogas during stillage processing. It was also significant that the fermentation process is highly dependent on the organic load and acidity - at high ORL and low pH the slowdown in the growth of anaerobic microflora was observed, which led to a longer hydraulic retention time. The average content of methane in biogas was 58%, which can be explained by the presence of large amounts of raw sugar. Processing of stillage allows to reduce COD and BOD by 91-97%. The obtained results correspond with data reported from other studies (Dubrovskis, and Plume, 2017; Sajbrt et al. 2010).

Digestate is a valuable by-product of stillage processing. It was analyzed for the content of macroelements (phosphorus, potassium, calcium, magnesium, etc.) and heavy metals (lead, nickel, chromium, copper, zinc etc.). The content of macroelements in the soil fertilized with digestate corresponded to their content in the soil fertilized with mineral fertilizers.

Conclusions

Considering the constant bombing of the energy infrastructure of Ukraine by Russia and, the destruction of ports, and energy infrastructure, the use of alternative energy sources becomes a priority. It helps reform the energy market, provides decentralization, and ensures stability. Stillage biomass was identified as a regional substrate for biogas production in Ukraine with high potential. It is easily degradable, with high biogas and biomethane yield, and produces digestate with good agricultural quality. The use of digestate from stillage in agriculture makes it possible to get rid of mineral fertilizers, which contributes to the development of sustainable agriculture.

Acknowledgements: This study is supported by the European Commission within the MSCA4Ukraine project "Biogas Solutions in overcoming the energy, climate and food crisis in EU and Ukraine" (ID number 1233009) and National Scholarship Program of the Slovak Republic under the project "Applying of digestate potential for sustainable agriculture development".

References

Mikucka, W., Zielińska, M., 2020. Distillery Stillage: Characteristics, Treatment, and Valorization. *Appl Biochem Biotechnol* 192, 770–793. https://doi.org/10.1007/s12010-020-03343-5.

Dubrovskis, V., Plume, I., 2017. Methane production from stillage. *Engineering for Rural Development* https://doi.org/10.22616/ERDev2017.16.N086.

Sajbrt, V., Rosol, M., Ditl, P. (2010). A Comparison of Distillery Stillage Disposal Methods. *Acta Polytechnica*. 50. https://doi.org/10.14311/1175.

Modelling Methane Emissions Resulting from Municipal Solid Waste Management: Reduction Options and Environmental Impact

D.Petrisor, C. Cirjan , D.Gavrilescu, C. Teodosiu

[1]Department of Environmental Engineering and Management, "Cristofor Simionescu" Faculty of Chemical Engineering and Environmental Protection, "Gheorghe Asachi" Technical University of Iasi, Iasi, Romania
Corresponding author's email: daniela.gavrilescu@academic.tuiasi.ro

keywords: *municipal solid waste; methane emissions; waste management operations; environmental impact.*

Introduction

Methane (CH_4) is one of the main contributors to the greenhouse gas emissions while waste management operations are the third anthropogenic source of CH_4 emissions. Any changes in the waste management planning and operations must consider not only waste valorization options, but also which of the valorization and treatment option ensures the lowest CH_4 emissions. The main objective of this study is to model and predict the CH_4 emissions coming as a result of various municipal solid waste (MSW) treatment alternatives. This study is performed for Bucharest, the capital city of Romania, a municipality with 1.87 million inhabitants and an annual waste generation rate of 642 tons/year.

Methodology

In Bucharest, the generated MSW is currently 9% recycled and 91% landfilled which translates into an annual CH_4 emission rate of 25353 ton/year resulted from its waste management operations. According to the Municipality Waste Management Plan (MWMP), by 2025 the distribution of waste management treatment options other than landfilling should be operational (described in Table 1 as Alternatives 0 to 4). While Alternative 0 represents the situation forecast for 2025 with no additional waste treatment infrastructure investments compared to 2019, Alternatives 1 to 3 put emphasis on further investments especially on waste recycling and biowaste treatment based on composting and anaerobic digestion.

By using the Decision Support Tool available in the Waste Methane Assessment Platform (WASTEMAP), the CH_4 reduction and its environmental impact has been modeled for the 4 alternatives having as the actual status of waste management in Bucharest as Reference Scenario. The main goal is to analyze which alternative ensures the highest CH_4 emission reduction as compared to the Reference Scenario- 9% waste recycling and 91% waste landfilling.

Table 1. *Municipal solid waste treatment options distribution (Reference Scenario-derived from WASTEMAP) and Alternative scenarios developed by MWMP*

Waste Management Operation	Reference Scenario WASTEMAP	Alternative 0	Alternative 1	Alternative 2	Alternative 3
Recycling	9	28.39	32.27	32.27	35.64
Composting	0	3.63	6.31	10.24	6.97
Anaerobic Digestion	0	0	12.28	6.46	7.99
Coincineration	0	1.19	12.29	13.05	12.67
Total	**9**	**33.21**	**63.15**	**62.02**	**63.27**

Results and discussion

The annual CH_4 generation from 2025 up to 2050 indicates that the minimum values are achieved in the case of Alternative 1 (Figure 1). In this modelling stage, the remaining waste is considered to be landfilled in a controlled landfill but with no landfill gas capture system. By 2050, the CH_4 emission reductions obtained are 41.66% in the case of Alternative 1, 41.28% in the case of Alternative 2 respectively 39.77% in the case of Alternative 3. Even though from this study, Alternative 1 ensures the maximum CH_4 reductions, due to technical and economic constraints, the municipality has selected Alternative 3 to be implemented by 2025.

Further CH_4 emission reduction options can be explored by considering the variation of the percentage of landfill with gas capture. Thus for Alternative 3, the investigated values of this parameter are 25%, 50%, 75% and 85% (the last being the technical current limitation). For the maxim captured methane, by 2050, the

CH_4 reduction percentage may achieve 43.39%. By contrast with the current practice (Reference Scenario) in 2050, Alternative 3 with 85% landfill gas capture gives a 65.91% CH_4 emission reduction.

The environmental impact of CH_4 emissions can be estimated by the Global Warming Potential indicator which can be calculated for a 20-year period (GWP 20) and a 100-year period (GWP 100). Considering that methane has an average atmospheric residence time of approximately 10 years, the GWP 20 has been selected for this study to translate the methane emissions into environmental impact (ton of CO_2e/year) (Figure 3). By 2050, the GPW 20 of Alternative 3 will be 1.33 million ton of CO_2e compared to 2.21 million ton of CO_2e in the case of the Reference Scenario. The maximum landfill gas capture percentage may facilitate further reduction up to 0.76 million tons of CO_2e.

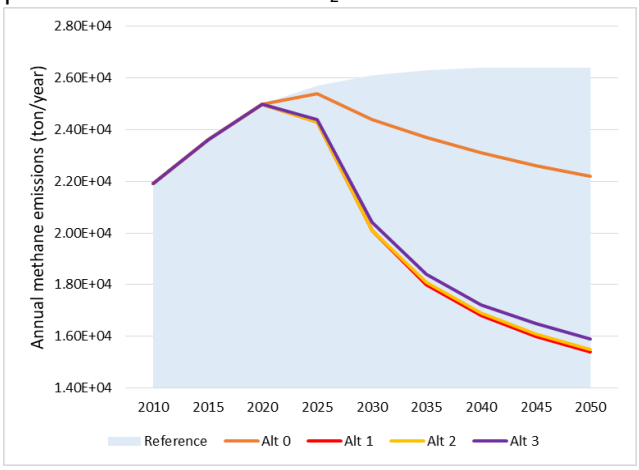

Fig 1. *Annual methane emissions for the city of Bucharest from various waste management operations.*

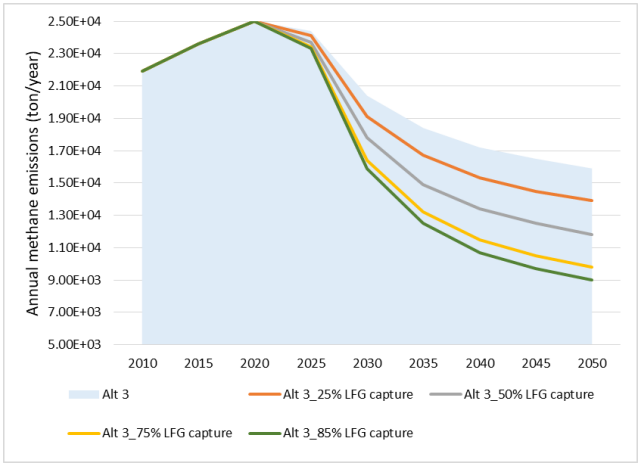

Fig. 2 *Annual methane emissions for the city of Bucharest, Alternative 3 and various landfill gas capture rates.*

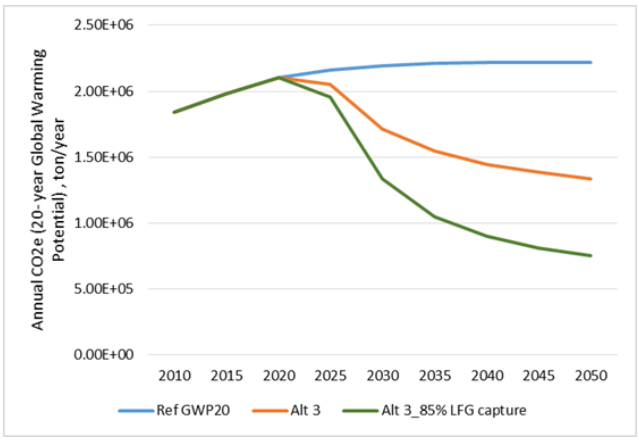

Fig. 3 *Environmental impact of methane in the case of Alternative 3 and Alternative 3 with 85% landfill gas capture compared to the Reference Scenario.*

Conclusions

The results obtained in the modelling of CH_4 emission for Bucharest for a 25 year period of time shows that, out of the 4 explored alternatives, Alternative 1 gives the maximum reduction in methane emissions. Alternatives 2 and 3 follow closely in terms of methane emission reductions, with Alternative 3 being selected by the municipality due to other technical and economic criteria. If landfill gas is captured, in all investigated alternatives further significant methane emission reduction may be achieved.

References

Bucharest Municipality Waste Management Plan, 2021.
Daniel A. Vallero, Chapter 8 - Air pollution biogeochemistry, in Air Pollution Calculations, 2019, Elsevier, pages 175-206, ISBN 9780128149348.
https://wastemap.earth/decision-support-tool.
https://www.iea.org/reports/methane-tracker-2021/methane-and-climate-change.

Modeling of Waste Electrical and Electronic Equipment Generation Rate using Multiple Regression Analysis

Marius Gavrilescu[1] and Daniela Gavrilescu[2]

[1]Faculty of Automatic Control and Computer Engineering,
[2] "Cristofor Simionescu" Faculty of Chemical Engineering and Environmental Protection,
"Gheorghe Asachi" Technical University of Iași, Romania
Corresponding author email: marius.gavrilescu@academic.tuiasi.ro

keywords: *Waste Electrical and Electronic Equipment; regression models; data augmentation;*

Introduction

Waste Electrical and Electronic Equipment (WEEE) generation trends are a multifaceted issue intertwined with economic activity, material consumption patterns, population dynamics, and educational levels. Understanding these relationships is essential in developing effective policies and practices to manage WEEE in a sustainable manner. In support of this important environmental issue, we develop several regression models that correlate the generation of WEEE with four social, economic and population-related metrics such as: gross domestic product (GDP) (Euro/capita), domestic material consumption (DMC) (t/capita), population density (PD) (inhabitants/km^2) and access to tertiary education (TE) (% population). The quantities of generated WEEE come from Eurostat database, while the GDP, DMC, PD and TE were selected from Our World in Data database. Using an augmentation strategy to boost the scarce data set, our regression models significantly minimize the mean squared error (MSE) to the point of accurately capturing the relationship between the aforementioned factors and the Waste Electrical and Electronic Equipment generation into the environment.

Materials and methods

Our original data consists in 15 instances, representing the values of GDP, DMC, PD, TE as inputs, and generated WEEE as output, as measured between 2007-2021 for the population of Romania (Figure 1). In order to develop a reliable regression model, we explore several regression methods: ElasticNet (a linear model with L1 and L2 regularization), K-Nearest Neighbors (KNN), Support Vector Machines (SVM), and Decision Trees. Due to the limited number of instances in the data series, we employ an augmentation strategy which consists in fitting a cubic spline to the data and sampling from the spline inbetween existing data points, therefore significantly extending our original data. We perform 3-fold cross-validation on each of the four regression methods using train-splits of both the augmented and non-augmented data, in order to find the best parameter values of each model. Finally, we fit and evaluate the models with the best parameters on a train-test split of both the non-augmented and augmented data in order to find the regressor with the best fit to our data set.

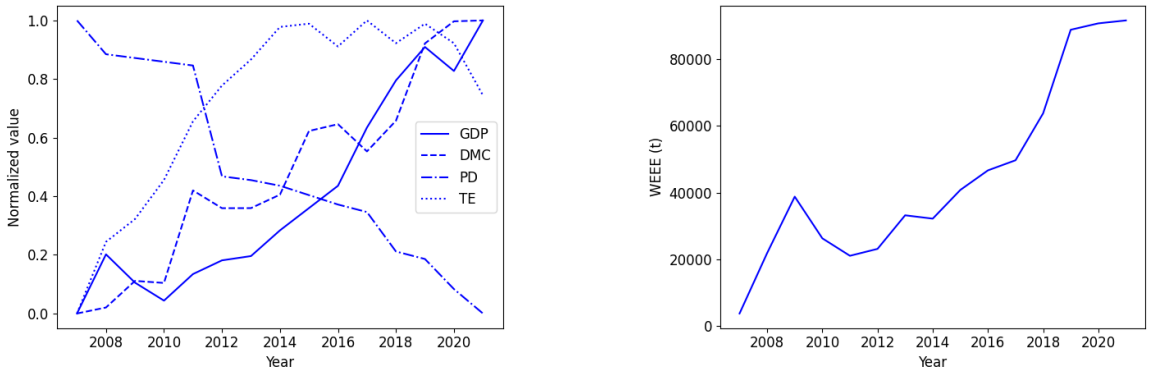

(a) **(b)**

Figure 1. *Plots of (a) input values of the four social-based parameters and (b) output values of WEEE, using linear interpolation inbetween data points.*

Results and discussion

We illustrate the results of our augmentation method in Figure 2, for each of the four input parameters. The larger, blue dots represent the original data, and the smaller red ones are the data points added by sampling from a cubic spline which interpolates the initial data points. We find that adding four instances between each pair of original points is enough for our purposes, extending the data from the original 15 instances to 57 ones in the augmented data set. We search for the best parameters of the four regression methods using cross-validation on both the augmented and non-augmented data, as shown in Table 1. We then train and evaluate the resulting models on a 70/30 train-test split of the data set show the resulting MSE values and coefficients of determination in Table 2. We find that the four regression methods provide acceptable regression models on the original data. However, by augmenting the original dataset we are able to considerably improve the metrics, the result of which are much better fitting models. We find that the best models are based on KNN and SVM regression, with R^2 values of 0.996 and 0.986, respectively. In particular, KNN regression with k = 3 neighbors, using Manhattan distance-weighted instances provides the best fit and therefore constitutes the most reliable regressor for our problem.

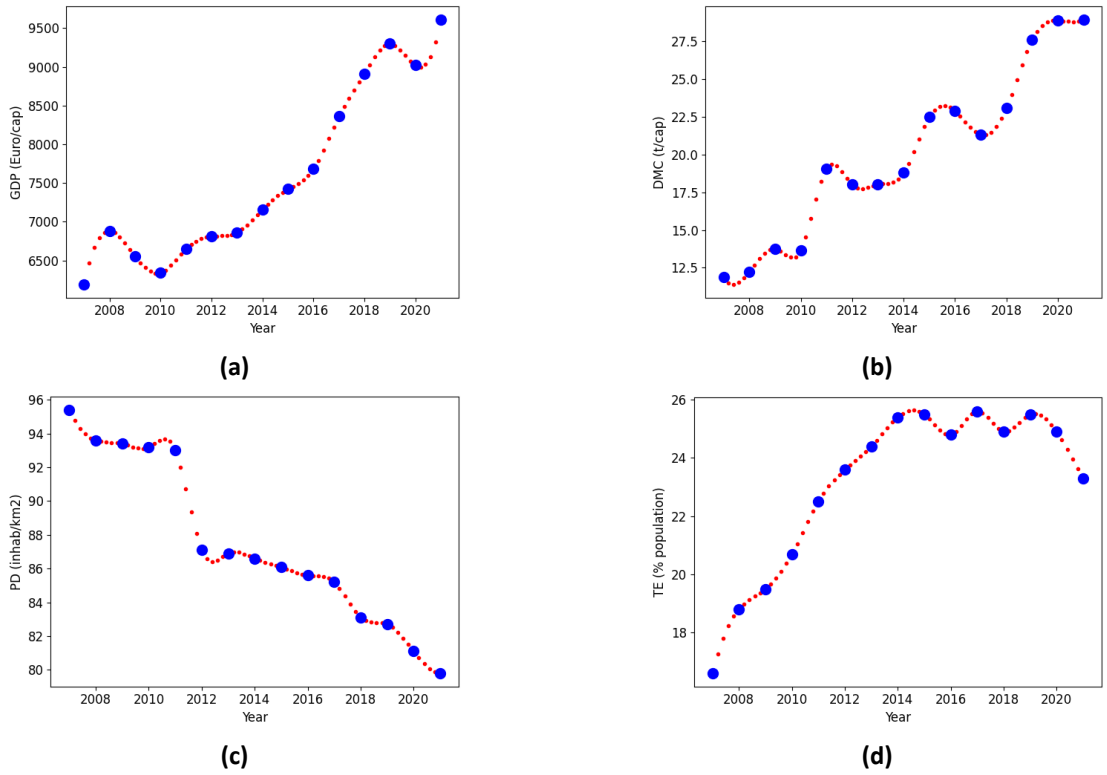

Figure 1. *Augmented and non-augmented plots of the four input parameters: (a) gross domestic product (GDP); (b) domestic material consumption (DMC); (c) population density (PD); (d) access to tertiary education (TE).*

Table 1. *Cross validation results of considered regression methods. MSE values with and without augmented data and hyperparameters of best corresponding models*

Method	CVMSE	CVMSE Aug	Best Parameters
ElasticNet	0.0704	0.0089	alpha = 1e-05; l1_ratio = 1e-04
KNN	0.0166	0.0025	n_neighbors = 3; p = 1; weights ='distance'
SVM	0.0052	0.0024	'C': 1000.0; 'epsilon': 0.0001; 'kernel': 'rbf'
Decision Tree	0.0096	0.0028	split_criterion = 'friedman_mse'; max_depth = 12

Table 2. *MSE and R^2 values of the best regression models, applied to non-augmented and augmented data*

Method	MSE	R^2	MSE Aug	R^2 Aug
ElasticNet	0.0443	0.709	0.0066	0.951
KNN	0.0203	0.874	0.0004	0.996
SVM	0.0171	0.904	0.0016	0.986
Decision Tree	0.0436	0.795	0.0043	0.946

Evaluation of Biochar from Sewage Sludge for Sustainable Carbon Adsorption

L. D. Tshenyego[1], P.T. Odirile[1]., A. Giannis[2] and P. Gikas[2]

[1]Department of Civil Engineering, Faculty of Engineering. University of Botswana
Private Bag 0061. Gaborone. Botswana.
[2]Department of Environmental Engineering, Technical University of Crete, Chania 17300, Greece
Corresponding author email: odirilep@ub.ac,bw

keywords: biochar, sewage sludge, carbon adsorption, pyrolysis, heavy metals.

Introduction

One of the most crucial problems in the world wastewater treatment cycle is how to handle sewage sludge (SS). For instance, sewage sludge production in the EU is expected to weigh 10.13 million tons annually in dry weight Odirile et al., (2021). Faecal matter with sewage sludge is a challenging waste to handle due to its fast production rates, high concentration of microorganisms, and high content of heavy metals. The objective of this research was to assess the potential for organic and inorganic carbon adsorption by using biochar made from micro sieved sewage sludge (MSS) Fernández-Gutiérrez et al., (2023).

Materials and methods

Micro sieved sewage sludge was taken from the municipal wastewater treatment plant in Chania, Crete. Municipal wastewater is treated secondarily at this facility using an activated sludge system, while sludge is treated using anaerobic digestion process Odirile et al., (2021) and belt-filter-press dewatering. The micro sieved, dewatered sludge was dried in an oven at 103 °C for 24 hours, then crushed to 56 microns using a milling crusher, sieved, and kept in an airtight plastic bag. Micro sieved municipal sewage sludge was pyrolyzed at a temperature of 600 °C to create biochar (MSSBC400).

Results and discussion

In the landfill leachate solution, the maximum adsorption capacities (qm) for total inorganic carbon (TIC) and total organic carbon (TOC) were 5.681 and 5.342 mg/g, respectively. Due to competitive adsorption, the leachate solution's TIC and TOC adsorption capabilities dropped. An essential process in the sorption of these carbons on MSSBC400 is surface precipitation. Lower adsorption capabilities for TIC and TOC on MSSBC400 were the result of competitive adsorption in the leachate solution. This shows that the leachate solution's other components interfere with the biochar's ability to absorb heavy metals Sanvong & Suppadit, (2013). The study also emphasizes the significance of surface precipitation as a mechanism for these carbons' sorption on MSSBC400.

Table 1. Table 1. Adsorption capacities for TIC and TOC

Component	Maximum Adsorption Capacity (mg/g)
Total Inorganic Carbon (TIC)	5.681
Total Organic Carbon (TOC)	5.342

Overall, the results show that applying sewage sludge biochar to co-contaminated soil may successfully immobilize heavy metals, making it a potential rehabilitation method.

Conclusions

This work demonstrates that biochar made from sewage sludge can lower the mobility of heavy metals in co-contaminated soils, indicating its potential as a remediation tool. The presence of other components in the

leachate solution affects the biochar's adsorption capabilities, highlighting the complexity of using biochar in real-world applications.

Acknowledgements:

This study is financed by the the erusmas student exchange program and the University of Botswana Organisation of research fund. Thank you also to my supervisor and the Department of Civil Engineering from Botswana and Create for their guidance and help in submitting to the SustEng Conference.

References

Fernández-Gutiérrez, D., Manali, A., Tsamoutsoglou, K., Gikas, P., & Guillén, A. L. (2023). Environmental life cycle assessment of an integrated biosolids microsieving-drying-gasification pilot plant from WWTP. *Green Energy and Sustainability*, 1–24. https://doi.org/10.47248/ges2303030004

Odirile, P. T., Marumoloa, P. M., Manali, A., & Gikas, P. (2021). Anaerobic digestion for biogas production from municipal sewage sludge: A comparative study between fine mesh sieved primary sludge and sedimented primary sludge. *Water (Switzerland)*, *13*(24). https://doi.org/10.3390/w13243532

Sanvong, C., & Suppadit, T. (2013). *The Characteristic of Pelleted Broiler Litter Biochar Derived from Pilot Scale Pyrolysis Reactor and 200-Liter-Oil-Drum Kiln*. *3*(10), 34–39.https://www.researchgate.net/profile/Tawadchai-Suppadit/publication/266203662

Unlocking the timeless wisdom of Athens: A journey towards sustainability through design

D. Tzourmakliotou[1] and E. Sourli[2]

[1]Department of Civil Engineering/School of Engineering, Democritus University of Thrace, Xanthi, Greece
[2]Hellenic-American Educational Foundation, Athens 154 52, Greece
Corresponding author email: dtzourma@civil.duth.gr

keywords: *sustainability; climate change; circular design; LCA; adaptation.*

Introduction

This research paper aims to integrate sustainable design principles in the contemporary civil engineering landscape. Sustainable design it's a philosophy that combines environmental, social and economic considerations into the design process. The main emphasis of this paper would be to conduct an analysis on the integration of traditional and modern techniques, resilience and adaptation to climate change, and circular economy principles (LCA). We will explore some exemplary sustainable building projects in Greece from the past, from the white island houses to the highly populated metropolis of Athens fuelled with historical landmarks such as the Parthenon. Previous projects employed methods that are crucial in modern engineering and architecture. Our main goal is to uncover the efficacy of traditional civil engineering techniques, which are still implemented nowadays in sustainable design. We are going to follow a practical approach drawing on case studies to expand, not only on the environmental impact, but also the effect on social equity these significant projects have.

References

UN. Transforming our world. (2015), The 2030 agenda for sustainable development. A/RES/70/1 United Nations. Retrieved on 27 May 2024 From https://sustainabledevelopment.un.org/content/documents/21252030%20Agenda%20for%20Sustainable%20Development%20web.pdf

Rosenlund, H. (2000). Climatic design of buildings using passive techniques. Building Issues, 10, 16–18.

Life Cycle Assessment (LCA) of PLA/MXene Nanocomposites

Vasileios Tzatzadakis[1], Alexandros Thomos[2], Franceska Gojda[2], Fanourios Krasanakis[2], Kiriaki Chrissopoulou[2], Spiros H. Anastasiadis[2], Evridiki Patelarou[1] and Minas M. Stylianakis[1,2]

[1]Department of Nursing, School of Health Sciences, Hellenic Mediterranean University, Heraklion, Greece.
[2]Institute of Electronic Structure & Laser, Foundation for Research & Technology-Hellas, Heraklion, Greece.
Corresponding author email: vtzatzadakis@hmu.gr

keywords: *LCA, MXene, PLA*

Introduction

The European Union has increasingly embraced Life Cycle Assessment (LCA) policies over the last decades to achieve sustainability goals. In this frame, LCA analysis on several well-known functional materials and (bio)composites is the new trend to evaluate toxicity, eco-friendliness and versatility, considering their production process. In this study, we developed functional nanocomposites of poly(lactic acid) (PLA) incorporating MXene flakes ($Ti_3C_2T_x$) to evaluate the impact of the followed experimental procedures on human health and the environment. To this end, we propose alternative strategies to optimize the top-down synthesis of $Ti_3C_2T_x$ and the development of PLA/$Ti_3C_2T_x$ nanocomposites, to mitigate the environmental impact.

Materials and Methods

The experimental data required for the production of a) the MAX phase, b) $Ti_3C_2T_x$ flakes and c) PLA/MXene nanocomposites to evaluate the total environmental impact were obtained from the literature. $Ti_3C_2T_x$ flakes were chemically synthesized by etching the MAX phase of the precursor Ti_3AlC_2 material, using hydrochloric acid (HCl) (6M) and NaF, according to the a chemical etching procedure, assisted by the production of in situ HF. This process involved multiple washes to neutralize the pH and the final dispersion was filtered and dried. The resulting $Ti_3C_2T_x$ was then used to prepare PLA/MXene nanocomposites by dispersing and delaminating the flakes into acetonitrile (ACN), followed by wet mixing with PLA dissolved in ACN.

Results and Discussion

The present LCA for the development of PLA/MXene nanocomposites reveals that the production of ACN is the largest contributor to global warming potential (GWP) and marine eutrophication, while the one of PLA exhibits negligible environmental impact. Our findings imply that significant reduction in the environmental burdens could be achieved either upon optimization of the synthetic procedure of $Ti_3C_2T_x$ flakes (MXenes) or by the selection of alternative “green” solvents, although the followed ones do not pose immediate threats to human health or ecosystems. To validate our findings, ReCiPe 2016 was used as the primary method due to its relevance to the EU context.

Conclusions

As the use of MXenes is the new trend in nanotechnology applications, their upscaling in an industrial level is undoubtedly inevitable and thus their commercialization necessitates to deeply explore their environmental impact on human health and the environment. Our findings are in full agreement with already anticipated values for environmental indicators like ALOP, MEP, and ODP, demonstrating that global warming potential (GWP100) for 1kg of PLA/$Ti_3C_2T_x$ estimated to be 214 kg of CO_2, while 1g of exfoliated $Ti_3C_2T_x$ may result in 382kg of CO_2 emissions. Although current findings do not indicate imminent harmful side effects on human health and ecosystems, future research should focus on the optimization of the MXenes synthesis conditions, as well as on the use of environmentally friendly solvents to further reduce the environmental footprint, ensuring a sustainable future for the MXene-related technology.

Acknowledgements: This study is financed by the Hellenic Mediterranean University (HMU), Project titled "Conducting Educational and Postdoctoral Research at the Hellenic Mediterranean University". The project is funded through the University’s budget with resources of the Ministry of Education and Religious Affairs. The

project has been approved by the HMU Senate decisions no. 2607/14-05-2022, no. 5994/13 09-2022 and no. 6514/03-10-2022.

References

Sala, S., Amadei, A.M., Beylot, A. and Ardente, F., 2021. The evolution of life cycle assessment in European policies over three decades. *Int. J. Life Cycle Assess*., 26, 2295–2314.

Niaounakis, M., 2013. Introduction to Biopolymers. *Biopolymers Reuse, Recycling, and Disposal*, William Andrew Publishing, 1–75.

Sonnemann, G., Gemechu, E.D., Sala, S., Schau, E.M., Allacker, K., Pant, R., Adibi, N. and Valdivia, S., 2018. *Life Cycle Thinking and the Use of LCA in Policies Around the World, in: Life Cycle Assessment*, Springer Int. Publishing, Cham, 429–463.

Tzatzadakis, V, Thomos, A., Gojda, F., Krasanakis, F., Chrissopoulou, K., Anastasiadis, S.H., Patelarou, E. and Stylianakis, M. M., 2024. The Environmental Footprint of MXenes and PLA/MXene Nanocomposites Production: Life Cycle Assessment. Submitted.

Decarbonisation of asphalt mix production

A. Woszuk[1], S. Malinowski[1] and R. Panek[1]

[1] Civil Engineering and Architecture Faculty/ Lublin University of Technology, Lublin Nadbystrzycka 38D, 20-628, Poland
Corresponding author email: a.woszuk@pollub.pl

keywords: *asphalt, zeolite, foamed asphalt,* emission

Introduction

Warm Mix Asphalt (WMA), as well as Hot Mix Asphalt (HMA), provide surface durability, comfort and safety for users. A decrease of asphalt mix production temperature causes reduction of carbon dioxide (CO_2) and other hazardous compounds emitted to the atmosphere by factories by approx. 40% and 70%, respectively. A decrease in asphalt mix production temperature by only 10°C brings about 50% reduction in emission of fumes and aerosols [1]. In WMA production can be applied both synthetic and natural zeolites [2, 3]. Thanks to gradual release of zeolite water, decrease in viscosity and improvement of workability are possible during asphalt mix production, placement and compaction [4, 5].

This paper evaluates the effect of zeolite-silane composites on bitumen foaming. In the process of modification of zeolite materials, silane compounds with different sulfur content were used. Based on investigation of the bitumen properties (dynamic viscosity and penetration, softening temperature) foamed with zeolite-silane composites the their usefulness in bitumen foaming technology was determined.

Materials and methods

Synthetic (NaP1) and natural –(clinoptilolite)zeolites were modified with silanes (TEOS, MPTS and TEST) by hydrolysis of modifier and its bonding to zeolite external functional groups. The obtained zeolite-silane composites were characterized in terms of their chemical and phase content with application of following methods: XRF, SEM-EDS, XRD, FTIR.

Experimental design covered the assessment of reference and zeolite-silane composite foamed bitumen The investigation was carried in parallel for road and Polymer Modified (PMB) Bitumen. To estimate bitumen foaming process effectiveness bitumen dynamic viscosity changes in time (measured after 30 and 45 minutes of mixing) were done. The dynamic viscosity tests were performed using a Brookfield's viscometer according to ASTM D 4402, at a temperature of 135°C. In addition, for foamed asphalt binders, their softening point and penetration were determined in accordance with the following standards: PN-EN 1427:2009 and PN-EN 1426:2009.

Results and discussion

The successful synthesis zeolite-silane composites was confirmed by XRF, SEM-EDS, XRD, FTIR results. XRF analysis of the composites (Table 1) showed different Si and S contents depending on the type of silane used in the modification process. The Si content of the synthesized composites increased from about 33% for unmodified NaP1 zeolite to more than 37% for composites containing silanes. For composites received based on clinoptilolite matrix, the increase in Si content compared to unmodified zeolite was about 15%. In addition, XRF analyses confirmed the increased S content in the investigated composites. The highest S content was found in composites obtained using TESPT silane having a 4-atom sulfide bridge in its structure.

As a result of foaming process of 35/50 bitumen with zeolite-silane composites, a decrease in dynamic viscosity is visible in most cases (Figure 1). Whereas, for PMB bitumen, a decrease in dynamic viscosity was observed only for unmodified zeolites and the NaP1-TEOS composite. Regardless of the zeolite type and test conditions, a decrease in dynamic viscosity in time was observed. This is due to the gradual release of "zeolite water" from the material structure and is consistent with the results of previous studies. Considering the obtained results as well as the visually observed increase of bitumen foam, it is expected that adhesion of foamed asphalt to aggregates will improve lower production temperature.

Table 1 Chemical composition of zeolites and zeolite-silane composite

	Na2O	MgO	Al2O3	SiO2	SO3	K2O	CaO	TiO2	Cr2O3
NaP1	6,124	0,741	17,757	33,428	0,144	0,417	2,933	1,372	0,031
NaP1-TEOS	4,835	0,753	18,612	37,135	0,088	0,45	2,561	1,333	0,029
NaP1-MPTS	6,759	0,774	17,965	37,327	2,516	0,46	2,797	1,248	0,025
NaP1-TESPT	4,314	0,551	14,488	37,462	8,442	0,382	2,195	1,113	0,023
CLIN	-	0,583	8,08	55,76	0,886	2,807	2,726	0,189	-
CLIN-TEOS	-	0,737	9,824	70,795	0,921	3,392	3,206	0,220	-
CLIN-MPTS	-	0,763	9,933	70,527	1,324	3,343	3,223	0,211	-
CLIN-TESPT	-	0,669	9,431	69,023	3,469	2,964	3,122	0,258	-

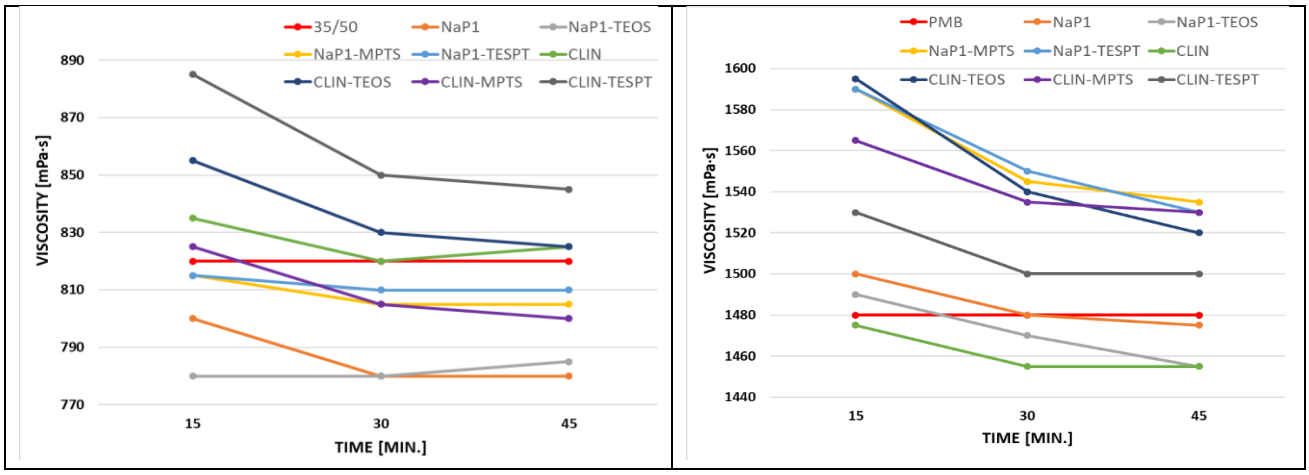

Figure 1. *The results of dynamic viscosity tests*

Conclusions

The chemical and mineralogical analysis confirmed successful zeolites modification with silanes differing in chemical structure. The observed changes of dynamic viscosity indicate that the foaming effect depends on both the type of zeolite-silane composite and the type of bitumen. The obtained results clearly confirm applicability of zeolit-silane composites in the bitumen foaming process, enabling reduction of asphalt mix production temperatures and simultaneous reducing the emission of hazardous compounds into the atmosphere.

Acknowledgements:

The research leading to these results has received funding from the commissioned task entitled 'VIA CARPATIA Universities of Technology Network named after the President of the Republic of Poland Lech Kaczyński,' under the special purpose grant from the Minister of Education and Science, contract no. MEiN/2022/DPI/2575, as part of the action 'ISKRA – building inter-university research teams.'

References

1. Woszuk A., Franus W. 2017. A review of the application of zeolite materials in Warm Mix Asphalt technologies. *Applied sciences*, 7, 293.

2. Liu N., Liu L., Li M., Sun, L., 2023, Effects of zeolite on rheological properties of asphalt materials and asphalt-filler interaction ability. *Construction and Building Materials*, 382, 131300.

3. Sanchez-Alonso E, Valdes-Vidal G, Calabi-Floody A., 2020, Experimental study to design warm mix asphalts and recycled warm mix asphalts using natural zeolite as additive for sustainable pavements. *Sustainability*. 12(3):980.

4 Zou F., Leng Z., Cao R., Li G., Zhang Y., Sreeram A., 2022, Performance of zeolite synthesized from sewage sludge ash as a warm mix asphalt additive, Resources, *Conservation and Recycling*, 181,106254.

5. Woszuk A., Zofka A. , Bandura L., Franus W., 2017 Effect of zeolite properties on asphalt foaming. *Construction and Building Materials*, 139, 247-255.

Exploring innovative cathodes based on perovskites in Microbial Fuel Cells

L. Skopas[1], G. Bampos[1], I. Apostolopoulos[1], S. Bebelis[1], G. Antonopoulou[2,3,*]

[1]Department of Chemical Engineering, University of Patras, Caratheodory 1, GR 26504, Patras, Greece
[2] Department of Sustainable Agriculture, University of Patras, 2 Georgiou Seferi st., GR 30100, Agrinio, Greece
[3]Institute of Chemical Engineering Sciences, 1 Stadiou st., Platani, GR 26504, Patras, Greece

Corresponding author email: geogant@upatras.gr

keywords: *perovskites, microbial fuel cells, cathodes, non-noble metals, low cost cathodes*

Introduction

Microbial fuel cells (MFCs) which generate electricity through the decomposition of organic compounds have gained considerable scientific interest in the last 10 years (Bose et al., 2019). Power production in MFCs is due to the electrocatalytic activity of specific microbial consortia (exo-electrogens), which typically colonize in the anodic electrode and consume the organics, generating electrons (Antonopoulou et al., 2023). Various factors, such as the adhesion of bacteria, the electron transfer mechanism, and the pH value, influence the performance of the MFC (Mohyudin et al., 2022). However, the MFC design and its characteristics, such as the electrocatalytic anode or cathode material, also influence its efficiency. The dual-chamber MFC, which consists of two compartments separated by a proton exchange membrane (PEM), has the advantage of a simple configuration, which usually operates in batch mode to determine the optimal operating conditions (Antonopoulou et al., 2010).

To increase the rate of oxygen reduction, high-cost Pt catalysts are used in the cathodes of the MFCs. However, to decrease the costs for the MFCs and facilitate their future market penetration, the Pt load should be kept at low levels (< 0.1 mg cm^{-2}) or new types of inexpensive catalysts should be explored. In the present study, the use of perovskites with low noble metal content, as alternative electrocatalysts in the cathodic electrode of dual-chamber MFCs is explored for the first time and its performance is compared with that of the reference electrode, based on Pt. Perovskites are low-cost mixed oxides with the general formula ABO_3 where A denotes a site typically occupied by an alkali or alkaline earth metal cation and B stands for a site typically occupied by a transition metal cation, that can fine-tune their catalytic properties by tailoring their composition. Partial substitution of cations at the A or/and B sites by foreign cations having a different oxidation state or radius may further improve the catalytic performance because it may result in increased oxygen mobility and/or synergy effects between the two metals. Towards the direction of investigating the effect of the partial substitution of Ni in the B sites of the $La_{0.8}Sr_{0.2}NiO_3$ perovskite with noble metals, in the present work, a series of $La_{0.8}Sr_{0.2}Ni_{1-y}M_yO_3$ (M = Rh, Ru, Pt, Pd) perovskite-type oxides have been synthesized, physicochemically characterized, and tested as cathode electrodes in dual chamber MFCs.

Materials and methods

Perovskites preparation

The parent $La_{0.8}Sr_{0.2}NiO_3$ (LSNi) sample and the partially substituted $La_{0.8}Sr_{0.2}Ni_{1-y}M_yO_3$ (M = Rh, Ru, Pt, Pd) perovskite-type oxides, where $La_{0.8}Sr_{0.2}$ and $Ni_{1-y}M_y$ denote the A- and B-sites, respectively, were prepared in powder form employing the *in situ* combustion synthesis method (Safakas et al., 2019). The metal precursor salts used were $Sr(NO_3)_2$, $La(NO_3)_3{\cdot}6H_2O$, $Ni(NO_3)_2{\cdot}6H_2O$, N_3O_9Rh, $Ru(NO)(NO_3)_3$, $(NH_3)_4Pt(OH)_2$ και $PdCl_2$.

Cathodes preparation

Mechanical mixtures of these perovskite oxides with carbon black (CB, Vulcan XC72R), in a mass ratio equal to 3:1, were used to prepare $La_{0.8}Sr_{0.2}Ni_{0.95}M_{0.05}O_3$/CB electrocatalysts. These mixtures were suspended in isopropanol and triple distilled water in order to be deposited on carbon fiber cloth (Carbon Cloth, CC) (3 cm × 3 cm) corresponding to a B-site metal loading equal to 0.5 $mg_{B\text{-}site\ met}$ cm^{-2}. Measurements were also performed with a commercial Pt reference cathode electrode (ETEK, 0.5 mg_{Pt} cm^{-2}). Table 1 shows the specific surface area values of the prepared perovskites. It can be observed that the partial substitution of Ni in the

$L_{0.8}S_{0.2}N$ perovskite led to a significant increase in the specific surface area from 5 m^2 g^{-1} in the case of the reference perovskite to 11 m^2 g^{-1} for the $L_{0.8}S_{0.2}N_{0.95}Pd_{0\ .05}$, and 22 m^2 g^{-1} for the $L_{0.8}S_{0.2}N_{0.95}Rh_{0\ .05}$ perovskite material.

Table 1. *Specific surface area of the perovskite material*

Perovskite	Composition	Surface Area (m^2 g^{-1}))	
$L_{0.8}S_{0.2}N$	$La_{0.8}Sr_{0.2}NiO_3$	5	
$L_{0.8}S_{0.2}N_{0.95}Ru_{0.05}$	$La_{0.8}Sr_{0.2}Ni_{0.95}Ru_{0.05}O_3$	18	MFC1
$L_{0.8}S_{0.2}N_{0.95}Rh_{0.05}$	$La_{0.8}Sr_{0.2}Ni_{0.95}Rh_{0.05}O_3$	22	MFC2
$L_{0.8}S_{0.2}N_{0.95}Pt_{0.05}$	$La_{0.8}Sr_{0.2}Ni_{0.95}Pt_{0.05}O_3$	21	MFC3
$L_{0.8}S_{0.2}N_{0.95}Pd_{0.05}$	$La_{0.8}Sr_{0.2}Ni_{0.95}Pd_{0.05}O_3$	11	MFC4

MFCs

Five identical H-type MFC devices (Bampos et al., 2024) were used, working with the 4 different cathode electrodes based on perovskite oxides (symbols MFC1, MFC2, MFC3 and MFC4) and one with the commercial Pt reference cathode electrode (MFC5). A graphite rod was used as an electron collector in the anodes, using graphite granules (GG). Both electrodes were connected to a resistance decade box, which closed the circuit and was connected in parallel to a recording system (ADAM 4017).

The MFCs were operated using a synthetic medium based on acetate for two operating cycles as described in Apostolopoulos et al. (2021) and Bampos et al. (2024). The impedance spectroscopy (EIS) measurements were carried out as described in Bampos et al. (2024).

Results and discussion

In Figure 1, the U_{cell}, versus time during the two operating cycles of all MFCs is depicted, while in Table 2 the performance of the cells in terms of Chemical oxygen demand (COD) removal efficiency and Coulombic efficiency, CE is presented.

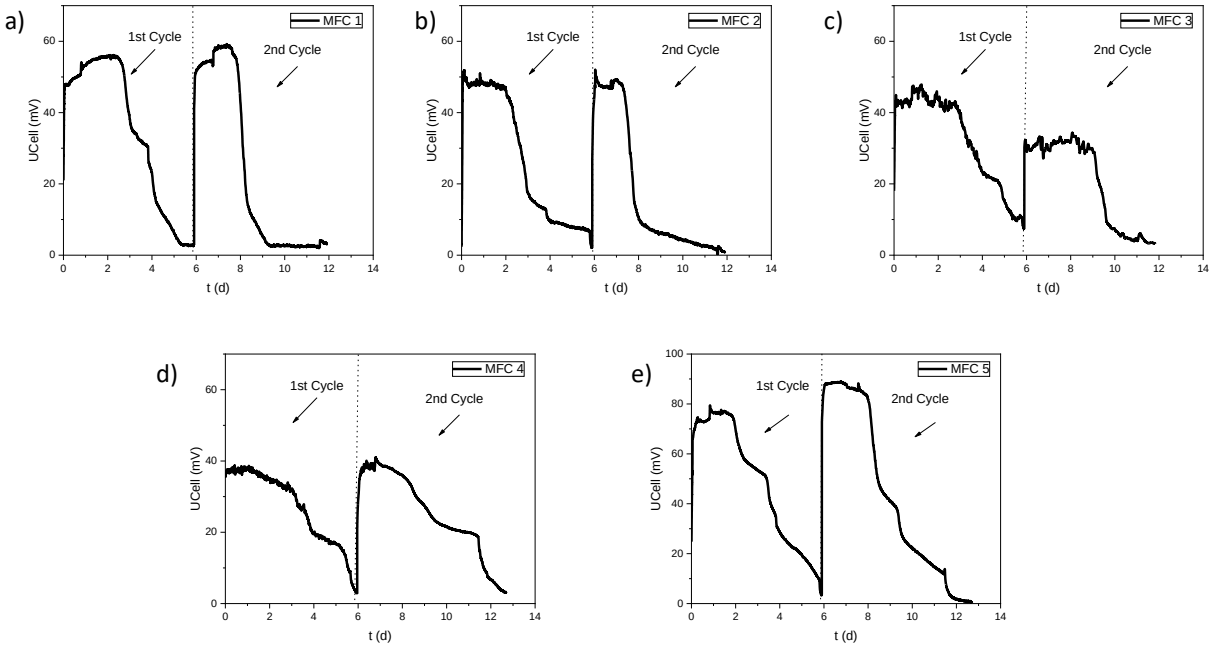

Figure 1*. MFC voltage during the two operating cycles of the MFCs, using different cathode electrodes.*

Table 1. *Characteristics of the MFCs*

MFC	COD removal efficiency (%)	CE(*%)
MFC1	73.5	28.6

MFC2	84.3	21.3
MFC3	82.7	26.3
MFC4	81.9	26.6
MFC5	87.3	33.8

In Figure 2, the Nyquist and Bond plots of the five MFCs at the beginning of the first operating cycle and when applying voltage of -0.4 V, is presented. The ohmic resistance value for MFC1, MFC2, MFC3, MFC4 and MFC5 was equal to 468.2 Ω, 347 Ω, 592 Ω, 480 Ω and 398 Ω, respectively whereas the polarization resistance value was 55.1 Ω, 47.6 Ω, 281 Ω, 86 Ω and 71 Ω, respectively.

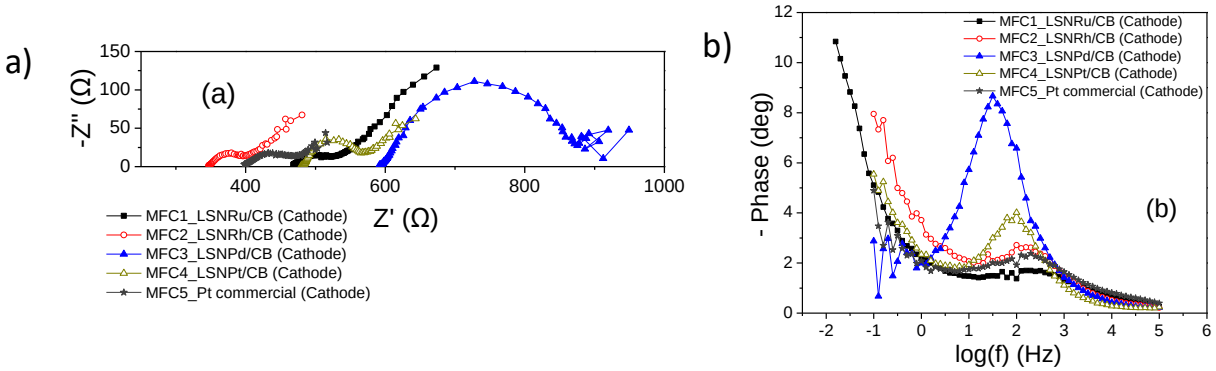

***Figure 2**. Nyquist (a) and Bode plots (b) for all MFCs, at the beginning of the first operating cycle, when applying a voltage of -0.4 V.*

Acknowledgments: This work has been partially financed by the funding programme "MEDICUS", of the University of Patras (Principal Investigator G. Antonopoulou) and the project "Perovskitic electrocatalysts for integrated systems of microbial electrolysis cells and anion exchange membrane fuel cells (Acronym: PERFORMANCE, project code: 82242)", which was supported by the 3rd Call of Hellenic Foundation of Research and Innovation (H.F.R.I.) Research Projects for the support of Post-doctoral Researchers (fellowship of Dr. G. Bampos).

References

1. Bose, D.; Gopinath, M.; Vijay, P.; Sridharan, S.; Rawat, R.; Bahuguna, R. Bioelectricity generation and biofilm analysis from sewage sources using microbial fuel cell. *Fuel* **2019**, *255*, 115815. https://doi.org/10.1016/j.fuel.2019.115815.
2. Antonopoulou, G.; Bampos, G.; Ntaikou, I.; Alexandropoulou, M.; Dailianis, S.; Bebelis, S.; Lyberatos, G. The biochemical and electrochemical characteristics of a microbial fuel cell used to produce electricity from olive mill wastewater. Energy 2023, 282, 128804. https://doi.org/10.1016/j.energy.2023.128804.
3. Mohyudin, S.; Farooq, R.; Jubeen, F.; Rasheed, T.; Fatima, M.; Sher, F. Microbial fuel cells a state-of-the-art technology for wastewater treatment and bioelectricity generation. *Environ. Res.* **2022**, *204*, 112387. https://doi.org/10.1016/j.envres.2021.112387
4. Antonopoulou, G.; Stamatelatou, K.; Bebelis, S.; Lyberatos, G. Electricity generation from synthetic substrates and cheese whey using a two chamber microbial fuel cell. *Biochem. Eng. J.* **2010**, *50*, 10–15. https://doi.org/10.1016/j.bej.2010.02.008.
5. Safakas, A.; Bampos, G.; Bebelis, S. Oxygen reduction reaction on La0.8Sr0.2CoxFe1-xO3-Δ perovskite/carbon black electrocatalysts in alkaline medium. *Appl. Catal. B Environ.* **2019**, *244*, 225–232, https://doi.org/10.1016/j.apcatb.2018.11.015.
6. Bampos, G., Gargala, Z., Apostolopoulos, I., Antonopoulou, G. Electrochemical characteristics of microbial fuel cells operating with various food industry wastewaters. Processes **2024**, 12, 1244. https://doi.org/10.3390/pr12061244
7. Apostolopoulos, I.; Bampos, G.; Soto Beobide, A.; Dailianis, S.; Voyiatzis, G.; Bebelis, S.; Lyberatos, G.; Antonopoulou, G. The effect of anode material on the performance of a hydrogen producing microbial electrolysis cell, operating with synthetic and real wastewaters. *Energies* **2021**, *14*, 8375. https://doi.org/10.3390/en14248375.

Hydrocyclone for the treatment of municipal primary wastewater

K. Tsamoutsoglou[1], A. Kechagias[1], and P. Gikas[1]

[1] School of Chemical and Environmental Engineering, Technical University of Crete, 73100 Chania, Greece
Corresponding author email: pgikas@tuc.gr

keywords: *wastewater; primary treatment; hydrocyclone*

Conventional wastewater treatment is widely recognized for its high energy consumption (Metcalf & Eddy et al., 2007; Tchobanoglous et al., 2003). Several wastewater treatment plants (WWTPs) in Europe are aging. As a result, many WWTPs do not meet performance requirements due to the expansion of sewerage networks and the rise of wastewater flow rates (Tsamoutsoglou et al., 2024). This study examines the use of hydrocyclones for early removal of suspended solids present in primary municipal wastewater. A hydrocyclone with maximum hydraulic capacity of 50 m^3/d, was installed downstream of the primary clarification at the WWTP of Chania, Greece (Figure 1). An efficiency estimation method was employed to assess the effectiveness of hydrocyclone. It was shown that the hydrocyclone achieved a TSS removal rate ranging from 9% to 48%, with an average of 33%, resulting to effluent TSS concentrations varying from 74 to 285 mg/L. The average biological oxygen demand (BOD_5) removal rate of the hydrocyclone was 19%, with a range of 6% to 42%, achieving effluent BOD_5 concentrations between 154 and 395 mg/L. The hydrocyclone chemical oxygen demand (COD) removal rates were estimated to vary from 2% to 39%, with an average of 13%, and the effluent COD concentrations from 252 to 782 mg/L.

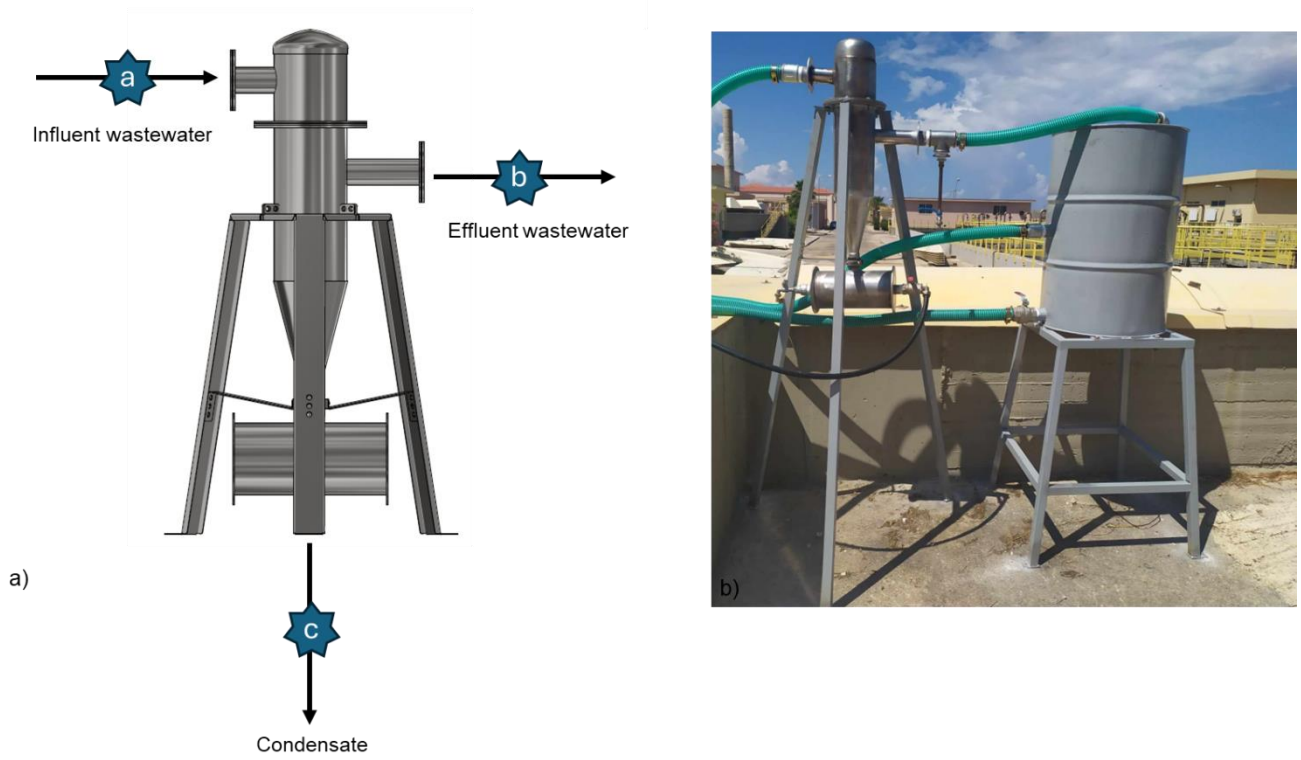

Figure 1. (a) Flow diagram and sample points of the hydrocyclone (with marked sampling points: (a) Primary influent to hydrocyclone, (b) hydrocyclone effluent, (c) Condensate of hydrocyclone) (b) Photograph of the hydrocyclone at the WWTP of Chania.

The hydrocyclone is a cost-effective unit operation that can be used to enhance the conventional treatment process in WWTPs. Potential reductions in the operating expenses of a WWTP may be achieved by employing the hydrocyclone as the primary wastewater system in full-scale applications, as a result of the reduced organic load entering the aeration tank. Hydrocyclones are a viable option for industrial wastewater applications because of their compact size, cost-effectiveness in terms of initial investment and ongoing operation costs, and lack of moving components.

References

Metcalf & Eddy, I. an A.C., Asano, T., Burton, F., Leverenz, H., 2007. Water Reuse: Issues, Technologies, and Applications, First edit. ed. McGraw-Hill Education, New York.

Tchobanoglous, G., Burton, F.L., Stensel, H.D., 2003. Metcalf & Eddy wastewater engineering: treatment and reuse. Int. Ed. McGrawHill 4, 361–411.

Tsamoutsoglou, K., Katzourakis, V.E., Chrysikopoulos, C. V, Gikas, P., 2024. Performance evaluation and parameter estimation of the advanced primary filtration (APF) process in wastewater treatment plants. Sep. Purif. Technol. 127106.

The impact of substrate extrusion on the energy and economic efficiency of biogas plant operation

K. Kupryaniuk[1], K. Witaszek[1], P. Pochwatka[2], J. Mazurkiewicz[1], I. Vaskina[1], D. Janczak[1] and J. Dach[1]

[1]Department of Biosystems Engineering, Poznań University of Life Sciences, Poznań, Poland
[2]Department of Environmental Engineering and Geodesy, University of Life Sciences in Lublin, Lublin, Poland
Corresponding author email: karol.kupryaniuk@up.poznan.pl

keywords: *substrates; extrusion; anaerobic digestion; energy efficiency.*

Introduction

One of the pre-treatment methods is extrusion. Extrusion is a HTST (High Temperature Short Time) type of process due to the fact that the material in the extruder stays in it from several seconds to several minutes and is exposed to high temperature. During this time, the material inside is mixed, compacted, compressed, sheared, liquefied and plasticized in the final zone [Oniszczuk et al., 2012]. Specific processing conditions contribute to the disintegration of lignin, facilitating access to cellulose and hemicellulose for bacteria [Oniszczuk and Pilawka, 2013]. The high pressure and temperature during extrusion contribute to the hydrolysis of lipids, proteins, carbohydrates, hemicellulose, cellulose and the disruption of the cell wall, thanks to which the material becomes plastic.

Agricultural biomass with an increased content of ligni-cellulose compounds is not normally used in biogas plants due to decomposition problems (straw has a structure that is difficult to access for fermentation bacteria). However, their use can bring a significant effect by increasing the energy efficiency and profitability of biogas plants. As research has shown [Rodiahwati and Sriariyanun, 2016], the use of the extrusion process in the preparation of raw materials for anaerobic digesion may be justified.

The aim of the work was to investigate the impact of extrusion of two types of straw (cereal and rapeseed) on increasing the efficiency of methane production and the energy and economic efficiency of the operation of a biogas plant with a capacity of 0.5 MW.

Materials and methods

In the research, two types of extruded substrates were used to power the biogas plant: cereal straw and rapeseed straw. Both types of straw were extruded, and then all substrates were tested for methane efficiency and compared with tests on straw without pre-treatment.

In the calculation of the efficiency of the biogas plant operation, two variants of biogas plant power supply were tested:

1. Variant 1: cereal straw + pig slurry and extruded cereal straw + pig slurry;
2. Variant 2: rapeseed straw + pig slurry and extruded rapeseed straw + pig slurry.

Energetic and economic calculations were carried out according to a standard methodology, based on market prices in Poland in May 2024 and taking into account the additional amount of electricity used during the extrusion of both types of straw.

Results and discussion

The results of anaerobic digestion tests and preliminary energetic and economic analysis are presented in Table 1.

Table 1. *Methane efficiency of the tested substrates and preliminary energetic and economic analysis for variants I and II*

Substrate	**D.M.**	**Methane efficiency**	**Substrate use**	**Electric energy spent for extrussion**	**Electric energy to use**	**Substrate cost (straw)**	**Revenue from electricity sold**
Variant I	**%**	**$m^3 \cdot Mg^{-1}$**	**Mg/a**	**MWh**	**MWh**	**EUR**	**EUR**
Wheat straw	88.51	197.18	5150	0	3854.50	301,678	879,450
Wheat straw after extrusion	91.96	213.72	4750	1220.75	2632.69	278,246	600,680
Variant II							
Rapeseed straw	90.70	205.07	4950	0	3853.14	289,962	879,141
Rapeseed straw after extrusion	90.62	228.79	4440	888.00	2967.84	260,087	677,148

In both variants, an increase in methane production from straw was observed, but this increase was relatively small (8.4% in the case of wheat straw and 11.6% in rapeseed straw). The increase in the efficiency of methane production from the same amount of straw resulted in a decrease in the mass necessary to power a biogas plant with a capacity of 0.5 MW, from 5150 to 4759 Mg/year in the case of wheat straw and from 4950 to 4400 Mg in the case of rapeseed straw, respectively. In this case, there are savings due to the smaller amount of straw needed, at the level of 23.4 kEUR in variant I and 29.9 kEUR in variant II.

However, during further calculations, it must be taken into account that the extrusion process requires additional electricity, which increases the cost of this technology. Therefore, taking into account the cost of electricity necessary for the extrusion process, it should be concluded that in both variant I and variant II, the revenue from the sale of electricity from a biogas plant powered by straw is higher in the variant without extrusion, respectively 278.7 kEUR in the case of wheat straw and 202 kEUR in the case of case of rapeseed straw.

Conclusions

The extrusion process increases the efficiency of CH_4 production during anaerobic digestion of lignocellulosic substrates such as various types of straw. However, various parameters of the extrusion process influence the increase in productivity. In the studies discussed, the increase in CH_4 production was so low (8.4% in the case of cereal straw and 11.6% in rapeseed straw) that it did not cover the increase in electricity consumption resulting from the operation of the extruder. As a consequence, the use of the extrusion process in the analyzed variants of biogas plants gave a negative economic result. Therefore, it should be concluded that further research is necessary on the optimization of the extrusion process in order to increase the efficiency of CH_4 production from straw with reduced energy demand.

References

Oniszczuk T., Wójtowicz A., Mitrus M., Mościcki L., Combrzyński M., Rejak A., Gładyszewska B. 2012. Influence of process conditions and fillers addition on extrusion-cooking efficiency and SME of thermoplastic potato starch. TEKA Commission of Motorization and Energetics in Agriculture, 12(1), 181-184.

Oniszczuk T., Pilawka R. 2013. Wpływ dodatku włókien celulozowych na wytrzymałość termiczną skrobi termoplastycznej. Przemysł Chemiczny, 2, 265-269.

Rodiahwati W., Sriariyanun M. 2016. Lignocellulosic biomass to biofuel production: integration of chemical and extrusion (screw press) pretreatment. KMUTNB Int. J. Appl. Sci. Technol., 9, 289-298. https://doi.org/10.14416/j. ijast.2016.11.001

Quality criteria for water reuse in the Mediterranean basin

E. Gika[1], V. Tzika[1], F. Ranieri [2], A.C. Ranieri[3], E. Ranieri[2] and P. Gikas[1]

[1] School of Chemical and Environmental Engineering, Technical University of Crete, 73100 Chania, Greece
[2] Department of Social Sciences, University of Foggia, 71121 Foggia, Italy
[3] Department of Physics, Polytechnic University of Bari, 70126 Bari, Italy
[4] Department of Biosciences, Biotechnologies and Environment, University of Bari, 70125 Bari, Italy
Corresponding author email: pgikas@tuc.gr

keywords: *water reuse; quality criteria; regulations*

Water scarcity is the main reason for water reclamation and reuse, particularly for agricultural applications (Ungureanu et. Al., 2020). The present paper examines the regulations, practices and applications related to wastewater reuse around the Mediterranean region, with emphasis on reuse practices for non-potable urban and agricultural applications. Due to severe water scarcity in the Mediterranean region and the increasing demand for freshwater, most Mediterranean countries have established quality criteria for water reuse.

A comprehensive overview of the guidelines and regulations enforced in the Mediterranean countries is presented. Each country has instituted its own regulations and threshold values regarding wastewater reuse, tailored to the intended application. As a rule of thumb, the most developed countries have adopted stricter regulations, while, on the other hand, countries with severer water scarcity tend to apply looser criteria (Angelakis and Gikas, 2014). Israel, Cyprus and Malta reuse the larger fractions of wastewater treatment plant effluents for agricultural applications, while, Spain is the leader for urban and recreational reuse applications. Due to the pressing necessity for the utilization of reclaimed water, national or regional regulations in the Mediterranean region have been less stringent compared to those implemented in other parts of Europe.

The most commonly regulated characteristics for water reuse are turbidity, TSS concentration, BOD concentration and concentration of pathogenic microorganisms (Müller and Cornel, 2017). For the later, is mostly regulated by measuring the colonies of *E. coli*, while some countries are also enforcing the measurement of enterococci colonies. Since June 2023, a new EU regulation (EU 2020/741) has been enforced (in the EU countries) which apart of *E. coli*, regulates also the concentration of *Legionella* spp. (where there is a risk of aerosolisation) and helminth eggs (for irrigation of pastures or forage). The EU regulation is enforced, in the EU countries along, with the national regulations. Specifically, the new EU regulation classifies reclaimed water in four categories according to the intended use (Table 1). The quality criteria imposed by the EU regulation (EU 2020/741) are shown in Table 2. Moreover, EU 2020/741, while the minimum monitoring frequencies are shown in Table 3.

All things considered, water reclamation and reuse is practiced in all Mediterranean countries with various intensities and various criteria. The recently enforced EU regulation (EU 2020/741) attends to unify the water reuse criteria in the EU member states, while it is expected that sooner or later the non-EU Mediterranean countries shall adopt the regulations imposed bt EU 2020/741.

Table 1. *Classes of reclaimed water quality and permitted agricultural use and irrigation method (EU/2020/741)*

Minimum reclaimed water quality class	Crop category (*)	Irrigation method
A	All food crops consumed raw where the edible part is in direct contact with reclaimed water and root crops consumed raw	All irrigation methods
B	Food crops consumed raw where the edible part is produced above ground and is not in direct contact with reclaimed water, processed food crops and non-food crops including crops used to feed milk- or meat-producing animals	All irrigation methods
C	Food crops consumed raw where the edible part is produced above ground and is not in direct contact with reclaimed water, processed food crops and non-food crops including crops used to feed milk- or meat-producing animals	Drip irrigation (**) or other irrigation method that avoids direct contact with the edible part of the crop

Table 2. *Reclaimed water quality requirements for agricultural reuse (EU/2020/741)*

Reclaimed water quality class	Indicative technology target	Quality requirements				
		E. coli (number/100 ml)	BOD_5 (mg/l)	TSS (mg/l)	Turbidity (NTU)	Other
A	Secondary treatment, filtration, and disinfection	≤ 10	≤ 10	≤ 10	≤ 5	*Legionella* spp.: < 1 000 cfu/l where there is a risk of aerosolisation Intestinal nematodes (helminth eggs): ≤ 1 egg/l for irrigation of pastures or forage
B	Secondary treatment, and disinfection	≤ 100	In accordance with Directive 91/271/EEC (Annex I, Table 1)	In accordance with Directive 91/271/EEC (Annex I, Table 1)	-	
C	Secondary treatment, and disinfection	≤ 1 000			-	
D	Secondary treatment, and disinfection	≤ 10 000			-	

Table 3. *Minimum frequencies for routine monitoring of reclaimed water for agricultural reuse (EU 2020/741)*

Reclaimed water quality class	Minimum monitoring frequencies					
	E. coli	BOD_5	TSS	Turbidity	*Legionella* spp. (when applicable)	Intestinal nematodes (when applicable)
A	Once a week	Once a week	Once a week	Continuous	Twice a month	Twice a month or as determined by the reclamation facility operator according to the number of eggs in waste water entering the reclamation facility
B	Once a week	In accordance with Directive 91/271/EEC (Annex I, Section D)	In accordance with Directive 91/271/EEC (Annex I, Section D)	-		
C	Twice a month			-		
D	Twice a month			-		

References

Ungureanu, N., Vlăduț, V. and Voicu, G., 2020. Water Scarcity and Wastewater Reuse in Crop Irrigation. *Sustainability*. 12(21), 9055.

Angelakis, A. N. and Gikas, P., 2014. Water reuse: Overview of current practices and trends in the world with emphasis on EU states. *Water Utility Journal*. 8(67), e78.

Müller, K. and Cornel, P., 2017. Setting water quality criteria for agricultural water reuse purposes, *Journal of Water Reuse and Desalination*. 7 (2), 121–135.

EU 2020/741, 25-5-2020. Minimum requirements for water reuse. *Official Journal of the European Union*, L 177/32

Carbon dioxide capture from actual industrial flue gas using microalgae

G. Makaroglou, D. Mitrogiannis and P. Gikas

School of Chemical and Environmental Engineering, Technical University of Crete, Kounoupidiana, Greece
Corresponding author email: gmakaroglou@tuc.gr

keywords: *Stichococcus sp.; photo-bioreactors; flue gas; CO_2 fixation; high added value products.*

Introduction

Microalgae have emerged as a promising solution for addressing environmental challenges, particularly in the context of carbon capture and utilization. These microscopic, photosynthetic organisms are highly efficient at sequestering carbon dioxide (CO_2) from the atmosphere, making them a valuable tool in mitigating climate change. One innovative application of microalgae is in the sequestration of flue gas, a major byproduct of industrial processes such as power generation, which is a significant source of anthropogenic CO_2 emissions (Chia et al., 2021).

Flue gas typically contains high levels of CO_2 along with other pollutants like sulfur oxides (SO_x) and nitrogen oxides (NO_x). Microalgae can thrive in such environments by utilizing the CO_2 for growth, effectively reducing greenhouse gas emissions (Razzak et al., 2019). Moreover, microalgae cultivation can produce valuable byproducts, including biofuels, animal feed, and biochemicals, offering a sustainable and economically viable approach to carbon management (Zhao et al., 2020).

As research advances, optimizing microalgae-based sequestration systems could play a critical role in reducing industrial carbon footprints and supporting the transition to a low-carbon economy (Chia et al., 2021).

Materials and methods

The purpose of the research is the reduction of CO_2 emissions from flue gases with the use of microalgae and their bioconversion into high-value products. The present study took place in one of Greece's largest Public Power Corporation power plant. Two closed type photo-bioreactors (15 L each) were utilized for microalgae cultivation, in which the cells were cultivated attached on sandblasted glass tiles (at the bottom of the photo-bioreactors), as a means to reduce biomass harvesting costs (Makaroglou et el., 2021). The photo-bioreactors were housed inside a small shelter to provide protection from weather conditions and other limiting factors.

The experiments were conducted with the microalgal strain *Stichococcus* sp., which had been recovered from Souda bay in Greece. Flue gas from the combustion of natural gas was provided as a carbon source into each photo-bioreactor at a rate of 0.6 L min^{-1}. Three types of cultures were examined: cultivation with i) continuous light, ii) flashing light (1,000 Hz), and iii) continuous light + nitrogen starvation ($NaNO_3$ deficiency) applied three days prior to harvesting. Cultures were illuminated by LED lamps at 6,600 lux for cultivation with continuous and flashing light. However, microalgae cultivation under nitrogen starvation was illuminated by only 3,300 lux to promote lipids production. Furthermore, the temperature of the culture was controlled by an A/C unit (25 ± 1 °C). Microalgae were cultivated in artificial seawater + Bold's Basal Medium with the composition of NaCl and $NaNO_3$ being 35 g L^{-1} and 0.75 g L^{-1}, respectively.

After 26 days of cultivation, collection of the microalgae was conducted by scraping of the biomass attached to the sandblasted glass tiles and was used to quantify dry weight and high added value products, namely lipids, pigments, proteins and carbohydrates.

Results and discussion

During the experiment, microalgae adapted well to the flue gas environment, capturing approximately 1.8 kg of CO_2 per 1 kg of biomass. The results of *Stichococcus* sp. cultivation for biomass production were 50.5, 47.9 and 38.3 g m^{-2} for cultivation with continuous light, flashing light, and with continuous light + nitrogen starvation, respectively. The bioproducts content of *Stichococcus* sp. (Fig. 1) were approximately 80-90%, measured from a sum of bioproducts including carbohydrates, lipids, proteins, and total chlorophyll. The

highest bioproduct was carbohydrates being 24.8, 23.4, and 11.9 g m^{-2}, respectively. The lipid content was found to be 6.6, 6.8 and 11.0 g m^{-2}, showing that flashing lights and especially nitrogen starvation increased lipids production. The proteins were measured as 8.3, 7.6, and 6.1 g m^{-2} and the total chlorophyll found to be $19.1 \cdot 10^{-2}$, $23.0 \cdot 10^{-2}$, $12.0 \cdot 10^{-2}$ g m^{-2}. The application of flashing lights showed a slight decline in biomass productivity, but promoted pigments production. Constant lighting consumed 33.1 kWh, while flashing lights required 25.7 kWh during the 26 days of cultivation, reducing the cost of cultivation.

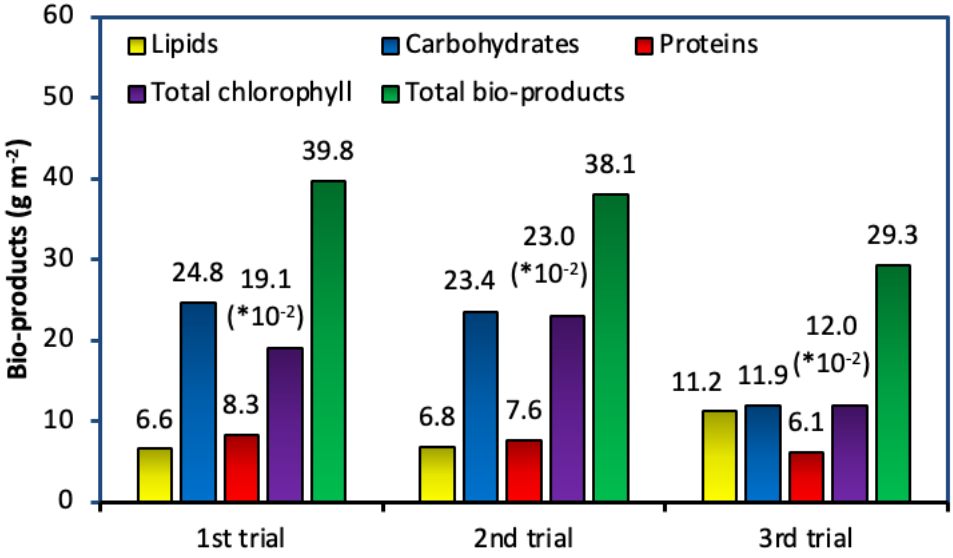

Figure 1. *Stichococcus sp. bioproducts (in g m^{-2}) for each trial. 1st trial was conducted with continuous light at 6,600 lux, 2nd trial with flashing light (1,000 Hz) at 6,600 lux, and 3rd trial with continuous light at 3,300 lux and nitrogen starvation 3 days prior to harvesting.*

Conclusions

Based on the findings, *Stichococcus* sp. was effectively cultivated using industrial flue gas from a natural gas-powered plant. This highlights the potential of microalgae as a viable solution for reducing CO_2 emissions from flue gases before they are emitted into the environment. The resulting biomass offers the possibility for conversion into valuable products. In summary, implementing large-scale microalgae photo-bioreactors could play a crucial role in decreasing CO_2 levels, thereby contributing to the reduction of the greenhouse effect.

Acknowledgements: This study was co-financed by the European Regional Development Fund of the EU and Greek national funds through the Operational Program Competitiveness, Entrepreneurship and Innovation, under the call "Research-Create-Innovate" (project code: T1EDK-02681). Project title: "Bioconversion of CO_2 into high-added value bioproducts through sustainable microalgae cultivation processes (CO_2-BioProducts)".

References

Chia, S. R., Chew, K. W., Show, P. L., Yap, Y. J., Ling, T. C. and Nguyen, T. H. P., 2021. Sustainable utilization of biowaste for biofuel production. *Bioresour. Technol.*, 319, 124210.

Makaroglou, G., Marakas, H., Fodelianakis, S., Axaopoulou, V. A., Koumi, I., Kalogerakis, N. and Gikas, P., 2021. Optimization of biomass production from *Stichococcous* sp. biofilms coupled to wastewater treatment. Biochem. Eng. J., 169, 107964.

Razzak, S. A., Hossain, M. M., Lucky, R. A., Bassi, A. S. and DeLasa, H., 2019. Integrated CO_2 capture, wastewater treatment and biofuel production by microalgae culturing—A review. *Renew. Sustain. Energy Rev.*, 82, 319-327.

Zhao, B., Su, Y. and Zhang, Y., 2020. Biosequestration of carbon dioxide by microalgae: Assimilation principle, leading microorganisms, and application. *Appl. Biochem. Biotechnol.*, 191(1), 160-177.

Full papers

Early-stage Mathematical Modeling of Solution Spray Pyrolysis for the Fabrication of Functional Ceramic Films

Natalia Fotiadi[2], Dimitris Lazaridis[1], Nikolaos Rigakis[3] and Nikolas Kiratzis[1]

[1]Laboratory of Advanced Materials and Electrochemical Technology (ElectrocheMat Lab)/Department of Mineral Resources Engineering/School of Engineering, University of Western Macedonia, Kozani, Greece
[2]Department of Chemical Engineering/School of Engineering, University of Western Macedonia, Kozani, Greece
[3]1st General Secondary Education Lyceum of Grevena, Grevena, Greece
Corresponding author email: nkiratzis@uowm.gr

ABSTRACT
Fabrication of ceramic or composite ceramic-metallic films form the functional basis of several devices such as ceramic fuel cells or electrolyzers, gas sensors, and ceramic membranes. In particular, the fabricated film thickness, porosity, and tortuosity dictate the extent and relative contribution polarization losses in electrochemical reactions in ceramic fuel cells and electrolyzers. Thus, it is essential to control the morphology of the produced film structure, early during the fabrication stage in order to achieve optimal values of electrochemical reaction and diffusion rates. Toward this end, molecular deposition methods such as Solution Spray Pyrolysis (SAT), in which the film formation is determined by a series of physicochemical processes of the precursor molecules suitably modulated by the deposition process parameters, offer a promising fabrication route for optimal morphology and functionality of the final film. The SAT tecchnique, entails the fabrication of thin simple and/or mixed inorganic oxide films by spraying a solution of salts with appropriate ions and in suitable molecular ratios within a thermal field and on a suitable substrate for a certain time necessary for the decomposition into the appropriate oxides. The technique is of low cost, done in an open atmosphere and offers precise control of stoichiometry at a droplet level along with t direct correlation of the solution's physicochemical properties and the process parameters with the properties of the final ceramic film (morphology, particle size). Modeling efforts of this technique are certainly required, starting from the early stages during droplet evaporation. In the present contribution we formulate the basis of a mathematical model during these early stages of the process that essentially determine final film morphology.

Keywords: Ceramic film; Spray Pyrolysis; Mathematical Modeling.

1. INTRODUCTION

Ceramic or composite ceramic-metallic membranes (cermets) are widely used as electrodes in various devices such as ceramic fuel cells or electrolyzers, gas sensors, and ceramic membranes. Parameters such as membrane thickness, porosity, and tortuosity regulate the extent and relative contribution of concentration and activation polarization losses in electrochemical reactions in ceramic fuel cells and electrolyzers (He et al. 2010). It is crucial during the fabrication of such structures to control the morphology of the produced film structure to achieve optimal values of electrochemical reaction and diffusion rates (He and Goodenough 2014).

Recent research efforts in developing the aforementioned devices have focused on innovative fabrication methods that allow control over the morphological characteristics of the produced thin ceramic membranes according to their required functional properties. Such methods mainly belong to the category of molecular deposition methods where the film formation is determined by a series of physicochemical processes of the precursor molecules suitably regulated by the deposition method parameters in such a way that the fabricated film acquires the required morphological and functional characteristics (Krestou et al., 2018).

One of the promising methods in this category is the technique of solution spray pyrolysis (SAT), which essentially involves the preparation of thin simple and/or mixed inorganic oxide films by spraying a solution of salts with appropriate ions in suitable molecular ratios within a thermal field and on a suitable substrate for

the time required for the decomposition of salts into the appropriate oxides (Kiratzis, 2016). A typical experimental set-up is shown in Figure 1.

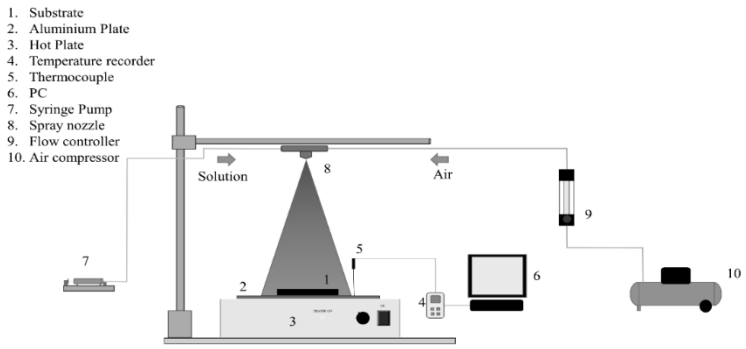

Figure 1. A typical Experimental Set-up of the Solution Spray Pyrolysis (SAT) process.

The advantages of the method, besides its low cost, lie in its simplicity since it operates in an open atmosphere, precise control of stoichiometry at a droplet level, and the direct correlation of the solution's physicochemical properties and the process parameters with the properties of the final ceramic film (morphology, particle size). A limited number of modeling efforts of this technique have appeared in the literature, mostly considering the droplet behavior for the production of ceramic powders rather than films. Thus, Messing et al. (1993) and Jayanthi et al. (1993) examine the initial droplet evaporation stage, Eslamian et al. (2006) concentrate to sub-micron and nanosized droplets and Nakaruk and Sorrell (2010) present a conceptual model for film formation that includes the annealing stage.

In the present contribution, we apply the approach of Jayanthi et al. (1993) using a commercial software (Wolfram Mathematica) and check its applicability in the case of the same solution model used by the above authors i.e. aqueous solution of zirconium hydroxyl chloride (ZHC) for the production of ZrO_2 particles. The validity and limitations of the approach is discussed as well as its extension to other systems where relevant data on the solute equilibrium saturation (ES) and critical supersaturation points (CSS) exist.

2. MODEL CONSTRUCTION AND ASSUMPTIONS

Following Jayanthi et al. (1993), spherical geometry of droplets is assumed with a radius R(t) that is changing with time (t) as solvent evaporation proceeds (Fig.2). Within the droplet and along with the spherical coordinate r (0<r<R) the solute concentration is denoted as C and is a function of both time and r due to concentration gradients formed within the droplet as it moves through the temperature field (Fig.1). Thus,

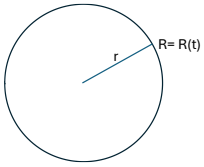

Figure 2. *Spherical geometry of droplets with variable radius R and coordinate r.*

$$C = C(r,t) \quad (1)$$

Obviously, 0<r/R<1 and the initial conditions are designated as:

$$R(0) = R_o$$
$$C(0,r) = C_o \quad for\ 0 \le r \le R_o \quad (2)$$

i.e. a uniform solute concentration is assumed throughout the droplet initially.

In addition, we also assume a uniform temperature throughout the whole volume of the droplet and thus, temperature is only a function of time t, i.e. a

$$T = T(t) \quad for\ all \quad 0 \le r \le R \qquad with\ T(0) = T_o \tag{3}$$

We also assume a constant temperature surroundings for the droplet i.e. T_∞

The droplet radius is a function of the solute concentration and assuming ideal solution a linear dependence is predicted as

$$\rho = 1 + 0.1196C \qquad \text{and therefore } \rho = \rho(r,t) \qquad (\text{in g/cm}^3) \tag{4}$$

The mass of the sphere is also a function of time as the droplet continuously shrinks due to solvent evaporation as it moves through the temperature field i.e.

$$m = m(t) \text{ with initial value } \quad m(0) = m_0 = \frac{4}{3}\pi R_0^3 \rho_0 \tag{5}$$

with ρ_0 being the initial droplet density which according to (4) should be given by

$$\rho_0 = \rho(r,0) \text{ for } 0 \le r \le R_0 \text{ and apparently } \quad \rho_0 = 1 + 0.1196C_0 \tag{6}$$

At each time point the mass of the sphere should be given by integrating over the droplet radius for this particular time point i.e.

$$m(t) = \int_o^{R(t)} 4\pi r^2 \rho \, dr \tag{7}$$

Following Jayanthi et al. (1993) it is reasonable to assume that the rate determining processes (i.e. the slowest) of the initial stage of droplet evaporation as it enters the temperature filed are the solute diffusion inside the droplet and droplet shrinkage. Vapor diffusion and heat conduction in air are 3 to 4 orders of magnitude faster while heat conduction within the droplet is faster but still lower by 2 to 3 orders of magnitude so it can be assumed that the temperature profile inside the droplet is essentially flat resulting in a constant temperature.

Further in formulating the droplet mass and energy balances, we assume that the vapor concentration profile has reached a steady-state so that the solvent vapor concentration gradient at the droplet surface (i.e. at $r = R$) is constant and constitutes the driving force for diffusion. The same can be assumed for the vapor phase temperature profile and the corresponding temperature gradient at the droplet surface.

Thus the pseudo-steady state evaporation rate at time t can be written as

$$\frac{dm}{dt} = -4\pi R \rho_{gas} D_V (\omega_{VR} - \omega_{V\infty}) \tag{8}$$

where ρ_{gas} refers to the total (i.e. including solvent vapor and ambient air) gaseous density and ω_{VR} and $\omega_{V\infty}$ relate to the mass fractions of solvent vapor at the droplet surface and the ambient air respectively. Substituting then, the expressions for the mass fractions and the total gas density assuming ideal gas behavior i.e.

$$\omega_V = m_V/(m_V + m_{air}) \qquad \text{and} \quad \rho_{gas} = (m_V + m_{air})/V_{gas} \tag{8a}$$

one expresses equation (8) above in terms of the solvent molecular weight M and the solvent partial pressures at the droplet surface and ambient as

$$\frac{dm}{dt} = -\frac{4\pi R D_V M}{R_{con}} \left(\frac{P_{VR}}{T_R} - \frac{P_{V\infty}}{T_\infty} \right) \tag{9}$$

assuming implicitly average values of ρ_{gas} and D_V for r between $[R, \infty]$ and D_V denoting the diffusion coefficient of solvent vapor in air while P_V , T correspond to the vapor partial pressure (which can be

approximated with the solution vapor pressure at the surface droplet temperature and at pressure of 1 atm) and absolute temperature at the droplet surface (i.e. R) and ambient (i.e. ∞) and R_{con} is the ideal gas constant. Note that P_{VR} can be related to the pure solvent equilibrium vapor pressure via Rault's law despite its limited applicability at higher solution concentrations (Jayanthi et al., 1993) i.e.

$$P_{VR} = P_{satR}\,\gamma_s x_s \tag{9a}$$

Where γ_s and x_s correspond to the activity coefficient and mole fraction of the solvent in the aqueous solution at the droplet surface while P_{satR} denotes the equilibrium vapor pressure of the solvent (i.e. in this case water) at the droplet surface temperature. For ideal and dilute solutions, the activity coefficient can be taken as $\gamma_s = 1$ and it is a function of the type the diluted salt.

One then, needs to express the equilibrium vapor pressure of the pure solvent as a function of temperature and for this purpose the Clapeyron-Clausius equation was mostly used:

$$ln\frac{P_{sat}}{P^o} = \frac{\overline{\Delta H}_V}{R_{con}} \cdot \left(\frac{1}{298} - \frac{1}{T}\right) \tag{10}$$

Where $\overline{\Delta H}_V$ is the enthalpy of vaporization of water taken as approximately constant between 24-147°C and $\overline{\Delta H}_V = 2.36 \times 10^{10}\ erg/g$ varying within a range of $\overline{\Delta H}_V = (2.44 - 2.12) \times 10^{10} erg/g$ respectively. The reference temperature was taken at 298K in which $P^o = 0.0313\ atm$.

As an alternative equation the Antoine Vapor-Pressure correlation was used (Reid et al., 1977):

$$lnP_{sat} = 18.3036 - \frac{3816.44}{T - 46.13} \tag{11}$$

in mmHg with T in degrees K. This is expected to be more accurate due to a third constant included and modifies the previous expression (9a) (for $\gamma_s = 1$ and $x_s = \frac{C_s}{C + C_s}$ where C_s the solvent concentration) as

$$P_{VR} = 1.316 \times 10^{-3} \left(\frac{C_s}{C + C_s}\right) exp\left(18.3036 - \frac{3816.44}{T - 46.13}\right) \tag{12}$$

Next an energy balance is done for the droplet in terms of heat lost due to vaporization and gained by the difference between the droplet temperature and that of the surroundings which is actually the heat conduction within the gaseous atmosphere as the droplet temperature is assumed constant as stated previously:

$$mc_P \frac{dT}{dt} = \overline{\Delta H}_V \frac{dm}{dt} + 4\pi R k (T_\infty - T) \tag{13}$$

where c_P is the solution specific heat and k the thermal conductivity of the gaseous phase. Here we have also assumed a quasi steady-state situation for the heat flux resulting in a constant temperature profile around the droplet.

The diffusion equation for solute transport inside the droplet becomes complicated due to the moving outer boundary as the droplet evaporates and shrinks.

The diffusion equation in terms of spherical coordinates and for binary diffusion within the liquid droplet is for the water (van der Lijn, 1976):

$$\frac{\partial \omega_{Ls}}{\partial t} = D_L \frac{1}{r^2} \frac{\partial}{\partial r}\left\{r^2 \cdot \frac{\partial \omega_{Ls}}{\partial r}\right\} \tag{14}$$

where ω_{Ls} refer now to mass fractions in the liquid phase of solvent (i.e. water) and D_L is the binary diffusion coefficient in the liquid phase (i.e. within the droplet) which is the same for the two components. Further, following van der Lijn (1976), we transform the equation in solute fixed coordinates.

Thus, a change in the independent variable from r to s can be defined as:

$$s = \frac{y}{y_o} = \frac{\int_0^r 4\pi r^2 \rho_L \omega_L \, dr}{\int_0^R 4\pi r^2 \rho_L \omega_L \, dr} = \frac{\int_0^r r^2 \rho_L \omega_L \, dr}{\int_0^R r^2 \rho_L \omega_L \, dr} \quad (15)$$

where ω_L is the solute mass fraction at radius r within the droplet (i.e. liquid phase) and ρ_L is the density of the liquid droplet solution. Apparently then, y denotes the total mass of the solute contained within a radius r and therefore, y_o refers to the total mass of the solute within the whole droplet (i.e. for $r = R$). Then, after these definitions, $s = 0$ at $r = 0$ and $s = 1$ at $r = R$ and always $0 \le s \le 1$ and is independent of R which is decreasing with time due to droplet shrinkage. In addition, the dependent variable is transformed as:

$$z = \frac{\omega_{Ls}}{\omega_L} = \frac{\omega_{LA}}{1-\omega_{LA}} \quad (16)$$

Then, the final form of (14) after these transformations becomes:

$$\frac{\partial z}{\partial t} = \frac{16\pi^2}{y_o^2} \cdot \frac{\partial}{\partial s}\left(D_L \left(\frac{\rho_L^2}{(1+z)^2}\right) s^4 \cdot \frac{\partial z}{\partial s}\right) \quad (17)$$

with the initial condition at *t=0:*

$$z_o = \frac{\omega_{Lso}}{\omega_{Lo}} = \frac{\omega_{Lso}}{1-\omega_{Lso}}, \quad m = m_0 \,, \; R = R_0 \text{ and } T = T_0 \quad (18)$$

and boundary conditions:

at $s = 0$ $\quad \frac{\partial z}{\partial s} = 0$ and at

$s = 1$ $\quad \frac{4\,\pi \cdot R^2 \rho_L^2 \cdot D_L}{y_0 (1+z)^2} \cdot \frac{\partial z}{\partial s} = \frac{dm}{dt} \cdot \frac{1}{4\pi R^2}$ (19)

and from (15) and (16) we obtain

$$R^3 = \left[\frac{3y_o}{4\pi} \int_0^1 \frac{1+z}{\rho_L} ds\right] \quad (20)$$

3. RESULTS AND DISCUSSION

The solution of the above system has been performed by Jayanthi et al. (1993) by applying an explicit first order finite difference method to calculate time derivatives from initial values of $z(s)$, m,T and R and using equations (9), (13), (17) and (20). Convergence was achieved by decreasing the steps of ds and dt. Nevertheless, van der Lijn, J., (1976) warns of the case of confronting instabilities particularly at low values of r (or s). Messing et al., (1993) reports that an unequally spaced grid with more points toward the surface of the droplet works without instabilities. Here, we feed the equations to a commercial software (Wolfram, Mathematica). Mathematica is quite widespread in most academic institutions (since about the 2000s) and it is based on an interactive style of programming easily approachable by students. As a starting point, we use the same model solution as the above authors (i.e. ZrO(OH)Cl or ZHC) with the following parameter values (Lijn, J. van der, 1976):

$D_V = 0.22 + 0.0015 \cdot \theta \; (in \; cm^2/s) \; ; \; c_P = 418.4 \times 10^5 ergs/g/℃ \; ;$
$k = (5.77 + 0.016 \cdot \theta) \times 418.4 \; ergs/(s \; ℃ \; cm); \; D_L = 1 \times 10^{-5} \; cm^2/s; \; M = 18 \; g/mole;$
$R_{con} = 82.056 \; cm^3 \; atm/mole/K$ (21)
Equilibrium Saturation Concentration= (ES)=5.7 mol/L,
Supersaturation Concentration= 8 mol/L

where here we designate as θ the droplet temperature in (°C). Typical runs are shown in Figure 2 (Georgiadou, A., 2009):

$$\theta_\infty = 50 \, ℃, C_o = 1 mol/L, R_o = 10 \mu m$$

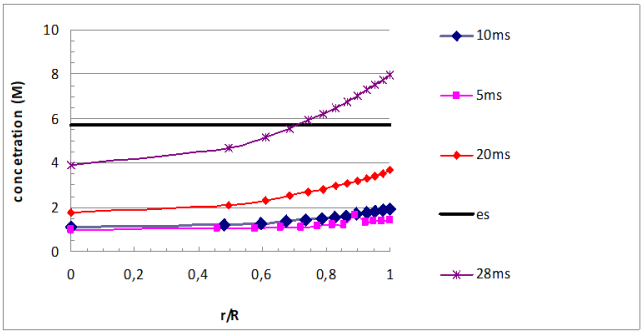

Figure 3. *Typical computational runs with spraying times as parameter.*

Certainly, the behavior captures that reported by van der Lijn, J., (1976), however, faster evaporation rates were calculated resulting in instabilities not encountered by the above authors. Improvements in the program efficiency are certainly required to further increase its usefulness and generality.

4. CONCLUSIONS-FUTURE WORK

A mathematical model was presented for the initial stages of evaporation of solution droplets in the technique of Solution Spray Pyrolysis (SAT). A student-friendly commercial software (wolfram Mathematica) was implemented to check its validity and generality for a studied physical system based on spraying of a solution of zirconyl hydroxychloride. While the simulation captures the general behavior observed by a more sophisticated model by Jayanthi et al., (1993) it fails at higher spraying times possibly due to inherent program instabilities. Future work will focus on improving the stability and generality of the program as well as extending its application to other physical systems.

REFERENCES

Eslamian, M.,Ahmed, M., and Ashgriz, N.,2006. Modelling of nanoparticle formation during spray pyrolysis. *Nanotechnology,* 17,1674–1685.

Georgiadou, A.,2009. Modeling of the fabrication of ceramic electrolytic films by the method of spray pyrolysis for use in solid electrolyte fuel cells. *Student Thesis*, University of Western Macedonia, Greece.

He, W., Yoon K.J., Eriksen, R.S., Gopalan, S., Basu, S.N., and Pal, U.B., 2010. *Journal of Power Sources*, 195,532-535.

He, W. and Goodenough, J.B., 2014. *Journal of Power Sources*, 251,108-112.

Jayanthi, G.V, Zhang, S-C., Messing, G.L.,1993. *Aerosol Science and Technology,* 19,478-490.

Kiratzis, N.E., 2016. *Ionics*, 22,751-770.

Krestou, A., Giozis, I., Maroulis, G., Barbatsis, A., Tsanaktsidis, C., Kyriakou, V. and Kiratzis N.E., 2018. *ECS Journal of Solid State Science and Technology*, 7 (11), P660-P670.

Lijn, J. van der, 1976. *Simulation of Heat and Mass transfer in Spray Drying*, Agricultural Research Reports, No. 845.

Messing, G.L., Zhang, S-C., Jayanthi, G.V., 1993. *J Am Ceram Soc.*, 76(11),2707 – 2726.

Nakaruk, A., Sorrell, C. C.,2010. Conceptual model for spray pyrolysis mechanism: fabrication and annealing of titania thin films. *J. Coat. Technol. Res.*, 7 (5), 665–676.

Reid,R.C., Prausnitz, J.M., Sherwood, T.K., 1977. *The Properties of Gases and Liquids*, 3rd ed., McGraw Hill: New York, NY, USA.

Life Cycle Assessment to address key environmental impact elements of ERASE, an innovative in situ remediation technology

Gabriele Beretta[1], Elena Sezenna[1], Giovanni Dolci[1], Lucia Rigamonti[1], Sabrina Saponaro[1], Claudio Carnabuci[2], Daniele Vezzoli[2]

[1]Department of Civil and Environmental Engineering, Politecnico di Milano, Milano, Italy
[2]HPC Italia srl, Milano
Corresponding author email: gabriele.beretta@polimi.it

ABSTRACT

The remediation of contaminated sites supports the goal of sustainable development but may also have environmental impacts at local, regional, and global scales. Life Cycle Assessment (LCA) is increasingly used to support decision-making in site remediation. ElectRode-Aided Soil rEmediation (ERASE) technology, developed from laboratory-scale proof of concept to pilot field tests, as part of Research & Development related to the Polluted Site Decontamination Pre-Commercial Procurement (POSIDON PCP), combines physical, chemical, and biological processes by powering electrodes in a porous medium, such as soil or backfilling materials, contaminated with organic and inorganic substances. Along with operational conditions to increase efficiency, reduce cleanup time, and improve overall cost-effectiveness, the environmental footprint of this technology was evaluated through LCA. Based on the plant equipment installed at a pilot site in Bilbao and the operating conditions, the LCA study compared different field-scale pilot plant solutions, considering key impact elements for the technology, such as electrode material and energy supply. The results highlighted the potential benefits of using renewable energy sources, particularly photovoltaic panels, in reducing the overall environmental impacts. Graphite electrodes showed promising environmental performance, although corrosion remains a concern. This approach led to pinpointing key factors contributing to significant environmental impacts, guiding future efforts in optimizing an efficient and sustainable remediation intervention.

Keywords: *Electrode-aided remediation; soil; LCA; sustainable remediation.*

1. Introduction

Economic and social development has caused impacts on the quality of soil and groundwater. Soil is a non-renewable resource and, together with groundwater, needs to be preserved for the next generations and eventually restored from negative impacts through appropriate remedial measures and interventions.

The main goal of soil and groundwater remediation is to mitigate contamination and effectively reduce/control the associated risks, but attention should be paid to minimize the environmental footprint of remediation activities. Therefore, it is crucial to consider the potential environmental impacts that may arise from remediation activities to maximize the overall benefits of the intervention.

In the framework of the Polluted Site Decontamination Pre-Commercial Procurement (POSIDON PCP), HPC Italia srl and Politecnico di Milano – Civil and Environmental Engineering Department proposed and developed, from the laboratory proof of concept up to field testing, an in situ remediation technique (ERASE - ElectRode-Aided Soil rEmediation). ERASE is based on the integration and simultaneous exploitation of physical, chemical, and biological mechanisms induced by properly powering at least one pair of electrodes installed in a porous medium (heterogeneous soil/backfilling materials, under saturated or unsaturated conditions), contaminated by organic and inorganic pollutants. Direct current (DC) electric fields promote electrokinetic mechanisms (electromigration, electroosmosis, and electrophoresis), driving mass transport towards the electrodes and facilitating the distribution of injected chemical substances (e.g., oxidants, reductants, substrates, nutrients), supporting pollutant degradation and/or recovery. Conversely, alternating current (AC) power induces soil heating through the Joule effect, up to 30° - 40°C, enhancing biological and/or chemical degradation rates of organic pollutants and thermally activating chemical oxidants such as persulfate. Electrochemical reactions also occur near the electrodes, with the production of hydrogen peroxide (H_2O_2) or high-energy free radicals

($O_2^{-\bullet}$ or $^{\bullet}OH$) and water hydrolysis, which modifies the pH and can increase the availability of oxygen or hydrogen, thereby favoring aerobic or anaerobic biodegradation, respectively (Beretta et al., 2019).

Throughout the technology development process, alongside studying the effectiveness of contaminant removal, evaluating site-specific operational conditions, and assessing costs and time required to achieve clean-up goals, a Life Cycle Assessment (LCA) of the proposed solution was performed to evaluate its environmental impacts. The LCA identified key impact factors, highlighting the electrodes life cycle (production, installation, decommissioning, and end-of-life) and electricity consumption as the most relevant environmental burdens (Beretta et al. 2023). This paper analyses in more detail such elements, focusing on the outcomes of pilot testing in Bilbao and comparing through LCA different electrode materials and different electrical energy sources.

2. Overview of pilot test in Bilbao

The ERASE pilot testing in Bilbao (ES) took place in a small portion of the former Zorrotzaurre industrial area, highly contaminated with Total Petroleum Hydrocarbons (TPHs), Polycyclic Aromatic Hydrocarbons (PAHs), and Inorganics (such as As, Pb, and Cd). The site is an artificial island inside the Deusto Canal connecting Bilbao to the sea. Accordingly, the water table at the site is 1.0 - 1.75 m b.g.s, depending on tides, and the unsaturated soil is a coarse-grained filling material (47 - 67% gravel, 16 - 34% sand, <25% fines).

The pilot plant consisted of an electrical unit, a hydraulic unit, and a monitoring unit (Figure 1). The electrical unit included 18 electrode pairs and the power supply system in DC or AC mode. The electrodes were installed in the unsaturated soil (down to 1 m b.g.s.) in boreholes at a distance of 3 m from each other. The hydraulic unit included an injection system (injection wells - IWs, an injection unit for dosing water and chemicals), and an extraction system (extraction wells - EWs, an extraction unit for removing interstitial water). The monitoring unit included devices for monitoring electrical parameter values (current intensity, voltage, power), monitoring points in the unsaturated porous medium (thermocouples, lysimeters, tensiometers, probes for soil gas), and monitoring points in the saturated porous medium (thermocouples, piezometers).

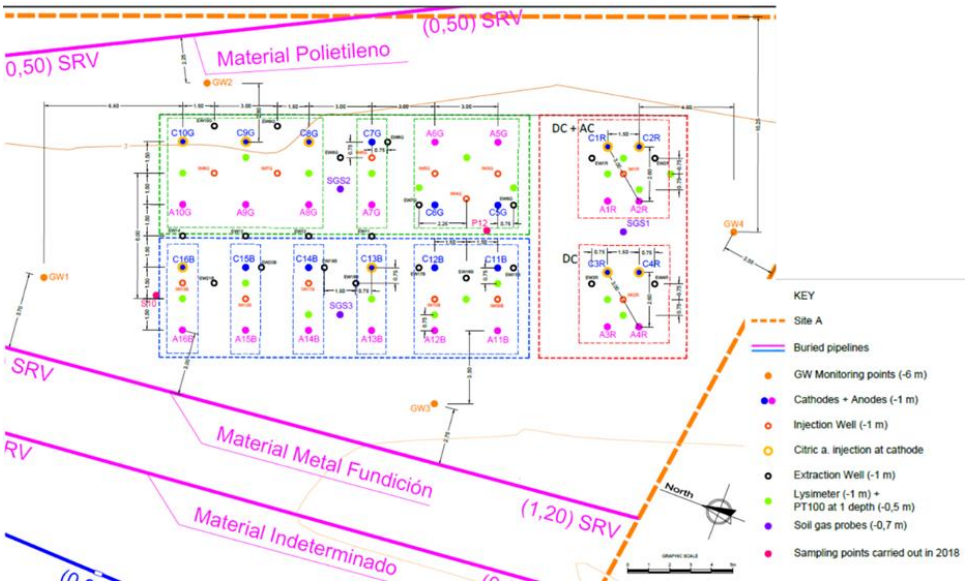

Figure 1 *– Pilot plant layout*

The field strategy was structured according to the following phases: a) installation of the plant, preliminary checks, and tuning; b) DC operation and dosing of persulfate, to promote electrokinetic transport mechanisms of inorganic pollutants and the distribution of the oxidant; c) AC operation to heat the soil to 30° - 40°C and thermally activate the oxidant.

During the test duration, a comprehensive monitoring program was conducted. From test site baseline to the final characterization, many parameters were periodically checked (e.g., soil temperature, interstitial water, soil gas, and groundwater quality).

3. LCA

3.1. Method

The LCA was performed according to the ISO 14044 and 14040 standards (ISO, 2006a; ISO, 2006b).

The selected functional unit (FU) was the overall pilot test including preliminary activities, operational activities, and the decommissioning of the pilot plant.

The Environmental Footprint 3.0 (Fazio et al., 2018) method was selected. It includes 16 impact categories on human health and environment (Climate change - CC; Ozone depletion - OD; Ionizing radiation, human health - IR; Photochemical ozone formation - POF; Particulate matter/respiratory inorganics - RI; Human toxicity, non-cancer effects - HTNC; Human toxicity, cancer effects - HTC; Acidification – A; Eutrophication, aquatic freshwater - EAF; Eutrophication, aquatic marine - EAM; Eutrophication, terrestrial - ET; Ecotoxicity freshwater - EF; Land use - LU; Water use - WU; Resource use, energy carriers - RUE; Resource use, mineral, and metals - RUM). Normalization and weighting stages were not performed.

Based on the pilot test data, performed by using titanium electrodes and the national power grid as the electricity source, the assessment aimed to investigate the effects of the electrode material and the electricity source on the environmental performance of the cleanup system. In particular, three different scenarios were evaluated for each of them: 1) titanium; 2) chromium steel, and 3) graphite, as the electrode material (Table 1 -Stage A); plant powered: a) entirely by the national power grid; b) by the national power grid and on site energy production through photovoltaic panels (PPs) installed in the area under treatment (75 m^2, covering approximately 40% of the plant energy requirements; c) by on site energy production through PPs over about 185 m^2, covering the overall energy requirement of the pilot plant (Table 1 - Stage G). Table 1 summarizes the main inventory data and assumptions for the pilot plant installation and the scenarios evaluated in the LCA. The system was modeled considering the European context (the Spanish context was considered to model the electricity production). The ecoinvent database (version 3.8 allocation, cut-off by classification system model) was used to support the analysis (ecoinvent centre, 2021). The systems were modeled with the SimaPro software (9.3 version).

Table 1 *Inventory data, assumptions, calculations, and ecoinvent processes considered in modelling the pilot test.*

	PRELIMINARY ACTIVITIES Stage – data
A	**Installation of electrodes** • Drilling: number (36), boreholes dimension and depth (Ø 76 mm; 1 m), material for the boreholes filling (70% silica sand and 30% kaolin). Diesel consumption for drilling: 1.63 kg/m^3 soil • Electrodes material: Scenario 1: titanium, as actually used at the field, 1 inch - 25 mm, 1 m long Scenario 2: chromium steel, 1 inch - 25 mm, 1 m long Scenario 3: graphite, 2 inches - 50 mm, 1 m long • Number of electrodes: 36 • Specific weights*: soil: 1970 kg/m^3; silica sand: 1.75 g/cm^3; kaolin: 2.6 g/cm^3; titanium: 4.5 g/cm^3; graphite: 1.7 g/cm^3; chromium steel: 7.86 g/cm^3. • Transportation of extracted soil for 75 km by lorry.
B	**Installation of injection wells (IWs)/extraction wells (EWs)** IWs and EWs: Drilling: number (34), borehole dimension and depth (Ø 178 mm; 1 m), material for the borehole filling (gravel from the borehole bottom up to 30 cm below the ground surface and sealed with bentonite in the last 30 cm). Screened pipes: material (PVC), dimension (4 inches - 100 mm, 1 m long). Specific weights*: silica gravel: 1.5 g/cm^3; bentonite: 2.6 g/cm^3; Weight of PVC pipe - 100 mm: 3.13 kg/m.
C	**Installation of monitoring points of unsaturated soil: lysimeters (LYS)/nesty probes (SGS)** LYS: Drilling: number (20), boreholes dimension and depth (Ø 76 mm; 1 m), drains and filling material: silica sand. Material (PVC), dimension (1 inch - 25 mm, 1 m long). SGS: Drilling: number (3), borehole dimension and depth (Ø 76 mm; 0.7 m), material for the borehole filling (gravel from the borehole bottom up to 30 cm below the ground surface and sealed with bentonite in the last 30 cm). Material (PVC), dimension (0.5 inches - 13 mm, 0.3 m long). Weight of PVC pipe - 25 mm: 0.94 kg/m; Weight of PVC pipe - 13 mm: 0.49 kg/m.

D	**Installation of monitoring points of saturated soil** Drilling: number (6), borehole dimension and depth (Ø 178 mm; 6 m), material for borehole filling (gravel from the borehole bottom up to 30 cm below the ground surface and sealed with bentonite in the last 30 cm). Screened pipes: material (PVC), dimension (4 inches - 100 mm, 6 m long). Weight of PVC pipe - 100 mm: 3.45 kg/m.
E	**Installation of pilot clean-up system** • Transformation and power supply unit including the injection/pumping system control unit and all the installations for energy supply to the electrodes (low voltage distribution panels, transformers, inverter/rectifier units, cables/connections). • Injection unit for water supply and dosage of chemicals: pumping system at the injection/extraction wells, nutrients/reagents dosage system (dedicated pumping system including a tank for dosing and mixing chemicals with water). • Pumping unit for the recovery of interstitial water (e.g. electroosmotic flow). Among the consumable materials, the use of pipes for the connection of the injection/extraction wells is considered. Pipes: material (HDPE), A - dimension (0.5 inches - 13 mm), length (300 m) + B - dimension (9×12), length (500 m) Weight of HDPE pipe A: 0.28 kg/m; Weight of HDPE pipe B: 0.048 kg/m
OPERATIONAL ACTIVITIES Stage – data	
G	Electricity consumption for electrodes, pumps, etc.: overall electricity consumption: 20,700 kWh Scenario a) National grid, as actually used at the field Scenario b) Area covered with photovoltaic panels (PPs): 75 m^2 (i.e., 37 panels; 0.309-0.415 kW/PP; 1300 h/y) → 8,130 kWh/6 months. Remaining consumption: national grid Scenario c) Only PPs: 185 m^2 (i.e., 95 panels; 0.309-0.415 kW/PP; 1300 h/y)
H	Water consumption: amount (1.6 m^3/month), supply (tap water). Total water consumption: 10 m^3
I	Dosage of chemicals: type (sodium persulfate), amount (12.5 kg/m^3 of soil treated). Sodium persulfate consumption: 900 kg
DECOMMISSIONING Stage – data	
L	**Final Soil sampling** Drilling: number (15), borehole dimension and depth (Ø 152 mm, 1 m), material for the borehole filling (bentonite). Mass of soil sent to disposal: 35.7 kg/borehole. Mass of bentonite: 47.2 kg/borehole
A	**Electrodes decommissioning** Mechanical removal of installations and restoration of boreholes with cement mortar. End-of-life treatment of electrodes. Specific weight: cement mortar: 2.1 g/cm^3
B	**Decommissioning of injection wells (IW)/extraction wells (EW)** Injection of cement mortar in each well. Mass of cement mortar (IW + EW): 16.5 + 16.5 kg/borehole.
C	**Decommissioning of monitoring points of unsaturated soil: lysimeters (LYS)/nesty probes (SGS)** LYS and SGS: Installations mechanically removed (drilling as modeled in the installation stage), boreholes restored with cement mortar. End-of-life treatment of lysimeter and nesty probes.
D	**Decommissioning of monitoring points of saturated soil** Injection of cement mortar in each well. -> Mass of cement mortar: 98.9 kg/borehole.
E	**Decommissioning of the clean-up system** End-of-life treatment of pipes used for the connection of the injection/extraction wells. Mass of pipe A sent to disposal: 84.0 kg/300 m. Mass of pipe B sent to disposal: 24.0 kg/500 m.

** Assumed for all the stages*

4. Results: potential environmental impacts

Figure 2 shows the impacts related to the production of one electrode (unit impact) for the different electrode materials considered. When chromium steel is used compared to titanium, impacts decrease in all the impact categories with reductions in the range of 9.8 - 97%. Greater reductions, between 61.5 and 99.8%, are obtained by using graphite. However, graphite is poorly resistant to corrosion during the process, and, despite the use of thicker electrodes, testing would be required especially in the DC phase.

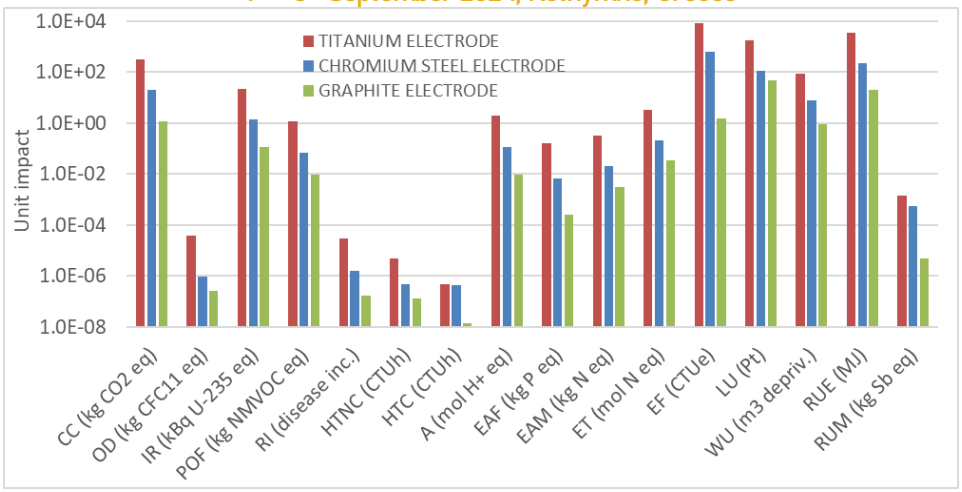

Figure 2 *Impacts of single electrode production (unit impact) as a function of component material. For impact categories acronyms, see Table 2*

Table 2 compares the potential impacts of the overall pilot test using chromium steel electrodes with different electricity sources. The use of photovoltaic energy in scenarios b) and c) allows for the reduction of potential impacts in all the impact categories excluding RUM. RUM impact category is strictly related to the production of PPs and might be mitigated by reusing PPs for other reclamation interventions.

Table 2 *Potential impacts (referred to the FU considered) for scenarios a, b, and c (electricity source). Chromium steel (scenario 2) was considered as the electrode material.*

Impact category	Unit	Scenario			Impact variation	
		a	b	c	100 x (b–a)/a	100 x (c-a)/a
Climate change (CC)	kg CO_2 eq	1.03E+04	8.17E+03	4.88E+03	-21%	-53%
Ozone depletion (OD)	kg CFC11 eq	1.16E-03	1.05E-03	8.83E-04	-9.4%	-24%
Ionizing radiation, human health (IR)	kBq U-235 eq	5.32E+03	3.48E+03	6.53E+02	-34%	-88%
Photochemical ozone formation (POF)	kg NMVOC eq	3.69E+01	2.90E+01	1.67E+01	-22%	-55%
Particulate matter/respiratory inorganics (RI)	disease inc.	3.97E-04	3.70E-04	3.28E-04	-6.8%	-17%
Human toxicity, non-cancer effects (HTNC)	CTUh	1.67E-04	1.59E-04	1.47E-04	-4.6%	-12%
Human toxicity, cancer effects (HTC)	CTUh	2.23E-05	2.16E-05	2.07E-05	-2.8%	-7.1%
Acidification (A)	mol H^+ eq	8.36E+01	6.44E+01	3.48E+01	-23%	-58%
Eutrophication, aquatic freshwater (EAF)	kg P eq	3.89E+00	3.20E+00	2.14E+00	-18%	-45%
Eutrophication, aquatic marine (EAM)	kg N eq	1.26E+01	9.59E+00	5.01E+00	-24%	-60%
Eutrophication, terrestrial (ET)	mol N eq	1.30E+02	9.88E+01	5.08E+01	-24%	-61%
Ecotoxicity freshwater (EF)	CTUe	1.89E+05	1.67E+05	1.34E+05	-11%	-29%
Land use (LU)	Pt	4.75E+04	3.92E+04	2.64E+04	-17%	-44%
Water use (WU)	m^3 depriv.	8.78E+03	7.42E+03	5.34E+03	-15%	-39%
Resource use, energy carriers (RUE)	MJ	2.14E+05	1.59E+05	7.42E+04	-26%	-65%
Resource use, mineral and metals (RUM)	kg Sb eq	1.32E-01	1.56E-01	1.93E-01	18%	46%

From the detailed analysis of the impact categories of each stage of the pilot plant, considering chromium steel electrodes - scenario 2, and electricity source of scenario b (Figure 3), the most relevant burden is related to "Electricity consumption" (stage G, up to 85% of overall contribution in the category IR), followed by "Production, installation, decommissioning, end-of-life of electrodes" (stage A, up to 74% of overall contribution in HTC) and "Production and use of chemicals" (Stage I, up to 31% in OD). About stage A, most of the potential impacts are related to the production of the electrodes. The choice of on site renewable energy can, however, partially mitigate the impacts of this electrode material.

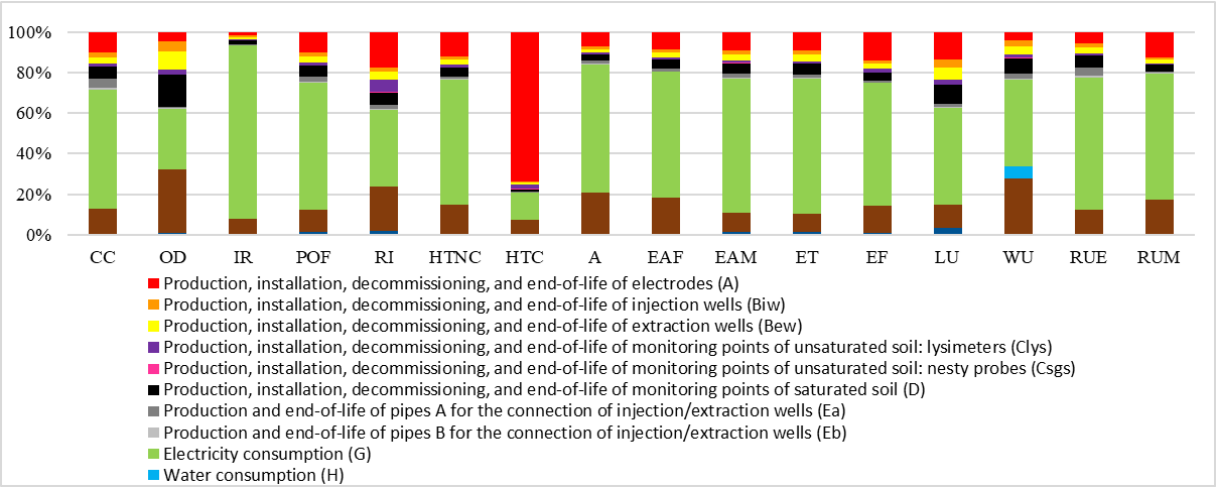

Figure 3 *Impacts contributions for the overall pilot test with chromium steel (scenario 2) as the electrode material and use of PPs + national grid electricity (scenario b). For impact categories, see Table 2.*

5. CONCLUSIONS

LCA allowed identifying the field-scale pilot test key elements that might be improved to reduce the environmental impacts and increase the ERASE technology's environmental performance. In detail, the main contributions of the potential impacts of the technology are related to “Electricity consumption”, “Production, installation, decommissioning, and end-of-life of electrodes” and “Production and use of chemicals”. Useful suggestions came from the outcomes of the comparison of different electrode materials (titanium, chromium steel, and graphite) and electricity sources (grid energy, photovoltaic energy, or a combination of them). Chromium steel electrodes, better than graphite in terms of resistance to corrosion, and energy partially from renewable sources (photovoltaic panels) ensure a significant reduction in the potential impacts of the remediation intervention (between -6 to -74% when compared to titanium electrodes and pilot plant entirely powered by the national grid).

6. ACKNOWLEDGEMENTS

This work was part of the POSIDON project, which received funding from the Horizon 2020 research and innovation program of the European Union (under grant agreement No. 776838). It reflects only the views of the authors.

REFERENCES

Beretta G., Mastorgio A.F., Pedrali L., Saponaro S., and Sezenna E. (2019) *The effects of electric, magnetic, and electromagnetic fields on microorganisms in the perspective of bioremediation*. Reviews in Environmental Science and Bio/Technology, 18, 29-75.

Beretta G., Sezenna E., Dolci G., Rigamonti L., Saponaro S., Carnabuci C., and Vezzoli D. (2023). LCA in the development of an in-situ innovative remediation technology: the case of ERASE-ElectRode-Aided Soil rEmediation. In L'innovazione per la sostenibilità ambientale nell'epoca della multitransizione (pp. 377-380). Cnr Edizioni.

ISO (2006b) ISO 14040:2006 Environmental management - Life cycle assessment - Principles and framework. (ISO 14044:2006 + Amd1:2017 + Amd2:2020).

ISO (2006a) ISO 14044:2006 Environmental management - Life cycle assessment - Requirements and guidelines. (ISO 14040:2006 + Amd1:2020)

Fazio S., Castellani V., Sala S., Schau E.M., Secchi M., and Zampori L. (2018) Supporting information to the characterization factors of recommended EF Life Cycle Impact Assessment methods. EUR 28888 EN, European Commission, Ispra, 2018, ISBN 978-92-79-76742-5, JRC109369

Ecoinvent centre (2021) Ecoinvent Version 3.8 database. Available at: http://www.ecoinvent.org/

Joint Research Center, EU Science HUB, Photovoltaic Geographical Information System (PVGIS) tools. Available at: https://re.jrc.ec.europa.eu/pvg_tools/en/

The impact of substrate extrusion on the energy and economic efficiency of biogas plant operation

K. Kupryaniuk[1], K. Witaszek[1], P. Pochwatka[2], J. Mazurkiewicz[1], I. Vaskina[1], D. Janczak[1] and J. Dach[1]

[1]Department of Biosystems Engineering, Poznań University of Life Sciences, Poznań, Poland
[2]Department of Environmental Engineering and Geodesy, University of Life Sciences in Lublin, Lublin, Poland
Corresponding author email: karol.kupryaniuk@up.poznan.pl

keywords: *substrates; extrusion; anaerobic digestion; energy efficiency.*

Introduction

The agricultural sector currently underutilises organic waste in the form of so-called lignocellulosic biomass, which can include maize straw, rapeseed straw, leaves and hay (Panigrahi and Dubey, 2019). In recent years, technologies to manage these wastes have been increasingly developed. As an example, they can be used in agricultural biogas plants, where heat or electricity can be produced. By carrying out a methane fermentation process, it is possible to dispose of biodegradable substances that are a burden on the ecosystem. The full utilisation of these raw materials as a substrate for biogas production is only possible after pretreatment, which allows the lignocellulosic structures to be broken down. This has the effect of increasing the efficiency of biogas production, including methane (Tong et al. 1990; Kozlowski et al. 2018; Dach et al. 2014). One of the pre-treatment methods is extrusion. Extrusion is a HTST (High Temperature Short Time) type of process due to the fact that the material in the extruder stays in it from several seconds to several minutes and is exposed to high temperature. During this time, the material inside is mixed, compacted, compressed, sheared, liquefied and plasticized in the final zone (Oniszczuk et al., 2012). Specific processing conditions contribute to the disintegration of lignin, facilitating access to cellulose and hemicellulose for bacteria (Oniszczuk and Pilawka, 2013). The high pressure and temperature during extrusion contribute to the hydrolysis of lipids, proteins, carbohydrates, hemicellulose, cellulose and the disruption of the cell wall, thanks to which the material becomes plastic.

Agricultural biomass with an increased content of ligni-cellulose compounds is not normally used in biogas plants due to decomposition problems (straw has a structure that is difficult to access for fermentation bacteria). However, their use can bring a significant effect by increasing the energy efficiency and profitability of biogas plants. The methane fermentation process is highly dependent on conditions, availability and type of substrate. Depending on the raw materials used, the gas mixture resulting as a final product can have different contents of methane, carbon dioxide and other components. It is possible to use agricultural by-products such as cereal straw, corn and cotton waste, plant stalks, animal residues (manure, slurry, poultry manure, litter) and others (Gregersen and Raven 2007; Kalina and Skorek 2002; Lantza et al. 2007; Rasi et al. 2007). The production of methane in the anaerobic digestion process is a proven technology, but it is characterized by low profitability. Biogas installations without financial initiative in the form of green and yellow certificates or fixed feed-in tariffs for the sale of electricity and heat would not be cost-effective and could not compete with conventional fuels such as coal or natural gas. There are a lot of factors causing this state of affairs, e.g., the high costs of substrates for biogas production, a limited supply of local raw materials, and limited availability of innovations that would make biogas energy production cost-effective (Witaszek et al. 2020). Lignocellulose found in plant raw materials is a polymer consisting of three main fractions: cellulose (40-55% DM), hemicellulose (24-40% DM) and lignin (18-25% DM). Because they belong to long-chain polysaccharides that are hydrolysed to a mixture of pentoses and hexoses, they can be used as a substrate for biogas production (Tan et al. 2008). As research has shown (Rodiahwati and Sriariyanun, 2016), the use of the extrusion process in the preparation of raw materials for anaerobic digesion may be justified. Several factors influence the extrusion process: the degree of comminution of the raw materials, the speed of the extruder screw, the plasticising system used, the use of a suitable extruder (single-screw, twin-screw), the appropriate level of wetting of the raw material and the process temperature. An important parameter affecting the extrusion process is the degree of fineness of the substrates, which affects their more effective mixing and

obtaining a homogeneous mixture (e.g. for chopped rye straw the lengths are assumed to be: 1-3 mm, 8-11 mm, 10-15 mm and 20-40 mm) (Kupryaniuk et al. 2020). The processing of the raw material, regardless of its structure, is only possible through the use of optimal wetting. A difference in the moisture content of the raw material of even 1% can increase the energy intensity of the process by up to 100%. In this case, additional pressure-thermal treatment of the lignocellulosic pulp may not be economically justified.

The aim of the work was to investigate the impact of extrusion of two types of straw (cereal and rapeseed) on increasing the efficiency of methane production and the energy and economic efficiency of the operation of a biogas plant with a capacity of 0.5 MW.

Materials and methods

In the study, 2 types of extruded substrates were used to feed the biogas plant: cereal straw and rapeseed straw. Both types of straw were shredded using a CF420B flail shredder (Pavolt, Zrębice, Poland) to particle sizes below 10mm and then extruded using a TS-45 single-screw extruder (Z.M.Ch Metalchem, Gliwice, Poland), and then all substrates were tested for methane yield according to standard methodologies (DIN 38414/S8 and VDI 4630) (Dach et al. 2014) and contrasted with tests on straw without pretreatment. Biogas yield testing was conducted under standard methane fermentation conditions in sets of 3 tank biofermenters (Czekała 2017). The 2 dm3 fermentation reactors were first filled with inoculum (a dose of microorganisms from a working biogas plant) and raw materials processed under different conditions. The organic dry matter content of the inoculum varied from 1.5 to 2%. Dry matter and organic dry matter were checked before testing and the substrates were placed in an airtight digestion reactor. The reactors were placed in temperature-controlled water (approximately 39°C), which simulated the actual operating conditions of commercial biogas plants. The volume and qualitative composition of the gases produced were measured every 24 hours. The fermentation process was stopped when the daily biogas production was less than 1% of the total biogas production. Samples were tested in triplicate. Biogas yield (m3 Mg^{-1}) was expressed in terms of fresh matter, dry matter and dry organic matter, as described by Dach et al. (2014).

In the calculation of the efficiency of the biogas plant operation, two variants of biogas plant power supply were tested:

1. Variant 1: cereal straw + pig slurry and extruded cereal straw + pig slurry;
2. Variant 2: rapeseed straw + pig slurry and extruded rapeseed straw + pig slurry.

Energetic and economic calculations were carried out according to a standard methodology, based on market prices in Poland in May 2024 and taking into account the additional amount of electricity used during the extrusion of both types of straw.

Results and discussion

The results of anaerobic digestion tests and preliminary energetic and economic analysis are presented in Table 1.

Table 1. *Methane efficiency of the tested substrates and preliminary energetic and economic analysis for variants I and II*

Substrate	**D.M.**	**Methane efficiency**	**Substrate use**	**Electric energy spent for extrussion**	**Electric energy to use**	**Substrate cost (straw)**	**Revenue from electricity sold**
Variant I	**%**	**$m^3 \cdot Mg^{-1}$**	**Mg/a**	**MWh**	**MWh**	**EUR**	**EUR**
Wheat straw	88.51	197.18	5150	0	3854.50	301.678	879.450
Wheat straw after extrusion	91.96	213.72	4750	1220.75	2632.69	278.246	600.680
Variant II							
Rapeseed straw	90.70	205.07	4950	0	3853.14	289.962	879.141
Rapeseed straw after extrusion	90.62	228.79	4440	888.00	2967.84	260.087	677.148

In both variants, an increase in methane production from straw was observed, but this increase was relatively small (8.4% in the case of wheat straw and 11.6% in rapeseed straw). The increase in the efficiency

of methane production from the same amount of straw resulted in a decrease in the mass necessary to power a biogas plant with a capacity of 0.5 MW, from 5150 to 4759 Mg/year in the case of wheat straw and from 4950 to 4400 Mg in the case of rapeseed straw, respectively. In this case, there are savings due to the smaller amount of straw needed, at the level of 23.4 kEUR in variant I and 29.9 kEUR in variant II.

However, during further calculations, it must be taken into account that the extrusion process requires additional electricity, which increases the cost of this technology. Therefore, taking into account the cost of electricity necessary for the extrusion process, it should be concluded that in both variant I and variant II, the revenue from the sale of electricity from a biogas plant powered by straw is higher in the variant without extrusion, respectively 278.7 kEUR in the case of wheat straw and 202 kEUR in the case of case of rapeseed straw.

Conclusions

The research presented above confirms that it is possible to process lignocellulosic materials using a TS-45 single-screw extruder. On the basis of the research carried out, it was observed that the application of the extrusion technique to lignocellulosic raw materials had a differential effect on the properties of potential substrates for biogas plants. The extrusion process increases the efficiency of CH_4 production during anaerobic digestion of lignocellulosic substrates such as various types of straw. However, various parameters of the extrusion process influence the increase in productivity. Problems have been observed due to the dosage of raw material. In the studies discussed, the increase in CH_4 production was so low (8.4% in the case of cereal straw and 11.6% in rapeseed straw) that it did not cover the increase in electricity consumption resulting from the operation of the extruder. As a consequence, the use of the extrusion process in the analyzed variants of biogas plants gave a negative economic result. Therefore, it should be concluded that further research is necessary on the optimization of the extrusion process in order to increase the efficiency of CH_4 production from straw with reduced energy demand. It would be desirable to extend the scope to include further publicly available raw materials. A second direction for extending the research is the selection of appropriate process variables (temperature, extruder screw speed, raw material moisture content), as well as the selection of a suitable screw for the extruder. The next step could be the use of advanced technologies such as heat recovery systems (recuperators) or efficient cooling systems. The use of modern process monitoring technologies is crucial for their ability to provide precise control over the course of the esctrusion process. They enable the key parameters of the process to be monitored in real time, identify potential problems and respond quickly to any irregularities. As a result, they will contribute to the efficiency, quality and profitability of the process.

References

1. Panigrahi, S.; Dubey, B.K. A critical review on operating parameters and strategies to improve the biogas yield from anaerobic digestion of organic fraction of municipal solid waste. *Renew. Energy* 2019, *143*, 779–797.
2. Tong M., Smith LH., McCarty PL. 1990. Methane fermentation of selected lignocellulosic materials. Biomass, 21: 239-255.
3. Kozłowski K., Dach J., Lewicki A., Cieślik M., Czekała W., Janczak D., Brzoski M. 2018. Laboratory simulation of an agricultural biogas plant start-up. Chem. Eng. Technol., 41(4): 711-716. https://doi.org/10.1002/ceat.201700390
4. Dach J., Czekała W., Boniecki P., Lewicki A., Piechota T. 2014. Specialised internet tool for biogas plant modelling and marked analysing. Adv. Mater. Res., 909, 305–310. https://doi.org/10.4028/www.scientific.net/AMR.909.305.
5. Gregersen K.H., Raven R.P.J.M. 2007. Biogas plants in Denmark: successes and setback. Renew. Sust. Energ. Rev., 11, 116-132. https://doi.org/10.1016/j.rser.2004.12.002
6. Kalina J., Skorek J. 2002: Paliwa gazowe dla układów kogeneracyjnych; Seminarium cykliczne „Elektroenergetyka w procesie przemian" - Generacja rozproszona, Politechnika Śląska, 11-26.
7. Lantza M., Svenssonb M., Bjornssonb L., Borjessona P. 2007. The prospects for an expansion of biogas systems in Sweden-Incentives, barriers and potentials. Energy Policy, 35, 1830-1843.

8. Rasi S., Veijanen A., Rintala J. 2007. Trace compounds of biogas from different biogas production plants. Energy, 32, 1375-1380.
9. Witaszek K., Pilarski K., Niedbała G., Pilarska A. A., Herkowiak M. Energy Efficiency of Comminution and Extrusion of Maize Substrates Subjected to Methane Fermentation. *Energies*. 2020; 13(8):1887. https://doi.org/10.3390/en13081887
10. Oniszczuk T., Wójtowicz A., Mitrus M., Mościcki L., Combrzyński M., Rejak A., Gładyszewska B. 2012. Influence of process conditions and fillers addition on extrusion-cooking efficiency and SME of thermoplastic potato starch. TEKA Commission of Motorization and Energetics in Agriculture, 12(1), 181-184.
11. Oniszczuk T., Pilawka R. 2013. Wpływ dodatku włókien celulozowych na wytrzymałość termiczną skrobi termoplastycznej. Przemysł Chemiczny, 2, 265-269.
12. Rodiahwati W., Sriariyanun M. 2016. Lignocellulosic biomass to biofuel production: integration of chemical and extrusion (screw press) pretreatment. KMUTNB Int. J. Appl. Sci. Technol., 9, 289-298. https://doi.org/10.14416/j. ijast.2016.11.001
13. Czekała W. 2017. Concept of in oil project based on bioconversion of by products from food processing industry. J. Ecol. Eng., 18, 180–185. https://doi.org/10.12911/22998993/76211.

A Review of EU Refineries Oily Sludge Waste Production, Management Options and Sustainability Assessment of Traditional and Emerging Oily Sludges Treatment Techniques

Alfio Mianzan[1], William Odle[2], Jacob Oerig[2], Eleni Vaiopoulou[3], Konstantinos Sakkalis[4]

[1]NewFields UK, Bradford, United Kingdom
[2]NewFields LLC, Atlanta, United States
[3] Concawe, Brussels, Belgium
[4]bp, London, United Kingdom
Corresponding author email: Waste@Concawe.eu

ABSTRACT

This study presents the results of a survey of EU refineries waste types' production, their sources and management options, with focus on oily sludges and a sustainability assessment of selected traditional versus emerging treatment options for oily sludges wastes. It provides a statistical analysis of waste production by Concawe[3] member company refineries in the years 2019, 2020 and 2021, based on survey data returned from 68 refineries (70.1% response rate) situated in the EU-27 countries + UK, Norway and Switzerland. It includes a breakdown of oily sludge waste tonnage according to its origin and how it was managed. A literature review of emerging and traditional oily sludges treatment technologies provided a selected list of treatment options for detailed assessment of their sustainability. The assessment consisted of a semi-quantitative multi-criteria analysis including criteria assigned to the three main pillars of sustainability: environment, social and economics. A fourth pillar (waste circularity) was added to assess technologies based on their preservation of resources and minimisation of waste generation. Each criterion was given a score with a higher score indicating technologies more favorable for each of the selected criteria. The scores were weighted allowing comparison of the assessed technologies for each of the four pillars. The assessment identified overall better sustainability performance for emerging technologies pyrolysis, solvent extraction and biopiles than for more traditional technologies such as incineration in municipal solid waste incinerators, at cement works and disposal to landfill.

Keywords: refinery oily sludges, waste management options, waste treatment and disposal, sustainability

1. INTRODUCTION

The European Commission (EC) has been adopting a 'Circular Economy package' aimed to develop a more circular economy (European Commission, 2020). Traditional oily sludge treatment/disposal technologies such as incineration and landfilling involve high treatment costs and sit low in the waste hierarchy. They are also becoming less desirable as environmental regulations become more stringent.

A previous review of European refineries waste data (Concawe Report 12/17) showed that Waste Water Treatment (WWT) and hydrocarbon sludges were the most significant part of refinery waste sludges in tonnages. A survey on oily sludges was undertaken of European refineries that reported waste production, sources and management options from 2019 to 2021. The survey identified current pre-treatment techniques and final management options for refinery oily sludges such as incineration, and landfill. These techniques are associated with adverse environmental and human health impacts and high costs. Also, oily sludges can be a potential energy source considering its production quantity and calorific value.

Energy recovery has received particular attention given that it can recover valuable resources as well as mitigate potential impacts by reducing disposal volumes of these type of waste. Recent developments present different treatment mechanisms, resource recovery performance, energy consumption and environmental impacts (Hu et al., 2013). Their success depends on the substantial reduction of oily sludge volumes, the recovery of energy from the sludge and the final treatment of the unrecoverable residue. Oily sludge treatment technologies can be divided into those that focus on the recovery of the oil contained in the oily

[3] Concawe is the technical branch of the Fuels Manufacturers Association operating in Europe.

sludges and those considered traditional disposal/treatment methods currently used by the industry (Figure 1).

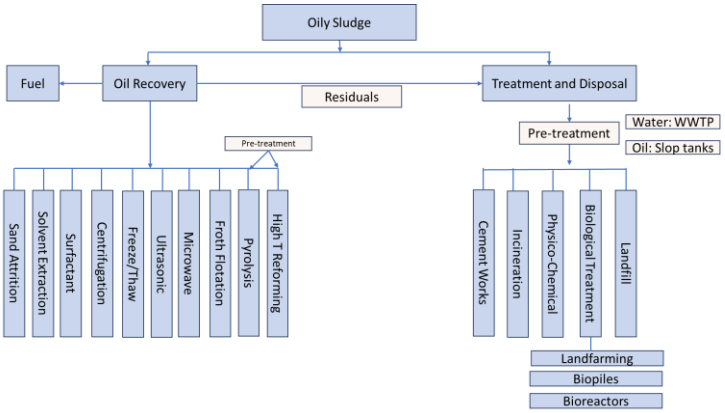

Figure 1. *Oil Sludge Treatment and Disposal Technologies (adapted from Murungi et al, 2022)*

As new technologies have been developed to recover oil in sludge, reduce the amount of waste needing additional treatment or disposal, and potentially having lower environmental and social impacts, to gain further insights into the overall sustainability of traditional vs emerging techniques, a sustainability assessment is undertaken herein considering the three pillars of sustainability: environment, social and economics. A fourth pillar, waste circularity, was added to assess technologies based on their preservation of resources and minimisation of waste generation.

2. MATERIALS AND METHODS

Data on refinery waste production and management options were collected via a survey of European refineries who were asked to provide data for the years 2019, 2020 and 2022. Data was returned by 68 Concawe members' refineries (70.1% response rate) situated in the EU-27 countries + UK, Norway and Switzerland. Survey included questions on historic throughput and waste quantities reported were normalized to the years reported. Normality was tested using Q-Q plots. Waste data is presented as total waste tonnage (reflecting the environmental burden) and tonnes per kilotonne of refinery feedstock throughput (a measure of efficiency) and include an analysis of differences in waste production and management between different European regions. Wastes are reported based on their European Waste Catalogue codes (EWC codes). To identify emerging technologies for oily sludges treatment a thorough literature search was conducted using different sources. Also, interviews with technical experts from Concawe Member Companies were conducted to identify new technologies being sought or tested by refineries and to seek clarification on current technologies used. Findings are summarized in Figure 2.

To select technologies for the sustainability assessment, advantages and disadvantages of each technology were identified and their applicability evaluated to a refinery context and their stage of development (i.e., laboratory, field scale, fully implemented). The technologies selected were: pyrolysis, solvent extraction, cement works, biological treatment (biopiles), landfilling and incineration with energy recovery. A qualitative/semi-quantitative multicriteria analysis was chosen to undertake the sustainability assessment, broadly aligned with ISO 18504 (on sustainable contaminated soil remediation). This approach helped with the identification of relevant "categories of indicators" (assessment criteria) of the three pillars of sustainability plus the fourth pillar (waste circularity). Environmental, and some social indicators were selected from the EU Reference Document on Economics and Cross-Media Effects (ECME June 2006) along with indicators from US EPA's Tool for the Reduction and Assessment of Chemical and other environmental Impacts (EPA 2012). Indicators were global warming potential (GWP), acidification (AP) and eutrophication potential (EP), air quality indicators such as respiratory effects (RE) and smog formation (SM), ecotoxicity effects (ECT) and human toxicity/carcinogenic effects (CAR and NCAR) (Table 1). Weightings were applied between 0 and 5, where 0 was considered not specifically relevant or lacks data to make an assessment. One (1) indicates low importance or data were not conclusive, and 5 indicates high importance.

Table 1. *Assessment Criteria and Associated Weightings*

Pillar	Assessment Criteria	Media Affected	Assigned Weighting	Key Relevant Indicators
Environmental	Ozone Depletion Potential (ODP)	Air	0	Bromofluoroethanes, CFCs
	Global Warming Potential (GWP)	Air	5	CO_2 eq. per ton of sludge
	Acidification Potential (AP)	Air, water	1	SOx, NOx
	Euthrification Potential (EP)	Water	1	Phosphate, Nitrates
	Ecotoxicity Effects (ECT)	Air, water, soil	1	Metals, PAHs
	Further disposal/treatment of residues	Air, water, soil	5	N/A
	Energy Recovery (ER)		5	kW/h
Social	Onsite vs Offsite Treatment	N/A	3	Noise, Vibrations
	Carcinogenic Effects (CAR)	Air, water, soil	0	Cr VI
	Non-carcinogenic Effects (NCAR)	Air, water, soil	0	Metals, PAHs
	Respiratory Effects (RE)	Air	1	PM2.5, SOx
	Smog Formation (SM)	Air	1	NOx, O3
Financial	Commercial Availability	N/A	3	NA
	Disposal/Treatment Cost	N/A	5	€/ton of waste
Circularity Efficiency	Waste Hierarchy	N/A	5	Disposal, Recovery, Recycling

3. RESULTS

3.1 EUROPEAN REFINERIES OILY SLUDGES SOURCES, QUANTITIES AND MANAGEMENT OPTIONS

Sludges are semi-liquid residue from industrial processes and wastewater treatment. Different types of sludges are generated in refinery operations including crude and product tanks bottoms sludges, sludges from API separation units, flocculation and flotation units. (Best Available Techniques Reference Document for the Refining of Mineral Oil and Gas, 2015).

In total, the 68 refineries produced some 3600 kt of hazardous and non-hazardous waste between 2019-2021 thus, an average of 3.15 t of waste per kt of throughput. The largest amount of total waste originates from refinery operations (~62%), followed by re-construction works (~13%), diverse sources (~9.7%) and remediation activities (~8%). Non-hazardous soils and stones waste associated with construction works were the largest waste type produced in the period with ~850 kt. Sludges from waste water treatment containing hazardous substances (~240 kt), and soil and stones containing hazardous substances (~180 kt), were the second and third largest categories overall (Figure 2).

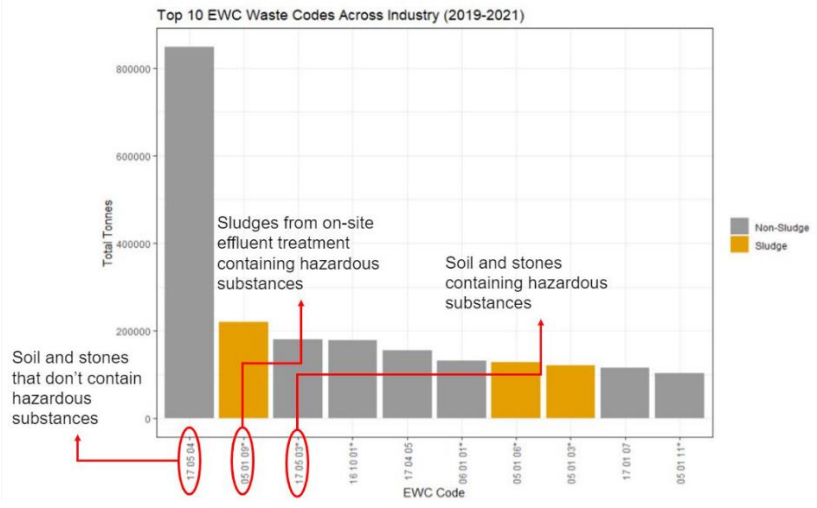

Figure 2. *Top Ten EWC Waste Categories by Tonnage (2019-2021)*

The percentages of sludges in relation to the total amounts of wastes produced were 22.17% (277,137 t) in 2019, 20.61% (237,466 t) in 2020 and 19.61 % (236,647 t) in 2021. The majority of the sludges produced (81.5%) were classified as hazardous. The greatest tonnage (~85%) of sludge wastes reported originated from refinery operations. The three largest waste sludge categories reported were sludge from waste water

treatment plants, oily sludges from maintenance operations and tank bottom sludges and represent 72% of the top ten waste sludge categories (62% of the total amount of sludges produced in the period).

The Waste Framework Directive (2008/98/EC) sets out a waste hierarchy, or priority order of what constitutes the best overall environmental option in waste legislation and policy. It places prevention then reuse, recycling, recovery and disposal from most to least desirable management option. To facilitate the analysis, sludge waste management options reported in the survey were grouped into disposal or recovery options to reflect the EU Waste Hierarchy. As such, disposal categories included incineration (D10), landfill (D1/5) and treatment (such as D9 for physicochemical treatment). Recovery options included incineration with energy recovery (R1), recycling (R3/R4/R5 for recycling and R9 for reuse) and recovery other such as regeneration (R2/R6).

Hazardous sludges constituted the majority of the waste sludge. Incineration and incineration with energy recovery were the two largest management options by weight. Only 2.6 % of the sludges managed by these options were classified as non-hazardous. These two incineration options were followed by landfill, recycling and treatment, all with similar tonnages of hazardous sludges and less amounts of non-hazardous sludges. The recovery-other option is the only option with a larger quantity of non-hazardous sludges in relation to the hazardous fraction (Figure 3).

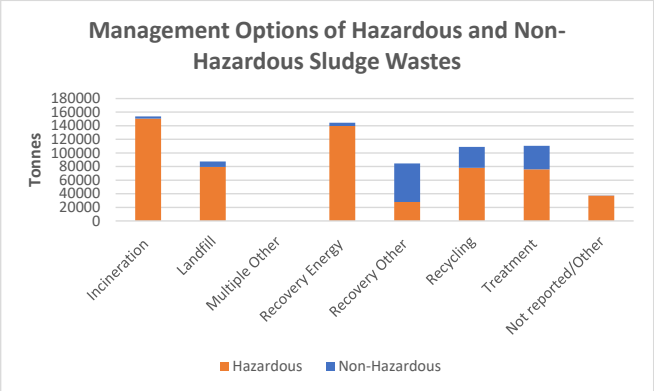

Figure 3. *Hazardous and Non-Hazardous Sludge Wastes by Management Option*

There are regional differences in the management options, this might reflect the availability of waste management options and local policy enforced. Approximately 44% of the wastewater treatment (WWT) sludges received no treatment prior to final disposal or the information was not provided. All regions reported a mixture of treatment/separation and no treatment prior to final disposal with the exception of UK/Ireland/Northern Europe which reported all WWT sludges treated by thickening (centrifugal, flotation and gravity thickening). Energy recovery (R1) was the main management option for this type of sludge waste with a reported 25.2% of the total volume. This was followed by physico-chemical treatment (~14.4%) and recycling (~6.8%)[4]. Disposal into landfill constituted only 1.7% of the total. Overall, more volume of waste water sludge was treated than not treated prior to incineration (D10) and energy recovery (R1), while more sludge volume was not treated than treated when the management option selected was physicochemical treatment (D9).

The largest management option (~15%) for maintenance sludges was physico-chemical treatment (D9), followed in decreasing volume by recycling (R3/4/5), energy recovery (R1), incineration (D10) and oil re-refining (R9), with percentages of between approximately 10% and 13%. The disposal into landfill (D1/5) was low, with approximately 1.8% of the total maintenance sludge managed by this option (in UK/Ireland/Northern Europe, Central/Eastern Europe and Iberia Country Regions). For maintenance sludges it is unclear the pattern in final management options and sludge separation or lack of separation onsite.

The highest tonnage of tank bottom sludges was managed by Landfill (25%) followed by Incineration (24%) and Energy Recovery (23%). Recycling was the main management option for maintenance sludges (26%) followed by Landfill (24%) and Treatment (18%). Wastewater sludges were mainly managed by Incineration (34%) and Energy Recovery (26%), followed by Treatment (16 %) and Recycling (11%).

[4] Examples of category D9, physico-chemical treatment, includes oxidation/reduction, precipitation, neutralisation, immobilisation, etc. Examples of recycling options include composting, anaerobic digestion, gasification and pyrolysis.

3.2 SUSTAINABILITY ASSESSMENT OF TRADITIONAL AND EMERGING REFINERY OILY SLUDGES MANAGEMENT OPTIONS

The sustainability assessment consisted of a comparison between traditional oily sludge treatment/disposal technologies and emerging technologies. The assessment used does not follow a Life Cycle Assessment (LCA) method, but helps identifying system boundaries of the selected management options helping to better understanding of which parts of the alternatives are responsible for the higher impacts. In general, the processes considered are those from the beginning of the oily sludge treatment to the final landfilling or treatment of the residual solids. The technologies assessed included incineration, landfilling, solvent extraction, pyrolysis, biopiles and cement kilns.

The scores were applied on a relative basis, with reference to the relevant indicators in Table 1. The scores range between 1 and 5, where 1 represents the least favorable technique and 5 is the most favorable for that particular criterion (i.e., causes the least impact, has the lower cost, etc). For each pillar (environmental, social, finance and waste circularity) a percentage score was calculated (percentage of maximum possible score, reflecting the number of assessment criteria). The assessment then combined (and normalised) the score for the four pillars, to provide a balanced overall score for each management option. For a given option, this balance overall score can be compared against the other options and assists with the identification of the most favorable options. The results of the assessment are shown in Figure 4. The most favorable management options are biopiles, followed by solvent extraction and pyrolysis. These options are more favorable from a sustainability and circularity point of view than traditional options such as landfilling, cement works and incineration with energy recovery. However, these are considered as emerging techniques and their degree of application to refineries varies, with some technologies only tested at laboratory or pilot scale. Therefore, a conclusion can only be drawn once their availability, cross media effects and applicability restriction are determined.

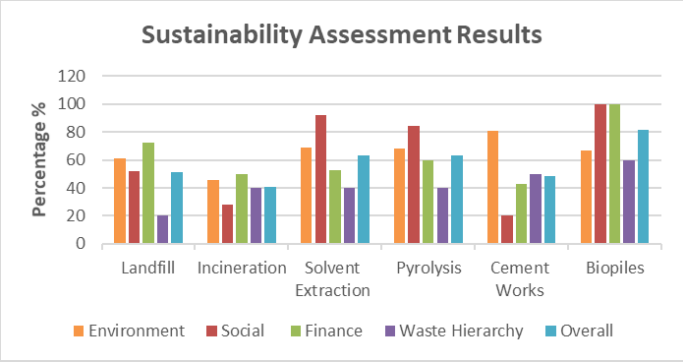

Figure 4. *Sustainability Assessment Results (High bar is judged more sustainable)*

Regarding the environmental pillar, the emission of greenhouse gases is an important environmental impact for all options, primarily associated with CO_2 emissions from combustion and biological degradation, and methane emissions in the case of landfilling. Biological degradation options are favourable with some 300 kg of CO_2 eq. per ton of sludge (Tsiligiannis et al 2020), while incineration is the least favourable option with 1000 to 2000 kg/ton of CO_2 eq. per ton of sludge and much higher when the use of auxiliary fuels to achieved required combustion temperatures is considered. Pyrolysis also scores less favourable when combustion of py-gas and py-oil is considered together with the energy required to maintain the temperature in the pyrolysis reactor. Environmental criteria of Ecotoxicity criteria (ECT), Acidification potential (AP) and Eutrophication potential (EP) were given low weightings given the lack of quantified data encountered during the literature review. The final treatment/disposal of solid residues considers the additional potential environmental impacts from the need to dispose/treat residues (ash, wastewater, solids) from the selected management options. Pyrolysis and cement works resulted the most favourable options. Solids residues from pyrolysis are essentially a char that can be used for soil conditioning while in cement works solid residues are incorporated into clinker. Biopiles have no solid residues since after degradation in the biopiles the remaining soil can be used as a soil conditioner. However, biopiles and landfill produce leachate that requires treatment. Incineration and solvent extraction scored the least favourable due to the amounts of solid residues produced by these options (between 10 and 20% of the original sludge) and the amounts of separated water that needs

to be treated in a waste water treatment plant in the case of solvent extraction. Finally, the Energy Recovery criterion includes the use of energy from waste as a substitute for fossil fuel. Landfill (without CH_4 capture) and biopiles are the least favourable, whilst incineration and cement works obtained higher scores with over 1300 kW/h of produced energy per ton of sludge. Solvent extraction and pyrolysis result in similar production of grid electricity of between 1000 and 1150 kW/h per ton of (oily) sludge using the heat energy from the combustion of recovered oil.

Regarding the social pillar, criteria refer to impacts to people due to emissions. Emissions refer not only to emissions to air and water but also nuisance issues such as noise, vibrations and odours. As such, options requiring offsite transport were selected as the least favourable ones as they can cause additional nuisance due to transport such as noise, dust, vibrations, etc. Onsite treatment was not considered to increase existing refinery impacts on neighbourhoods in any significant way. Most oily sludges are currently disposed or treated offsite. However, handling more waste onsite has the potential to increase overall sustainability and circularity as long as proper management of the waste can be achieved in a cost-effective way. Options such as solvent extraction and pyrolysis can be scaled up to operate within a refinery depending on permitting requirements given contractors are available who can build these plants to various capacities. Biopiles are already used by one Company Member, but availability of space in the refinery is paramount to make them viable. Incineration, cement works, and landfilling are clearly offsite options unlikely to be viable or permitted in refineries and therefore received a lower score. Air emissions causing air quality issues with consequences for people, such as respiratory effects and/or smog formation, were also considered in this category. Cement works was found to be the least favourable option with landfill and biopiles the most favourable. Toxic, carcinogenic effects of emissions from the selected management options are criteria commonly used in LCA studies. However, these criteria were not considered for the assessment.

Regarding the financial pillar, gate costs for disposal or treatment of hazardous waste are difficult to calculate without actual analysis of the waste received by waste managers. Consequently, costs (in €/ton of waste) were obtained from interviews that provided ranges of costs for disposal of oily sludges in general. Other costs were obtained from the literature review and do not necessarily represent commercial rates. Costs for solvent extraction and pyrolysis are operational costs and exclude capital costs (no information). Biopiles assigned costs also represents operational costs only. Solvent extraction costs are based on pilot tests. Commercial availability was not considered, because some options (landfill, incineration) are widespread available to compare against selected emerging options. The low scores in solvent extraction are linked to lack of information and lesser widespread availability.

Re the circularity pillar, each Waste Hierarchy was allocated a score of 1 to 5 in ascending order, i.e., 1 for disposal and 5 for prevention. In this way, landfill (D1/5) was provided a score of 1 and incineration with energy recovery (R1) a score of 2. Incineration without energy recovery (D10) would have been assigned a score of 1. Pyrolysis (R3) and solvent extraction (R3) also falls into the recovery hierarchy and are assigned a score of 2. The co-processing of wastes in cement kilns is a mix of recycling and thermal recovery. The mineral portion of the waste is reused during the process and replaces virgin raw materials. At the same time, the energy content of the waste is very efficiently recovered into thermal energy (R1), thus saving conventional fuels. Therefore, in the waste hierarchy co-processing of waste in cement works generally has a position just below recycling (R5, recycling of inorganic materials) as it is more beneficial than incineration with energy recovery (Cement Sustainability Initiative, CSI). Accordingly, the cement works option was assigned a score of 2.5.

4. CONCLUSIONS

Oily sludges are significant wastes in refinery operations in the 2019-2021 period, oily sludges in European refineries ranged between 19.6 and 22.2 wt% of total produced wastes. The main three types of oily sludges produced by weight were tank bottom sludges, refinery maintenance sludges and WWTP sludges. Incineration with and without energy recovery, followed by landfill, treatment and recycling were the main management options.

The sustainability assessment indicated that biopiles are the most favourable management option, followed by solvent extraction and pyrolysis. However, these are considered as emerging techniques and their degree of application to refineries varies, with some technologies only tested at laboratory or pilot scale. Therefore, a conclusion can only be drawn once their availability, cross media effects and applicability restriction are determined, and the specificities of the refinery are taken into account.

Finally, the sustainability assessment provided a rapid, semiquantitative method to compare overall sustainability of different technologies. More quantitative sustainability appraisal tools, such as LCA tools, can be beneficial in the understanding of impacts and benefits from emerging technologies in comparison to traditional approaches. They can also help quantify possible cross-media effects and avoid unintended consequences of improving one or more of the evaluated pillars to the detriment of others.

REFERENCES

A new Circular Economy Action Plan for a cleaner and more competitive Europe, European Commission COM 2020 (98).

Best Available Techniques (BAT) Reference Document for the Refining of Mineral Oil and Gas, 2015, and its accompanied BAT, 2014.

Best Available Techniques (BAT) Reference Document for Common Wastewater and Waste Gas Treatment/Management Systems in the Chemical Sector, 2010.

Best Available Techniques (BAT) Reference Document for Waste Incineration, 2019.

Best Available Techniques (BAT) Reference Document for the Production of Cement, Lime and Magnesium Oxide, 2013.

Best Available Techniques (BAT) Reference Document for Waste Treatment, 2018.

Best Available Techniques (BAT) Reference Document for Large Combustion Plants, 2017

Concawe (2017). 2013 Survey of Waste Production and Management at European Refineries. Concawe Report No 12/17.

Concawe Waste Survey Data 2019-2021 (Report in preparation).

Directive (EU) 2018/851 of the European Parliament and of the Council of 30 May 2018 amending Directive 2008/98/EC on waste.

Directive 2010/75/EU of the European Parliament and of the Council of 24 November 2010 on industrial emissions (integrated pollution prevention and control).

Directive 2008/50/EC of the European Parliament and of the Council of 21 May 2008 on ambient air quality and cleaner air for Europe.

EPA, 2012. Tool for the Reduction and Assessment of Chemical and other Environmental Impacts (TRACI).

EU Council Directive on the landfill of waste, 1999.

EU Reference Document on Economics and Cross-Media Effects, June 2006.

ISO, 2017. ISO 18504:2017, Soil Quality: Sustainable Remediation. ISO, Geneva

Murungi P.I., Sulaimon A. A., 2022. Petroleum sludge treatment and disposal techniques: a review. *Environmental Science and Pollution Research (2022) 29:40358-40372. https://doi.org/10.1007/s11356-022-19614-z.*

Tsiligiannis A., Tsiliyannis C., 2020. Oil refinery sludge and renewable fuel blends as energy sources for the cement industry. *Renewable Energy 157 (2020), https://doi.org/10.1016/j.renene.2020.03.129.*

United Nations, 2020. CCET guideline series on intermediate municipal solid waste treatment technologies: Waste-to-Energy Incineration.

Soil Improvement by Electro Carbonation Induced Calcite Precipitation (ECICP) from the Seawater

Hamed Abdeh Keykha[1], Maria Mavroulidou[1]*, Hadi Mohamadzadeh Romiani[2]

[1] Division of Civil and Building Services Engineering, BEA, London South Bank University, 103 Borough Road, London, SE1 0AA, UK
[2] Departments of Civil Engineering, Buein Zahra Technical University, Buein Zahra, Qazvin, Iran

Corresponding author email: mavroum@lsbu.ac.uk

ABSTRACT

This paper explores the potential of using captured CO_2 to generate carbonates, towards the production of sustainable binders for soil stabilization. In this study, seawater was used in an electrokinetic process to produce sodium hydroxide, which reacted with CO_2 in the presence of Ca^{+2}, resulting in the precipitation of $CaCO_3$. A downward flow injection method was employed to introduce carbonate produced from CO_2 and calcium solutions into sand column specimens. Permeability and unconfined compressive strength (UCS) tests were conducted to evaluate the effectiveness of the method as soil stabiliser. Scanning electron microscope (SEM) images and energy dispersive X-ray spectroscopy (EDX) spectra confirmed the precipitation of calcite crystals in soil pores, thereby enhancing strength. This method has the potential of using captured industrial CO_2 to rapidly produce high concentrations of $CaCO_3$, which can potentially serve as a sustainable soil binder.

Keywords: Carbon dioxide, Electro-carbonation, Calcite, Soil stabilization.

1. INTRODUCTION

Chemical soil stabilizers such as cement and lime are commonly used to enhance the engineering properties of soils, as well as povide dust and erosion control (Kichou et al, 2023). However, the production of both materials releases considerable amounts of carbon dioxide (CO_2) into the atmosphere. For this reason, extensive international effort targets the production of alternative cements such as alkali-activated cements (Mavroulidou et al, 2022,2023) or biocements (Keykha et al, 2017,2018; Safdar et al, 2021, 2022, Mwandira et al, 2023) towards the development of more sustainable soil stabilisation techniques.

In this context, this paper studies instead the development of binders based on mineral carbonation as a promising technique, which could potentially use captured CO_2 from industries, while developing eco-friendly soil stabilisers. The technique produces carbonates or bicarbonates, which can combine with calcium ions in the system to precipitate calcium carbonate ($CaCO_3$) (Romiani et al. 2019). $CaCO_3$ is an economical, non-toxic, environmentally friendly, and durable product capable of physically and chemically bonding soil particles, thereby enhancing compressive strength. Therefore, efforts to utilize CO_2 for developing new soil stabilizers are of significant scientific interest.

It is well understood that when CO_2 interacts with seawater, carbonic acid (H_2CO_3) is formed, although this reaction is reversible. With aqueous sodium hydroxide (NaOH), the solubility of CO_2 increases. The reaction between H_2CO_3 and NaOH produces Na_2CO_3 (Equations 1 & 2), which can be precipitated as $CaCO_3$ if a calcium ion source -in our case calcium chloride ($CaCl_2$) solution- is provided (Equation3). The $CaCO_3$ can then bind soil particles, thereby enhancing the engineering properties of soils.

$$CO_2 + H_2O \rightleftharpoons H_2CO_3 \rightleftharpoons H^+ + HCO_3 \rightleftharpoons 2H^+ + CO_3^{-2} \quad (1)$$

$$H_2CO_{3\,(aq)} + NaOH_{(aq)} \rightarrow Na_2CO_{3(aq)} + H_2O \quad (2)$$

$$Na_2CO_3 + CaCl_2 \rightarrow CaCO_3 + NaCl_{(aq)} \quad (3)$$

Electrolysis of concentrated sodium chloride solutions produces chlorine gas, hydrogen gas and aqueous sodium hydroxide (Equation 4).

$$2NaCl_{(aq)} + 2H_2O_{(l)} \rightarrow H_{2(g)} + Cl_{2(g)} + 2NaOH_{(aq)} \quad (4)$$

Sodium chloride (NaCl) and the reduction process through electrolysis can be further used to generate aqueous NaOH (Du et al. 2018). Various types of electrolytic cells, including the Castner-Kellner cell, Nelson diaphragm cell, or membrane cell, can be utilized for this purpose. Among these, the membrane cell is preferred for NaOH production as it does not produce hazardous by-products and requires minimal energy (Hou et al. 2018). In the membrane cell, an ion-exchange membrane selectively allows Na^+ and water to pass into the cathode compartment while blocking the movement of products between compartments. Saturated brine enters the anode compartment, and concentrated NaOH is produced in the cathode compartment (Luo et al. 2018).

This current study aims to prove the technique and the produced $CaCO_3$ as a soil stabiliser, towards the development of sustainable binders, with the potential of using waste CO_2 from industries. This mechanism is called "Electro carbonation induced calcite precipitation (ECICP)" for soil treatment.

2. EXPERIMENTS

2.1 Electorkinetic cell

Figure 1 shows a schematic diagram of the experimental setup, consisting of a 20-cm long, 10-cm wide and 10-cm high plexiglas, graphite plates with a surface area of 60 cm^2 used as electrodes, a power supply useed to generate a direct current (DC) voltage of around 10 V at 25 °C and atmospheric pressure, and a ceramic membrane with pore size less than 0.2 µm between cathode and anode electrodes to minimise the possibility of back reactions (e.g. sodium ions). To increase the contact area between CO_2 bubbles and absorbent produced by electrolysis, the CO_2 was injected in the cathode chamber.

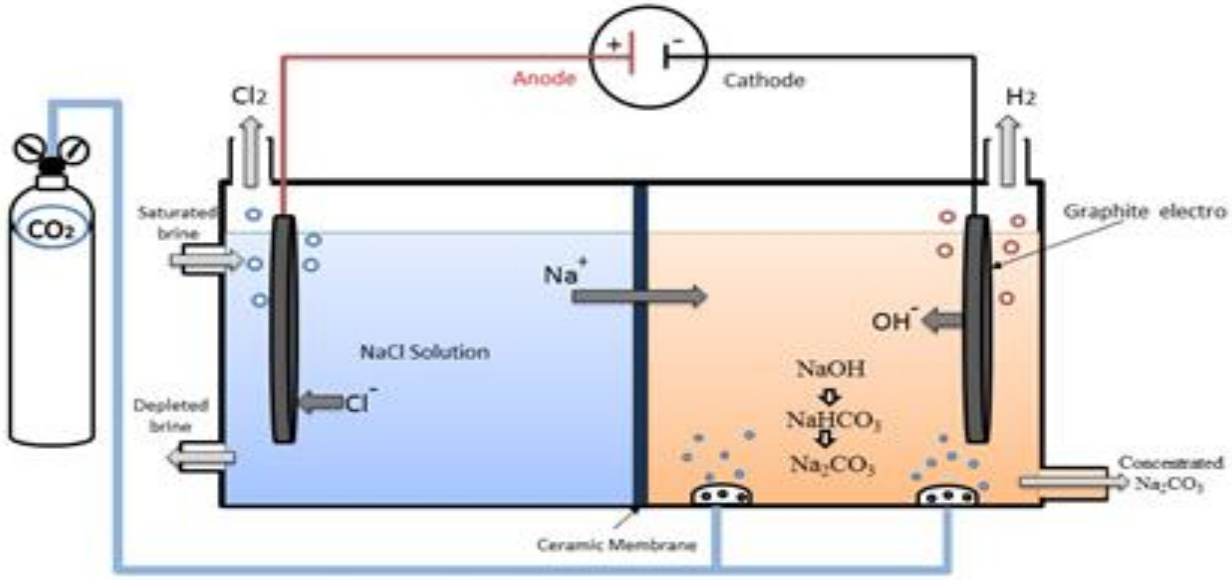

***Figure 1**. Electrolysis cell for CO_3^{-2} preparation*

2.2. Preparation of free carbonate (CO_3^{-2}) and Calcium carbonate ($CaCO_3$)

To generate free carbonate ions (CO_3^{2-}), distilled water was mixed with NaCl to replicate seawater, resulting in solutions with concentrations of 5%, 10%, and 20%. Subsequently, an electrolysis cell was connected to a CO_2 cylinder, and CO_2 gas was injected into the solution at a rate of 5 ml/min. The solutions underwent electrolysis at a voltage gradient of approximately 10 V, at a temperature of around 25 °C, and at atmospheric pressure for varying durations of up to 96 hours. The concentration of CO_3^{-2} ions was measured by Thomas Combination Carbonate Ion Selective Electrode (ISE) at different period of times during the electrolysis process. 1M $CaCl_2$ solution was used to provide the required calcium ions.

a. Soil sample preparation and stabilizing procedure

A clean uniform medium silica sand was used in this study, with maximum and minimum void ratios e of 0.91 and 0.57, respectively. Air-dry sand column specimens of a relative density of 60% (e=0.72) were prepared by dry pluviation (Presti et al., 1992) into 50 mm diameter split moulds of 100 mm length.The produced free carbonate (CO_3^{-2}) and $CaCl_2$ solution (1M) were then added to the top of the sand and the effluent was collected from the bottom of the specimens (i.e. downward flow injection method) (Figure 2). The treatment with the cementation solution was repeated (one and three times respectively) to achieve different degrees of cementation. A constant degree of saturation was kept throughout the tests by managing the volume of effluent solution to be equal to that of the injected solution. The specimens were left to cure at room temperature for a period of 7 days to allow for precipitation of calcite before testing.

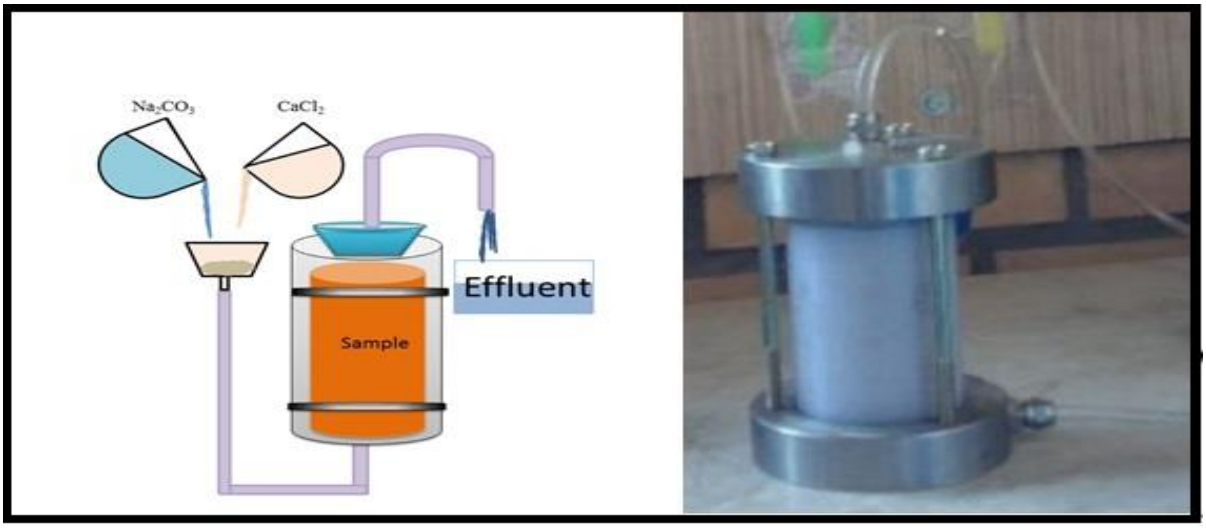

***Figure 2**. Injection and stabilizing procedure*

b. Soil testing and material analysis

Tests consisted of constant head permeability testing according to BS 1377-5:1990) and unconfined compression testing according to ASTM D2166/D2166M-16 (2016) conducted in triplicate on untreated and treated samples. Scanning electron microscope (SEM) and energy dispersive X-ray (EDX) analyses were conducted on crushed UCS specimens after 7 days of curing to characterize the crystalline formation and elemental composition of the $CaCO_3$ crystals present in the sand matrix. $CaCO_3$ content tests were also conducted on ECICP specimens through the washing technique (Keykha et al. 2017). In this technique, the oven dried mass of the soil specimens across the specimen was measured before and after an acid wash in a 2M solution of hydrochloric acid. The dissolved calcium chloride was filtered after treatment. The difference in the two measured masses before and after treatment was taken as the mass of $CaCO_3$.

3. RESULTS and DISCUSSION

Figure 3 shows changes in CO_3^{-2} concentration at different NaCl percentages, over a period of time up to 96h. As can be seen at a constant voltage gradient of 10V and a constant inlet CO_2 rate of 5ml/min, a higher CO_3^{-2} concentration of 1.08 mol/kg was achieved when a NaCl concentration of 20% was used compared to the use of lower NaCl concentrations (i.e. 5 and 10%).

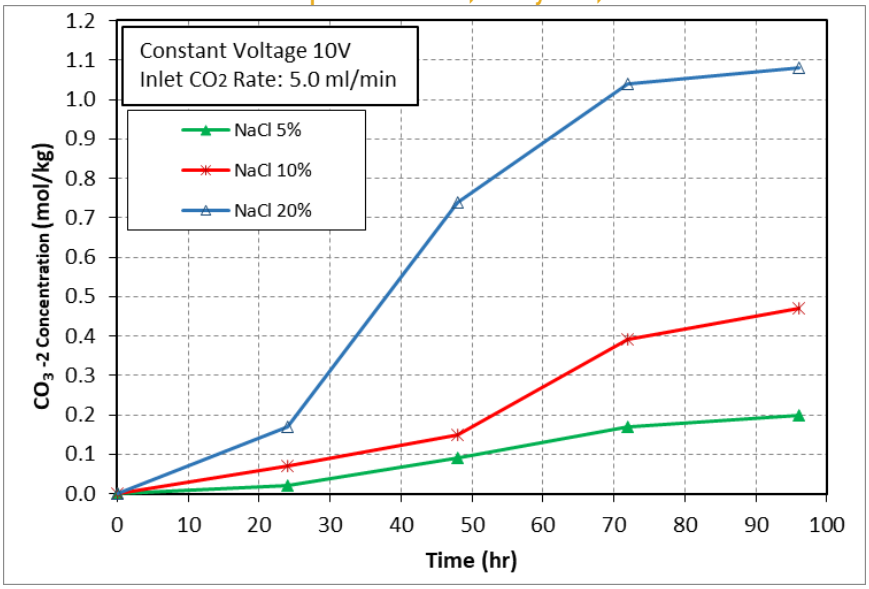

***Figure 3**. CO_3^{-2} concentration during EK process and CO_2 injection*

Figure 4 presents the outcomes of UCS and permeability tests conducted on sand samples treated with ECICP. The figure indicates that the ECICP-treated samples acquired varying amounts of $CaCO_3$ when the cementation solution treatment was repeated more than once on individual sand columns. It is evident that an increase in $CaCO_3$ content resulted in higher UCS values. The treated samples achieved a maximum UCS strength of approximately 182 kPa with a $CaCO_3$ content of 0.045 g/g sand. Additionally, the treated samples exhibited a reduced permeability, particularly at higher $CaCO_3$ contents, reaching a minimum of 5.2×10^{-6} m/s (compared to 9.2×10^{-6} m/s for the untreated soil) corresponding to 0.045 g/g sand calcite content.

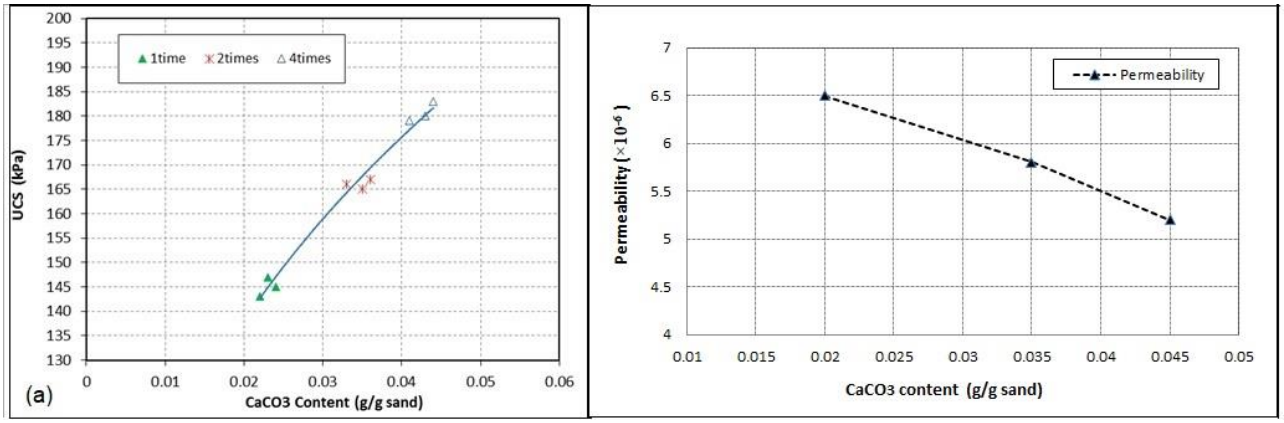

***Figure 4.** UCS (a) and permeability (b) of treated specimens with electro carbonation induced calcite precipitation (ECICP)*

The SEM image of Figure 5a shows that large calcite crystals precipitated at the soil pore throats covering the gap between the sand particles, thus providing an increase in soil strength. The EDX analysis in Figure 5b confirms the presence of calcium (10 %), carbon (9 %), and oxygen (70 %) in the ECICP treated sand matrix, consistent with the composition of calcite ($CaCO_3$), while silicon (11 %) was derived from the quartz (SiO_2), which is the main component of silica sand used in the current study.

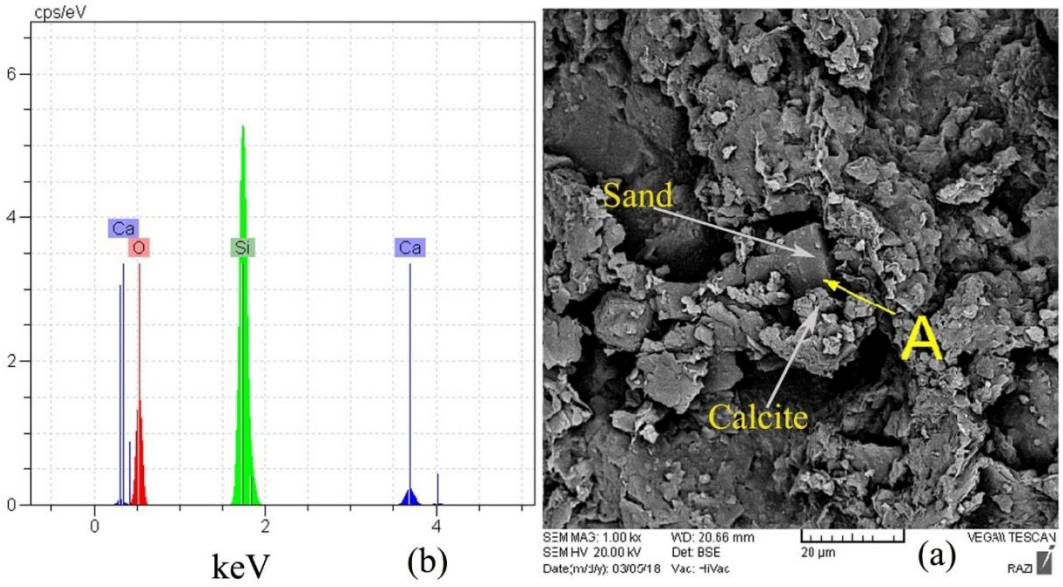

***Figure 5**. (a) SEM image of calcite precipitation between sand particles; (b) EDX analysis of calcite-sand matrix.*

4. CONCLUSIONS

The laboratory-scale experimental results in this study confirmed that the electro-carbonation induced calcite precipitation (ECICP) is a feasible method for soil improvement. The ECICP-treated sand column specimens gained UCS of around 182 kPa with 0.045 $CaCO_3$ content (g/g sand) and had a permeability reduced to 5.2×10^{-6} m/s. SEM and EDX analyses confirmed the precipitation of calcite crystals in the calcite-sand matrix. The findings of this study should encourage futher study and development of the technique as a new sustainable stabilization method with positive environmental impact.

5. ACKNOWLEDGEMENTS

The research on this topic currently carried out by Dr Keykha at London South Bank University is linked to the UKRI-funded MSCA-PF project COSMIC (Grant EP/Y029607/1).

REFERENCES

ASTM D2166, A. 2016. Standard test method for unconfined compressive strength of cohesive soil.

Bai, Y., and Bai, Q. 2018. Subsea engineering handbook. Gulf Professional Publishing.

Du, F., Warsinger, D. M., Urmi, T. I., Thiel, G. P., Kumar, A., and Lienhard V, J. H. 2018. Sodium hydroxide production from seawater desalination brine: process design and energy efficiency. *Environmental science & technology*, 52(10), 5949-5958. https://doi.org/10.1021/acs.est.8b01195.

Hou, M., Chen, L., Guo, Z., Dong, X., Wang, Y., and Xia, Y. 2018. A clean and membrane-free chlor-alkali process with decoupled Cl2 and H2/NaOH production. Nature communications, 9(1), 438. https://doi.org/10.1038/s41467-018-02877-x

Kichou, Z.,Mavroulidou M., Gunn, M.J. (2023) Investigation of the strength evolution of lime-treated London Clay soil. Ground Impovement, 176 (5), 321-352

Keykha, H. A., Asadi, A., and Zareian, M. 2017. Environmental factors affecting the compressive strength of microbiologically induced calcite precipitation-treated soil. *Geomicrobiology journal*, 34(10), 889-894.http://www.tandfonline.com/loi/ugmb20.

Keykha, H. A., Asadi, A., Huat, B. B., and Kawasaki, S. 2018. Microbial induced calcite precipitation by Sporosarcina pasteurii and Sporosarcina aquimarina. *Environmental Geotechnics*, 6(8), 562-566.https://doi.org/10.1680/jenge.16.00009.

Mavroulidou, M., Gray, C., Gunn, M.J. and Pantoja-Muñoz L. 2022b A Study of Innovative Alkali-Activated Binders for Soil Stabilisation in the Context of Engineering Sustainability and Circular Economy. Circular Economy and Sustainability. 2: 1627–1651. https://doi.org/10.1007/s43615-021-00112-2.

Mavroulidou M, Gray C, Pantoja-Muñoz L, Gunn MJ 2023. An assessment of different alkali-activated cements as stabilisers of sulphate-bearing soils. Quarterly Journal of Engineering Geology and Hydrogeology. doi: 10.1144/qjegh2022-057

Mwandira W., Mavroulidou M, Satheesh A, Gunn MJ, Gray C., Purchase D., Garelick J. (2023a) An electrokinetic-biocementation study for clay stabilisation using carbonic anhydrase-producing bacteria Environmental Science and Pollution Research, 30: 104916–104931 https://doi.org/10.1007/s11356-023-29817-7

Romiani, H. M., Keykha, H. A., Talebi, M., Asadi, A., and Kawasaki, S. 2021. "Green soil improvement: using carbon dioxide to enhance the behaviour of clay". Proc. Inst. Civ. Eng. Ground Improvement, 1-26. https://doi.org/10.1680/jgrim.20.00073.

Safdar, M.U., Mavroulidou, M., Gunn, M.J., Purchase D., Payne I., and Garelick, J. 2021 Electrokinetic biocementation of an organic soil. Sustainable Chemistry and Pharmacy, 21: 100405 https://doi.org/10.1016/j.scp.2021.100405

Safdar, M.U., Mavroulidou, M., Gunn, M.J., Purchase D., Gray C., Payne I., and Garelick, J. 2022. Towards the Development of Sustainable Ground Improvement Techniques—Biocementation Study of an Organic Soil. Circ. econ. sustainability. 2: 1589–1614. https://doi.org/10.1007/s43615-021-00071-8

Luo, T., Abdu, S., and Wessling, M. 2018. Selectivity of ion exchange membranes: A review. Journal of membrane science, 555, 429-454. https://doi.org/10.1016/j.memsci.2018.03.051

Park, H. S., Lee, J. S., Han, J., Park, S., Park, J., and Min, B. R. 2015. CO2 fixation by membrane separated NaCl electrolysis. *Energies*, 8(8), 8704-8715.. https://doi:10.3390/en8088704.

Presti, D. L., Pedroni, S., and Crippa, V. 1992. Maximum dry density of cohesionless soils by pluviation and by ASTM D 4253-83: A comparative study. *Geotechnical testing journal*, 15(2), 180-189.https://doi.org/10.1520/GTJ10239J.

Biocementation via microbial induced struvite precipitation: A mini review on cleaner method of soil stabilization

Sumit Joshi, Maria Mavroulidou* and Michael J Gunn

School of Build Environment and Architecture, London South Bank University, SE1 0AA, London, U.K
Corresponding author email: mavroum@lsbu.ac.uk

ABSTRACT

Biological mineralization is a widespread natural phenomenon, in which over sixty distinct biominerals of biogenic origin are produced. A novel and effective research method that draws inspiration from nature is microbially induced calcium carbonate precipitation (MICP). A wide range of MICP based engineering applications have been studied, including soil stabilisation, stone monument restoration and improving the durability properties of concrete. To date, ureolysis-based metabolic process of urease producing bacteria is the most widely used for rapid and controlled precipitation of calcium carbonate as a cementing agent. Despite the benefit of being a biomimetic and potentially sustainable process, the MICP process using enzymatic hydrolysis of urea generates ammonia (NH_4^+ (aq) & NH_3 (g)) posing threat to groundwater and ecosystems. To overcome this, a novel technique known as the microbial induced struvite precipitation (MISP) mechanism has recently been developed to manage the ammonium and ammonia byproducts. In MISP treatment, ammonium ions are utilized in the presence of magnesium and phosphate ions to precipitate bio-struvite minerals that have shown promise of providing effective cementation in construction materials and geotechnical applications. In this comprehensive review, bio-struvite through phosphate biomineralization is presented as an alternative and efficient breakthrough in ammonia free bio-cementation. The cost- effectiveness in bio-struvite precipitation with the use of recovered phosphorous/ammonium ions from various waste sources are also discussed in this review.

Keywords: biomineralization; struvite; ammonium; phosphate; soil improvement.

1. INTRODUCTION

All over the world, the demand for infrastructure expansion has led to intensive large-scale construction activities. A significant amount of infrastructure is constructed using concrete; existing concrete infrastucture also needs regular maintenance and repairs. This leads to a yearly consumption of concrete of ca. 30 billion tons (Monteiro et al, 2017). Different conventional methods are used in concrete research to improve durability properties and retrofitting of deteriorated concrete structures. Surface treatments of concrete with synthetic agents for the remediation of permeability of concrete, different chemical additives as an admixture to improve strength properties of concrete, and different organic agents are used to heal the concrete cracks are reported (Pan et al, 2017). The conventional practices are being scrutinized due to constructability constraints, capital cost and environmental safety (Fu et al, 2023). As a result, biocement, which is produced based on the natural process of biomineralization has been welcomed as an innovative and potentially more sustainable way of building self-healing concretes or producing biocement grouts to seal concrete cracks. Similarly, biocement was met with enthusiasm by the geotechnical engineering community as a potential alternative to Portland cement for soil stabilisation or grouting. The most commonly researched and used biocement is calcium carbonate in the form of calcite or aragonite minerals, produced as a result of microbially-induced calcium carbonate precipitation (MICP).

In nature, biomineralization by different microbial species like photosynthetic organisms (cyanobacteria and algae), sulfate reducing bacteria (SRB) (dissimilatory reduction of sulfates), organisms utilizing organic acids, heterotrophic carbonic anhydrase producing bacteria and urea hydrolyzing bacteria in diverse environments under different pathways has been reported. Among the abovementioned microbial pathways, ureolytic pathway of calcium carbonate precipitation is the most frequently employed biological process to drive $CaCO_3$ biocementation in concrete for concrete strength improvement, concrete crack healing, restoration of heritage buildings, soil stabilisation, beachrock formation, dust erosion resistance and bioremediation (Joshi

et al, 2017, Mwandira et al, 2023). MICP via urea hydrolysis is an easily controlled mechanism in which high amounts of carbonates are produced by the ureolytic bacteria in a short time period. In ureolysis, degradation of urea is catalyzed by microbial urease enzyme into carbonate and ammonium. One mole of urea is hydrolyzed intracellularly into one mole of carbonate and two mole of ammonium (Joshi et al, 2018). The precipitation of calcium carbonate through ureolysis is shown in the equations 1-2 below.

$$CO(NH_2)_2 + H_2O \xrightarrow{Bacteria} NH_2COOH + NH_3 \quad \text{Eq. 1}$$

$$NH_2COOH + H_2O \rightarrow NH_3 + H_2CO_3 \quad \text{Eq. 2}$$

These products further equilibrate in water to form bicarbonate and two moles of ammonium and hydroxide ions (Eq. 3 – 4).

$$2NH_3 + 2H_2O \rightarrow 2NH_4^+ + 2OH^- \quad \text{Eq. 3}$$

$$2OH^- + H_2CO_3 \rightarrow CO_3^{2-} + 2H_2O \quad \text{Eq. 4}$$

The presence of calcium ions in the microenvironment around the bacterial cell wall results into the precipitation of calcium carbonate as the super-saturation is reached as shown in Eq. 5.

$$CO_3^{2-} + Ca^{2+} \leftrightarrow CaCO_3 \quad \text{Eq. 5}$$

Although the ureolytic pathway is easy, straightforward and high-$CaCO_3$ yielding, the produced ammonium resulting from microbial urea hydrolysis may have human health and environmental impacts if left untreated. During the biotreatment, a considerable amount of toxic NH_3 gas is discharged into the environment and NH_4^+ (aq) ions adsorbed in the treated soils can be harmful to the surface water and may result in eutrophication (Yu et al, 2021). The European Union regulation of ammonium concentration (~0.03 mM) for drinking water reflects the effects of ammonium on human health. Therefore, its removal following MICP requires careful monitoring (European Union 2020). As the ammonium generation is a major disadvantage in ureolytic based MICP applications, an alternative pathway with desirable biocementation is discussed in this paper. The precipitation of struvite (magnesium ammonium phosphate hexahydrate, $MgNH_4PO_4{\cdot}6H_2O$) via biomineralization is identified as an alternative to MICP which tackles the generation of ammonium. This paper discusses the mechanism of microbially induced struvite precipitation (MISP), the recovery of phosphorous and ammonium from waste materials and the application of MISP as a sustainable biocementation method for soil improvement.

2. STRUVITE – Mechanism of precipitation

Struvite, is a white colored, orthorhombic crystalline mineral formed of Mg^{2+}, NH_4^+ and PO_4^{3-} ($MgNH_4PO_4{\cdot}6H_2O$) in equal molar concentrations. As the concentration of phosphates, magnesium, and ammonium exceeds the solubility product in an alkaline environment, struvite precipitation occurs (Hao et al, 2013). Struvite is the most ideal mineral obtained chemically or biologically usually from the wastewater treatment plants, showing the recovery of 51.8% of phosphates based on its chemical composition. The chemical equation of the formation of struvite is given in Equation 6 below:

$$Mg^{2+} + NH_4^+ + PO_4^{3-} + 6H_2O \rightarrow MgNH_4PO_4.6H_2O \quad \text{Eq. 6}$$

The nucleation and the growth of crystals are the two main phases of the struvite crystallization process. In the nucleation phase, the ions combine with each other and form a crystalline embryo. The growth of crystals ends when equilibrium is reached in the reaction mixture.

Chemical precipitation of struvite is a well-known mechanism to recover PO_4^{3-}/NH_4^+ from the wastewater as a value-added product. Recovery of phosphorous from municipal waste water or sludge dewatering liquors with struvite precipitation is reported extensively (Siciliano et al, 2020). For spontaneous struvite precipitation, a minimum of 100 mg PO_4-P/L is reported; however in municipal waste water PO_4-P is 10 times less. Also pH adjustment around the value of 8.5 is required along with the equimolar concentration of magnesium and

phosphorous. The factors like pH adjustment and maintaining molar concentrations of magnesium and phosphorous in chemical precipitation of struvite precipitation are the limiting factors (Leng and Soares, 2023).

Another method of biological struvite is proposed as a key route to recover phosphorous and ammonium from the waste water. It has the advantage of no pH-adjustment and recovering PO_4^{3-}/NH_4^+ even at low concentrations when compared with conventional chemical precipitation. A diverse range of microbial strains have been documented to modify solution chemistry (such as pH and $NH4^+$) through their metabolic processes, hence fostering supersaturation conditions that lead to the formation of bio-struvite. The process of bio-struvite crystallization was also reported as a link of electrostatic interaction of cations (Mg^{2+}, NH_4^+) in solution with microbial cells/microbial extracellular polymeric secretions. The capability of different microbial strains in precipitation of bio-struvite is discussed in the next section.

3. BIO-STRUVITE – Microbial mineralization

Microbial mediated precipitation of bio-struvite by different microbial strains is an innovative process to recover phosphorous and ammonium from the waste water stream. Different microbial strains have been reported to recover phosphorous and ammonium from the waste water stream/synthetic waste water medium with efficient precipitation of bio-struvite. The precipitation of bio-struvite in sludge dewatering liquor was investigated with *Bacillus pumilus, Halobacterium salinarum and Brevibacterium antiquum* bacterial strains between pH of 5.7 to 9.1 (Simoes et al, 2018a). It was reported that all the strains could grow at pH range of 5.7 to 9.1 but the highest production of bio-struvite (135-198 mg/L) was observed at pH range of 7.3 to 8.3. In a different study, *Shewanella oneidensis* MR-1 (ATCC 700550) strain was used to precipitate bio-struvite with cheap magnesium source (MgO) in organic growth medium (Luo et al, 2018). It was reported that 97% of magnesium was transformed into bio-struvite precipitation. *Brevibacterium antiquum* strain was reported to precipitate bio-struvite in sludge dewatering liquor (Simoes et al, 2018b). In another study, halophilic bacterial strain *Microbacterium marinum* sp. nov. H207 was used to induce bio-struvite under different percentages of salinity (ranging 0% to 4%) (Zhao et al, 2019). In this study, 90.8% of phosphorous removal in the form of bio-struvite was reported. Leng and Soares (2021) reported that bacterially-induced mineralization of bio-struvite was observed in H. salinarum, B. pumilus and M. Xanthus bacterial strains. Heterogeneous sizes of bio-struvite were observed and 63-71% phosphorous and 94-99% magnesium was recovered from the synthetic medium. Biomineralization of struvite through *Enterobacter cloacae* and *Bacillus pumilus* was reported in synthetic waste water medium (Kumari and Jagadevan, 2022).

4. BIO-STRUVITE – Application in geotechnical engineering

In the field of soil biocementation, the potential of phosphate biomineralization generated by microbes has been demonstrated. Biogenic struvite minerals have advantages over ureolytic-based calcium carbonate minerals: (a) bio-struvite precipitation does not entail ammonium byproducts, (b) bio-struvite crystals have low solubility and (c) there is potential of using waste phosphorous resources to bioprecipitate struvite. To improve the engineering properties of construction materials through microbial induced struvite precipitation, different studies proposed by researchers are discussed below. An overview of different approaches of MISP is shown in Table 1.

The use of *Sporoscarcina pasteurii* bacterial strain to biocement loose sand using microbially produced struvite was reported (Yu et al, 2016). Biocementation was carried out in a sand column using solutions comprising $MgCl_2$, urea, and $K_2HPO_4.3H_2O$ in varying concentrations. The microbial struvite precipitation led to a considerable decrease in ammonia and an increase in strength (1.59 MPa) in biocemented loose sand. The wind erosion of loose sand was reported to be significantly suppressed as a bio-struvite crust formed a solidified layer on the sand.

Table 1. *Overview of different biocementation application through MISP*

Microorganism / Material	Application	Phosphate mineral	References
Sporoscarcina pasteurii	Loose sand	Struvite	Yu et al, 2016
S. pasteurii	Loose desert sand	Struvite	Yu et al, 2019a
S. pasteurii	Quartz sand	Magnesium carbonate, Struvite	Yu et al, 2019b
S. pasteurii	Ottawa sand	Struvite	Yu et al, 2022
Synthetic effluent	Fine sand	Struvite	Mohsenzadeh et al, 2022
S. pasteurii	Ottawa sand	Struvite	Yu and Yang, 2023
S. pasteurii	Waste mud	Struvite	He et al, 2023

In a different study, spraying treatments with *Sporoscarcina pasteurii* and solutions comprising urea, $MgCl_2$, and $K_2HPO_4.3H_2O$, resulted into the suppression of desert sand following cementation with bio-struvite precipitation. Significant improvements in the mechanical properties and decreased porosity of biocemented desert sand were reported after three times of media spraying treatment (Yu et al, 2019a). An average wind speed of 12.0 m/s was used to measure wind erosion for the biocemented desert sand. The wind erosion rate of untreated desert sand was reported to be 798 $g/m^2/h$. However, after 3 spray treatment of media and *S. pasteurii* culture results into 0 $g/m^2/h$ wind erosion rate of biocemented desert sand.

The optimization of bio-magnesium phosphates for the treatment of sand particles was also reported, in which a ratio of 1:2:2 for bio-carbonate cement: $MgCl_2$: $K_2HPO_4.3H_2O$, respectively was recommended (Yu et al, 2019b). In this study, a reduction in the average permeability and a strength gain of the sand cemented by bio-struvite was reported. This study also reported the fixation of 88% of ammonia into struvite crystals.

In another bio-struvite study, columns made of Ottawa sand were treated with the microbially induced struvite precipitation also employing the *S. pasteurii* strain (Yu et al, 2022). The bacterial culture was injected into a two-stage injection treatment in which a first cycle using 2M dipotassium hydrogen phosphate was followed by a second cycle using 1M urea and 2M magnesium chloride solution after 6 hours. Bio-struvite precipitation was found to be quicker, more effective in reducing specimen porosity, and needed less injection cycles when compared to microbially produced $CaCO_3$ precipitation.

An alternative method of using synthetic effluent, whose composition is comparable to that of the effluent produced when soil is treated ureolytically was reported (Mohsenzadeh et al, 2022). This work described the successful removal of ammonium ions via struvite precipitation. After passing the synthetic effluent through the sand columns for a full day, the adsorbed ammonium ions in the soil were removed using washing solutions (NaCl, $CaCl_2$, and $MgCl_2$). Using $MgCl_2$ and Na_2HPO_4, the ammonium ion-rich washing solutions were utilised to chemically precipitate struvite. The study's key findings indicate that at pH 8.5 and with the molar ratio of 1.2:1:1 of Mg^{2+}:NH^{4+}:PO_4^{3-}, 86.8% of the ammonium ions were recovered as very pure struvite precipitate in the synthetic effluent.

The combined effects of a one-phase MICP treatment and a two-phase microbial struvite treatment were documented in a recent study on Ottawa sand columns (Yu and Yang, 2023). A grown culture of *S. pasteurii* containing a solution of urea and calcium chloride/calcium acetate at low pH 6 was introduced into the sand column during the MICP treatment. The collected effluent, referred to as the "biocementation waste solution," was utilized to create two distinct solutions of $K_2HPO_4.3H_2O$ and $MgCl_2$. The prepared solutions were then injected into the sand columns to induce struvite by bacteria. It has been reported that the struvite and calcium carbonate crystals effectively precipitated in the sand grains and greatly decreased the permeability of the biocemented sand.

In a recent study, MISP was applied with *S. pasteurii* culture to treat engineering waste mud to induce solid settling (He et al, 2023). In this study, optimum concentration of bacterial cell (8.36×10^6 cell.ml^{-1}), urea (10 mM), phosphate buffer saline (20 mM, pH7) and $MgCl_2$ (25 mM) were used. Under this optimum concentration, kaolin suspension was reported to be effectively flocculated with flocculation rate of 87.2%.

5. CONCLUSIONS

Microbially induced struvite precipitation has emerged as a feasible and promising alternative to the ureolytic pathway of biocementation by calcite precipitation for geotechnical applications. The literature study indicates that MISP-based soil treatments are still in their infancy. Some encouraging results of bio-struvite precipitation during laboratory-scale studies have given rise to novel ideas about how to solve the geotechnical issues in an environmentally responsible and sustainable manner. MISP mechanism of treatment effectively mitigates the undesirable release of ammonium which is a major disadvantage in ureolytic treatment of soils at field scale. The extensive studies of phosphorous and ammonium recovery from the waste water streams through bio-struvite precipitation also provide a value addition in economical operations of MISP in ground improvement at large scale. MISP could also be an effective technique to deal with different applications such as soil contamination and concrete crack healing in the future.

6. ACKNOWLEDGEMENTS

This paper is supported by the UKRI-funded MSCA-PF project “BIOPHILIC: BIOprecipitated PHosphates for Improved Low-carbon Innovative Cements” (EP/Y029615/1).

REFERENCES

European Union 2020., Directive (EU) 2020/2184 of the European parliament and of the Council of 16 December 2020. On the quality of water intended for human consumption (No. 435). Off. J. Eur. Union.

Fu, T., Saracho, A. C., Haigh, S. K., 2023. Microbially induced carbonate precipitation (MICP) for soil strengthening: A comprehensive review. *Biogeotechnics*., 1, 100002.

Hao, X., Wang, C., Van Loosdrecht, M. C., Hu, Y., 2013. Looking beyond struvite for P-recovery. *Environ. Sci. Technol.,* 47, 4965-4966.

He, Y., Liu, S., Shen, G., Pan, M., Cai, Y., Yu, J., 2023. Treatment of engineering waste slurries by microbially induced struvite precipitation mechanisms. *Front. Bioeng. Biotechnol*., 11, 1109265.

Joshi, S., Goyal, S., Mukherjee, A., Reddy, M. S., 2017. Microbial healing of cracks in concrete: a review. *J. Indus. Microbiol. Biotechnol.* 44(11), 1511-1525.

Joshi, S., Goyal, S., Reddy, M. S. 2018. Influence of nutrient components of media on structural properties of concrete during biocementation. *Constr Build. Mater*., *158*, 601-613.

Kumari, S., Jagadevan, S., 2022. Phosphorus recovery from municipal wastewater through struvite biomineralization using model gram-negative and gram-positive bacterial strains. *J Clean Prod*., 366, 132992.

Leng, Y., Soares, A., 2021. Understanding the mechanisms of biological struvite biomineralisation. *Chemosphere*., 281, 130986.

Leng, Y., Soares, A., 2023. Microbial phosphorus removal and recovery by struvite biomineralisation in comparison to chemical struvite precipitation in municipal wastewater. *J.Environ. Chem. Eng*., 11, 109208.

Luo, Y., Li, H., Huang, Y. R., Zhao, T. L., Yao, Q. Z., Fu, S. Q., Zhou, G. T., 2018. Bacterial mineralization of struvite using MgO as magnesium source and its potential for nutrient recovery. *Chem. Eng. J.,* 351, 195-202.

Mohsenzadeh, A., Aflaki, E., Gowthaman, S., Nakashima, K., Kawasaki, S., Ebadi, T., 2022. A two-stage treatment process for the management of produced ammonium by-products in ureolytic bio-cementation process. Int. J. Environ. Sci. Te., 19, 449–462.

Monteiro, P. J., Miller, S. A., Horvath, A., 2017. Towards sustainable concrete. *Nat. Mater*., 16, 698-699.

Mwandira, W., Mavroulidou, M., Gunn, M. Purchase, D., 2023. Concurrent Carbon Capture and Biocementation through the Carbonic Anhydrase (CA) Activity of Microorganisms -a Review and Outlook, *Environ. Process*. 10 (56).
Pan, X., Shi, Z., Shi, C., Ling, T. C., Li, N., 2017. A review on surface treatment for concrete–Part 2: Performance. *Constr Build. Mater*., 133, 81-90.
Siciliano, A., Limonti, C., Curcio, G. M., Molinari, R., 2020. Advances in struvite precipitation technologies for nutrients removal and recovery from aqueous waste and wastewater. *Sustainability*., 12, 7538.
Simoes, F., Vale, P., Stephenson, T., Soares A., 2018a. The role of pH on the biological struvite production in digested sludge dewatering liquors. *Sci. Rep.,* 8, 7225.
Simoes, F., Vale, P., Stephenson, T., Soares, A., 2018b. Understanding the growth of the bio-struvite production Brevibacterium antiquum in sludge liquors. *Environ. Technol*., 39, 2278-2287.
Yu, X., Qian, C., Xue, B., 2016. Loose sand particles cemented by different bio-phosphate and carbonate composite cement. *Constr Build. Mater*., 113, 571-578.
Yu, X., Qian, C., Jiang, J., 2019a. Desert sand cemented by bio-magnesium ammonium phosphate cement and its microscopic properties. *Constr Build. Mater*., 200, 116-123.
Yu, X., Zhan, Q., Qian, C., Ma, J., Liang, Y. 2019b. The optimal formulation of bio-carbonate and bio-magnesium phosphate cement to reduce ammonia emission. *J. Clean. Prod*., 240, 118156.
Yu, X., Chu, J., Yang, Y., Qian, C., 2021. Reduction of ammonia production in the biocementation process for sand using a new biocement. J. Clean. Prod., 286, 124928.
Yu, X., Yang, H., Wang, H., 2022. A cleaner biocementation method of soil via microbially induced struvite precipitation: A experimental and numerical analysis. *J. Environ. Manage*., 316, 115280.
Yu, X., Yang, H., 2023. One-phase MICP and two-phase MISP composite cementation. *Constr Build. Mater*., 409, 133724.
Zhao, T. L., Li, H., Huang, Y. R., Yao, Q. Z., Huang, Y., Zhou, G. T., 2019. Microbial mineralization of struvite: salinity effect and its implication for phosphorus removal and recovery. *Chem. Eng. J*., 358, 1324-1331.

Unseen Processes in Freeze Desalination: Molecular Dynamics of Nucleation, Crystal Growth, and Ion Entrapment – A Short Review

Khadije El Kadi[1,2] and Isam Janajreh[1,2]

[1]Mechanical and Nuclear Engineering Department, Khalifa University, Abu Dhabi, United Arab Emirates
[2]Center for Membrane and Advanced Water Technology, Khalifa University, Abu Dhabi, United Arab Emirates
Corresponding author email: isam.janajreh@ku.ac.ae

ABSTRACT
Freeze desalination (FD) presents a promising path for sustainable and energy-efficient freshwater production. This emerging technology leverages the physical principles of crystallization to form ice crystals from supercooled saline solutions, followed by the melting of ice to produce freshwater. Despite its potential, FD faces challenges related to capital costs and more importantly to its process complexity. Understanding the intricate freezing process is essential for optimizing FD efficiency. Molecular dynamics (MD) simulations offer a powerful tool to study FD phenomena at the molecular level, providing insights into ice nucleation, crystal growth, and surface interactions. This short review highlights recent advancements in MD simulations for FD, categorizing them into three main areas: crystal growth and salt ion rejection, homogeneous ice nucleation kinetics, and freezing on solid surfaces. While MD simulations hold promise for enhancing FD understanding, significant knowledge gaps persist. Future research directions include investigating the dynamics of hydrogen bonding during ice nucleation, elucidating ion entrapment mechanisms, and quantifying ion rejection rates during ice growth.
Keywords: Molecular dynamics; Freeze desalination; Ice nucleation; Ion entrapment; Ice crystallization.

1. INTRODUCTION

While several desalination methods are currently mature and abundant, freeze desalination (FD) is an emerging technology that has the potential to be a more sustainable and energy efficient alternative. FD is a freezing-melting process in which ice crystals are formed from a supercooled saline solution and further melted to produce freshwater. The technology is based on the physical nature of crystallization in which impurities, e.g., salts and dissolved solids, are excluded during the formation of ice lattice (Saji et al., 2020). One notable advantage of FD is the potential for brine valorization in the form of salt hydrates, particularly when operating at the eutectic point condition, i.e., highly concentrated brine (Nathoo et al., 2009; Pangborn, 1963; Stepakoff et al., 1974). This offers another possibility of utilizing the byproduct of the current desalination plants in a valuable way, contributing to the overall sustainability of the operation. Meanwhile, the capital cost and complexity of the process are two factors affecting the deployment of FD in the desalination industry (Kucera, 2019). The process of freezing saline water follows the NaCl-water binary phase diagram, depicted in ***Figure 4***. As the temperature drops below the liquidus line, ice crystals emerge in the liquid phase, expelling out salt ions and forming a concentrated brine solution. Conversely, if the salt-water mixture exceeds the solubility line at a given temperature, it becomes supersaturated, indicating an excess of dissolved salt. This can occur through cooling, such as in FD, or through evaporation, causing salt crystals to precipitate from the solution. When saline water cools, salt hydrates crystallize, a phenomenon referred to as eutectic point freezing at the eutectic point temperature. The shape of the ice, the degree of ice growth, and the rejection of brine hinge on various factors, including the mixture's composition, initial salinity, cooling/heat removal speed, and physical traits such as density, viscosity, surface tension, and temperature.

Understanding the freezing process is crucial for optimizing FD. Heat and mass transfer occur simultaneously between solid and liquid phases, particularly at the interface. Heat transfer triggers phase change, forming ice. The rate of heat removal influences phase transition and ice formation patterns. Kinetic factors at the ice-liquid interface impact ice growth quality and thickness. Mass transfer of solutes during freezing alters liquid composition and final ice appearance. Comprehending interconnected mass and heat transfer at the interface is vital for controlling ice quality (Elif Genceli Güner et al., 2015; Kalista et al., 2018).

Continuum approaches commonly used to describe freezing processes often fail to accurately capture the intricate transport phenomena at the ice-liquid interface, which typically spans several molecular diameters (Slattery et al., 2007). These approaches assume fluid continuity and homogeneity, overlooking the non-uniform nature of the ice-liquid interface. Moreover, they rely on assumptions to approximate the complex phenomena of ice nucleation at nano-time and space scales, a stochastic process involving the formation and aggregation of water molecule clusters into ice crystals. In contrast, molecular dynamics (MD) simulations offer a promising tool to study freezing processes at the molecular level, capturing individual molecule behavior. MD simulations provide insights into thermodynamics and kinetic factors at the interface, including ice nucleation and growth, by considering intermolecular and intramolecular forces. They offer valuable information that is not easily predictable or easy to capture through continuum models or experiments, such as nucleation and recalescence. Thus, MD simulations complement experimental and numerical continuum studies, enhancing understanding of parameters in saline water freezing and facilitating more efficient and sustainable desalination processes.

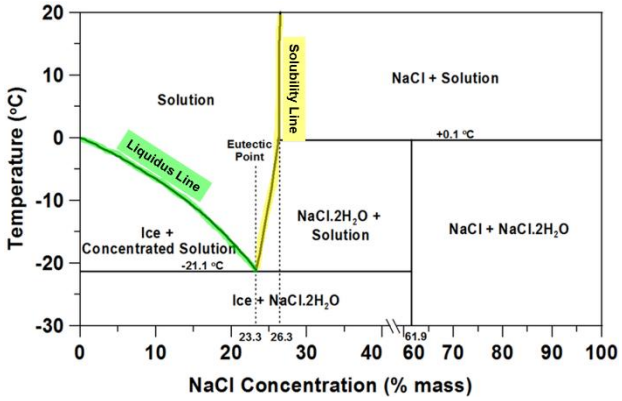

Figure 9. *Phase diagram of NaCl-H_2O mixture*

2. MD for FD

MD simulation has emerged as a powerful tool for studying phenomena occurring during ice crystallization process, which has been of particular interest in various applications such as desalination, cryopreservation, food concentration, and pharmaceutical purposes (Englezos, 1994; Izutsu, 2018; Sánchez et al., 2009; Whaley et al., 2021; Williams et al., 2015). Recent advances in MD simulations for FD technology are highlighted in this work. Literature review categorizes MD work into three areas: (1) crystal growth and salt ion rejection, (2) homogeneous ice nucleation kinetics, and (3) solid surface freezing effects. Despite some studies, significant knowledge gaps persist in simulating seawater freezing using MD.

2.1 Crystal growth and Ion rejection

Studying the behavior of ions and impurities during ice growth is an important aspect to understand the FD process and determining their mechanisms and eventually efficiency. In such MD studies, the simulation box is typically initiated with two distinct equilibrated regions, namely an ice region and a liquid water region, as seen in Figure 5. This approach has been widely adopted by researchers in this field (Conde et al., 2018; Rozmanov and Kusalik, 2011; Tsironi et al., 2020; Wu et al., 2017). For instant, (Vrbka and Jungwirth, 2005) have performed extensive MD simulations of ice growth in an aqueous sodium chloride (NaCl) solution. They have reported the change in water oxygen density and ion density profiles along the direction of crystal growth. Similarly, (Carignano et al., 2006) have investigated the growth of hexagonal ice structure from a brine solution. (Fatemi and FOROUTAN, 2016) were able to simulate crystal growth in a brine solution (salinity = 14%) using the coarse-grained mono-atomic water (mW) model, where radial distribution function (RDF) was utilized to describe the relationship between oxygen water molecules and dissolved ions. It was found that Na+ ions are more likely to be closer to liquid molecules than Cl- ions. Additionally, Na^+-ice interactions were much weaker than Na^+-water interactions (Luo et al., 2021). These results suggest higher entrapment of Cl- ions in the ice phase compared to Na+, similar findings were reported by (Luo et al., 2021; Tsironi et al., 2020). For NaCl-water mixture, it was found that ice growth rate is slower at higher concentrations due to the ion-water interactions. Other results revealed that the accumulation of specific anions, e.g., F^-, on the ice-liquid interface critically influence ice structure and growth rates (Zhang et al., 2021).

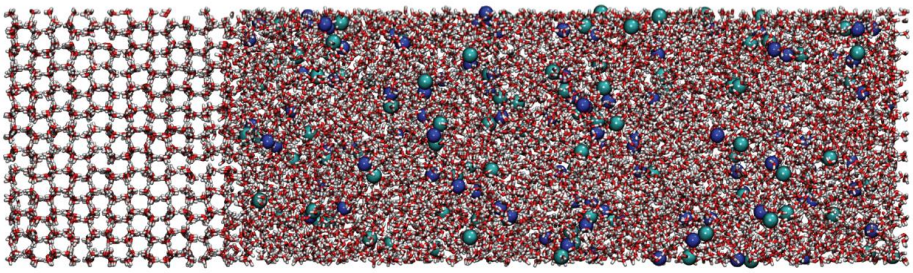

Figure 10. *Initial simulation setup of ice crystal (left) growth in a 0.53M saline water solution (right) with PBC (Color codes: Na+: Dark blue, Cl-: Light blue, H: White, O: Red). Retrieved from* (Tsironi et al., 2020)

2.2 Ice nucleation and surface interactions

Information about the structure and morphology of ice nuclei, the kinetics of nucleation, as well as the role of impurities are important factors in determining the FD performance and can be obtained through MD simulations. However, simulating the nucleation process accurately can be computationally challenging, and many factors can influence the outcome of simulations. This is because ice nucleation exhibits a stochastic nature, with a characteristic time of orders of magnitude longer than those of classical MD simulations (Limmer and Chandler, 2013; Naullage et al., 2020). To initiate the nucleation process in pure water, either deep supercooling or rare event simulations (via enhanced sampling methods) are necessary to overcome the large free energy barriers associated with ice nucleation (Naullage et al., 2020). Water stays supercooled, trapped in a high-energy state (state A), even below the melting point, hindered by an energy barrier (ΔG) from transitioning to stable ice (state B) (Barahona, 2015) (see **Figure 6 (a)**). One of the early studies on homogenous ice nucleation using MD was conducted by Matsumoto et al. (Matsumoto et al., 2002). In this study, water was firstly thermalized at a high temperature, followed by quenching it to a low temperature of 230 K at time t = 0 resulting in a supercooled state of water. As seen in **Figure 7 (a)**, the freezing process of water went into four stages: (1) a long quiescent period (supercooled water), (2) a slow decrease in potential energy, (3) a rapid decrease in potential energy, and a (4) final period where the ice structure fully forms, with intermittent collective motions and energy fluctuations associated with hydrogen bond rearrangements (see **Figure 7 (b)**) occurring during the supercooled liquid state in the quiescent period.

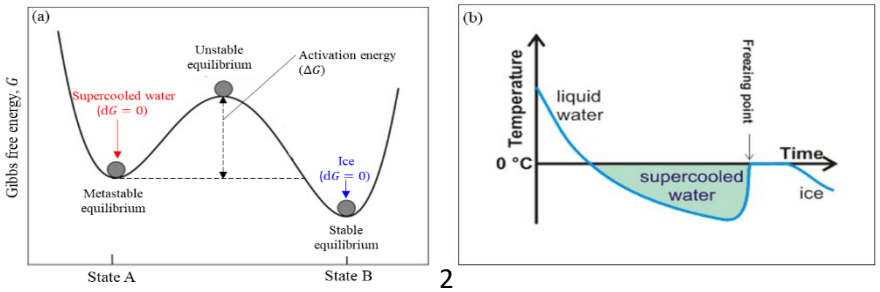

2

Figure 11. *(a) Free energy as a function of the arrangement of atoms in phases: State A: metastable configuration (supercooled water), State B: stable configuration (ice), (b) cooling curve of pure water*

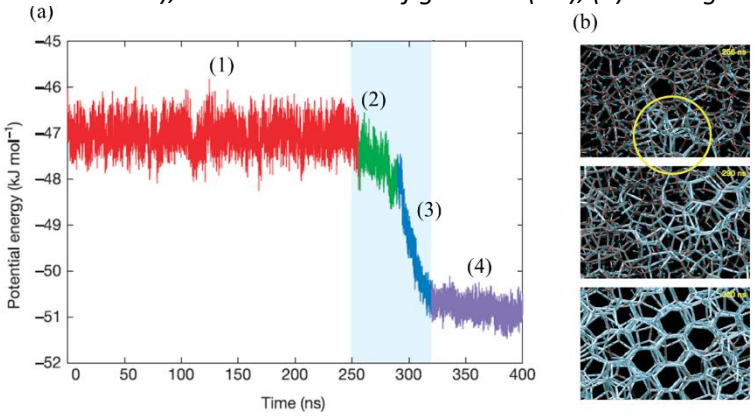

Figure 12. *(a) The total potential energy of the system showing the four stages of water freezing, and (b) the development of "long lasting" hydrogen bond network as developed by* (Matsumoto et al., 2002)

Despite that, if ice nucleation occurs heterogeneously, meaning water is no longer pure and contains dissolved ions/particles or in a direct contact with solid surface, the formation of a metastable state may be inhibited (Langham et al., 1997). In this case, ions can provide nucleation sites to form ice crystals, thus reducing the free energy barrier. Understanding the interaction between the solid surface and the saltwater solution during freezing can help in the design and optimization of FD processes, more specifically for the indirect FD configuration. The surface morphology and properties, e.g., wettability and surface roughness, can affect the ice nucleation (heterogenous nucleation) and growth process, and therefore, the efficiency of the desalination process. Despite the potential of MD simulations in providing atomic-level insights into such phenomenon, the literature on this topic is still relatively scarce. Only a few studies have focused on the behavior of freezing of saline water on solid surfaces using MD (Li et al., 2018; Metya et al., 2016; Metya and Singh, 2018; Moore et al., 2010; Naullage et al., 2020; Ren et al., 2020; Sayer and Cox, 2019; Zielke et al., 2016). This highlights the need for further research efforts to address the knowledge gap in this area and to fully utilize the capabilities of MD simulations in elucidating the underlying physics of FD.

The group of (Metya et al., 2016; Metya and Singh, 2018) have explored the nucleation behavior of a supercooled water (pure water droplet (Metya et al., 2016) and saline bulk solution (Metya and Singh, 2018)) on a nanotextured (Metya et al., 2016) and smooth (Metya and Singh, 2018) graphene surfaces. They found that the ice nucleation rate is enhanced with increasing surface fraction for the Cassie-Baxter state, while the nucleation rate decreases for the Wenzel state with increasing surface fraction (see ***Figure 8***). Moreover, ice adhesion was found to be significantly higher for the Wenzel states compared to the Cassie-Baxter states. Such different wetting states of rough surfaces can give a sense of surface wettability. The authors also showed that a hydrophobic surface is a better nucleating surface when the salinity is above 5%. Heterogeneous ice nucleation occurs at the liquid-solid interface, leading to phase-segregated brine near the liquid-vapor interface. On the other hand, Li et al. (Li et al., 2018) found that the presence of nanogrooves on a surface can have a significant impact on the ice nucleation rate, either enhancing or delaying nucleation depending on the width of the grooves. The study provides critical insights for designing surfaces that can effectively control ice nucleation (Li et al., 2018).

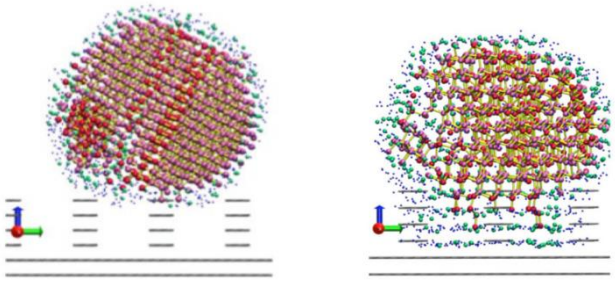

Figure 13. *Water droplet interaction with Cassie-Baxter (left) and Wenzel (right) rough surfaces during ice nucleation* (Metya et al., 2016).

Another important factor that can affect ice formation on surfaces is the presence of ice-nucleating agents (also referred as Ice-binding molecules (IBMs)), which are substances that promote the formation of ice nuclei and facilitate the transition of liquid water to solid ice by lowering the energy barrier for ice nucleation (Abdelmonem et al., 2015; Naullage et al., 2020; Qiu et al., 2019). Ren et al. (Ren et al., 2020) investigated the influence of inorganic salts (LiI, LiCl, NaI, NaCl, KI, KCl, and NH_4I) on the heterogeneous ice nucleation on kaolinite surface ($Al_2Si_2O_5(OH)_4$). The interaction between salts and ice-binding surfaces was found to be relatively weak and non-specific, which can improve the quality of frozen ice. Both Zielke et al. (Zielke et al., 2016) and Sayer et al. (Sayer and Cox, 2019) have investigated ice nucleation on AgI surface using the all-atom TIP4P/2005 water model. The presence of ions (Na^+ and Cl^-) at a water/solid interface have significantly impact the mechanism of ice formation by stabilizing a proton ordered contact layer, potentially leading to more efficient ice nucleation (Sayer and Cox, 2019).

The exact effect of ions on the nucleation process is dependent on several factors, including the ion concentration composition, as well as the temperature and pressure conditions. For instance, it was found that the nucleation rate slows down with salt due to a significant increase in the ice-fluid interfacial free energy, despite the higher thermodynamic driving force for ice nucleation in salty water for a given supercooling (Soria et al., 2018). In another earlier study (Bauerecker et al., 2008), antifreeze effect of adding salt (NaCl: 1 M) on ice nucleation and freezing was investigated, and the molecular mechanisms behind the

corresponding slow down were revealed. On the other hand, Espinosa et al. (Espinosa et al., 2017) reported that increasing operating pressure and solute concentration hinder ice formation by increasing the energy requirement of creating the ice-liquid interface.

3. FUTURE DIRECTIONS

Despite significant advancements in the application of MD simulations to study FD, several research gaps persist, offering substantial opportunities for further exploration. While MD simulations have elucidated the formation and rearrangement of hydrogen bonds of water molecules during the formation of ice crystals, the intricate details of these processes during different stages of freezing require further investigation. Firstly, the transient dynamics of hydrogen bonding during ice nucleation and growth, particularly under varying salinity and temperature conditions, remain underexplored. Secondly, the mechanisms underlying ice entrapment of ions, such as the preferential entrapment of certain ions over others, are not yet fully understood. Identifying the specific molecular interactions and conditions that influence ion entrapment is critical. This includes examining the roles of different ionic species, concentrations, and impurities present in the water. Advanced MD simulations, supplemented with experimental validation, could help elucidate the precise conditions that promote or inhibit ion entrapment during ice crystallization. In addition, there is a need to investigate the rejection rates of various ions during the ice growth process. The interplay between ion-water interactions and hydration energy significantly impacts these rates. Current studies have highlighted that ion-water interactions slow down ice growth at higher concentrations, but a comprehensive understanding of how these interactions affect different ions under diverse operational conditions is lacking. Future research should aim to quantify the impact of specific ion-water interactions on rejection rates and crystal growth dynamics, potentially leading to optimized desalination processes.

MD simulations also have the potential to provide detailed information about ice nucleation and growth on surfaces and the behavior of water molecules and ions at the interface. The knowledge gained from such simulations can be applied to optimize FD processes and mitigate scaling effects caused by impurities. However, simulating freezing on surfaces using MD is computationally challenging, and many factors can influence the simulation results. Despite the promising capabilities of MD, the literature on this topic is still relatively limited, indicating the need for further research efforts. Such efforts will bridge existing knowledge gaps and advance the understanding and efficiency of FD processes.

4. CONCLUSIONS

In conclusion, the application of MD simulations has provided valuable insights into freeze desalination processes, ranging from crystal growth dynamics to surface interactions. However, substantial research gaps remain, necessitating further exploration to unlock the full potential of MD in advancing FD technology. Future research efforts should focus on unraveling the transient dynamics of hydrogen bonding, and explaining ion entrapment mechanisms for various ionic compositions and concentrations. By addressing these knowledge gaps, MD simulations can play a pivotal role in optimizing FD processes and advancing sustainable freshwater production.

5. ACKNOWLEDGEMENTS

This publication is based on the work supported by the Khalifa University under Award No. ESIG-2023-013/847001 and Award No. RIG-2023-107

6. REFERENCES

Abdelmonem, A., Lützenkirchen, J., Leisner, T., 2015. Probing ice-nucleation processes on the molecular level using second harmonic generation spectroscopy. Atmos. Meas. Tech. 8, 3519–3526. https://doi.org/10.5194/amt-8-3519-2015

Barahona, D., 2015. Thermodynamic derivation of the activation energy for ice nucleation. Atmos Chem Phys 15, 13819–13831. https://doi.org/10.5194/acp-15-13819-2015

Bauerecker, S., Ulbig, P., Buch, V., Vrbka, L., Jungwirth, P., 2008. Monitoring Ice Nucleation in Pure and Salty Water via High-Speed Imaging and Computer Simulations. The Journal of Physical Chemistry C 112, 7631–7636. https://doi.org/10.1021/jp711507f

Carignano, M.A., Baskaran, E., Shepson, P.B., Szleifer, I., 2006. Molecular dynamics simulation of ice growth from supercooled pure water and from salt solution. Ann Glaciol 44, 113–117.

Conde, M.M., Rovere, M., Gallo, P., 2018. Molecular dynamics simulations of freezing-point depression of TIP4P/2005 water in solution with NaCl. J Mol Liq 261, 513–519.

Elif Genceli Güner, F., Wåhlin, J., Hinge, M., Kjelstrup, S., 2015. The temperature jump at a growing ice–water interface. Chem Phys Lett 622, 15–19. https://doi.org/10.1016/J.CPLETT.2015.01.013

Englezos, P., 1994. The freeze concentration process and its applications. Developments in Chemical Engineering and Mineral Processing 2, 3–15.
Espinosa, J.R., Soria, G.D., Ramirez, J., Valeriani, C., Vega, C., Sanz, E., 2017. Role of Salt, Pressure, and Water Activity on Homogeneous Ice Nucleation. J Phys Chem Lett 8, 4486–4491. https://doi.org/10.1021/acs.jpclett.7b01551
Fatemi, S.M., FOROUTAN, M., 2016. Molecular dynamics simulations of freezing behavior of pure water and 14% water-NaCl mixture using the coarse-grained model.
Izutsu, K., 2018. Applications of freezing and freeze-drying in pharmaceutical formulations. Survival Strategies in Extreme Cold and Desiccation: Adaptation Mechanisms and Their Applications 371–383.
Kalista, B., Shin, H., Cho, J., Jang, A., 2018. Current development and future prospect review of freeze desalination. Desalination 447, 167–181. https://doi.org/10.1016/j.desal.2018.09.009
Kucera, J., 2019. Desalination: water from water. John Wiley & Sons.
Langham, E.J., Mason, B.J.-N., Bernal, J.D., 1997. The heterogeneous and homogeneous nucleation of supercooled water. Proc R Soc Lond A Math Phys Sci 247, 493–504. https://doi.org/10.1098/rspa.1958.0207
Li, C., Tao, R., Luo, S., Gao, X., Zhang, K., Li, Z., 2018. Enhancing and Impeding Heterogeneous Ice Nucleation through Nanogrooves. The Journal of Physical Chemistry C 122, 25992–25998. https://doi.org/10.1021/acs.jpcc.8b07779
Limmer, D.T., Chandler, D., 2013. Corresponding states for mesostructure and dynamics of supercooled water. Faraday Discuss 167, 485–498. https://doi.org/10.1039/C3FD00076A
Luo, S., Jin, Y., Tao, R., Li, H., Li, C., Wang, J., Li, Z., 2021. Molecular understanding of ion rejection in the freezing of aqueous solutions. Physical Chemistry Chemical Physics 23, 13292–13299.
Matsumoto, M., Saito, S., Ohmine, I., 2002. Molecular dynamics simulation of the ice nucleation and growth process leading to water freezing. Nature 416, 409–413. https://doi.org/10.1038/416409a
Metya, A.K., Singh, J.K., 2018. Nucleation of Aqueous Salt Solutions on Solid Surfaces. The Journal of Physical Chemistry C 122, 8277–8287. https://doi.org/10.1021/acs.jpcc.7b12495
Metya, A.K., Singh, J.K., Müller-Plathe, F., 2016. Ice nucleation on nanotextured surfaces: the influence of surface fraction, pillar height and wetting states. Physical Chemistry Chemical Physics 18, 26796–26806. https://doi.org/10.1039/C6CP04382H
Moore, E.B., de la Llave, E., Welke, K., Scherlis, D.A., Molinero, V., 2010. Freezing, melting and structure of ice in a hydrophilic nanopore. Physical Chemistry Chemical Physics 12, 4124–4134. https://doi.org/10.1039/B919724A
Nathoo, J., Jivanji, R., Lewis, A.E., 2009. Freezing your brines off: eutectic freeze crystallization for brine treatment, in: International Mine Water Conference. pp. 431–437.
Naullage, P.M., Metya, A.K., Molinero, V., 2020. Computationally efficient approach for the identification of ice-binding surfaces and how they bind ice. J Chem Phys 153, 174106. https://doi.org/10.1063/5.0021631
Pangborn, J.B., 1963. Observations of the eutectic freezing of salt solutions. Report to AJ Barduhn, Department of Chemical Engineering, Syracuse University.
Qiu, Y., Hudait, A., Molinero, V., 2019. How Size and Aggregation of Ice-Binding Proteins Control Their Ice Nucleation Efficiency. J Am Chem Soc 141, 7439–7452. https://doi.org/10.1021/jacs.9b01854
Ren, Y., Bertram, A.K., Patey, G.N., 2020. Effects of Inorganic Ions on Ice Nucleation by the Al Surface of Kaolinite Immersed in Water. J Phys Chem B 124, 4605–4618. https://doi.org/10.1021/acs.jpcb.0c01695
Rozmanov, D., Kusalik, P.G., 2011. Temperature dependence of crystal growth of hexagonal ice (I h). Physical Chemistry Chemical Physics 13, 15501–15511.
Saji, V.S., Meroufel, A.A., Sorour, A.A., 2020. Corrosion and fouling control in desalination industry. Springer.
Sánchez, J., Ruiz, Y., Auleda, J.M., Hernández, E., Raventós, M., 2009. Freeze concentration in the fruit juices industry. Food Science and Technology International 15, 303–315.
Sayer, T., Cox, S.J., 2019. Stabilization of AgI's polar surfaces by the aqueous environment, and its implications for ice formation. Physical Chemistry Chemical Physics 21, 14546–14555. https://doi.org/10.1039/C9CP02193K
Slattery, J.C., Sagis, L., Oh, E.-S., 2007. Interfacial transport phenomena. Springer Science & Business Media.
Soria, G.D., Espinosa, J.R., Ramirez, J., Valeriani, C., Vega, C., Sanz, E., 2018. A simulation study of homogeneous ice nucleation in supercooled salty water. J Chem Phys 148, 222811.
Stepakoff, G.L., Siegelman, D., Johnson, R., Gibson, W., 1974. Development of a eutectic freezing process for brine disposal. Desalination 15, 25–38.
Tsironi, I., Schlesinger, D., Späh, A., Eriksson, L., Segad, M., Perakis, F., 2020. Brine rejection and hydrate formation upon freezing of NaCl aqueous solutions. Physical Chemistry Chemical Physics 22, 7625–7632.
Vrbka, L., Jungwirth, P., 2005. Brine rejection from freezing salt solutions: A molecular dynamics study. Phys Rev Lett 95, 148501.
Whaley, D., Damyar, K., Witek, R.P., Mendoza, A., Alexander, M., Lakey, J.R.T., 2021. Cryopreservation: an overview of principles and cell-specific considerations. Cell Transplant 30, 0963689721999617.
Williams, P.M., Ahmad, M., Connolly, B.S., Oatley-Radcliffe, D.L., 2015. Technology for freeze concentration in the desalination industry. Desalination 356, 314–327.
Wu, S., Zhu, C., He, Z., Xue, H., Fan, Q., Song, Y., Francisco, J.S., Zeng, X.C., Wang, J., 2017. Ion-specific ice recrystallization provides a facile approach for the fabrication of porous materials. Nat Commun 8, 15154.
Zhang, S., Zhang, C., Wu, S., Zhou, X., He, Z., Wang, J., 2021. Ion-specific effects on the growth of single ice crystals. J Phys Chem Lett 12, 8726–8731.
Zielke, S.A., Bertram, A.K., Patey, G.N., 2016. Simulations of Ice Nucleation by Model AgI Disks and Plates. J Phys Chem B 120, 2291–2299. https://doi.org/10.1021/acs.jpcb.5b06605

Rethymno City map – SUSTENG 2024

Contact

Professor Petros Gikas
Design of Environmental Processes Laboratory
School of Chemical and Environmental Engineering, Technical University of Crete, Greece
T: +30 28210 37836
E: pgikas@tuc.gr, secretariat.susteng@tuc.gr
W: www.deplab.tuc.gr, www.susteng2024.tuc.gr

SUSTENG 2024